Les multiples facettes des adénovirus : Focus à travers les dodécaèdres de l'Ad3 humain

Pascal Fender

HAL Id: tel-01063446

https://tel.archives-ouvertes.fr/tel-01063446

Submitted on 12 Sep 2014

Université Joseph Fourier de Grenoble

HABILITATION A DIRIGER
DES RECHERCHES

Pascal FENDER

Chargé de recherche au CNRS

Les multiples facettes des adénovirus :
Focus à travers les dodécaèdres de l'Ad3 humain

Soutenance 16 juin 2006

Dr Hugues Lortat-Jacob	**Président**
Dr Yves Gaudin	**Rapporteur**
Dr Saw See Hong	**Rapporteur**
Dr Emmanuelle Vigne-Dedieu	**Rapporteur**
Dr Jadwiga Chroboczek	**Examinateur**

Institut de Biologie Structurale (CNRS/CEA/UJF), 41 rue Jules Horowitz
38027 Grenoble Cedex 9

Remerciements

2

Je tiens à exprimer ma reconnaissance aux différentes personnes qui chacune à leur manière m'ont aidé. Que vous soyez mes proches, mes collègues de tous les jours, membres du jury ou collaborateurs : Merci !

The study of biology is partly an exercise in natural esthetics. We derive much of our pleasure as biologists from the continuing realization of how economical, elegant and intelligent are the accidents of evolution that have been maintained by selection. A virologist is among the luckiest of biologists because he can see into his chosen pet down to the details of all of its molecules. The virologist sees how an extreme parasite functions using just the most fundamental aspects of biological behavior.

DAVID BALTIMORE (Nobel Lecture, December 12, 1975)

Résumé :

Les adénovirus sont le fil conducteur du travail présenté dans ce rapport. Une partie importante est dédiée à une particule « pseudo-virale » non pathogène appelée le dodécaèdre de l'Ad3. Plusieurs aspects sont abordés dans ce mémoire. Nous verrons tour à tour, des aspects de virologie fondamentale tels que les mécanismes d'entrée des virus dans les cellules, des aspects structuraux avec l'étude de ces complexes par cryomicroscopie ou encore des aspects d'applications biotechnologiques. L'adénovirus est un bon exemple montrant que les connaissances dérivant d'un organisme aussi petit dépassent largement le simple cadre de la particule mais viennent s'intégrer dans le contexte général du fonctionnement cellulaire. L'étude de ces particules hyperspécialisées dans l'attachement et la pénétration des cellules permet non seulement d'approfondir les connaissances mais ouvre également des perspectives biotechnologiques notamment dans le domaine de la vectorisation de molécules thérapeutiques.

SOMMAIRE

PREMIERE PARTIE

PRESENTATION DU CANDIDAT

Curriculum, Synopsis de carrière, Production scientifique

Etat Civil

Pascal FENDER
Né le 2 juin 1970 à Brive la gaillarde (19)
Vie Maritale, 2 enfants

Adresse personnelle :
35, rue Thiers
38000 GRENOBLE
Tel : 04 76 17 09 06

Adresse professionnelle :
Institut de Biologie Structurale
41, rue Jules Horowitz
38027 Grenoble
Tel : 04 38 78 95 78
fender@ibs.fr

Cursus universitaire

1990 DEUG de Biologie (Chimie-Biochimie)- Mention AB – Université de Limoges
1991 Licence de Biochimie – Mention AB – Université Paul Sabatier de Toulouse
1992 Maîtrise de Microbiologie – Mention AB - Université Paul Sabatier de Toulouse
1993 DEA de Biologie Moléculaire et Cellulaire – Mention B – Université Joseph Fourier de Grenoble
1997 Doctorat de Biologie – Mention très honorable avec les félicitations - Université Joseph Fourier de Grenoble
« Etude Structurale et Fonctionnelle des dodécaèdres de l'adénovirus de sérotype 3 – Elaboration d'un nouveau vecteur de transfert de gènes»

Fonctions, Financements

Bourse du ministère de la recherche (MRT) ; Oct 1994 à Sept 1997
Financement d'Ingénieur de Recherches CNRS (en CDD) ; Oct 1997 à Juillet 1998
Financement de Post Doctorat (CNRS-Rhône Poulenc Gencell) ; Août 1998 à Sept 1999

Chargé de Recherche 2ème classe au CNRS ; Octobre 1999
Chargé de Recherche 1ère classe depuis Octobre 2003

Obtention d'un contrat « Emergence » de la région Rhône-Alpes en 2001 (23.000 €)

Membre de la commission de spécialistes de l'UFR de Biologie de l'Université Joseph Fourier de Grenoble depuis 2003

Rapporteur pour les revues « Gene Therapy » et « Journal of Gene Medicine »

Diffusion des connaissances

Auteur de 15 publications internationales
Auteur de 2 publications francophones
Détenteur de 2 brevets d'invention internationaux
Présentations orales dans 3 congrès internationaux

Enseignement de la Virologie et de la Vectorologie en 2ème et 3ème cycle universitaire

Porteur du projet « Virologie et applications au domaine des biotechnologies médicales » dans le cadre de la Fête de la Science

SYNOPSIS DE CARRIERE

<u>Sept 1992 – Sept 1993</u>

DEA de Biologie Moléculaire et Cellulaire, Université de Grenoble
Institut de Biologie Structurale de Grenoble (Groupe de Jadwiga Chroboczeck)

Expression et caractérisation du domaine « tête » de la fibre de l'Ad2.
Expression dans le système de baculovirus et purification de ce domaine trimérique responsable de la reconnaissance du récepteur (non identifié à cette époque). Caractérisation structurale (microscopie électronique, pontage chimique) et fonctionnelle (attachement aux cellules). Production d'anticorps monoclonaux dirigés contre ce domaine. Détermination des sites antigéniques et caractérisation d'anticorps neutralisants.

<u>Oct 1993 – Juillet 1994</u>
Service national

<u>Oct 1995 – Oct 1997</u>

Doctorat de Biologie, Université de Grenoble
Institut de Biologie Structurale de Grenoble (Groupe de Jadwiga Chroboczeck)

Caractérisation structurale et fonctionnelle du dodécaèdre de l'Ad3. Elaboration d'un nouveau vecteur de transfert de gènes.
- Coexpression de la base du penton et de la fibre de l'Ad3 dans le système de baculovirus.
- Caractérisation structurale par microscopie électronique (obtention d'un complexe symétrique : le dodécaèdre). Structure à moyenne résolution par cryomicroscopie. Détermination de l'importance de la base du penton de l'Ad3 dans l'auto-assemblage des particules et comparaison avec la base du penton de l'Ad2.
- Caractérisation fonctionnelle. Suivi de l'attachement et de l'entrée des dodécaèdres dans les cellules. Détermination de l'importance relative de la protéine « base du penton » et de la protéine « fibre » dans les processus d'attachement et d'endocytose. Création de dodécaèdres « chimériques » portant la fibre d'un sérotype différent de l'Ad3.
- Applications biotechnologiques. Elaboration d'un système permettant d'utiliser la haute capacité d'endocytose des dodécaèdres pour apporter de l'ADN plasmidique dans les cellules.

Caractérisation physique de ce système par diffusion de lumière et corrélation avec son efficacité dans différentes conditions d'utilisation (tampon, temps d'incubation, stoechiométrie des différents composants).

<u>Nov 1997 – Juillet 1998</u>

Post-doctorant. (Ingénieur de recherche au CNRS en CDD)

Institut de Biologie Structurale de Grenoble (Groupe de Jadwiga Chroboczeck)

Caractérisation d'un peptide transfectant dérivé de l'adénovirus

Utilisation d'un peptide composé des 20 acides aminés N-terminaux de la fibre de l'Ad3 prolongé par 20 lysines pour condenser de l'ADN plasmidique et transfecter des cellules en culture. Suivi du peptide seul ou des complexes peptides/ADN par microscopie confocale.

<u>Août 1998 - Sept 1999</u>

Post-doctorant (CNRS- Rhône Poulenc Gencell)

Laboratoire de Génétique de la Neurodégénérescence, Hôpital de la Pitié Salpétrière à Paris (dirigé par Jacques Mallet)

Rhône-Poulenc Gencell, groupe «Vector development/ Vector design », Centre de Recherche de Vitry-Alfortville (dirigé par Mitch Finner)

Elaboration d'adénovirus recombinants de « troisième génération » régulables par la tétracycline.

Production d'adénovirus recombinants plus surs et moins immunogènes (délétés des régions précoces E1, E3 et E4) dits de « troisième génération ». Adaptation du système « Tet-On » pour la régulation de l'expression des transgènes sur un système 2 virus (virus régulateur et virus opérateur) et sur un virus unique (régulateur et opérateur). Caractérisation de ces adénovirus régulables dans le cerveau (voie nigro-striée) et dans le muscle. Détermination du rôle des promoteurs utilisés et de la stoechiométrie transactivateur/opérateur sur le bruit de fond en absence d'inducteur et sur le taux d'induction obtenu en présence d'inducteur. Construction d'adénovirus de troisième génération codant le facteur neurotrophique GDNF (Glial Derived Neurotrophic Factor) sous la dépendance du promoteur « cellule-spécifique » GFAP (Glial Fibrillary Acidic Protein) exprimé spécifiquement dans les cellules gliales.

Chargé de recherche 2ème classe au CNRS

Institut de Biologie Structurale de Grenoble (Groupe de Jadwiga Chroboczeck)

Etude de la formation des dodécaèdres dans les cellules infectées par l'Ad3. Création d'un vecteur de transfert de protéines dans les cellules.

- Etude cinétique et localisation de la biogénèse des dodécaèdres et des virions dans les cellules infectées par l'Ad3. Quantification du nombre de dodécaèdres produits par cellule infectée et détermination du ratio dodécaèdres/virion.

- Production d'anticorps monoclonaux dirigés contre la base du penton de l'Ad3. Démonstration que les dodécaèdres décorés par certains anticorps monoclonaux pénètrent efficacement dans les cellules vectorisant ainsi ces protéines multimériques de haut poids moléculaire.

- Conception d'un système universel d'attachement permettant l'apport de protéines d'intérêt dans les cellules par les dodécaèdres: les modules WW. Etude de l'efficacité de ce système sur des lignées humaines immortalisées ou sur des cultures primaires.

Depuis Sept 2004

Chargé de recherche 1ère classe au CNRS

Institut de Biologie Structurale de Grenoble (Groupe d'Hugues Lortat-Jacob)

Caractérisation des mécanismes d'entrée des dodécaèdres dans les cellules. Importance relative des intégrines et des protéoglycanes dans l'attachement et l'internalisation.

- Mise en évidence d'une voie d'endocytose des dodécaèdres dépendante des héparanes sulfate. Calcul des constantes d'affinité et de la démonstration de la spécificité de l'interaction des dodécaèdres pour les héparanes sulfate. Détermination du rôle respectif de la base et de la fibre dans les chemins d'endocytose.

- Recherche des séquences peptidiques responsables de l'interaction avec les HS. Etude structurale par cryomicroscopie et cristallographie des interactions dodécaèdres-HS.

- Détermination du rôle respectif des HS et des intégrines dans l'attachement et l'internalisation des dodécaèdres. Etude de la régulation de ces composants au cours du cycle cellulaire.

DEUXIEME PARTIE

PRODUCTION SCIENTIFIQUE

Publications, Brevets, Encadrement, Enseignements, Fonctions

PUBLICATIONS

Pubications internationales:

1. Garcel, A, Gout, E, Timmins, J, Chroboczek J, and Fender P. Protein transduction into human cells by adenovirus dodecahedron using WW domains as universal adaptors. **J. Gene Med, 2006; 8(4): 524-31**

2. Fuschiotti P, Schoehn, G, Fender, P, Fabry, C, Hewat, E, Chroboczek, J, Ruigrok, R and Conway J. Structure of the dodecahedral penton particle from human adenovirus type 3. **J Mol Biol, 2006; 356 (2): 510-20**

3. Vivès, R, Lortat-Jacob, H, and Fender P. Heparan Sulfate Proteoglycans and viral vectors: ally or foe? **Curr Gene Ther, 2006; 6 (1): 35-44.**

4. Fender P, Boussaid A, Mezin P, and Chroboczek J. Synthesis, cellular localisation and quantification of penton-dodecahedron in serotype 3 Adenovirus infected cells. **Virol**, **2005; 340(2): 167-173**

5. Mahot S, Fender P, Vivès R, Caron C, Perrissin M, Gruffat H, Sergeant A and Drouet E. Cellular Uptake of the EBV transcription factor EB1/Zta. **Virus Res, 2005; 110:187-93.**

6. Szolajska E, Poznanski J, López Ferber M, Michalik J, Gout E, Fender P, Bally I, Dublet B and Chroboczek J. Poneratoxin, a neurotoxin from ant venom: structure, expression in insect cells and construction of a bio-insecticide. **Eur J Biochem, 2004; 271(11):2127-36**

7. Fender P. Recombinant adenoviruses and adenovirus penton vectors: from DNA transfer to direct protein delivery into cell. **Gene Ther Mol Biol, 2004 ; 8: 85-90.**

8 : Vivès R, Lortat-Jacob , Chroboczek J and Fender P. Heparan Sulphate Proteoglycan mediates the selective attachment and internalisation of serotype 3 adenovirus dodecahedron. **Virol, 2004; 321(2): 332-340.**

9 : Fender P, Schoehn G, Foucaud-Gamen J, Gout E, Garcel A, Drouet E, and Chroboczek J. Adenovirus dodecahedron allows large multimeric protein transduction in human cells. **J.Virol, 2003 ; 77(8): 4960-4964.**

10: Fender P, Jeanson L, Ivanov MA, Colin P, Mallet J, Dedieu JF, Latta-Mahieu M. Controlled transgene expression by E1-E4-defective adenovirus vectors harbouring a "tet-on" switch system. **J Gene Med. 2002 ; 4(6): 668-75.**

11: Zhang F, Andreassen P, Fender P, Geissler E, Hernandez JF, Chroboczek J. A transfecting peptide derived from adenovirus fiber protein. **Gene Ther. 1999;6(2):171-81.**

12: Fender P, Ruigrok RW, Gout E, Buffet S, Chroboczek J. Adenovirus dodecahedron, a new vector for human gene transfer. **Nat Biotechnol, 1997; 15(1): 52-6.**

13: Schoehn G, Fender P, Chroboczek J, Hewat EA. Adenovirus 3 penton dodecahedron exhibits structural changes of the base on fibre binding. **EMBO J, 1996; 15(24): 6841-6.**

14: <u>Fender P</u>, Kidd AH, Brebant R, Oberg M, Drouet E, Chroboczek J. Antigenic sites on the receptor-binding domain of human adenovirus type 2 fiber. **Virol, 1995; 214(1): 110-7.**

15: Louis N, <u>Fender P</u>, Barge A, Kitts P, Chroboczek J. Cell-binding domain of adenovirus serotype 2 fiber**. J Virol, 1994; 68(6): 4104-6.**

<u>Publications francophones :</u>

16: <u>Fender P,</u> Garcel A, Gout E, Timmins J, Weissenhorn W, Chroboczeck J. Vectorisation de protéines thérapeutiques par les dodécaèdres de l'adénovirus. **Bulletin du cancer, 2004; 91 (6) : 475**

17: Lortat-Jacob, H,   <u>Fender P</u> and Vivès, R. Virus et héparane sulfate : des mécanismes d'adsorption cellulaire à l'entrée virale. **Virologie, 2005; 9: 315-325.**

<u>Publication en cours :</u>

18. Fuschiotti P, <u>Fender P</u>, Schoehn G, & Conway J.F. Development of the dodecahedral penton particle from Adenovirus 3 for therapeutic application. **(in press, J Gen Virol).**

BREVETS

<u>Brevets internationaux:</u>

1:      Fender et Chroboczek (CNRS, CEA) 1997 et 2000
        Complexe protéique dodecaèdrique adénoviral, procédé de préparation, composition le contenant et ses applications
        (US6083720/ WO9718317/EP0861329)

2:      Fender et Chroboczek (CNRS/CEA) 1997 et 2004
        Peptide transfectant adénoviral, composition le contenant et applications.
        (US6750058/ WO9923237/EP1029070/FR2770537)

ENCADREMENT

J'ai encadré de nombreux étudiants de différents niveaux universitaires (DUT à DEA) et de différentes formations (biologiste, physicien). L'encadrement d'étudiants en troisième cycle est mis en évidence par les rectangles de couleur.

1995   Wendy Mona - *Licence de Biochimie* - 2 mois

1996   Anita Adrets   - *IUT de Biologie Animale* - 3 mois

1997-1998   Stéphane Pons - *Maîtrise de Physique* - 6 mois

1999-2000   Laurence Jeanson - *Co-encadrement du DEA ENS-Cachan* « Développement de vecteurs adénoviraux de troisième génération : Régulation pharmacologique de l'expression des transgènes » Publication commune :   Fender *et al*., Journal of Gene Medicine, 2002

2000   Soléne Chambert. - *3ème année de Pharmacie* - 2 mois

2000-2001   Mike Failly - *Encadrement du DEA de Biologie Structurale et Fonctionnelle* « Etude structurale de la stabilité des dodécaèdres de l'Ad3. Dissociation et réassociation. »

2002   Christine Suchier - *Maîrise de Biologie* - 2 mois (remerciée pour son aide dans Vivès *et al.*, Virology 2004)

2002-2003   Aude Garcel - *Encadrement du DEA de Génie Biologique et Médicale* « Développement et optimisation d'un nouveau vecteur de transfert de protéines » Publications communes :   Fender *et al.*, Journal of Virology 2003   Garcel *et al.*, Journal of Gene Medicine 2006

2004   Ali Boussaid - *Encadrement du D.U de Biotechnologie de l'Université de Rennes.* Localisation et quantification des dodécaèdres au cours du cycle viral de l'Ad3 Publication commune :   Fender *et al.*, Virology, 2005

2005   Alexandre Dias : Stage M1 de Biologie - 2 mois

2006   Katherine Boardman – Stage M1 de Biologie – 2 mois

2006   Romain Blanchet – Stage M1 de Biologie – 2 mois

2006   Charles Vragniaud – BTS Analyses Biologiques – 3 mois

ENSEIGNEMENTS

J'ai assuré des enseignements essentiellement sous forme de **cours magistraux en Virologie et Vectorologie** en deuxième et troisième cycle universitaire.

- Travaux pratiques en Enzymologie. Maîtrise de Biochimie de la Faculté des Sciences de Grenoble (36H)
- Cours de Virologie. 3ème année de la Faculté de Pharmacie de Grenoble (8H)
- Cours de Vectorologie en DEA « Génie Biologique et Médical » (6H)
- Cours de Virologie au module de virologie de l'école doctorale de chimie et des sciences du vivant (16H)

FONCTIONS

Rédacteur de projet

Dans le cadre de la valorisation de mes projets de recherches, j'ai soumis en 2001 une demande de financement à la région Rhône-Alpes. Ce projet **« Emergence 2001 »** visant à développer des vecteurs de transfert de protéines dans les cellules humaines a été retenu à hauteur du financement demandé **(150.000 F, 23000€)**.

Rapporteur pour des journaux scientifiques

Je suis régulièrement sollicité comme **« rapporteur »** pour deux prestigieux journaux de thérapie génique : « Journal of Gene Medicine » et « Gene Therapy » .

Membre de la commission de spécialistes de l'UFR de Biologie de l'UJF

Depuis 2003, je suis **membre nommé de la commission de spécialistes** de l'UFR de Biologie (sections 64 à 69 du CNU) de l'Université Joseph Fourier de Grenoble.

Porteur de projets

J'ai porté le projet « Virologie et applications au domaine des biotechnologies médicales » dans le cadre de la **fête de la science 2004 et 2005**. Ce projet consistait en une journée porte ouverte de l'Institut de Biologie Structurale avec des animations interactives avec le grand public autour des moyens d'étude en virologie et les applications virales en thérapie génique.

TROISIEME PARTIE

EXPOSE DES TRAVAUX PRINCIPAUX

Les multiples facettes des adénovirus.
Focus à travers le dodécaèdre de l'Ad3

PREAMBULE

Dans l'exposé suivant, je ferai ressortir les principales découvertes issues de mon travail de recherche. Les détails opératoires ne seront pas mentionnés ceux-ci étant accessibles dans les publications. Il en est de même pour la bibliographie qui sera limitée à un minimum de références essentielles pour la compréhension du rapport. La plupart de mes articles décrits dans ce mémoire sont donnés en annexe du document.

Le fil conducteur des recherches est l'adénovirus. Celui-ci sera vu sous des aspects purement fondamentaux comme l'étude de ses protéines de structure, la recherche de partenaires cellulaires ou encore l'étude des mécanismes d'endocytose mais également sous des aspects d'utilisations biotechnologiques en tant que vecteur de transfert. Si la plupart des recherches sur l'adénovirus humain utilisent les modèles des sérotype 2 ou 5, notre modèle d'étude repose essentiellement sur une particule originale associée à l'adénovirus de sérotype 3 : le dodécaèdre de l'adénovirus.

Le plan du rapport s'attachera à mettre en valeur d'une part les recherches « fondamentales », et d'autre part les aspects « applications » et ne suivra donc pas toujours la chronologie des découvertes.

Plan

Généralités
- Généralités sur les adénovirus
- Aperçu sur les dodécaèdres

Formation des dodécaèdres
- Expression des dodécaèdres dans baculovirus
- Eléments structuraux de la formation des dodécaèdres
- Expression des dodécaèdres au cours du cycle viral

Propriétés biologiques des dodécaèdres
- Les dodécaèdres entrent dans les cellules
- Le dodécaèdre base
- La base du penton interagit avec les héparanes sulfate
- Survie des dodécaèdres dans les cellules

Vectorologie
- Régulation de l'expression d'un transgène dans le contexte des Rads
- Vectorisation d'ADN par les dodécaèdres
- Vectorisation de protéines par les dodécaèdres

Projets en cours et à venir
- Localisation structurale des sites d'interaction des HS sur les Dds
- Détermination du rôle respectif des HS et des intégrines
- Compréhension du rôle biologique des dodécaèdres

GENERALITES

Généralités sur les adénovirus

Les adénovirus ont été identifiés en 1953 à partir d'amygdales d'enfants infectés (Rowe et al., 1953). Les adénovirus peuvent infecter les mammifères (Mastadénovirus), les oiseaux (Aviadenovirus) et animaux à sang froid classés chez les Atadénovirus ou les Siadénovirus (Davison, Benko, and Harrach, 2003). Chez l'homme, la cinquantaine de sérotypes répertoriés est divisée en six sous-groupes de A à F, selon des critères biochimiques, génétiques et structuraux. Les sérotypes les plus étudiés sont l'adénovirus de sérotype 2 (Ad2) et l'adénovirus de sérotype 5 (Ad5 : utilisé en thérapie génique) appartenant au sous-groupe C. L'Ad3, objet de mes travaux appartient au sous-groupe B.

D'un point de vue structural, les adénovirus sont des virus icosaédriques à ADN dont les facettes triangulaires sont composées d'une protéine trimérique appelée l'hexon (240 copies). Une protéine pentamérique, la base du penton, compose les sommets de l'icosaèdre et interagit de façon non-covalente avec une protéine trimérique en forme d'antenne : la fibre. Le complexe formé de la base du penton et de la fibre est appelé : le penton. Si le domaine globulaire externe de la fibre appelé « domaine tête » est structuralement proche d'un sérotype à l'autre, la longueur de la partie allongée (la tige) varie suivant les sous-groupes. Cette variation vient du nombre de domaines structuraux répétés constituant cette tige (Green et al., 1983). Ainsi, la fibre de l'Ad3 contenant 9 éléments répétés présente une longueur d'environ 16 nm alors que celle de l'Ad2 qui en contient 22 présente une longueur d'environ 37 nm (Ruigrok et al., 1990).

Les étapes précoces de l'infection

Lorsque j'ai commencé mon travail de recherche au cours de mon DEA en 1992, un certain nombre d'éléments essentiels de l'adénovirus n'était pas connus. Aucun récepteur adénoviral n'était identifié ce qui justifie le choix de nous être intéressé particulièrement à la fibre et à la base du penton . Depuis l'ores, de nombreux travaux ont éclairé les étapes précoces de l'internalisation des adénovirus. En 1993, deux publications ont décrit qu'une séquence « RGD » conservées dans la plupart des bases du penton des sérotypes adénoviraux humains (à l'exception du sous-groupe F : Ad40 et Ad41) était responsable de la reconnaissance des intégrines $\alpha v\beta 3$ et $\alpha v\beta 5$ et que cette interaction induisait l'internalisation

du virus (Belin and Boulanger, 1993; Wickham et al., 1993). Cette même année, le « déshabillage » progressif du virus à l'intérieur de la cellule et le transport de son génome vers le noyau ont été disséqués (Greber et al., 1993). Ce processus fait apparaître l'endocytose du virus par des vésicules à clathrine, un relargage très précoce de la fibre et de la base du penton (10 et 20 minutes respectivement) au cours de l'acidification de ces vésicules et une « endosomolyse » rapide permettant au génome viral d'aller vers les pores nucléaires *via* les microtubules en une quarantaine de minutes. Il est à noter que pour les adénovirus du sous-groupe B comme l'Ad3, objet de mes études ou encore l'Ad7, ce mécanisme est très différent de celui du sous-groupe C comme l'Ad2 ou l'Ad5 (Fig 1). Ces adénovirus sont incapables de se libérer des endosomes et suivent la voie lysosomiale (Miyazawa et al., 1999). Cependant, si le temps nécessaire à ces sérotypes pour délivrer leur information génétique dans les noyaux est nettement supérieur (entre 2 et 8 heures), leur efficacité réplicative est comparable.
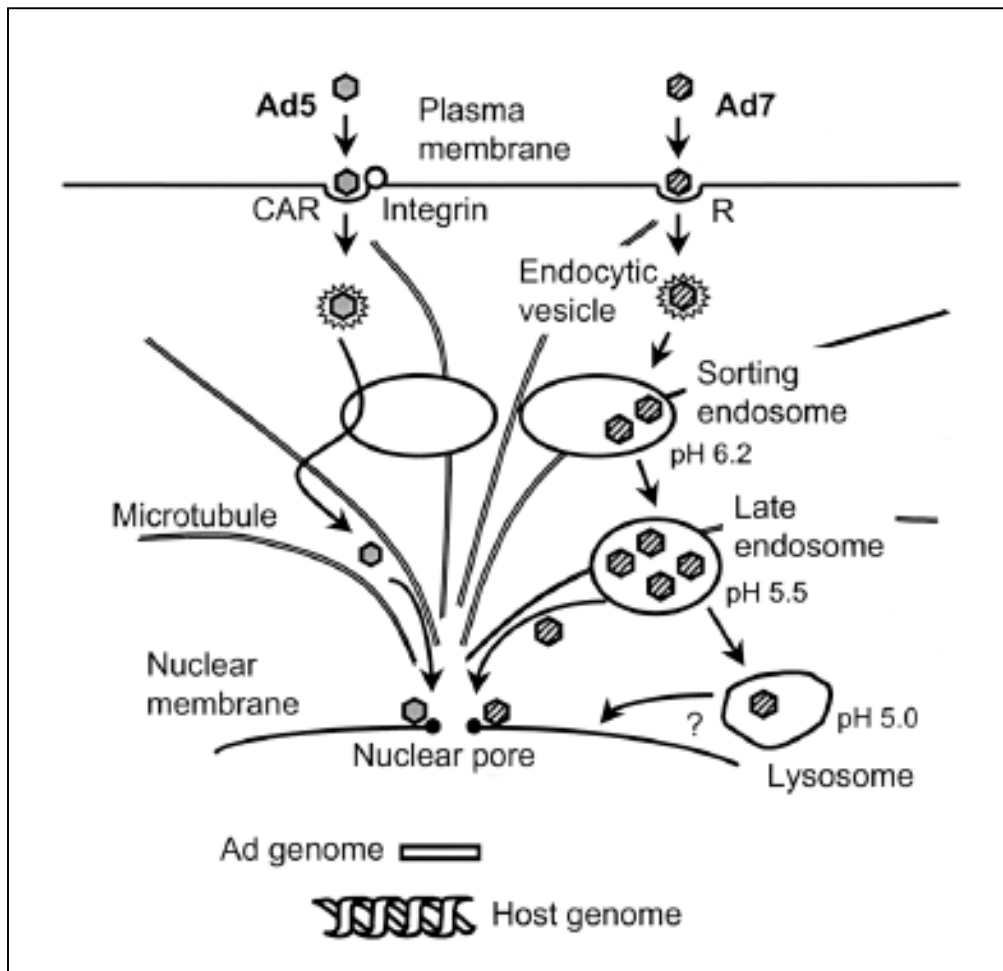

Figure 1 : Shéma présentant les chemins d'endocytose respectivement suivis par les adénovirus du sous-groupe C (Ad5) et du sous-groupe B (Ad7). D'après Miyazawa et al., 1999.

Les récepteurs adénoviraux

Malgré d'intenses recherches dans différents groupes, il aura fallu attendre 1997 pour voir l'identification des premiers récepteurs adénoviraux. C'est ainsi qu'il a été montré que le domaine α2 du complexe majeur d'histocompatibilité de classe I (MHC-I) interagissait avec les domaines globulaires de la fibre de l'Ad5 (Hong et al., 1997).

Un autre récepteur commun au cocksackie virus et à l'adénovirus nommé CAR (Cocksakie and Adenovirus Receptor) a été identifié de façon concomitante (Bergelson et al., 1997). Ce récepteur semble être commun à la plupart des sérotypes humains à l'exception du sous-groupe B dont fait partie l'Ad3 (Roelvink et al., 1998). Ceci explique la différence de tropisme des sérotypes appartenant à ce sous-groupe ainsi que le changement de chemin intracellulaire décrit ci-dessus (confère Fig 1) (Miyazawa, Crystal, and Leopold, 2001; Miyazawa et al., 1999).

Plus récemment, un nouveau type de récepteur, les « héparane sulfate protéoglycanes » (HSPG) ont été décrits pour l'Ad2 (Dechecchi et al., 2001; Dechecchi et al., 2000). Cette reconnaissance est responsable de l'internalisation de 50% de l'Ad2 sur des cellules épithéliales en culture et n'est pas sensible à l'ajout de CAR soluble. L'interaction entre ces récepteurs portant des chaînes d'oligosaccharides fortement sulfatés et la fibre interviendrait non pas sur le domaine globulaire de celle-ci mais sur sa tige. La fibre de l'Ad3 possédant une tige plus petite et plus rigide (Wu et al., 2003) n'interagit pas avec les HSPG (Dechecchi et al., 2000).

Concernant plus spécifiquement le sous-groupe B, l'usage des récepteurs est plus complexe ce qui nécessite une sous-classification des sérotypes en B1 et B2. Les sérotypes appartenant à B1 reconnaissent un récepteur unique alors que ce du groupe B2 reconnaissent ce même récepteur et un récepteur additionnel (Segerman et al., 2003a). Plusieurs groupes ont identifié de façon concomitante CD46 comme étant le récepteur de certains sérotypes du sous-groupe B (Gaggar, Shayakhmetov, and Lieber, 2003; Segerman et al., 2003b; Sirena et al., 2004). Une incertitude persiste pour l'Ad3 (sous groupe B1), car un travail lui attribue CD46 comme récepteur (Sirena et al., 2004), alors que d'autres travaux excluent la possibilité que CD46 soit le récepteur commun au groupe B1 (Marttila et al., 2005). Des molécules exprimées à la surface des lymphocytes B et des cellules dendritiques matures telles que CD80 et CD86 peuvent également servir de récepteurs pour le sous groupe B (Short et al., 2004; Zhang and Bergelson, 2005).

Les vecteurs adénoviraux

Du fait de leur facilité de production à haut titre et de leur grande efficacité de pénétration dans les cellules, les adénovirus sont des vecteurs de choix pour l'apport d'ADN à des fins biotechnologiques ou thérapeutiques. Je ne rentrerai pas dans le détail de leur production et dans les différentes générations d'adénovirus recombinants existantes, ces renseignements se trouvant dans la revue (Fender P, Gene Ther Mol Biol, 2004, en annexe). Brièvement, les vecteurs adénoviraux sont délétés d'une région précoce (E1) indispensable à la réplication du virus. Cette région est apportée en *trans* dans les cellules HEK-293 afin de permettre la production des adénovirus recombinants. La place libérée par cette région (et éventuellement par la région E3 non indispensable pour la réplication du virus sur des cultures cellulaires) permet l'apport du transgène. Des générations plus évoluées ont été élaborées en délétant la région précoce E4 ou en utilisant une région précoce E2 thermosensible. Ceci permettait non seulement de libérer de la place pour l'apport du transgène et surtout d'éviter l'apparition d'adénovirus compétants pour la réplication (RCA : replication competent adenovirus) qui polluaient les stocks d'adénovirus de première génération. Finalement, une dernière génération d'adénovirus dite « gutless » conservant uniquement les séquences ITR et la séquence d'encapsidation et ne possédant aucune séquence codante du virus est apparue. Ces virus moins immunogènes permettent en théorie l'apport de transgène d'environ 30 kpb au lieu de 7 kpb pour les générations précédentes.

Aperçu sur les dodécaèdres de l'adénovirus

Géométrie

D'un point de vue purement géométrique, un dodécaèdre est un solide composé de 12 faces pentagonales et possédant 20 sommets. Il est intéressant de noter que ce solide est complémentaire de l'icosaèdre qui lui, est composé de 20 faces triangulaires et possède 12 sommets. Ces deux solides appartiennent aux solides de Platon (avec le cube, le tétraèdre et l'octaèdre) car leurs côtés sont isométriques, tous les angles sont égaux et ils sont inscriptibles dans une sphère. Le dodécaèdre et l'icosaèdre sont dits « dual » car il est possible de les inscrire l'un dans l'autre (Fig 2). Ces solides possèdent des axes de symétrie 2, 3 et 5.
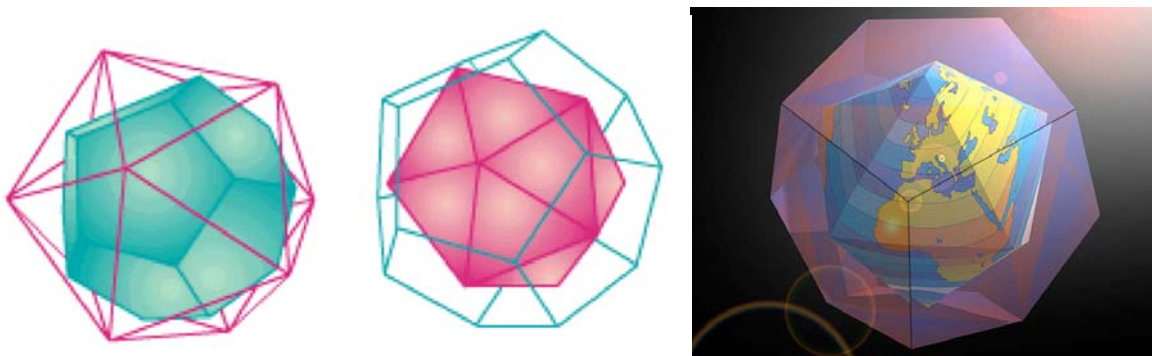
Figure 2 : Dualité des icosaèdres et des dodécaèdres. Un dodécaèdre peut être inscrit dans un icosaèdre (à gauche) et réciproquement (au milieu). D'un point de vue symbolique l' icosaèdre représente la terre inscrite dans l'univers dodécaèdrique.

Historique

La première mise en évidence des dodécaèdres adénoviraux date de 1966, une époque où la structure des adénovirus et de leurs constituants était peu connue. En purifiant les antigènes solubles produits lors de l'infection de cellules humaines par l'Ad3, Norrby a observé des structures présentant une symétrie dodécaèdrique ressemblant à une étoile à cinq ou six branches: les dodécaèdres. Ces dodécaèdres étaient formés d'après l'auteur par des protéines ayant une structure tubulaire et autour desquelles étaient retrouvés cinq ou six points (Norrby, 1966). Ces structures tubulaires correspondent à ce que nous appelons aujourd'hui les bases du penton et les points correspondent aux domaines tête de la fibre. Dans ce travail, Norrby remarquait que les composants formant le dodécaèdre (les pentons) étaient normalement présents aux 12 sommets de la capside virale.

La purification de ces structures reposait sur les propriétés hémagglutinantes que possèdent les dodécaèdres. Lors d'une première étape de purification sur gradient de chlorure de césium, les virus entiers et défectifs étaient éliminés. Le matériel recueilli au dessus des

bandes virales était purifié lors d'une seconde étape par ultracentrifugation sur gradient de saccharose. L'activité hémagglutinante des différentes fractions du gradient de saccharose a permis de déterminer que cet antigène se retrouvait uniquement dans les fractions lourdes et qu'il semblait posséder un coefficient de sédimentation de 50-60 S. L'observation de ce matériel en microscopie électronique a permis à Norrby de définir une taille de 22,5 à 27,5 nm pour le coeur du dodécaèdre (les bases du penton) et de 40 à 50 nm entre deux "points" opposés (les domaines tête des fibres).

Sérotypes et dodécamérisation

Depuis cette première description, d'autres travaux ont permis de mettre en évidence la présence ou l'absence de dodécaèdres dans des cellules infectées par différents sérotypes d'adénovirus humains. Ainsi le sérotype 4 (Norrby and Wadell, 1967), le sérotype 7 (Neurath and Rubin, 1968), le sérotype 11 (Norrby, 1968) et les sérotypes 9 et 15 (Norrby et al., 1967) sont connus pour donner des structures dodécaèdriques lors de leur cycle d'infection alors que la présence de dodécaèdres n'a jamais pu être détectée pour les sérotypes 1, 2, 5 et 6 (Wadell and Norrby, 1969), le sérotype 12 (Norrby and Ankerst, 1969) et le sérotype 16 (Norrby and Skaaret, 1968) ou pour les adénovirus entériques (Ad40 et Ad41).

La formation de dodécaèdres ne semble pas être dépendante des sous-groupes d'adénovirus (tableau 1). Il est intéressant de noter que si aucun sérotype du sous groupe C ne produit naturellement de dodécaèdre, la structure de la base de l'Ad2 a été résolue à partir d'un cristal de bases du penton s'étant dodécamérisées au cours de la cristallogénèse (Zubieta et al., 2005).

Sous-groupe	Sérotypes
A	**12**, 18, 31
B	**3**, **7**, **11**, 14, **16**, 21, 34, 35
C	**1, 2, 5 ,6**
D	8, **9**, 10, 13, **15**, 17, 19, 20, 22-30, 32, 33, 36-39, 42
E	**4**
F	**40**, **41**

Tableau 1 : Formation de dodécaèdres en fonction des sérotypes d'adénovirus. La formation de dodécaèdres a été observée pour les sérotypes indiqués en rouge alors que les sérotypes indiqués en bleu n'en forment pas. Pas de données pour les sérotypes indiqués en noir.

RECHERCHE

FORMATION DES DODÉCAÈDRES

Les dodécaèdres ont été observés pour la première fois en 1966 à partir de cellules infectées par l'Ad3. Depuis l'ores, quelques travaux ont mentionné la présence ou non de dodécaèdres dans le lysat de cellules infectées. Une partie de mon travail mené depuis 1994 a été consacrée à l'identification structurale des éléments nécessaires à la formation des dodécaèdres et à la détermination de leurs fonctions.

Expression des dodécaèdres dans baculovirus :

Publication de référence : Fender et al., Nat Biotech 1997

En coexprimant la base du penton et la fibre de l'Ad3 dans le système de baculovirus nous avons purifié sur gradient de sucrose une particule dodécamérique avec les fibres projetées vers l'exérieur. Cette particule à été nommée le dodécaèdre-fibre (DF) (Fender et al., 1997). L'expression simple de la base du penton de l'Ad3 à quant à elle permis de purifier une particule nommée le dodécaèdre-base (DB) (Fig 3). D'un point de vue structural, ceci démontre que l'information de dodécamérisation est contenue dans la base du penton et qu'aucun autre élément adénoviral n'est requis. L'expression de la base de l'Ad2 dans baculovirus (gracieusement donné par le groupe de Pierre Boulanger) nous a permis de confirmer que malgré une forte expression, les bases de ce sérotype ne pouvaient pas se dodécamèriser.
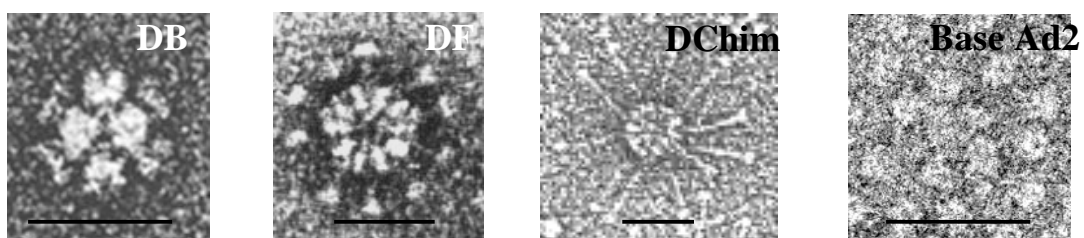
Figure 3 : Micrographies des différents dodécaèdres. Dodécaèdre composé uniquement de la base Ad3 (DB), dodécaèdre composé de la base et de la fibre Ad3 (DF), dodécaèdre chimérique composé de la base Ad3 et de la fibre Ad2 (DChim), et base pentamérique de l'Ad2. Les différentes photos ne sont pas présentées à la même échelle, la barre indique 30 nm.

Si l'interaction entre les bases pentamériques dépend des sérotypes, l'interaction base-fibre semble plus universelle. En incubant la fibre « longue » de l'Ad2 avec des DB de l'Ad3 nous avons pu obtenir des dodécaèdres chimériques. Réciproquement, l'incubation de la fibre courte de l'Ad3 avec des bases pentamériques de l'Ad2 permet l'obtention de penton chimérique.

En conclusion, nous pouvons dire que les interactions bases-fibres sont conservées entre plusieurs sérotypes. L'information de dodécamérisation est, quant à elle, contenue uniquement dans la base du penton de certains sérotypes. Aucun autre élément adénoviral n'est requis pour la formation des dodécaèdres.

### Eléments structuraux de la formation des dodécaèdres
Publications de référence : Schoehn et al., EMBO 1996 – Fuschiotti et al., JMB 2006

Nous avons résolu pour la première fois la structure des DB et des DF par cryomicroscopie à 20A de résolution (Schoehn et al., 1996). Ceci nous a permis de montrer qu'une cavité d'environ 8,7 nm de diamètre (350 nm^3) était présente dans les dodécaèdres. Ces particules sont donc des pseudovirus ne contenant aucune information génétique. De façon très intéressante, en présence de la fibre, une boucle de la base du penton contenant la séquence RGD se déplace de 15A vers l'extérieur de la structure. Il est donc envisageable que la reconnaissance des intégrines diffère entre le DB et le DF.

En 2004, la structure de la base du penton de l'Ad2 délétée de 49 acides aminés du côté N-terminal a été résolue par cristallographie aux rayonx X à 3,3A par le groupe de Stephen Cusack à l'EMBL de Grenoble (Zubieta et al., 2005). Etonnamment, cette base qui ne forme pas spontanément de dodécaèdres s'était dodécamérisée au cours de la cristallogénèse ce qui a permis l'identification des résidus impliquées dans la formation du complexe. En faisant correspondre cette structure cristallographique de la base Ad2 dans un modèle du dodécaèdre Ad3 obtenu par cryomicroscopie à 9A, nous avons pu mettre en évidence que l'architecture des dodécaèdres de l'Ad3 repose sur uniquement trois points de contact entre deux bases adjacentes. La séquence SDVS d'un pentamère « A » interagit avec son homologue sur un pentamère « B » voisin alors que la séquence NDFT du pentamère « A » interagit avec la séquence RSTR du pentamère « B » et que vice versa la séquence RSTR du pentamère « A » est en interaction avec la séquence NDFT du pentamère « B » (Fig 4).

En dehors de ces séquences d'interaction bien définies, nous avons montré qu'un clivage protéolytique joue sur la stabilité des dodécaèdres. Le monomère de la base Ad3 est composé de 544 acides aminés. Nous avions identifié au cours de mon doctorat qu'une coupure protéolytique partielle était observée du côté N-terminal (E37-A38). Depuis l'ores, nous avons montré que cette coupure joue un rôle sur la stabilité des dodécaèdres, la forme tronquée donnant des dodécaèdres très stables alors que la forme non protéolysée résulte essentiellement en la production de bases pentamériques ou de dodécaèdres très instables (Fuschiotti et al., 2006). Cette observation s'explique par le positionnnement du côté N-terminal de la base du penton dans la cavité du dodécaèdre. La « libération » des 37 premiers acides aminés de la base du penton sur les 60 monomères composant le dodécaèdre revient à enlever 2.220 résidus (244 kDa) au niveau de la cavité interne ce qui résulte en un moindre encombrement stérique et donc à une stabilisation du complexe.

Outre l'importance fondamentale des interactions « protéine-protéine », ces données structurales seront utiles à des fins biotechnologiques dans le domaine de la vectorisation.
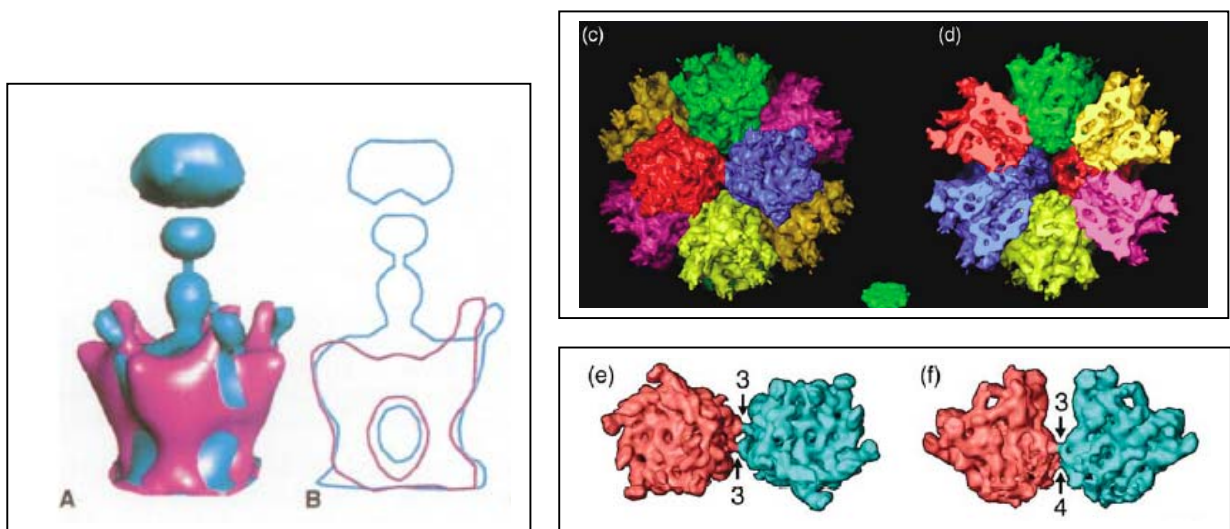
Figure 4 : Structure des dodécaèdres par cryomicroscopie. Changement de la structure de la base du penton (en rouge) en présence de la fibre (A et B). Structure du dodécaèdre-base à 9A de résolution (C) et coupe transversale montrant la cavité interne (D). Points de contact entre deux bases de l'Ad3 permettant la formation des dodécèadres (E et F). La vue « par dessus » montre les interactions entre les séquences RSTR et NDFT (marquées 3), la vue « de côté » montre l'interaction entre deux séquences SDVS adjacentes (marquée 4).

Expression des dodécaèdres au cours du cycle viral

Publication de référence : Fender et al., Virology 2005

L'étude des dodécaèdres peut se faire à partir de particules isolées produites dans un système d'expression tel que le baculovirus. Il n'en reste pas moins vrai que ces particules sont naturellement produites au cours du cycle viral de l'Ad3 et de quelques autres sérotypes adénoviraux (cf : tableau 1 page 23). Je me suis intéressé à leur production au cours du cycle infectieux du virus. Ce travail publié récemment (Fender et al., 2005) (en annexe) fait ressortir que la biosynthèse des monomères de la base du penton commence dans le cytoplasme des cellules 12 heures après infection. Ces polypeptides sont transportés rapidement dans le noyau où ils s'accumulent de façon diffuse alors que la traduction protéique continue dans le cytoplasme. Après 20 heures d'infection, il n'y a plus de néosynthèse dans le cytoplasme mais un arrangement du signal correspondant à la base du penton est observé le long de la membrane nucléaire côté interne. Il s'agit de dodécaèdres qui se sont assemblés dans le noyau. Il n'est malheureusement pas possible d'observer directement en microscopie électronique ces particules sur des coupes ultrafines de cellules infectées mais la corrélation de cette technique ultrastructurale avec la microscopie confocale fait apparaître une nette différenciation du signal dû aux bases dodécamérisées de celles présentent aux sommets des virus. Une quantification du nombre de dodécaèdres fait apparaître qu'en moyenne $7,5\ 10^5$ dodécaèdres sont produits par cellule. Ce nombre est bien supérieur au nombre de virions produits par cellule puisque nous avons estimé un ratio dodécaèdres/virion de l'ordre de 200. La fonction biologique des dodécaèdres n'est pas connue mais un tel excès suggère un rôle biologique important pour les dodécaèdres. (Cf : Compréhension du rôle biologique des dodécaèdres, page 39)

PROPRIÉTÉS BIOLOGIQUES DES DODÉCAÈDRES

Les dodécaèdres entrent dans les cellules

Publications de référence : Fender et al., Nat Biotech 1997

Le dodécaèdre-fibre (DF)

Comme nous l'avons vu dans l'introduction, les éléments clefs de l'entrée virale sont la base du penton et la fibre présentes aux douze sommets de la capside. Il était donc important d'étudier si ces protéines conféraient des propriétés d'endocytose aux dodécaèdres. Nous avons très rapidement montré que le DF était capable de s'attacher à 4°C aux cellules en culture. En incubant ensuite ces cellules à une température permissive pour l'endocytose (37°C), nous avons observé une internalisation très rapide de ces particules (Fender et al., 1997). En une dizaine de minutes seulement, la plupart des complexes se retrouvent autour du noyau mais ils ne semblent pas pénétrer dans celui-ci même après une heure d'incubation (Fig 5).
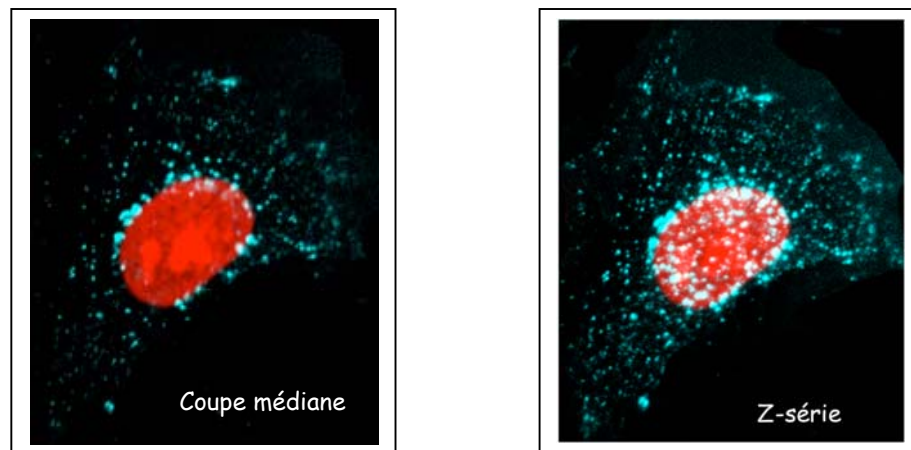
Figure 5 : Etude de l'entrée des dodécaèdres dans les cellules. Les dodécaèdres incubés pendant une heure à 37°C sur des cellules HeLa sont détectés en bleu, le noyau est marqué en rouge. La coupe médiane d'une cellule montre la concentration des vésicules autour du noyau. La série Z de la même cellule consiste en la projection de 8 coupes focales de 0,5 µm partant du plan médian en allant vers le haut de la cellule et donne l'aspect tridimensionnel de cette cellule.

Par analogie au virus Ad3 ou Ad7 (Miyazawa et al., 1999) (Fig 1, page 19), il est concevable d'imaginer un mécanisme d'internalisation du DF par des vésicules d'endocytose. Dans un premier temps, la fibre reconnaît un récepteur à haute affinité ce qui facilite une interaction secondaire de la base du penton avec les intégrines. Cette dernière déclenche l'endocytose (Mathias, Galleno, and Nemerow, 1998; Wickham et al., 1993) et les petites

vésicules ainsi obtenues fusionnent entre elles pour donner des endosomes tardifs qui se retrouvent près du noyau.

Le dodécaèdre-base (DB)

Les mécanismes d'internalisation en deux étapes avec la reconnaissance d'un récepteur d'attachement à haute affinité facilitant la reconnaissance d'un récepteur d'endocytose à plus basse affinité sont couramment observés chez les virus. Lorsque nous incubons des DB sur des cellules, nous observons une très forte internalisation de celui-ci montrant que la fibre n'est pas indispensable pour l'endocytose. Ceci suggére donc un mécanisme à une étape pour cette particule. En comparant l'efficacité d'entrée des DF et des DB, nous avons pu montrer que la fibre est très utile à faible concentration (0,3 nM) mais non indispensable à une concentration légèrement supérieure (3 nM) (Fender et al., 2003). A cette dernière concentration, l'internalisation du DB représente en effet 70% du signal obtenu pour le DF alors qu'il n'était que de 7% pour une concentration 10 fois moins élevée (Tableau 2).

	0,3 nM	3 nM
DB	7%	70%
DF	83%	100%

Tableau 2 : Efficacité d'internalisation des DB et des DF sur les cellules HeLa à deux concentrations différentes. Les résultats sont exprimés en pourcentage relatif par rapport à la valeur maximale observée.

Il existe donc une interaction de la base du penton avec les cellules permettant l'internalisation des complexes. D'après la littérature disponible, nous pouvions imaginer un passage direct par les intégrines. Des travaux sur la base du penton de l'Ad2 ont également montré que celle-ci pénétrait efficacement dans les cellules et que contrairement à la base Ad3, elle pouvait même atteindre le noyau (Hong et al., 1999b). Les auteurs discutaient le possible rôle de récepteurs auxiliaires aux intégrines dans l'endocytose de cette protéine. Nous avons étudié cette possibilité et caractérisé ainsi le rôle des héparanes-sulafte dans l'internalisation de la base du penton.

La base du penton interagit avec les héparanes sulfates

(Publications de référence : Vivès et al, Viorology 2004 – Lortat-Jacob et al., Virologie 2005 – Vivès et al., Curr Gene Ther 2006)

Les héparanes sulfates (HS) sont des chaînes de glycosaminoglycanes composées de la répétition d'un dissacharide sulfaté. Ces groupements peuvent être liés à un cœur protéique et forment alors un « protéoglycane ». De nombreux virus utilisent ces protéoglycanes et en particulier leurs chaînes d'HS pour s'attacher aux cellules (confère nos revues : (Vives, Lortat-Jacob, and Fender, 2006) et (Lortat-Jacob, Fende rand Vivès, 2005). Dans le cas de l'adénovirus, il a été montré que l'Ad2 et l'Ad5 utilisaient ces chaînes d'HS grâce à une interaction par les protéines « fibre ». L'Ad3, lui, n'utilise pas ces groupements HS pour son endocytose (Dechecchi et al., 2000).

De façon étonnante, nous avons pu mettre en évidence que les dodécaèdres se comportaient tout à fait différemment du virus dont ils sont issus. Nous avons ainsi montré qu'aussi bien les DF que les DB pouvaient se fixer à 4°C sur des cellules CHO exprimant des HS alors qu'ils ne se fixaient pas sur un clone de ces cellules n'exprimant pas d'HS à leur surface (Vives et al., 2004). Des caractérisations biochimiques par résonance plasmonique de surface, nous ont permis de confirmer que l'interaction se faisait par la base du penton avec une affinité pour les HS de l'ordre du nanomolaire. La fibre ne joue aucun rôle positif ou négatif dans cette interaction puisque les affinités trouvées étaient identiques pour le DB et le DF.

Des expériences de compétition avec de l'héparine soluble sur des cellules HeLa ont permis de déterminer que l'internalisation des DB était strictement dépendante d'une interaction avec les HS cellulaires. Ce résultat indique que l'internalisation des DB n'est pas due à une interaction directe de la base avec les intégrines mais à un processus séquentiel commençant par la reconnaissance des HS. Dans le cas du DF, l'ajout d'héparine soluble ne bloque que partiellement l'internalisation de ces particules montrant que parallèlement aux interactions base du penton/HS coexiste un mécanisme de reconnaissance « classique » fibre/récepteur qui lui est indépendant des HS.

Un schéma récapitulatif de ces interactions est présentés avec de nouvelles données sur la figure 9, page 38 de la partie « projet en cours ».

Survie des dodécaèdres dans les cellules
Publication de référence : non publié

Nous nous sommes intéressés au devenir intracellulaire des dodécaèdres dans les cellules et en particulier à leur survie. Pour cela, nous avons incubé des cellules HeLa pendant une heure avec des dodécaèdres et nous avons lysé ces cellules à différents temps pour quantifier la présence de la base ou de la fibre après immunotransfert en utilisant un anticorps reconnaissantces deux protéines. Une diminution du signal est observée avec le temps, avec en particulier, des sauts importants après 1, 4 et 6 heures (Figure 6). Aucun produit de protéolyse n'est observé que ce soit pour la base ou pour la fibre ce qui laisse à penser que la dégradation ne se fait pas par des coupures internes dans les polypeptides mais de façon processive et rapide. Ce mécanisme pourrait correspondre à une dégradation de type « protéasome ». Des expériences complémentaires en microscopie confocale nous ont permis de montrer que des signaux spécifiques des dodécaèdres étaient détectables autour du noyaux des cellules jusqu'à 8 heures d'incubation. Le signal est à peine détectable après 24 heures dans les cellules dans ce type d'expérience (incubation pendant 1 heure avec les particules puis lavage) alors que le signal est très visibles à 24 heures si les dodécaèdres sont laissés dans le milieu pendant toute la durée de l'expérience (non montré). Ceci suggère un mécanisme de recyclage permanent des récepteurs à surface des cellules.
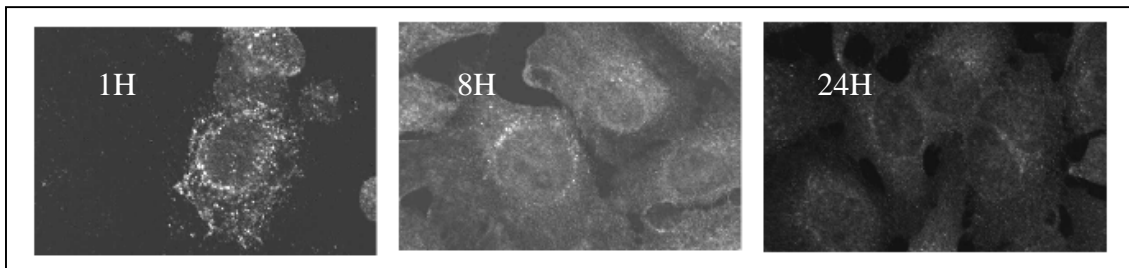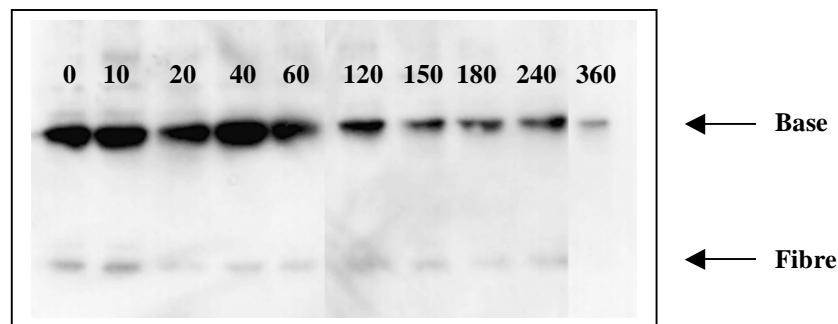
Figure 6 : Survie des dodécaèdres dans les cellules. En haut : les cellules HeLa incubées à 4°C avec le DF sont lavées puis incubées à 37°C pour les temps indiqués. Après lyse cellulaire, la présence de la base et de la fibre est détectée par western-blot (temps en minutes). En bas : immunodétection des dodécaèdres dans les cellules HeLa par microscopie confocale après 1, 8 ou 24 heures à 37°C.

VECTOROLOGIE

Régulation de l'expression d'un transgène dans le contexte des adénovirus recombinants

Publications de référence : Fender et al., J. Gene Med 2002 – Fender. Gene Ther Mol Biol 2004

Ce travail a été réalisé au centre de recherche de Rhône-Poulenc Gencell à Vitry et en collaboration avec le laboratoire de génétique de la neurodégénerescence de l'Hôpital de la Pitié Salpétrière à Paris.

Le but de ce travail était de construire des adénovirus recombinants qui pourraient recevoir des accords d'essais cliniques chez l'homme dans le cas des maladies neurodégénératives. Ceci nécessitait de travailler avec des vecteurs adénoviraux incapables de se multiplier dans les cellules. Ces virus délétés des régions précoces E1-E3-E4 étaient dits de troisième génération (cf Fender. Gene Ther Mol Biol 2004). Un deuxième prérequis pour obtenir cette autorisation était de pouvoir contrôler l'expression du transgène et notamment de pouvoir arrêter facilement son expression. Pour cela, nous nous sommes tournés vers le système « Tet On » qui permet d'allumer un promoteur régulable par l'ajout de tétracycline (Gossen et al., 1995). Ce système nécessite deux éléments distincts : des régions opératrices (Op7) en amont d'un promoteur minimal (CMV* ou TK*) et un transactivateur qui n'est actif qu'après s'être lié à la tétracycline le « rtTA » (Fig 7). L'ajout de tétracycline permet donc d'activer l'expression du gène et le retrait de l'inducteur permet un retour à un niveau minimum d'expression.
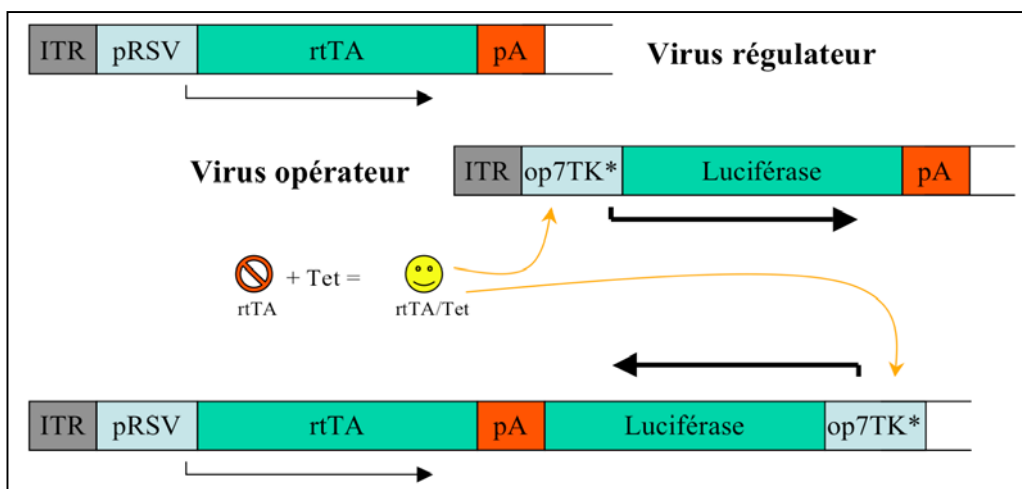

Figure 7 : Principe du système « Tet On ». Ce système peut être appliqué avec une stratégie deux virus (en haut) ou virus unique (en bas). En présence de tétracycline le transactivateur peut se fixer sur les région opératrices et déclencher la transcription du transgène.

Nous avons utilisé le gène reporteur de la luciférase que nous avons clonés en aval de deux promoteurs minimaux TK* et CMV* (promoteur de la Thymidine Kinase du virus Herpes Simplex et promoteur du Cytomégalovirus) précédés des régions opératrices Op7. Le transactivateur rtTA était pour sa part codé sous la dépendance d'un promoteur RSV entier (Rous Sarcoma Virus). Nous avons testé l'efficacité de régulation suivant une stratégie deux virus (virus régulateur + virus opérateur) ou virus unique (opérateur et régulateur).

Plusieurs enseignements ont été tirés de cette étude (Fender et al., 2002) :

- En absence d'inducteur, le promoteur minimal Op7-TK* donne peu de bruit de fond ce qui n'est pas le cas du promoteur minimal Op7-CMV* qui donne une expression basale 50 à 100 fois supérieure que ce soit sur des cultures cellulaires ou in vivo dans le cerveau de rat.

- La statégie « virus unique » donne de bons résultats. L'efficacité d'induction dépend du taux d'expression du transactivateur rtTA. Cette expression est variable d'un type cellulaire à un autre. La configuration choisie (Op7-TK* - luciférase/ RSV-rtTA) est optimum dans les cellules PC12 alors que dans les astrocytes primaires humains, le taux d'induction du virus unique de 80X peut atteindre 620X lors de l'apport d'un excès de virus codant le rtTA.

- Il est possible d'allumer et d'éteindre à façon l'expression d'un gène en ajoutant ou en enlevant l'inducteur sur les cultures de cellules.

- Pour les expériences *in vivo* dans le *striatum* de rat ou dans le muscle de souris nous avons montré qu'il était possible avec la stratégie « virus unique » d'obtenir des taux d'induction de 8X à 32X en apportant la doxycycline (analogue de la tétracycline) dans l'eau de boisson des animaux. L'ajout de virus codant le rtTA était bénéfique en petite quantité car il permettait d'augmentait le taux d'induction alors qu'un excès de ce virus résultait en l'augmentation du bruit de fond en absence d'inducteur traduisant ainsi une fixation non contrôlée du transactivateur sur les régions opératrices.

Vectorisation d'ADN par les dodécaèdres
Publication de référence : Fender et al., Nat Biotech 1997

La grande efficacité d'internalisation des dodécaèdres les rend intéressants pour la vectorisation de molécules dans les cellules. Dépourvus de matériel génétique, les dodécaèdres ne pose pas les mêmes problèmes que les adénovirus recombinants d'un point de vue sûreté. Le volume de la cavité interne par contre ne permet pas d'envisager son utilisation pour encapsider des acides nucléiques (Schoehn et al., 1996). Pour pallier ce

problème, nous avons élaboré un peptide bifonctionnel mimant la partie de la fibre de l'Ad3 interagissant avec la base (les 20 résidues N-terminaux) que nous avons prolongé par 20 lysines afin d'interagir avec les acides nucléiques. Ce peptide était capable d'interagir avec les DB mais également avec les DF car la fibre trimérique n'occupe que trois des cinq sites de liaison présents par base pentamérique. La partie polylysine quant à elle permettait d'attacher et de compacter l'ADN plasmidique.

Ce système nous a permis d'apporter des plasmides codant la luciférase dans des cellules en culture. L'expression de la luciférase qui était détectée de 9 à 72 heures après incubation prouvait que le plasmide avait réussi à franchir les membranes plasmiques et nucléaires et que le gène de la luciférase (sous la dépendance d'un promoteur SV40) avait été correctement transcrit puis traduit. Un effet dose-réponse était observé en augmentant le nombre de particules par cellule. L'efficacité du DB était nettement supérieure à celle du DF. Cette différence pouvait s'expliquer d'une part par le nombre de sites disponibles pour l'attachement du peptide sur le DB (12 fois 5 sites) contre (12 fois 2 sites demeurant libres) sur le DF, et d'autre part, par la gêne que provoque la fibre pour l'attachement des plasmides compactés.

Vectorisation de protéines par les dodécaèdres

Publications de référence : Fender et al., J. Virol 2003 – Fender. Gene Ther Mol Biol 2004 - Garcel et al., J. Gene Med 2006.

L'apport direct de protéines dans les cellules appelé également transduction de protéines est un champ émergent annexe à la thérapie génique. Il consiste à greffer une protéine d'intérêt incapable de franchir les barrières cellulaires à des protéines ou des peptides capables d'entrer dans les cellules. De façon intéressante, ces protéines ou peptides servant de vecteur sont souvent issus de protéines virales (ex : Tat de HIV ou VP22 de HSV ; confère la revue Fender - Gene Ther Mol Biol 2004) et entrent dans les cellules en utilisant une voie faisant intervenir les héparanes-sulfate (Console et al., 2003). Il était intéressant au vu de notre caractérisation des dodécaèdres d'explorer le potentiel de cette particule comme agent de transduction de protéines.

Dans un premier temps, nous avons élaboré des anticorps monoclonaux (MAbs) dirigés contre la base du penton. Nous avons sélectionné des clones capables de reconnaître aussi bien le DB que le DF et nous avons montré par microscopie électronique que ces anticorps décorés le pourtour des particules dodécaèdriques. L'incubation des complexes « dodécaèdre- MAbs » sur des cellules permettait une transduction rapide des anticorps qui

suivaient un chemin d'endocytose comparable à celui du dodécaèdre alors les anticorps seuls étaient incapables de pénétrer dans les cellules (Fender et al., 2003). Outre le fait que ces anticorps ne neutralisaient pas l'entrée des dodécaèdres, ce résultat apportait la preuve de principe de la transduction de protéines par nos vecteurs. L'efficacité du système est d'autant plus remarquable que les anticorps sont des protéines multimériques de grandes tailles (160 kDa).

Dans un deuxième temps, nous avons voulu généraliser notre système pour apporter n'importe quelle protéine d'intérêt. Il fallait donc trouver un système universel d'attachement qui remplacerait les interactions « antigènes-anticorps » utilisées lors de notre précédente étude. Pour cela, nous nous sommes penchés sur des résultats fondamentaux de notre laboratoire. La recherche de partenaires cellulaires de la base du penton en criblant une banque d'expression d'ADNc de poumons humains avec les dodécaèdres avait permis d'identifier plusieurs protéines qui possédaient toutes un point commun : des domaines WW (Galinier et al., 2002). Ces domaines structuraux WW sont composés d'environ 35 acides aminés et doivent leurs noms à deux résidus tryptophanes (W) conservés. Ils sont connus pour interagir avec des séquences complémentaires PPxY que l'on trouve conservées en deux exemplaires dans la séquence des bases du penton des différents sérotypes d'adénovirus.

Nous avons évalué l'utilisation de ces domaines WW pour greffer des protéines d'intérêt sur les dodécaèdres. Notre choix s'est porté sur une ubiquitine ligase (Nedd4) qui possède quatre domaines WW en tandem. Une caractérisation biochimique de ces domaines séparément ou en tandem nous a permis de conclure que, du fait d'une coopérativité d'interaction entre les domaines WW et les séquences PPxY, une construction contenant trois des quatres domaines (WW2,3,4) était optimale pour notre projet. Ce module WW2,3,4 peut être apporté en fusion N-terminale ou C-terminale avec des protéines d'intérêt ce qui permet leur attachement aussi bien au DB qu'au DF. Par microscopie confocale nous avons montré que la protéine d'intérêt était alors efficacement transduite dans les cellules ou elle colocalise avec le vecteur dodécaèdrique qui l'a délivrée (Garcel et al., 2006). Nous avons pu estimer qu'en moyenne 2. 10^7 protéines d'intérêt avaient été vectorisées par cellule après une heure d'incubation, démontrant le fort potentiel de nos vecteurs dans le domaine de la transduction de protéines.

PROJETS EN COURS ET A VENIR

Localisation structurale des sites d'interaction des HS sur les dodécaèdres

Nous cherchons à localiser les sites de fixation des HS sur la base de l'Ad3. Cette caractérisation devrait permettre d'apprendre d'une part s'il y a un ou plusieurs sites de fixation pour les HS par base pentamèrique et, d'autre part, si leur organisation ternaire dans le dodécaèdre facilite l'interaction. Ce dernier point pourrait en effet expliquer qu'il y ait une forte affinité des dodécaèdres pour les HS alors que le virus qui possède également douze base du penton est incapable d'interagir avec les HS (Dechecchi et al., 2000).

Un premier élément de réponse a été apporté par la microscopie électronique. En collaboration avec le Dr Guy Schoehn (IVMS-Grenoble), nous avons pu faire la reconstruction tridimensionnelle du DB avec un oligosaccharide d'HS composé de 8 saccharides (dp8). Ce dp8 donne une densité supplémentaire sur la boucle des dodécaèdres contenant la séquence RGD (Fig 8). Il se trouve que l'analyse de la séquence primaire de la base Ad3 nous avait fait suspecté cette région du fait de la présence de nombreux résidus basiques à proximité de la séquence RGD.
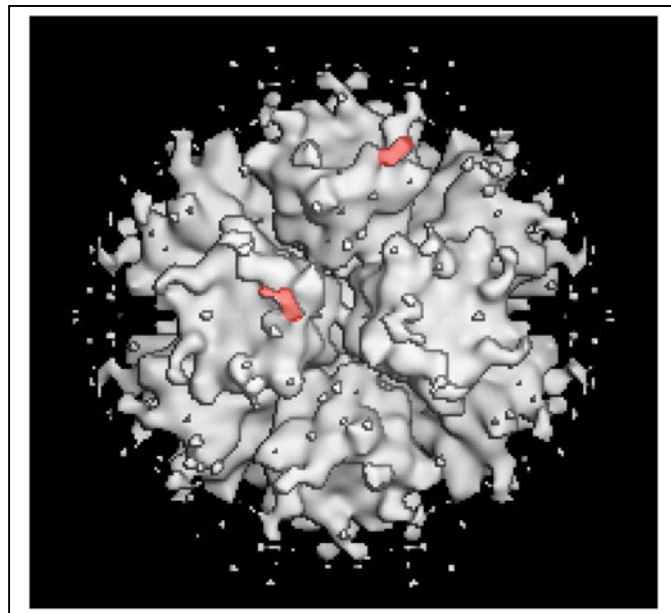
Figure 8 : Reconstruction du DB incubé avec un oligosaccharide d'héparane sulfate de 8 unités (dp8). Les densités supplémentaires (2 sont représentées en rose) dues a cette oligosaccharide sont localisées sur la boucle contenant la séquence RGD.

Cette étude sera poursuivie avec des oligosaccharides de plus grandes tailles. En effet, nous avons pu montrer par immunofluorescence que, contrairement à de l'héparine soluble de grande taille, la préincubation d'un excès de dp8 avec le DB n'empêchait pas sa fixation sur des cellules HeLa. Cela suggère soit une compétition entre les HS cellulaires et le dp8, soit l'existence d'un autre site de fixation des HS sur le dodécaèdre. Des données de suivi de l'attachement des dodécaèdres sur les cellules par immunofluorecence montrent un effet compétiteur brutal pour des oligosaccharide dp14 (7 unités disaccharidiques) alors qu'un oligosaccharide dp12 (6 unités disaccharidiques) ne neutralise pas l'attachement et l'internalisation des particules (résumé sur la figure 9, page suivante).

Cette étude sera complétée par une analyse structurale par cristallographie aux rayons X (collaboration avec les Dr Stephen Cusack et Elena Seiradake – EMBL Grenoble). Nous avons produit un dodécaèdre dont la partie N-terminale (les 37 premiers résidus) a été délétée. Ce dodécaèdre plus stable (cf : page 26), sera co-cristalisé avec des oligosaccharides de différentes tailles afin d'analyser finement l'interaction dodécaèdre-HS.

Détermination du rôle respectif des héparanes sulfate et des intégrines dans l'internalisation des dodécaèdres

Identification des protéoglycanes récepteurs

Il serait intéressant d'identifier le ou les protéoglycanes responsables de l'attachement des dodécaèdres à la surface des cellules. Du fait de la spécificité d'interaction avec les HS, il est envisageable que deux grandes familles de protéoglycanes soient impliquées dans cette reconnaissance : les syndécans (4 formes connues) et les glypicans (5 formes) connues. Nous avons montré par résonance plasmonique de surface (BIAcore) que certains anticorps monoclonaux que nous avions produits contre la base du penton de l'Ad3 ne neutralisaient pas les interactions dodécaèdres-HS. Ces MAbs nous serviront d'outils pour aller « pêcher » les complexes dodécaèdres - protéoglycanes obtenue en incubant nos particules pseudo-virales avec des préparations de protéines membranaires. L'identification des protéoglycanes impliquées pourra alors se faire de manière indirecte par immunodétection ou de manière directe par séquençage en spectrométrie de masse (ms/ms) (collaboration avec le Dr Michel Jaquinod au CEA grenoble).

Rôle des intégrines

Lors de nos précédents travaux (Vives et al., 2004), nous avions montré que les HS étaient primordiaux pour l'attachement des dodécaèdres, en particulier pour le DB qui ne peut pas utiliser la voie d'attachement de la protéine fibre. Il restait à déterminer si l'interaction avec les HS était suffisante pour permettre son endocytose. Nous avons pu montrer que les intégrines étaient indispensables pour déclencher l'endocytose. Pour cela, nous avons réalisé une mutation ponctuelle (D331 en E331) dans la séquence de la base. Le dodécaèdre ainsi obtenu appelé « mutant RGE » est toujours capable de se fixer aux cellules exprimant des HS mais ne peut pas pénétrer dans celles-ci. Ce résultat montrant la nécessité d'une interaction base-intégrines pour déclencher l'endocytose a été confirmé par l'utilisation d'une drogue « S36578 » gracieusement fourni par les laboratoires Servier. Cette drogue ne gêne pas la fixation des particules (DB et DF non muté) sur les HS mais empêche leur internalisation (Fig 9).
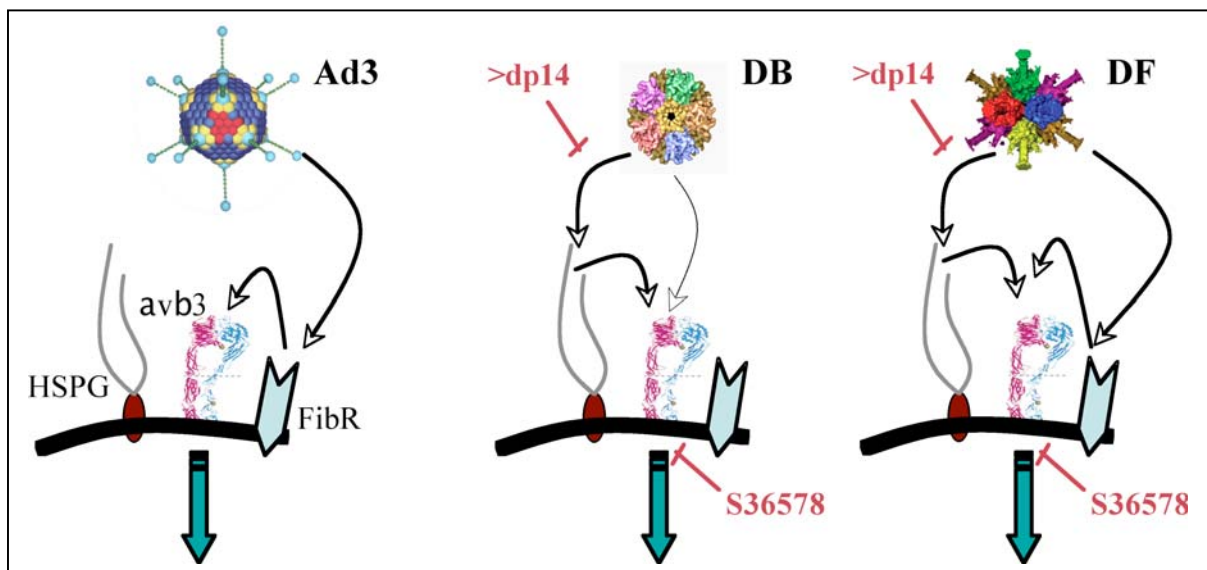
Figure 9 : Mécanismes d'attachement et d'internalisation des dodécaèdres. La base du penton interagit avec les HS ce qui facilite l'interaction avec les intégrines. L'attachement peut être bloqué par l'ajout d'oligosaccharides de tailles égales ou supérieures à quatorze unités saccharidiques (dp 14). En présence de la fibre un chemin indépendant des héparanes sulfate coexiste. Le bloquage des intégrines avec la drogue S36578 empêche aussi bien l'internalisation des DB et des DF. Le virus Ad3 n'interagit pas avec les HS.

L'incubation de dodécaèdres non mutés sur des cellules n'exprimant pas d'HS (CHO-2241) a permis de montrer une fixation très faible mais spécifique à 4°C des dodécaèdres sur ces cellules. Cela suggère qu'une interaction directe entre les séquences RGD des dodécaèdres et les intégrines existe. Un ciblage des intégrines par nos vecteurs est donc

possible mais celui-ci nécessiterait l'abrogation complète des interactions avec les HS. Ce travail est en cours d'élaboration avec la création de dodécaèdres mutées dans certaines séquences basiques comme KQKR ou KFKAR.

Compréhension du rôle biologique des dodécaèdres

Nous avons apporté de nombreux éléments nouveaux sur les dodécaèdres que ce soit au niveau biologique ou structural. Une question virologique fondamentale demeure : quel rôle joue les dodécaèdres au cours du cycle viral ? En effet, il est difficile d'imaginer qu'une particule aussi intrigante ait été conservée au cours de l'évolution si elle n'apporte pas d'avantage sélectif au virus. Cette question est extrêmement complexe à aborder.

- Une approche pourrait consister à comparer la réplication de l'Ad3 type sauvage avec celle d'un Ad3 dont les bases seraient mutées afin de ne plus se dodécamériser.

- Une approche similaire pourrait se faire avec des bases se dodécamérisant mais ne pouvant plus interagir avec les HS.

Pour cela, nous pourrions utiliser des Ad3 recombinants qui ont été récemment décrits (Sirena et al., 2005). Ces mutations ne devraient pas affecter la production des virus ainsi modifiés. En effet, dans le contexte viral, les bases ne sont pas dodécamériques et elles n'interagissent pas avec les HS. Nous pourrions alors étudier l'effet des bases mutées sur différents points du cycle viral tels que l'efficacité de la réplication, leur localisation dans les cellules au cours du cycle réplicatif, leurs rôles dans la diffusion du virus. Ce dernier point est extrêmement intéressant puisqu'il a été montré que l'excès de la fibre Ad2 produit au cours de la réplication de ce virus interagissait avec le récepteur CAR qui est un composant des jonctions serrées. Ce mécanisme permettait une meilleure diffusion des virions à partir de la première cellule infectée (Walters et al., 2002). Par analogie, nous avons montré que la base Ad3 était produite en excès et qu'elle interagissait avec les intégrines et les HS qui sont des éléments fondateurs de la cohésion cellulaire.

CONCLUSION

Les études que j'ai menées autour des adénovirus font intervenir différentes approches que sont la biologie structurale, la biologie cellulaire et les biotechnologies. Les virus peuvent être vus, tour à tour, comme des agents pathogènes, des agents thérapeutiques ou des outils de recherche fondamentale.

D'un point de vue structural, il est intrigant de remarquer qu'un virus icosaèdrique comme l'Ad3 produit au cours de sa réplication des particules dodécaèdriques qui sont les « dual » géométriques du virus. Si la production de particules pseudovirales (ou VLP : virus like particle) est fréquemment observée, le cas du dodécaèdre est particulier. En effet, les bases du penton n'interagissent pas naturellement entre elles au sein du virus alors qu'elles forment une particule hautement symétrique dans le cas du dodécaèdre. Cet assemblage confère de nouvelles propriétés à ces particules qui peuvent alors interagir fortement avec les héparanes sulfate et entrer dans les cellules par une voie que ne partage pas le virus. L'internalisation de ces particules dodécaèdriques est supérieure à l'adénovirus lui-même qui est pourtant à ce jour, un des modèles du genre dans ce domaine.

D'un point de vue vectorologie, il est intéressant d'utiliser les propriétés de ces particules. C'est ainsi que j'ai élaboré des systèmes permettant l'apport d'ADN plasmidique ou de protéines dans les cellules par l'intermédiaire des dodécaèdres. Pour ce faire, j'ai utilisé les connaissances fondamentales des interactions base du penton – fibre ou base du penton-domaines WW. La vectorologie consiste non seulement à créer des véhicules transportant des molécules dans les cellules, mais également à contrôler l'efficacité du système après transfert. La régulation de l'expression du transgène par le système « Tet On » représente le deuxième volet de cette science récente.

En poursuivant mes recherches sur les adénovirus, j'espère pouvoir non seulement continuer le développement de nouveaux concepts biotechnologiques mais également améliorer les connaissances des interactions entre ces « nano-objets » biologiques et les cellules.

REFERENCES BIBLIOGRAPHIQUES

Belin, M. T., and Boulanger, P. (1993). Involvement of cellular adhesion sequences in the attachment of adenovirus to the HeLa cell surface. *J Gen Virol* **74 (Pt 8),** 1485-97.

Bergelson, J. M., Cunningham, J. A., Droguett, G., Kurt-Jones, E. A., Krithivas, A., Hong, J. S., Horwitz, M. S., Crowell, R. L., and Finberg, R. W. (1997). Isolation of a common receptor for Coxsackie B viruses and adenoviruses 2 and 5. *Science* **275**(5304)**,** 1320-3.

Console, S., Marty, C., Garcia-Echeverria, C., Schwendener, R., and Ballmer-Hofer, K. (2003). Antennapedia and HIV transactivator of transcription (TAT) "protein transduction domains" promote endocytosis of high molecular weight cargo upon binding to cell surface glycosaminoglycans. *J Biol Chem* **278**(37)**,** 35109-14.

Davison, A. J., Benko, M., and Harrach, B. (2003). Genetic content and evolution of adenoviruses. *J Gen Virol* **84**(Pt 11)**,** 2895-908.

Dechecchi, M. C., Melotti, P., Bonizzato, A., Santacatterina, M., Chilosi, M., and Cabrini, G. (2001). Heparan sulfate glycosaminoglycans are receptors sufficient to mediate the initial binding of adenovirus types 2 and 5. *J Virol* **75**(18)**,** 8772-80.

Dechecchi, M. C., Tamanini, A., Bonizzato, A., and Cabrini, G. (2000). Heparan sulfate glycosaminoglycans are involved in adenovirus type 5 and 2-host cell interactions. *Virology* **268**(2)**,** 382-90.

Fender, P., Boussaid, A., Mezin, P., and Chroboczek, J. (2005). Synthesis, cellular localization, and quantification of penton-dodecahedron in serotype 3 adenovirus-infected cells. *Virology* **340**(2)**,** 167-73.

Fender, P., Jeanson, L., Ivanov, M. A., Colin, P., Mallet, J., Dedieu, J. F., and Latta-Mahieu, M. (2002). Controlled transgene expression by E1-E4-defective adenovirus vectors harbouring a "tet-on" switch system. *J Gene Med* **4**(6)**,** 668-75.

Fender, P., Ruigrok, R. W., Gout, E., Buffet, S., and Chroboczek, J. (1997). Adenovirus dodecahedron, a new vector for human gene transfer. *Nat Biotechnol* **15**(1)**,** 52-6.

Fender, P., Schoehn, G., Foucaud-Gamen, J., Gout, E., Garcel, A., Drouet, E., and Chroboczek, J. (2003). Adenovirus dodecahedron allows large multimeric protein transduction in human cells. *J Virol* **77**(8)**,** 4960-4.

Fuschiotti, P., Schoehn, G., Fender, P., Fabry, C. M., Hewat, E. A., Chroboczek, J., Ruigrok, R. W., and Conway, J. F. (2006). Structure of the dodecahedral penton particle from human adenovirus type 3. *J Mol Biol* **356**(2)**,** 510-20.

Gaggar, A., Shayakhmetov, D. M., and Lieber, A. (2003). CD46 is a cellular receptor for group B adenoviruses. *Nat Med* **9**(11)**,** 1408-12.

Galinier, R., Gout, E., Lortat-Jacob, H., Wood, J., and Chroboczek, J. (2002). Adenovirus protein involved in virus internalization recruits ubiquitin-protein ligases. *Biochemistry* **41**(48)**,** 14299-305.

Garcel, A., Gout, E., Timmins, J., Chroboczek, J., and Fender, P. (2006). Protein transduction into human cells by adenovirus dodecahedron using WW domains as universal adaptors. *J Gene Med* **8**(4)**,** 524-531.

Gossen, M., Freundlieb, S., Bender, G., Muller, G., Hillen, W., and Bujard, H. (1995). Transcriptional activation by tetracyclines in mammalian cells. *Science* **268**(5218)**,** 1766-9.

Greber, U. F., Willetts, M., Webster, P., and Helenius, A. (1993). Stepwise dismantling of adenovirus 2 during entry into cells. *Cell* **75**(3)**,** 477-86.

Green, N. M., Wrigley, N. G., Russell, W. C., Martin, S. R., and McLachlan, A. D. (1983). Evidence for a repeating cross-beta sheet structure in the adenovirus fibre. *Embo J* **2**(8)**,** 1357-65.

Hong, S. S., Galaup, A., Peytavi, R., Chazal, N., and Boulanger, P. (1999a). Enhancement of adenovirus-mediated gene delivery by use of an oligopeptide with dual binding specificity. *Hum Gene Ther* **10**(16)**,** 2577-86.

Hong, S. S., Gay, B., Karayan, L., Dabauvalle, M. C., and Boulanger, P. (1999b). Cellular uptake and nuclear delivery of recombinant adenovirus penton base. *Virology* **262**(1)**,** 163-77.

Hong, S. S., Karayan, L., Tournier, J., Curiel, D. T., and Boulanger, P. A. (1997). Adenovirus type 5 fiber knob binds to MHC class I alpha2 domain at the surface of human epithelial and B lymphoblastoid cells. *Embo J* **16**(9)**,** 2294-306.

Marttila, M., Persson, D., Gustafsson, D., Liszewski, M. K., Atkinson, J. P., Wadell, G., and Arnberg, N. (2005). CD46 is a cellular receptor for all species B adenoviruses except types 3 and 7. *J Virol* **79**(22)**,** 14429-36.

Mathias, P., Galleno, M., and Nemerow, G. R. (1998). Interactions of soluble recombinant integrin alphav beta5 with human adenoviruses. *J Virol* **72**(11)**,** 8669-75.

Miyazawa, N., Crystal, R. G., and Leopold, P. L. (2001). Adenovirus serotype 7 retention in a late endosomal compartment prior to cytosol escape is modulated by fiber protein. *J Virol* **75**(3)**,** 1387-400.

Miyazawa, N., Leopold, P. L., Hackett, N. R., Ferris, B., Worgall, S., Falck-Pedersen, E., and Crystal, R. G. (1999). Fiber swap between adenovirus subgroups B and C alters intracellular trafficking of adenovirus gene transfer vectors. *J Virol* **73**(7)**,** 6056-65.

Neurath, A. R., and Rubin, B. A. (1968). Interaction of p-chloromercuribenzoate with adenoviruses. Inactivation of haemagglutinins and degradation of virions of types 3, 4 and 7. *J Gen Virol* **2**(2)**,** 215-29.

Norrby, E. (1966). The relationship between the soluble antigens and the virion of adenovirus type 3. II. Identification and characterization of an incomplete hemagglutinin. *Virology* **30**(4)**,** 608-17.

Norrby, E. (1968). Identification of soluble components of adenovirus type 11. *J Gen Virol* **2**(1)**,** 123-33.

Norrby, E., and Ankerst, J. (1969). Biological characterization of structural components of Adenovirus type 12. *J Gen Virol* **5**(2)**,** 183-94.

Norrby, E., Nyberg, B., Skaaret, P., and Lengyel, A. (1967). Separation and characterization of soluble adenovirus type 9 components. *J Virol* **1**(6)**,** 1101-8.

Norrby, E., and Skaaret, P. (1968). Comparison between soluble components of adenovirus types 3 and 16 and of the intermediate strain 3-16 (the San Carlos agent). *Virology* **36**(2)**,** 201-11.

Norrby, E., and Wadell, G. (1967). Soluble components of adenovirus type 4. *Virology* **31**(4)**,** 592-600.

Roelvink, P. W., Lizonova, A., Lee, J. G., Li, Y., Bergelson, J. M., Finberg, R. W., Brough, D. E., Kovesdi, I., and Wickham, T. J. (1998). The coxsackievirus-adenovirus receptor protein can function as a cellular attachment protein for adenovirus serotypes from subgroups A, C, D, E, and F. *J Virol* **72**(10)**,** 7909-15.

Rowe, W. P., Huebner, R. J., Gilmore, L. K., Parrott, R. H., and Ward, T. G. (1953). Isolation of a cytopathogenic agent from human adenoids undergoing spontaneous degeneration in tissue culture. *Proc Soc Exp Biol Med* **84**(3)**,** 570-3.

Ruigrok, R. W., Barge, A., Albiges-Rizo, C., and Dayan, S. (1990). Structure of adenovirus fibre. II. Morphology of single fibres. *J Mol Biol* **215**(4)**,** 589-96.

Schoehn, G., Fender, P., Chroboczek, J., and Hewat, E. A. (1996). Adenovirus 3 penton dodecahedron exhibits structural changes of the base on fibre binding. *Embo J* **15**(24), 6841-6.

Segerman, A., Arnberg, N., Erikson, A., Lindman, K., and Wadell, G. (2003a). There are two different species B adenovirus receptors: sBAR, common to species B1 and B2 adenoviruses, and sB2AR, exclusively used by species B2 adenoviruses. *J Virol* **77**(2), 1157-62.

Segerman, A., Atkinson, J. P., Marttila, M., Dennerquist, V., Wadell, G., and Arnberg, N. (2003b). Adenovirus type 11 uses CD46 as a cellular receptor. *J Virol* **77**(17), 9183-91.

Short, J. J., Pereboev, A. V., Kawakami, Y., Vasu, C., Holterman, M. J., and Curiel, D. T. (2004). Adenovirus serotype 3 utilizes CD80 (B7.1) and CD86 (B7.2) as cellular attachment receptors. *Virology* **322**(2), 349-59.

Sirena, D., Lilienfeld, B., Eisenhut, M., Kalin, S., Boucke, K., Beerli, R. R., Vogt, L., Ruedl, C., Bachmann, M. F., Greber, U. F., and Hemmi, S. (2004). The human membrane cofactor CD46 is a receptor for species B adenovirus serotype 3. *J Virol* **78**(9), 4454-62.

Sirena, D., Ruzsics, Z., Schaffner, W., Greber, U. F., and Hemmi, S. (2005). The nucleotide sequence and a first generation gene transfer vector of species B human adenovirus serotype 3. *Virology.*

Vives, R. R., Lortat-Jacob, H., Chroboczek, J., and Fender, P. (2004). Heparan sulfate proteoglycan mediates the selective attachment and internalization of serotype 3 human adenovirus dodecahedron. *Virology* **321**(2), 332-40.

Vives, R. R., Lortat-Jacob, H., and Fender, P. (2006). Heparan sulphate proteoglycans and viral vectors: ally or foe? *Curr Gene Ther* **6**(1), 35-44.

Wadell, G., and Norrby, E. (1969). The soluble hemagglutinins of adenoviruses belonging to Rosen's subgroup 3. II. The slowly sedimenting hemagglutinin. *Arch Gesamte Virusforsch* **26**(1), 53-62.

Walters, R. W., Freimuth, P., Moninger, T. O., Ganske, I., Zabner, J., and Welsh, M. J. (2002). Adenovirus fiber disrupts CAR-mediated intercellular adhesion allowing virus escape. *Cell* **110**(6), 789-99.

Wickham, T. J., Mathias, P., Cheresh, D. A., and Nemerow, G. R. (1993). Integrins alpha v beta 3 and alpha v beta 5 promote adenovirus internalization but not virus attachment. *Cell* **73**(2), 309-19.

Wu, E., Pache, L., Von Seggern, D. J., Mullen, T. M., Mikyas, Y., Stewart, P. L., and Nemerow, G. R. (2003). Flexibility of the adenovirus fiber is required for efficient receptor interaction. *J Virol* **77**(13), 7225-35.

Zhang, Y., and Bergelson, J. M. (2005). Adenovirus receptors. *J Virol* **79**(19), 12125-31.

Zubieta, C., Schoehn, G., Chroboczek, J., and Cusack, S. (2005). The structure of the human adenovirus 2 penton. *Mol Cell* **17**(1), 121-35.

ANNEXE

Adenovirus 3 penton dodecahedron exhibits structural changes of the base on fibre binding

Guy Schoehn, Pascal Fender,
Jadwiga Chroboczek and
Elizabeth A.Hewat[1]

Institut de Biologie Structurale Jean-Pierre Ebel, 41 av. des Martyrs, 38027 Grenoble, France

[1]Corresponding author

It was recently shown that co-expression of adenovirus type 3 (Ad3) penton base and fibre in the baculovirus system produces dodecahedral particles, as does the expression of the penton base alone. The structure of both of these dodecahedral particles, with and without fibre, has been determined by cryoelectron microscopy and 3-dimensional reconstruction techniques to a resolution of 25 and 20 Å, respectively. The general form of the penton base resembles that of the base protein in the recent reconstruction of adenovirus type 2. There is a remarkable difference in the penton base structure with and without the fibre. The five small protuberances on the outer surface of each base move away from the 5-fold axis by ~15 Å when the fibre is present. These protuberances are of relatively low density and most probably represent a flexible loop possibly containing the RGD site involved in integrin binding. The fibre is apparently bound to the outer surface of the penton base, rather than inserted into it. The fibre is flexible and the shaft contains two distinct globular regions 26 Å in diameter. The volume of the inner cavity of the dodecahedron is 350 ± 100 nm^3. This small volume precludes the use of the inner cavity to house genetic information for gene therapy; however, the possibility remains of linking the gene to the dodecahedron surface in the hope that it will be internalized with the dodecahedron.
Keywords: adenovirus 3/cryo-electron microscopy/dodecahedron/gene therapy/3-D reconstruction

Introduction

Small dodecahedral particles were seen in adenovirus type 3 (Ad3) preparations by electron microscopy as early as 1964 (Norrby, 1964). These dodecahedron particles are apparently an association of 12 Ad3 pentons. Recently, the two penton proteins base and fibre of adenovirus 3 were co-expressed in a baculovirus system and dodecahedral particles formed spontaneously (Fender et al., 1997). This observation has opened up interesting possibilities not only for gene therapy (Fender et al., 1997), but also for the study of the penton base–fibre interaction. Infection by adenoviruses is unusual in that two cell recognition sites appear to be involved (Philipson et al., 1968; Wickham et al., 1993; Cuzange et al., 1994; Henry et al.,

1994; Louis et al., 1994). The first, on the knob of the fibre, recognizes a cell receptor. The second, probably involving an RGD sequence on the base, takes part both in the attachment to an integrin and in the virus internalization. The expressed dodecahedra are made of the viral proteins responsible for the attachment and internalization properties of the adenovirus.

Adenoviruses are non-enveloped double-stranded DNA viruses which are responsible for conjunctivitis, rhinopharyngitis and enteric disease in humans (Horwitz, 1990). They are of considerable use as model systems in molecular biology and have been extensively studied. The ability of the adenovirus to infect a wide range of cell types and their relatively large DNA capacity have made them of great interest as viral vectors in gene therapy (Fitzgerald et al., 1983; Yoshimura et al., 1993; Yang et al., 1995). The adenovirus capsid is ~900 Å in diameter with a fibre protein protruding outwards from each of the 12 icosahedral vertices. The virion contains at least 11 proteins (polypeptides II–IX, IVa, μ, terminal) whose position and role are becoming clearer (Stewart et al., 1991, 1993). The major capsid proteins are 240 hexons and 12 pentons at each of the 5-fold vertices. The pentons consist of a pentameric base to which a trimeric fibre protein is attached non-covalently. The fibre contains three regions: the N-terminal tail which is attached to the base, a shaft of serotype-dependent length and a globular C-terminal knob. The amino acid sequence of the shaft contains a repeat motif of ~15 residues (Green et al., 1983; Stouten et al., 1992). The length of the shaft ranges from six repeating motifs in Ad3 to 22 in Ad2 and Ad5, i.e. from 120 to 330 Å in length (Signäs et al., 1985; Devaux et al., 1987; Ruigrok et al., 1990; Chroboczek et al., 1995). The X-ray structures of the hexon of Ad2 (Roberts et al., 1986) and the knob of Ad5 fibre protein are known (Xia et al., 1994).

Stewart et al. determined the structure of the native Ad2 virion to 35 Å resolution (Stewart et al., 1991) and then to 25 Å resolution (Stewart et al., 1993) using cryo-electron microscopy and three-dimensional (3-D) reconstruction. They visualized the overall architecture of the virion, including the penton base and roughly the first 88 Å of the fibre at the same density level. The 330 Å long fibre of Ad2 is evidently very flexible and hence cannot all be seen in the reconstruction. By combining the cryo-electron microscope data with the X-ray structural data on the hexon to generate difference maps, Stewart et al. determined the form and location of six different proteins in the Ad2 capsid. In particular, they located four proteins involved in cementing and stabilizing the rather complex Ad2 capsid.

In this paper, we present the cryo-electron microscopy and 3-D reconstructions of the dodecahedron of the expressed Ad3 penton both with and without the fibre.
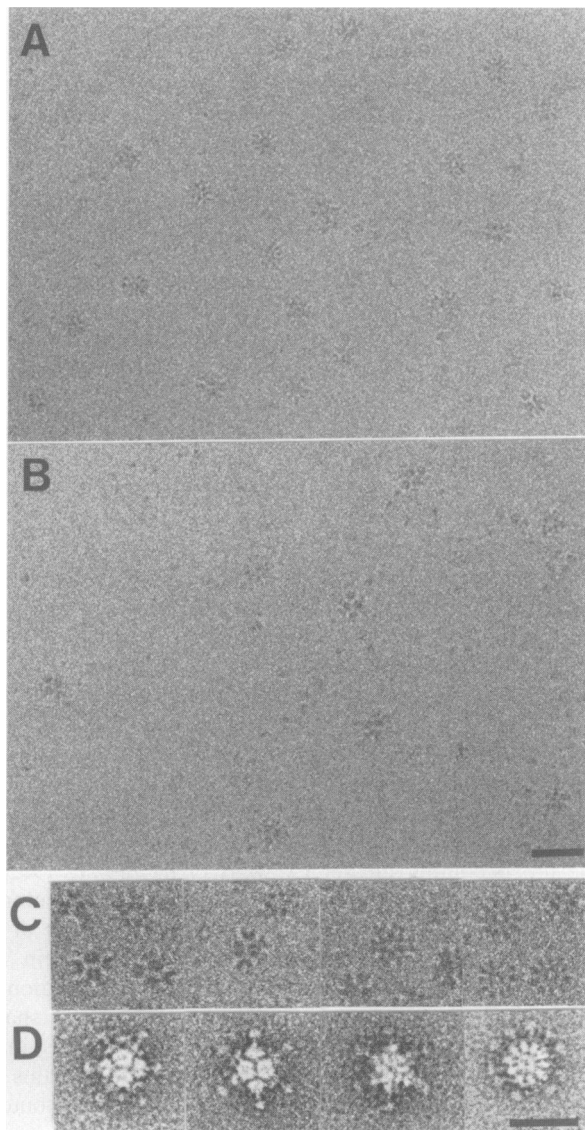
Fig. 1. Electron micrographs of frozen–hydrated Ad3 dodecahedra without (**A**) and with (**B**) fibre. They are the more highly defocused image pair used in the preliminary low-resolution reconstruction. The defocus is ~3.5 μm. (**C**) and (**D**) Enlargements of Ad3 dodecahedra seen down the 2-, 2-, 3- and 5-fold axis (from left to right). (C) Frozen–hydrated without fibre. (D) Negatively stained in uranyl acetate with fibre. Scale bars = 500 Å

The small diameter of the Ad3 dodecahedron, compared with the native virion, makes the Ad3 dodecahedron a more difficult object for structural studies than the large native virion, but the shortness of the Ad3 fibre allows visualization of its entire length. The aims of this study were to determine the size of the inner cavity of the dodecahedron because of its potential use as a gene carrier, to visualize the attachment of the fibre to the base and to determine whether structural changes occur on binding of the fibre to the base.

Results and discussion

Cryo-electron microscopy of Ad3 dodecahedra

The electron microscope images of frozen–hydrated Ad3 dodecahedra reveal well-formed particles with a highly textured surface (Figure 1). The knob, and in some cases

the fibre, is visible in high-defocus images and the orientations of some of the particles in high-symmetry orientations can be seen directly. The use of spun columns to remove isolated monomers was more effective in the case of dodecahedra without fibre than with fibre. Even after two passages through spun columns, monomers are visible in the background of the preparation with fibre. It appears that the equilibrium dodecahedra–penton is reached very rapidly and that the dodecahedra without fibre is more stable under the conditions used here.

Reconstructed density of the Ad3 dodecahedra

The isosurface representations of the reconstructed Ad3 dodecahedron with and without fibre (Figure 2A and B) reveal essentially the same external features as for the penton base of Ad2 (Stewart *et al.*, 1991, 1993). We have used this similarity to choose the hand of our reconstructions. Stewart *et al.* (1991) were able to determine the absolute hand of their reconstruction using additional information on the X-ray structure of the hexon and electron microscope data on a capsid dissociation fragment of Ad2, called the group of nine hexons (Laver *et al.*, 1969; Nermut, 1984; Furcinetti *et al.*, 1989). The diameter of the base at its widest point is 95 Å in both the dodecahedron with and without fibre, cf. 112 Å for the Ad2 base. The base height, including the five low-density protuberances, is roughly 124 Å, cf. 124 Å for Ad2. The penton base appears hollow inside, but there is no evidence of a 30 Å hole in the base into which the fibre is inserted, as was previously assumed (van Oostrum *et al.*, 1987; Ruigrok *et al.*, 1990; Stewart *et al.*, 1991). However, there is probably a communicating hole between the hollow interior of the base and the inner cavity of the dodecahedron. The internal cavity of the dodecaheron is ~8.7 nm in diameter so the volume is 350 ± 100 nm^3. In the dodecahedron, each penton base is bound to five neighbouring pentons, whereas in the adenovirus each penton is bound to five peripentonal hexons. The region of the penton involved in penton–penton and penton–hexon binding is roughly the same [Figure 3E and F, and Stewart *et al.* (1993) Figure 3C].

As for the Ad2 penton, there are five small protuberances on each penton base. The density in these protuberances is only 50% of the maximum density in the rest of the base (Figure 3). The contour threshold in Figure 3C has been chosen so that the total enclosed volume estimated for the dodecahedron equals the estimated volume, assuming a protein density of 1.3 g/cm^3 and a mol. wt of 430 kDa per penton. In all other isodensity figures, a slightly lower threshold has been used to show the low-density protuberances. An explanation for the low density is that the protuberances represent flexible loops. It will be recalled that the highly immunogenic loop of viral protein 1 of foot-and-mouth disease virus (FMDV) is a highly flexible loop which contains the RGD integrin receptor site and is seen by X-rays as a zone of low density. The structure of the FMDV serotype C 15 residue immunogenic loop complexed with a neutralizing Fab is known (Verdaguer *et al.*, 1995) and may be fitted (with room to spare) into the low-density protuberances of the Ad3 penton base (Figure 4). Mathias *et al.* (1994) used structure prediction algorithms which predicted that the conserved RGD sequence lies at the apex of two extended α helices.
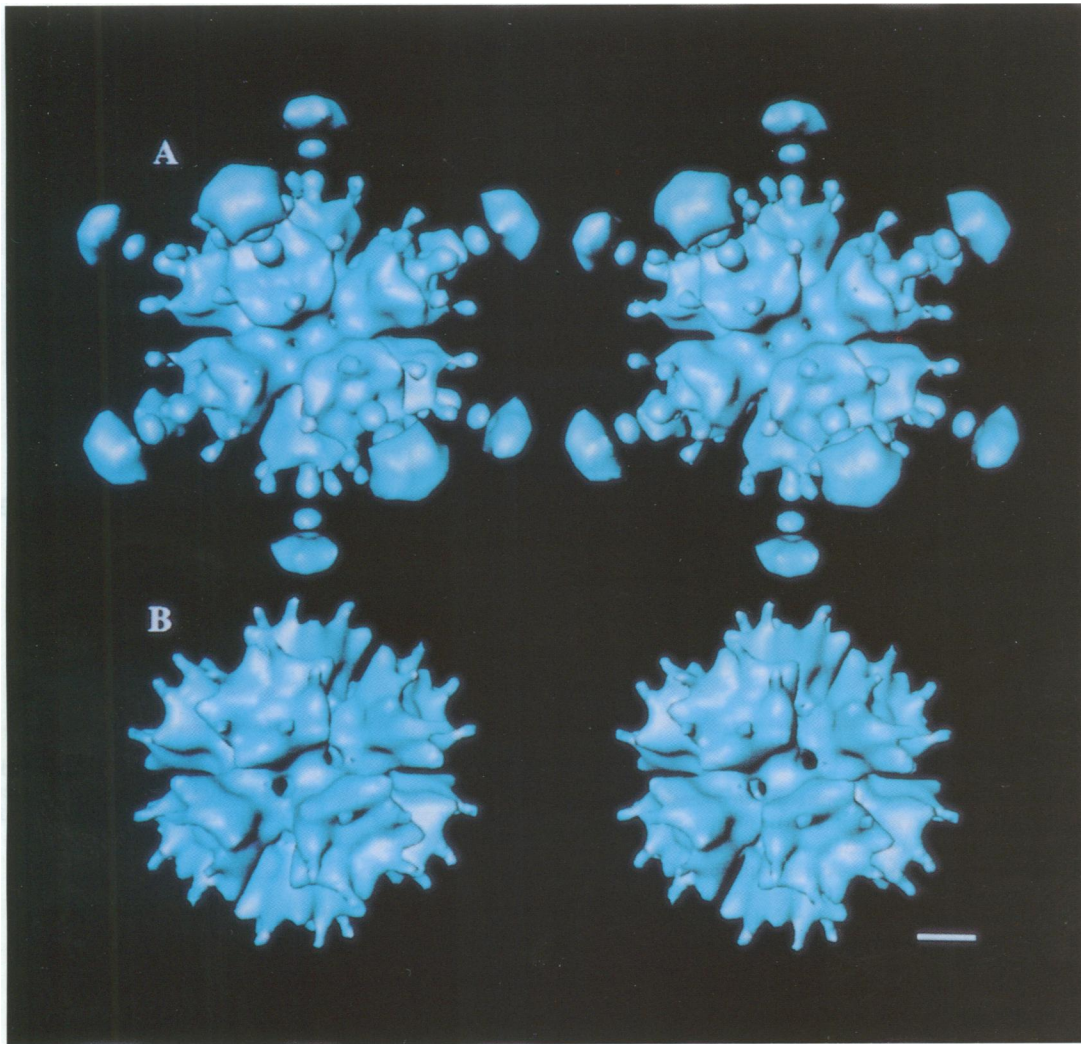
Fig. 2. Stereo views of the isosurface representations of the Ad3 dodecahedron with fibre, viewed down a 2-fold axis (**A**) and without fibre (**B**). Only the front half of the dodecahedra are represented. Scale bar = 50 Å.

This and the hydrophobic nature of the residues flanking the RGD sequence argue in favour of an exposed loop structure. Thus, it is possible that the five protuberances on each penton base each represent a flexible loop containing the RGD site.

The X-ray structure of the Ad5 knob (Xia *et al.*, 1994) fits well in size the Ad3 reconstructed density (Figure 4). The density of the knob has been 5-fold averaged so no detailed fit is possible. Also, the question of how the trimeric fibre binds to the pentameric base remains open. In reconstructing the dodecahedra, icosahedral symmetry is necessarily imposed. There is no obvious way of reconstructing the fibre with the correct 3-fold symmetry.

The fibre–base interaction

The fibre has a total length of 13.6 nm (Figure 3), cf. 16.0 ± 1.4 nm measured in negative stain (Ruigrok *et al.*, 1990). The tail of the fibre is spread out over a large area of the base at least 4.0 nm in diameter. It interacts with the outer surface of the base rather than being inserted into a pre-existing hole. The fibre shaft has a distinctly beaded appearance, as has been previously observed in shadowed images of Ad2 fibre (Ruigrok *et al.*, 1990) and

in the first 88 Å of the reconstructed Ad2 fibre (Stewart *et al.*, 1991). In fact, there is good agreement between the first 88 Å of the reconstructed Ad2 fibre (Stewart *et al.*, 1991) and the total length of the Ad3 fibre shaft (without the knob) which consists of two globular regions roughly 26 Å in diameter and separated by 35 Å. A beading pattern with a spacing of 35 Å was also observed in negatively stained isolated fibres of Ad2 (Ruigrok *et al.*, 1990). The relationship between this beaded fibre structure and the six hydrophobic repeating motifs in the fibre sequence (Kidd *et al.*, 1993) is not evident. There are apparently three motifs per globular (bead) domain.

The reconstructed map for the dodecahedron without fibre showed no change after about three cycles of refinement. On the contrary, the reconstructed map for the dodecahedron with fibre did not reach a completely stable result, particularly for the fibre density. The fibre density was more or less smeared out, as would be expected if the fibre was flexing from a point half way along its length. Stewart *et al.* (1991) observed a similar flexing of the Ad2 fibre, which smeared out all but the 88 Å of the fibre closest to the capsid. The final map was chosen on the basis of highest contrast in the fibre. The final
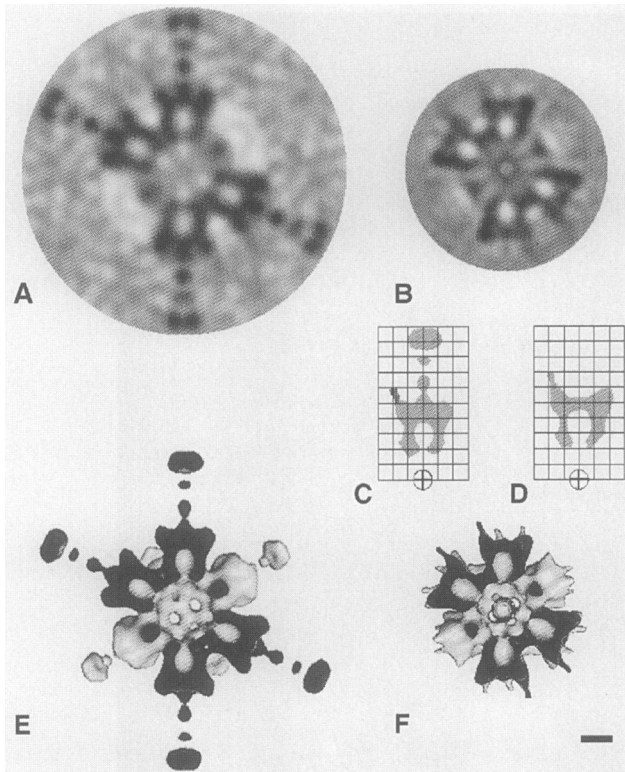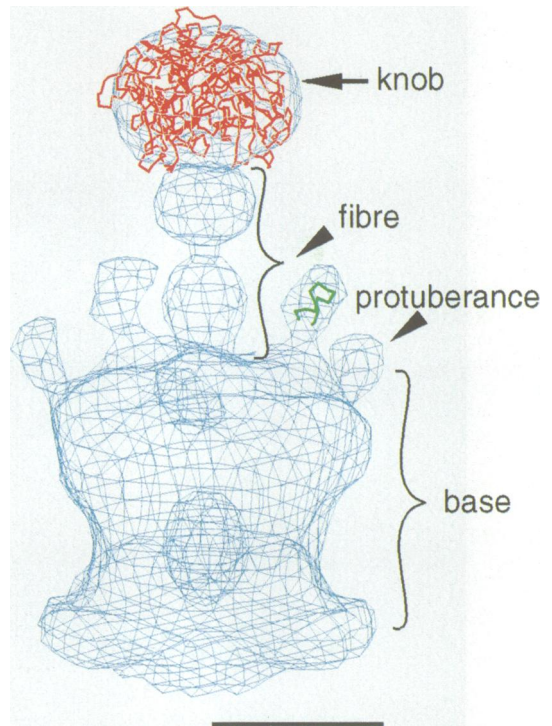
Fig. 3. Sections through the origin of the reconstructed density maps of the Ad3 dodecahedra with (**A**) and without (**B**) fibre, viewed down a 2-fold axis. A section through the penton which passes through the low-density protuberances on the dodecahedron with fibre (**C**) and without fibre (**D**). The hatched region in (C) represents the additional low-density protuberance visible when the threshold is lowered. The grid spacing is 25 Å. Isosurface representations of the Ad3 dodecahedron with fibre (**E**) and without fibre (**F**) viewed down a 2-fold axis. Only the back half of the dodecahedra are represented. The dark regions in (E) and (F) represent cut surfaces. Scale bar = 50 Å.

Fig. 4. Fit of the X-ray structures of the RGD-containing loop of FMDV (green) and the knob of Ad5 (red) to the cryo-electron microscope reconstructed density of Ad3 dodecahedron (blue). Scale bar = 50 Å.

reconstruction of the dodecahedron without fibre was made from 34 particles and included information to 20 Å resolution. The particle orientations were well dispersed over the asymmetric unit triangle (Figure 5). The phase residual went to 90° at roughly 20 Å^{-1} and all the inverse eigenvalues were <0.1. The final reconstruction of the dodecahedron with fibre was made from 26 particles and included information to 25 Å resolution. The phase residual went to 90° at 24 Å^{-1} and all the inverse eigenvalues were <0.1.
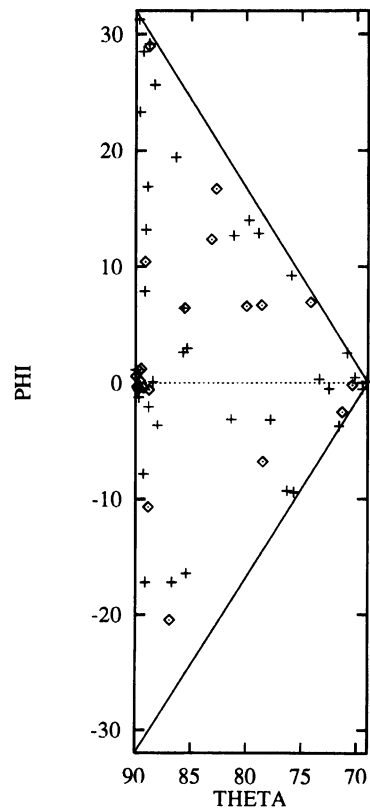
Effect of fibre binding on the structure of the penton base

Comparison of the reconstructions of the dodecahedron with and without fibre (Figure 6) reveals remarkable differences in the five protuberances on the penton base. They move away from the 5-fold axis by ~15 Å when the fibre is bound. If the assignment of these protuberances to a flexible loop containing the RGD integrin binding site is correct, it follows that the observed difference probably has a functional significance for the entry of the adenovirus into the cell.

Also, both density maps show the penton base to be hollow inside, but there is no hole in the base at the interface between the base and the fibre. The fibre is

Fig. 5. Refined orientation parameters, θ and φ of the 26 Ad3 dodecahedron with fibre (diamonds) used in the reconstruction shown in Figure 2A and of the 34 Ad3 dodecahedron without fibre (+) used in the reconstruction shown in Figure 2B.
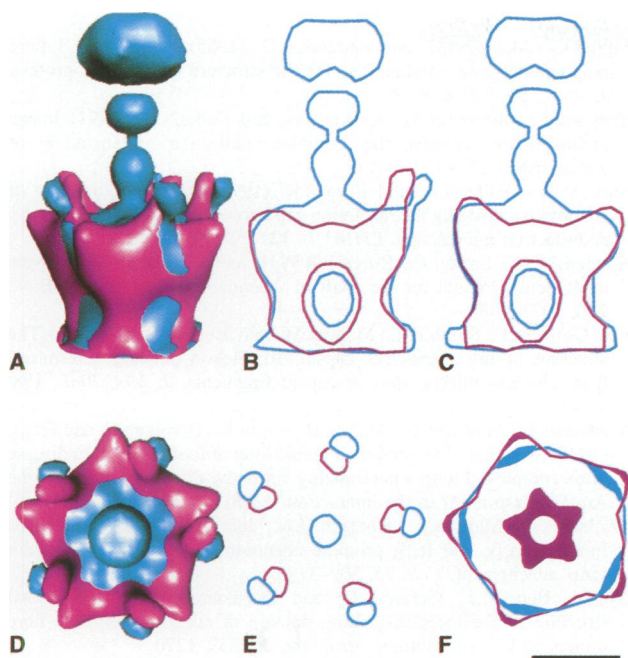
Fig. 6. Comparison of the reconstructed Ad3 penton with (blue) and without (magenta) fibre. For better comparison, both reconstructions are restricted to 25 Å resolution. Side view of one penton (**A**) and corresponding sections through the axis of the fibre showing the isodensity surfaces (**B** and **C**). Top view of one penton (**D**) and corresponding sections perpendicular to the axis of the fibre showing the isodensity surface through the low-density protrusions and through the widest section of the base (**E** and **F**). Scale bar = 50 Å.

apparently bound to the outer surface of the base. Given the change in position of the protuberances on binding of the fibre, there is clearly some rearrangement of the base. The difference in the maps at the inner cavity cannot be interpreted with certainty because the maps become less reliable towards the centre. Also, while a correction has been made to minimize the difference in contrast transfer function (CTF) of the images used in these two reconstructions, only reconstructions of both dodecahedra from the same image will completely eliminate all imaging-related differences. However, differences in the CTF will essentially cause differences in the size and not in the position of density regions. The CTF correction made to the reconstruction without fibre, for comparison with the reconstruction with fibre, did not change the position of the protuberance at all.

The inner cavity of the Ad3 dodecahedron

The volume of the inner cavity of the Ad3 dodecahedron at 350 ± 100 nm^3 is small compared with the Ad2 virion, which has a volume of ~165 000 nm^3 (Stewart *et al.*, 1991), and contains 36 000 bp. It follows that ~80 bp can fit into the Ad3 dodecahedron assuming the same DNA packing density. This precludes the use of the inner cavity of the dodecahedron to house genetic information for gene therapy; however, the possibility remains of linking the gene to the dodecahedron surface in the hope that it will be internalized with the dodecahedron.

Materials and methods

Growth and purification of adenovirus 3 dodecahedra

Dodecahedra were prepared after the method of Fender *et al.* (1997) using recombinant baculoviruses. Immediately prior to the preparation of frozen–hydrated specimens for electron microscopy, excess monomers were removed by passage through a Sepharose S300 spun column (Pharmacia).

Preparation and observation of electron microscope specimens

Negatively stained specimens of dodecahedron were prepared in uranyl acetate by standard techniques as described in Hewat *et al.* (1992a) and observed at 80 kV in a ZEISS 10C electron microscope.

Frozen–hydrated specimens were prepared on holey carbon films as described by Hewat *et al.* (1992a). A 4 µl sample of the specimen was applied to non-glow discharged holey carbon film on a 400 mesh copper grid, blotted with filter paper for 1–2 s and rapidly plunged into liquid ethane at –175°C. Specimens were observed at a temperature of close to –180°C using a Gatan 626 cryo-holder in a Phillips CM200 operating at 200 kV. Images were obtained under low-dose conditions (<10 e/Å^2) at a nominal magnification of ×27 500, and 1.2 and 3.5 µm underfocus. The images were recorded on KODAK SO163 electron image films and developed in full-strength D19 developer for 12 min at room temperature. The magnification was calibrated in an independent experiment using the 23 Å pitch of tobacco mosaic virus.

Image analysis

Preliminary selection of micrographs for analysis was performed as described previously (Hewat *et al.*, 1992b). Defocus pairs were digitized using an Optronics microdensitometer coupled to a PC, with a step size of 12.5 µm, which corresponds to a pixel size of 4.55 Å at the specimen, taking into account the corrected microscope magnification of ×28 500. Particle image selection and pre-processing were performed on a Silicon Graphics computer using the Semper 6 Plus image-analysis package. Images were re-interpolated to a pixel size of 1.5 times the original so that 128×128 files could be used. The selected particles were masked, normalized by subtracting the mean and any density gradient present, and normalizing the standard deviation. The particle images further from focus were pre-centred by cross-correlation with the radially averaged summation of several particle images. The particle images closer to focus had too little contrast for direct particle selection and centring. They were therefore selected and centred by cross-correlation with their high-defocus image pair.

Further image analysis was performed on a DEC Alpha using modified versions of the MRC icosahedral programs and model-based programs (Baker and Cheng, 1996) supplied by S.Fuller (Fuller *et al.*, 1996). The dodecahedron with fibre was the first to be analysed and the method of common lines (Crowther, 1971) was used for the determination of particle origins and orientations for the high-defocus image only. The model-based programs were used for all subsequent orientation and origin determinations. The reconstructed dodecahedron with fibre was used as a starting model for the analysis of the dodecahedron without fibre. In each case, the cycle of refinement consisted of: (i) determining the origins and orientations for the high-defocus image using the model-based approach; (ii) using the origins and orientations thus obtained to refine the low-defocus image using cross common lines (Simplex program); (iii) reconstructing an improved map from the low-defocus image which is used as a model for determining the origins and orientations for the high-defocus image in step (i). Using the low-defocus reconstruction as a model for directly refining the low-defocus data proved to be unsatisfactory. For the dodecahedron with fibre, the fibre density was not included in the model for orientation determination using the model-based programs, but it was included in the cross common lines refinement. For the final reconstruction in each case (Figure 2A and B), only particles from one negative were included and no correction for the CTF was made.

The reconstructions of the dodecahedra with and without fibre were made from micrographs with different defocus and hence different CTFs. Thus, in order better to compare the density maps, the average radial amplitude of the particle Fourier transforms for the reconstruction of dodecahedron without fibre were forced to that of the dodecahedron with fibre and the density map was recalculated to 25 Å resolution. The fibre density was not included in the comparison and the average radial density was slightly smoothed. This was not a complete CTF correction, just a minimal correction to bring the CTF of one reconstruction into line with another.

Isosurface representations of the reconstructed density were visualized using Explorer on an SGI.

References

Baker,T. and Cheng,R.H. (1996) A model-based approach for determining orientation of biological macromolecules imaged by cryoelectron microscopy. *J. Struct. Biol.*, **116**, 120–130.

Chroboczek,J., Ruigrok,R.W.H. and Cusak,S. (1995) Adenovirus fiber.In Doerfler,W. and Böhm,P. (eds), *Current Topics in Microbiology and Immunology. The Molecular Repertoire of Adenovirus I.* Vol. 199/I, Springer-Verlag, Berlin, pp. 164–200.

Crowther,R.A. (1971) Procedures for three-dimensional reconstruction of spherical viruses by Fourier synthesis from electron micrographs. *Phil. Trans. R. Soc. London Ser. B.*, **261**, 221–230.

Cuzange,A., Chroboczek,J. and Jacrot,B. (1994) The penton base of human adenovirus type 3 has the RGD motif. *Gene*, **146**, 257–259.

Devaux,C., Caillet-Boudin,M.-L., Jacrot,B. and Boulanger,P. (1987) Crystallization, enzymatic cleavage, and polarity of the adenovirus type 2 fiber. *Virology*, **161**, 121–128.

Fender,P., Ruigrok,R.W.H., Gout,E., Buffet,S. and Chroboczek,J. (1997) Adenovirus dodecahedron, a new vector for human gene transfer. *Nature Biotechnol.*, in press.

Fitzgerald,D.J.P., Padmanabhan,R., Pastan,I. and Wilingham,M.C. (1983) Adenovirus-induced release of epidermal growth factor and Pseudomonas toxin into the cytosol of KB cells during receptor-mediated endocytosis. *Cell*, **32**, 607–617.

Fuller,S.D., Butcher,S.J., Cheng,R.H. and Baker,T.S. (1996) Three-dimensional reconstruction of icosahedral particles. The uncommon line. *J. Struct. Biol.*, **116**, 48–55.

Furcinetti,P.S., van Oostrum,J. and Burnett,R.M. (1989) Adenovirus polypeptide IX revealed as capsid cement by difference images from electron microscopy and crystallography. *EMBO J.*, **8**, 3563–3570.

Green,N.M., Wrigley,N.G., Russell,W,C., Martin,S.R. and McLachlan,A. (1983) Evidence for a repeating cross-β sheet structure in the adenovirus fibre. *EMBO J.*, **2**, 1357–1365.

Henry,L., Xia,D., Wilke,M., Deisenhofer,J. and Gerard,R.D. (1994) Characterization of the knob domain of the adenovirus type 5 fiber protein expressed in *Escherichia coli. J. Virol.*, **68**, 5239–5246.

Hewat,E.A., Booth,T.F., Loudon,P.T. and Roy,P. (1992a) Three dimensional reconstruction of baculovirus expressed bluetongue virus core-like particles by cryo-electron microscopy. *Virology*, **189**, 10–20.

Hewat,E.A., Booth,T.F. and Roy,P. (1992b) Structure of bluetongue virus particles by cryoelectron microscopy. *J. Struct. Biol.*, **109**, 61–69.

Horwitz,M.S. (1990) Adenoviridae and their replication. In Field,B.N. and Knipe,D.M. (eds), *Virology.* Raven Press, New York, pp. 1680–1721.

Kidd,A.H., Chroboczek,J., Cusack,S. and Ruigrok,R.W.H. (1993) Adenovirus type 40 virions contain two distinct fibres. *Virology*, **192**, 73–84.

Laver,W.G., Wrigley,N.G. and Pereira,H.G. (1969) Removal of pentons from particles of adenovirus type 2. *Virology*, **39**, 599–605.

Louis,N., Fender,P., Barge,A., Kitts,P. and Chroboczek,J. (1994) Cell-binding domain of adenovirus serotype 2 fiber. *J. Virol.*, **68**, 4104–4106.

Mathias,P., Wickham,T., Moore,M. and Nemerow,G. (1994) Multiple adenovirus serotypes use αv integrins for infection, *J. Virol.*, **68**, 6811–6814.

Nermut,M.V. (1984) The architecture of adenoviruses. In Ginsberg,H.S. (ed.), *The Adenoviruses.* Plenum Press, New York, pp. 5–34.

Norrby,E. (1964) The relationship between the soluble antigens and the virion of adenovirus type 3. I. Morphological characteristics. *Virology*, **1**, 236–248.

Philipson,L., Lonberg-Holm,K. and Petterson,U. (1968) Virus-receptor interaction in an adenovirus system. *J. Virol.*, **2**, 1064–1075.

Roberts,M.M., White,J.L., Grütter,M.G. and Burnett,R.M. (1986) Three dimensional structure of the adenovirus major coat protein hexon. *Science*, **232**, 1148–1151.

Ruigrok,R.W.H., Barge,A., Albizes-Rizo,C. and Dayan,S. (1990)

Structure of adenovirus fibre. II. Morphology of single fibers. *J. Mol. Biol.*, **215**, 589–596.

Signäs,C., Akusjärvi,G. and Pettersson,U. (1985) Adenovirus 3 fibre polypeptide gene: implications for the structure of the fibre protein. *J. Virol.*, **53**, 672–678.

Stewart,P.L., Burnett,R.M., Cyrklaff,M. and Fuller,S.D. (1991) Image reconstruction reveals the complex molecular organization of adenovirus. *Cell*, **67**, 145–154.

Stewart,P.L., Fuller,S.D. and Burnett,R. (1993) Difference imaging of adenovirus: bridging the resolution gap between X-ray crystallography and electron microscopy. *EMBO J.*, **12**, 2589–2599.

Stouten,P.F.W., Sander,C., Ruigrok,R.W.H. and Cusack,S. (1992) New triple-helical model for the shaft of Adenovirus fibre. *J. Mol. Biol.*, **226**, 1073–1084.

van Oostrum,J., Smith,P.R., Mohraz,M. and Burnett,R.M. (1987) The structure of the adenovirus capsid. III. Hexon packing determined from electron micrographs of capsid fragments. *J. Mol. Biol.*, **198**, 73–89.

Verdaguer,N., Mateu,M.G., Andreu,D., Giralt,E., Domingo,E. and Fita,I. (1995) Structure of the major antigenic loop of foot-and-mouth disease virus complexed with a neutralizing antibody: direct involment of the Arg-Gly-Asp motif in the interaction. *EMBO J.*, **14**, 1690–1696.

Wickham,T., Mathias,P., Cheresh,D.A. and Nemerow,G.R. (1993) Integrins $\alpha_v\beta_3$ and $\alpha_v\beta_5$ promote adenovirus internalisation but not virus attachement. *Cell*, **73**, 309–319.

Xia,D., Henry,L.J., Gerard,R.D. and Deisenhofer,J. (1994) Crystal structure of the receptor-binding domain of adenovirus type 5 fibre protein at 1.7 Å resolution. *Structure*, **2**, 1259–1270.

Yang,Y., Li,Q., Ertl,H.C.J. and Wilson,J.M. (1995) Cellular and humoral immune response to viral antigens create barriers to lung-directed gene therapy with recombinanat adenoviruses. *J. Virol.*, **69**, 2004–2015.

Yoshimura,K., Rosenfeld,M.A., Seth,P. and Crystal,R.G. (1993) Adenovirus-mediated augmentation of cell transfection with unmodified plasmid vectors. *J. Biol. Chem.*, **268**, 2300–2303.

Adenovirus dodecahedron, a new vector for human gene transfer

Pascal Fender, Rob W.H. Ruigrok[1], Evelyne Gout, Sebastien Buffet, and Jadwiga Chroboczek*

*Institut de Biologie Structurale, 41 avenue des Martyrs, 38027 Grenoble, France. [1]European Molecular Biology Laboratory, Grenoble Outstation, BP 156, 38042 Grenoble Cedex 9, France. *Corresponding author (e-mail: wisia@ibs.fr).*

Recombinant adenovirus is one of most efficient delivery vehicles for gene therapy. However, the initial enthusiasm for the use of recombinant adenovirus for gene therapy has been tempered by strong immune responses that develop to the virus and virus-infected cells. Even though recombinant adenoviruses are replication-defective, they introduce into the recipient cell, together with the gene of interest, viral genetes that might lead to fortuitous recombination if the recipient is infected by wild-type adenovirus. We propose the use of a dodecahedron made of adenovirus pentons or penton bases as an alternative vector for human gene therapy. The penton is a complex of two oligomeric proteins, a penton base and fiber, involved in the cell attachment, internalization, and liberation of virus into the cytoplasm. The dodecahedron retains many of the advantages of adenovirus for gene transfer such as efficiency of entry, efficient release of DNA from endosomes, and wide range of cell and tissue targets. Because it consists of only one or two adenovirus proteins instead of the 11 contained in an adenovirus virion and it does not contain the viral genome, it is potentially a safer alternative to recombinant adenovirus.

Adenoviruses (Ad) are a family of nonenveloped icosahedral DNA viruses infecting humans as well as a variety of animals. On each of the 12 vertices of the Ad virion is a penton, a complex of two oligomeric proteins (the penton base anchored in the capsid and the antenna-like fiber[1]). The Ad penton plays a dual role in initiating the infection of host cells. Ad infection begins with the attachment of a viral particle to the cell surface, by interaction of the distal globular region of the fiber (C-terminal head domain) with an as yet unidentified cell receptor[2-5]. The role of the base protein is less clear, although it has been shown that for the internalization of serotypes 2, 3, 4, and 12, a second interaction step is needed between an Arg-Gly-Asp (RGD) sequence in the penton base and cellular integrins $a_v\beta_3$ and $a_v\beta_5$ (refs. 6, 7).

The Ad penton base protein is also implicated in the release of the virus from endosomes[8-11]. It has been suggested that the penton base undergoes an acid-induced conformational change in endosomes, resulting in the exposure of hydrophobic domains and leading to disruption of the endosomal membrane[12].

We have constructed a vehicle derived from Ad structural proteins that permits the attachment of plasmid DNA. As a result, gene transfer and expression were observed in human cells in culture.

Results

Production and electron microscopy of dodecahedra. A double expression transfer vector was used for the separate or simultaneous cloning of Ad3 base and fiber genes into the baculovirus genome. Lysates of infected *Trichoplusia ni* (High-Five) cells were separated on a sucrose gradient followed by analysis on denaturing polyacrylamide gels. Two gradient areas contained both the penton base and fiber proteins. At lower sucrose density the expressed proteins were recovered together with cellular proteins, and at higher sucrose density only the expressed proteins were found.

The heavy gradient fractions of coexpressed fiber plus base and of base alone were studied by negative stain electron microscopy.

Spherical particles were observed that were associated through their bases into regular dodecahedra (Fig. 1). There are 10 fibers visible in the fivefold view; the fiber at the top, extending away from the carbon film, and the fiber underneath the center of the structure are not visible. The pentons are packed as in the virus, on the 12 fivefold vertices of an icosahedron[13]. The diameter of the dodecahedra with the fibers (distance between tips of opposite fiber heads) is 49±0.7 nm; that of the base part, from top of base to top of opposite base, is 27.8±0.8 nm wide (n=number of measurements=43), which is almost identical to the diameter of the dodecahedra without the fibers (27.5±0.6 nm, n=49). Pentons of dissociated dodecahedra that could also be found had a length of 21.4±1 nm (n=24) measured from bottom of the base to the tip of the fiber head. This is somewhat smaller than the corresponding dimension of Ad3 penton isolated from Ad3 virus-infected cells, which was 22.7±1.1 nm[14]. Using 21.4 nm as the size of the dissociated recombinant penton, there is probably a cavity 6 to 7 nm wide inside the dodecahedron.

Role of penton base in dodecahedron formation. Dodecahedra of base and fiber (penton-dodecahedra) could be formed in insect cells not only by the coexpression from one baculovirus bearing two genes but also by coinfection of cells with two baculoviruses, each bearing one of the genes. When the Ad2 base protein either with Ad2 or Ad3 fiber was used instead of the Ad3 base, fractions recovered from the high sucrose concentration contained unstructured aggregates of pentons or of bases alone as observed with EM (data not shown). The formation of dodecahedra depends on the presence of the Ad3 base; the Ad2 base does not form regular dodecahedra.

Chimeric adenovirus pentons can be formed in vitro through incubation of purified fibers and penton bases derived from different serotypes[15]. Upon incubation of dodecahedra made of Ad3 bases with native Ad2 fibers, dodecahedra with the inserted heterologous long fibers were observed (Fig. 2). The interaction of bases

in preformed base-dodecahedra with heterologous fibers confirms the involvement of the conserved sequences in the N-termini of the fiber proteins in penton assembly[16,17].

Dodecahedron internalization and intracellular fate. We examined the uptake of penton proteins in HeLa cells by immunofluorescence. A penton-dodecahedra preparation was applied to cells at 4°C, a temperature that permits virus attachment but not internalization. Under these conditions both proteins were found at the cell surface, suggesting that attachment had occurred (Fig. 3A). Ten to twenty minutes after the cells were shifted to 37°C, the vast majority of immunofluorescent signal was seen in the vicinity of the nuclear membrane, creating a halo around the nucleus (Fig. 3C). No viral proteins were seen inside the nucleus, although they colocalized to some extent with lamin B (data not shown), one of the major proteins of the inner nuclear membrane[18]. Progressively the internalized dodecahedra gave a more diffuse signal, suggesting movement toward the cytoplasm (Fig. 3D, E, and F).

Electron microscopy of thin sections of HeLa cells after application of penton-dodecahedra showed, 3 min after the temperature shift, dense objects of the size of dodecahedra inside vesicles in the neighborhood of the plasma membrane (Fig. 4A). At 10 min numerous vesicles could be observed in the cytoplasm of the treated cell, each containing several dodecahedra (Fig. 4B). The images of the region near the nucleus showed disintegrating vesicles releasing the dodecahedra toward nucleus (Fig. 4C).

When entry of base-dodecahedra was tested, neither attachment nor internalization was seen at molar dodecahedron/cell ratios comparable to that used for penton-dodecahedra. However, when 10 to 20 times more base-dodecahedra was applied, a similar level of uptake as that seen for penton-dodecahedra was achieved (data not shown). It seems that the lack of fiber can be compensated for by a higher amount of dodecahedra-base. It should be noted that the binding affinity of the Ad2 fiber has been found to be about 30 times higher than that of the Ad2 penton base (K_d of 1.7 and 55 nM, respectively)[6].

The fate of internalized dodecahedra was studied by analyzing the kinetics of radioactive penton-dodecahedra in HeLa cells (data not shown). With time of internalization, a decrease in the amount of dodecahedra was observed accompanied by the appearance of lighter material. After 1 h about 60% of input dodecahedra was recovered in heavy sucrose fractions, and after 4 h about 25% of input dodecahedra seemed to be still intact. It should be noted, however, that at 3 h only about 70% of total applied radioactivity was recovered, which might suggest that low-molecular-weight material escapes from the cell.

These results indicate that after entry into the cell, Ad3 recombinant dodecahedra are targeted to the cytoplasmic face of the nuclear membrane. Some time after reaching the nuclear membrane they move away from the nucleus toward the cell inte-
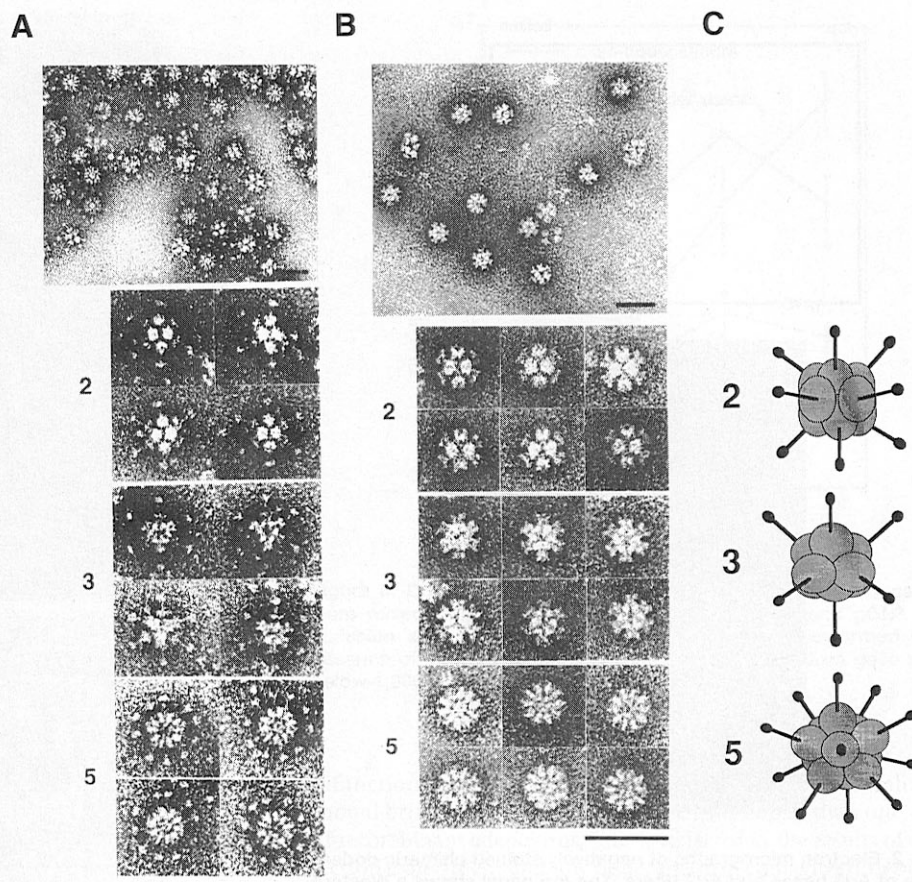
Figure 1. Electron micrographs of negatively stained Ad3 penton-dodecahedra (A) and base-dodecahedra (B). In (A) and (B) the top panels show dodecahedra in various orientations, the lower panels show the dodecahedra with their twofold, threefold and fivefold symmetry axes. The magnification bars represent 50 nm. (C) Schematic representation of twofold, threefold, and fivefold symmetry.

rior where they are depolymerized and probably degraded.

Dodecahedron-mediated gene tranfer. The small size of dodecahedron internal cavity as assesed by negative stain EM and confirmed in a reconstruction made by cryoelectron microscopy and image analysis[19] means that it is not feasible to pack more than 100 bases of DNA inside. We attached a luciferase reporter plasmid to the outside of the dodecahedron. Since in the penton, the fiber protein attaches to the penton base through its N-terminus[3], we have synthesized a bifunctional peptide composed of 20 amino acids corresponding to the N-terminus of Ad3 fiber with a C-terminal extension of 20 lysines. The electron microscopy analyses and DNA retardation gel performed with the mixture of plasmid DNA, peptide, and dodecahedra show that the bifunctional peptide can attach with the fiber-like N-terminus to the base and fix and condense DNA with the C-terminal polylysines. The DNA condensation is dependent upon the presence of the peptide (Fig. 5C). DNA fixation seems to be much weaker with penton-dodecahedra (Figs. 5A and C) in agreement with the transfection data (Fig. 6). Both penton-dodecahedra and base-dodecahedra when mixed with the peptide and plasmid DNA could enter cells and transfer DNA into the nucleus, resulting in gene expression (Fig. 6). The level of gene expression, and thus of transfer, was higher with base-dodecahedra, probably because this construct could accommodate more peptide with attached DNA than penton-dodecahedra. The level of transfection obtained with the recombinant adenovirus carrying the luciferase gene (Ad5luc), was lower at lower concentrations than that obtained with base-dodecahedra. At higher concentrations
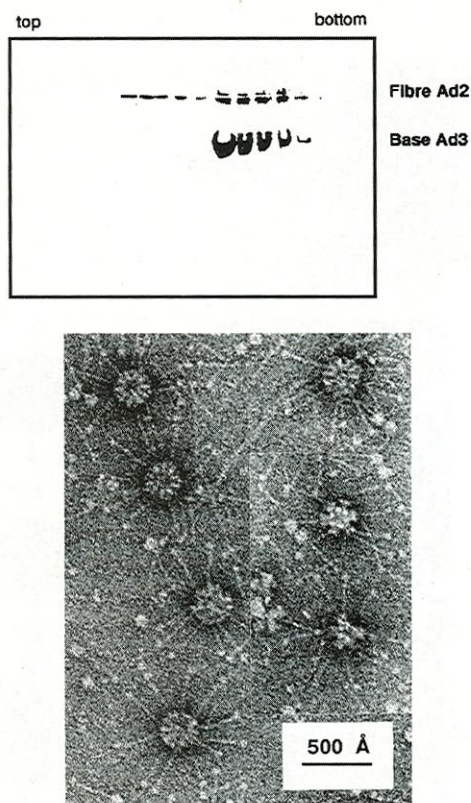
Figure 2. Electron micrographs of negatively stained chimeric dodec-ahedra of Ad3 bases and Ad2 fibers. The top panel shows a Western blot performed with anti-Ad2 fiber and anti-Ad3 base sera. Chimeric dodecahedra were made in vitro. The incubation mixture was fractionated on a sucrose density gradient. Aliquots of gradient fractions were run on a denaturing polyacrylamide gel, analyzed by Western blot performed consecutively with antibodies specific to Ad2 fiber and Ad3 penton base.
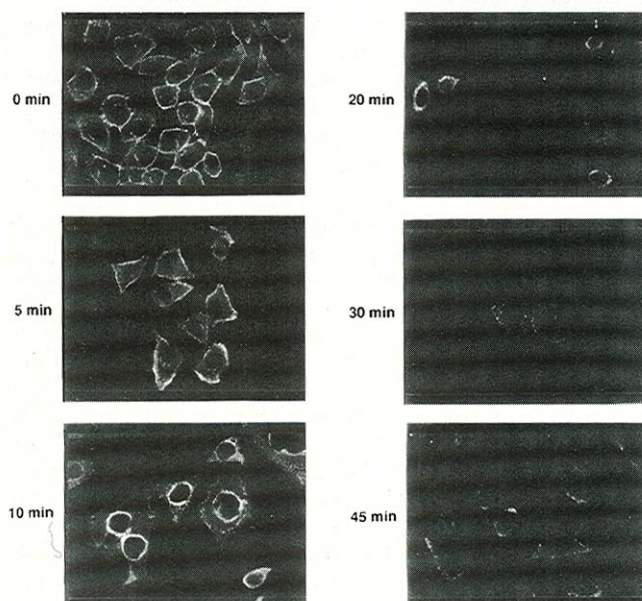

Figure 3. Dodecahedron internalization observed by confocal microscopy. Cells are stained with the anti-Ad3 fiber serum. Similar results were obtained with the anti-penton base antibody.
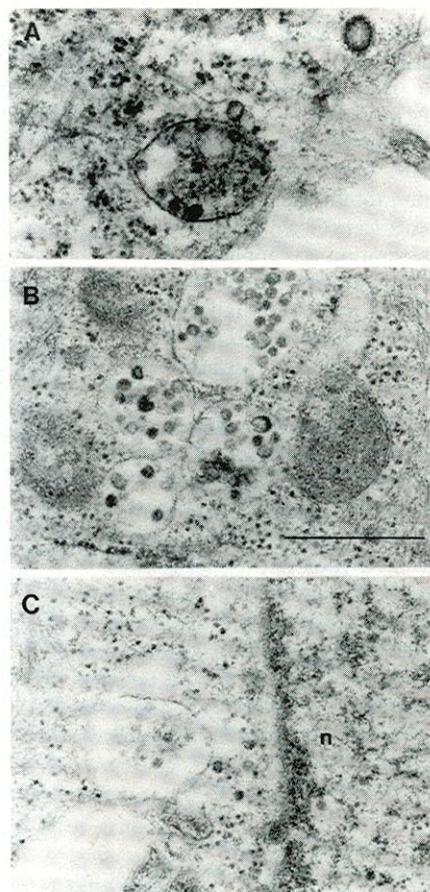

Figure 4. Dodecahedra observed in HeLa cells by electron microscopy of thin sections. The scale bar represents 500 nm. Treatment with penton-dodecahedra was for 3 min (A) and 10 min (B & C). n: nucleus.

the level of transfection was similar for both vectors. Both recombinant adenovirus and base-dodecahedron were much more efficient in gene transfer than DOTAP used under optimal conditions.

Discussion

Native penton-dodecahedra have been observed in the extracts of Ad3-, Ad4-, Ad7-, Ad9-, Ad11- and Ad15-infected cells[1,20-22]. Gelderblom et al.[21] described Ad3 as having a regular array of 12 morphological subunits arranged according to icosahedral symmetry. Through the coexpression of two structural Ad3 proteins we have recreated structures similar to those formed during biogenesis of Ad3. No such particles have been observed for serotypes 2 or 5[23,24] and we found that, when the Ad2 base was used instead of the Ad3 base, dodecahedra were not formed.

Formation of chimeric dodecahedra by inserting the Ad2 fiber into preformed Ad3 base-dodecahedra, confirms earlier results on formation of chimeric pentons[15-17]. The synthetic bifunctional peptide, containing 20 N-terminal amino acids of the Ad3 fiber, was able to attach to the dodecahedron. The first 20 amino acids of fiber protein are thus sufficient for the interaction with penton base, and this portion of the fiber probably does not have to be trimeric for the interaction to happen. The synthetic peptide can attach not only to base-dodecahedron but also to penton-dodecahedron, which has some implications concerning the interaction of fiber with base in the penton. The penton presents an interesting structural mismatch. The penton base is a homo-
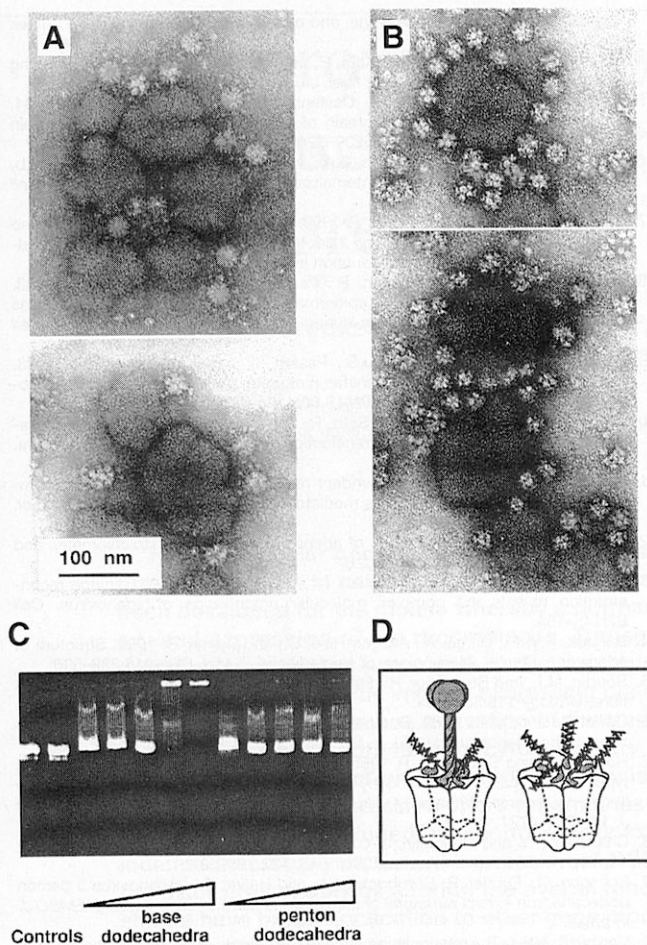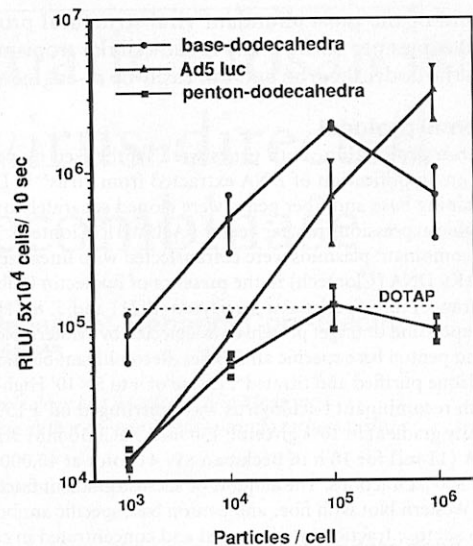
Figure 5. Interaction of bifunctional peptide with dodecahedron and plasmid DNA (pGL3). Electron micrographs of negatively stained complexes of (A) DNA/peptide/penton-dodecahedra and of (B) DNA/peptide/base-dodecahedra were prepared as for the transfection experiments, except without the addition of medium. The larger structures surrounded by the dodecahedra show the punctate appearance typical of negatively stained condensed DNA. (C) DNA retardation gel. Increasing amounts of base-dodecahedra were incubated with 250 ng peptide for 15 min at RT, 250 ng of plasmid DNA was added, and 5 min later the samples were applied to the 1% agarose gel made in TBE buffer and stained with ethidium bromide. Lane 1: plasmid DNA alone; lane 2: plasmid DNA with base-dodecahedron, no peptide; lanes 3–7: DNA, peptide and 1, 10, 100, 500 and 1,000 ng base-dodecahedron, respectively; lanes 8–12: DNA, peptide, and 1, 10, 100, 500, and 1,000 ng penton-dodecahedron, respectively. (D). Diagram of penton and penton base with a bifunctional peptide.

Figure 6. Dodecahedron-mediated gene transfection. Dodecahedra were mixed in vitro with the bifunctional peptide and pGL3. Light emission was measured 48 h later. Transfection performed in the absence of peptide or in the absence of dodecahedron gave values below 1,000 RLU.

pentamer and the fiber is a homo-trimer[14,25]. The results of transfection experiments (Fig. 6) show that the synthetic peptide attaches not only to the base-dodecahedra but also to penton-dodecahedra, suggesting that in the penton three fiber N-termini interact randomly with three base polypeptides, leaving two remaining base polypeptides available for the interaction with the synthetic peptide. The efficiency of transfection obtained with base-dodecahaedra was much higher than that observed for the penton-dodecahedra, suggesting that in the absence of fiber protein the penton base on penton-dodecahedron can probably attach five free fiber N-termini instead of the two attached with penton. This allows more of the attached bifunctional peptide to carry DNA because there is less steric hindrance in the absence of fiber protein.

If we assume full occupancy of pentons in the dodecahedron by

bifunctional peptide with attached DNA, each dodecahedron should bring 60 times more luciferase gene copies than one virion of recombinant adenovirus. This is reflected in the results of transfection experiment and low dodecahedron concentration but not at high dodecahedron concentration, possibly because one DNA molecule is then interacting with more than one dodecahedron. DNA attached externally to the dodecahedron may be less protected than DNA in the virion.

The initial kinetics of dodecahedron entry seem to be similar to those of the first steps of viral infection. Twenty minutes after attachment, over 50% of entering viral inoculum (Ad5) is seen at the nuclear periphery[26,27]. On the other hand, some characteristics of the Ad3 dodecahedron entry differ from wild-type adenovirus. During the stepwise dismantling of Ad2 accompanying virus entry, the first protein released is the fiber[28], however in the case of Ad3 dodecahedron entry, the dodecahedra remains intact during the first 20 min as proteins, fiber, and penton base reach the vicinity of the nuclear membrane. By comparing Ad2 entry with that of a temperature-sensitive mutant devoid of the L3/p23 protease adenovirus protease was shown to be required for virus entry into the cytosol[29]. Ad3 dodecahedra efficiently enter the cytosol without the adenovirus protease. Ad3 infection is very different from that of Ad2 under physiological conditions as well as in cell culture[30]. It is possible that the virus dismantling process is different for various Ad serotypes.

Gene therapy depends on efficient vectors. Viruses, transfer vehicles engineered by evolution, are the most efficient vectors. Ad are particularly attractive since they can incorporate about 8 kbp of foreign DNA, infect dividing and nondividing cells (in contrast to retroviruses), and can easily be cultivated in the laboratory to high titers. Recently a new adenoviral vector was constructed that consists of defective virus deleted of all viral coding sequences and that has to be grown in the presence of helper virus[31]. The use of Ads for gene transfer is accompanied by strong cellular and humoral immune response, which might be a barrier for therapy requiring repetitive applications[32]. A transfer vector consisting of base and fiber proteins will be safer than recombinant Ads because it does not contain viral DNA and it might be less immunogenic

RESEARCH

being devoid of the most abundant viral structural protein, the hexon (240 copies per virion). The broad cellular tropism of Ad is retained in the dodecahedron and can easily be re-engineered.

Experimental protocol

Dodecahedron production. Both genes were synthetized by polymerase chain reaction amplification of DNA extracted from virus[33–35]. DNA fragments containing base and fiber genes were cloned separately or together into the double expression transfer vector pAcUW31 (Clontech, Palo Alto, CA). The recombinant plasmids were cotransfected with linearized baculovirus Bac PAK6 DNA (Clontech) in the presence of lipofectin (Gibco, Cergy Pointoise, France) into *Spodoptera frugiperda* (Sf21) and *T. ni* (High-Five) cells[36]. The expression of target proteins was detected by Western blot analysis with fiber and penton base specific antibodies. Recombinant baculovirus isolates were plaque purified and titrated[37]. Lysate of 4 to 5×10^7 High-Five cells infected with recombinant baculovirus was centrifuged on a 15% to 40% sucrose density gradient in 10% glycerol; 150 mM NaCl; 10 mM Tris, pH 7.4; 2 mM EDTA (11 ml) for 18 h in Beckman SW 41 rotor at 40,000 rpm and harvested in 800 µl fractions. The aliquots of sucrose gradient fractions were analyzed by Western blot with fiber and penton base specific antibodies. The 31% to 38% sucrose fractions were pooled and concentrated in centriprep (Amicon, Epernon, France).

Electron microscopy. Negative staining with 1% sodium silicotungstate and low-dose electron microscopy were performed as described[14]. The magnification was calibrated with negatively stained catalase crystals, and measurements were made from positive prints with a magnification of 180K using an eye-piece giving additional magnification of 8x. HeLa cells grown in four-well Labtek chamber slides (Polylabo, Strasbourg, France) at 1.5×10^5 cells per well were incubated for 2 h at 4°C with 0.5 µg penton-dodecahedra in 200 µl PBS/3% BSA, then rinsed with cold PBS. One slide was incubated for 3 min and the other for 10 min at 37°C before cell fixation with 2.5% glutaraldehyde. The slides were embedded in Epon 812 after treatment with 1% osmium tetraoxide. Ultrathin sections were stained with saturated uranyl acetate in 50% ethanol and then with 1 M lead citrate. Observations were made with Philips CM10 microscope at 80 kV.

Dodecahedron internalization. 5×10^4 HeLa cells grown on coverslips were incubated for 2 h at 4°C with 1 µg penton-dodecahedra in 50 µl PBS-3% BSA. The cells were washed with cold PBS and incubated at 37°C in PBS-3% BSA. At different time-points cells were fixed and permeabilized with methanol and then incubated for 1 h at 37°C with rabbit anti-fiber or anti-base antibodies (both at 1:200, 50 µl in PBS-3%BSA/coverslip), washed with PBS, treated with a fluorescein-conjugated secondary antibody (1:250 for 30 min, 50 µl in PBS-3%BSA per coverslip). The coverslips were mounted on a microscope slide with 1,4-diazabicyclo[2.2.2]octane (Sigma, Verpillère, France) and observed in a MRC600 confocal microscope (Bio-Rad, Tory sur Seine, France).

Transfection experiments. Portions of dodecahedra were incubated in DMEM with 5 µg bifunctional peptide for 15 min at RT and then 1.5 µg pGL3 carrying luciferase reporter gene was added. The mixture of DOTAP (Behringer, Meylan, France) and 1.5 µg pGL3 was prepared as described by the supplier, at a 4:1 ratio of DOTAP:DNA (optimal in our hands). Duplicate portions of 10^5 HeLa cells per well in a 24-well plate were transfected in parallel with the above mixtures and with the recombinant adenovirus Ad5luc for 1 h at 37°C. Light emmission was measured in cell lysates (aliquots corresponding to 5×10^4 cells) 48 h later with the Promega (Madison, WI) kit.

1. Norrby E. 1969. The structural and functional diversity of adenovirus capsid components. *J. Gen. Virol.* **5:**221–236.
2. Philipson, L., Lonberg-Holm, K., and Pettersson, U. 1968. Virus-receptor interaction in an adenovirus system. *J. Virol.* **2:**1064–1075.
3. Devaux, C., Caillet-Boudin, M.-L., Jacrot, B., and Boulanger, P. 1987. Crystallization, enzymatic cleavage, and polarity of the adenovirus type 2 fiber. *Virology* **161:**121–128.
4. Louis, N., Fender, P., Barge, A., Kitts, P., and Chroboczek, J. 1994. Cell-binding domain of adenovirus serotype 2 fiber. *J. Virol.* **68:**4104–4106.
5. Henry, L., Xia, D., Wilke, M., Deisenhofer, J., and Gerard, R.D. 1994. Characterization of the knob domain of the adenovirus type 5 fibre protein expressed in *E. coli. J. Virol.* **48:**5239–5246.
6. Wickham, T., Mathias, P., Cheresh, D.A., and Nemerow G.R. 1993. Integrins a,b₃ and a,b₅ promote adenovirus internalization but not virus attachment. *Cell* **73:**309–319.
7. Bai, M., Harfe, B., and Freimuth, P. 1993. Mutations that alter an Arg-Gly-Asp (RGD) sequence in adenovirus type 2 penton base protein abolish its cell-rounding activity and delay virus reproduction in flat cells. *J. Virol.* **67:**5198–5205.
8. FitzGerald, D.J.P., Padmanabhan, R., Pastan, I., and Wilingham, M.C. 1983. Adenovirus-induced release of epidermal growth factor and Pseudomonas toxin into the cytosol of KB cells during receptor-mediated endocytosis. *Cell* **32:**607–617.
9. FitzGerald, D.J.P., Trowbridge, J.S., Pastan, I., and Wilingham, M.C. 1983. Enhancement of toxicity of antitransferrin receptor antibody-*Pseudomonas* exotoxin conjugates by adenovirus. *PNAS* **80:**4134–4138.
10. Yoshimura, V., Rosenfeld, M.A., Seth, P., and Crystal, R.G. 1993. Adenovirus-mediated augmentation of cell transfection with unmodified plasmid vectors. *J. Biol. Chem.* **268:**2300–2303.
11. Seth, P.J. 1994. Adenovirus-dependent release of choline from plasma membrane vesicles at an acidic pH is mediated by the penton base protein. *Virol.* **68:**1204–1206.
12. Wohlfart, C. 1988. Neutralization of adenoviruses: kinetics, stoichiometry, and mechanisms. *J. Virol.* **62:**2321–2328.
13. Stewart, P.L., Burnett, R.M., Cyrklaff, M., and Fuller, S.D. 1991. Image reconstruction reveals the complex molecular organization of adenovirus. *Cell* **67:**145–154.
14. Ruigrok, R.W.H., Barge, A., Albiges-Rizo, C., and Dayan, S. 1990. Structure of adenovirus fibre. II. Morphology of single fibres. *J. Mol. Biol.* **215:**289–596.
15. Boudin, M.L. and Boulanger, P. 1982. Assembly of adenovirus penton base and fibre. *Virology* **116:**589–604.
16. Caillet-Boudin, M.-L. 1989. Complementary peptide sequences in partner proteins of the adenovirus capsid. *J. Mol. Biol.* **208:**195–198.
17. Hong, S.S. and Boulanger, P. 1995. Protein ligands of the human adenovirus type 2 outer capsid identified by biopanning of a phage-displayed peptide library on separate domains of wild type and mutant penton capsomers. *EMBO J.* **14:**4714–4727.
18. Chaudhary, N. and Courvalin, J.-C. 1993. Stepwise reassembly of the nuclear envelope at the end of mitosis. *J. Cell Biol.* **122:**295–306.
19. Schoehn, G., Fender, P., Chroboczek, J., and Hewat E.A. Adenovirus 3 penton dodecahedron exibits structural changes of the base on fiber binding. *EMBO J.* In press.
20. Norrby, E. 1964. The relationship between the soluble antigens and the virion of adenovirus type 3. I. Morphological characteristics. *Virology* **1:**236–248.
21. Gelderblom, H., Bauer, H., Frank, H., and Wigand, R. 1967. The structure of group II adenoviruses. *J. Gen. Virol.* **1:**553–560.
22. Norrby, E. and Skaaret, P. 1968. Comparison between soluble components of adenovirus types 3 and 16 and of intermediate strain 3-16 (the San Carlos agent). *Virology* **36:**201–211.
23. Boulanger, P.A. and Puvion, F. 1976. Occurrence of a peculiar type of adenovirus 2 penton oligomer. *Intervirol.* **7:**126–134.
24. Karayan, L., Gay, B., Gerfaux, J., and Boulanger P. 1994. Oligomerization of recombinant penton base of adenovirus type 2 and its assembly with fibre in baculovirus-infected cells. *Virology* **202:**782–796.
25. Van Oostrum, J. and Burnett, R.M. 1985. Molecular composition of the adenovirus type 2 virion. *J. Virol.* **56:**439–448.
26. Chardonnet, Y. and Dales, S. 1970. Early events in the interaction of adenoviruses with HeLa cells. I. Penetration of type 5 and intracellular release of the DNA genome. *Virology* **40:**462–477.
27. Lyon, M., Chardonnet, Y., and Dales, S. 1978. Early events in the interaction of adenoviruses with HeLa cells. V. Polypeptide associated with the penetrating inoculum. *Virology* **87:**81–88.
28. Greber, U.F., Willetts, M., Webster, P., and Helenius, A. 1993. Stepwise dismantling of adenovirus 2 during entry into cells. *Cell* **75:**477–486.
29. Greber, U.F., Webster, P., Weber, J., and Helenius, A. 1996. The role of adenovirus protease in virus entry into cells. *EMBO J.* **15:**1766–1777.
30. Horwitz, M.S. 1990. Adenoviridae and their replication, pp. 1679–1721 in *Virology.* Fields, B.N. and Knipe, D.M. (eds.). Raven Press, New York.
31. Kochanek, S., Clemens, P.R., Mitani, K., Chen, H.-H., Chan, S., and Caskey, C.T. 1996. A new adenoviral vector: replacement of all viral coding sequences with 28 kb of DNA independently expressing both full length dystrophin and ß-galactosidase. *Proc. Natl. Acad. Sci. USA* **93:**5731–5736.
32. Yang, Y., Li, Q., Ertl, H.C.J., and Wilson, J.M. 1995. Cellular and humoral immune response to viral antigens create barriers to lung-directed gene therapy with recombinanat adenoviruses. *J. Virol.* **69:**2004–2015.
33. Petterson, U. and Sambrook, J. 1973. Amount of viral DNA in the genome of cells transformed by adenovirus type 2. *J. Mol. Biol.* **73:**125–130.
34. Cuzange, A., Chroboczek, J., and Jacrot, B. 1994. The penton base of human adenovirus type 3 has the RGD motif. *Gene* **146:**257–259.
35. Signäs, C., Akusjärvi, G., and Pettersson, U. 1985. Adenovirus 3 fibre polypeptide gene: implications for the structure of the fibre protein. *J. Virol.* **53:**672–678.
36. Kitts, P.A., Ayres, M.D., and Possee, R.D. 1990. Linearisation of baculovirus DNA enhances the recovery of recombinant virus expression vectors. *Nucleic Acid Res.* **18:**5667–5672.
37. King, L.A. and Possee, R.D. 1992. *The baculovirus expression system: a laboratory guide.* Chapman & Hall, London.

RESEARCH ARTICLE

Controlled transgene expression by E1-E4-defective adenovirus vectors harbouring a "tet-on" switch system

P. Fender[1]*,[†]
L. Jeanson[1]‡
M. A. Ivanov[1]
P. Colin[2]
J. Mallet[2]
J. F. Dedieu[1]
M. Latta-Mahieu[1]

[1]*Aventis-Gencell, CRVA, 94403 Vitry sur Seine, France*

[2]*CNRS-LGN, UMR 9923, Hôpital de la Pitie, 75013 Paris, France*

*Correspondence to: P. Fender, Laboratory of Molecular Virology, Institut de Biologie Structurale, 41 rue Jules Horowitz, 38027 Grenoble, France. E-mail: fender@ibs.fr

[†]Present address: IBS, 41 rue Horowitz, 38027 Grenoble, France.

[‡]Present address: CNRS UMR8532–39, rue Camille Desmoulins 94805 Villejuif, France.

Abstract

Background   The "tet switch system" was originally described under the tet-off configuration with its components encoded by two separate plasmids. Since then, many virus vectors harbouring tet-off components have been designed and their regulation by tetracycline is widely reported. On the contrary, tet-on regulation by viral vectors is poorly documented.

Methods   E1-E4-defective adenoviruses harbouring either rtTA or the luciferase gene under a minimal inducible promoter (TK* or CMV*) or both components in a single genome were produced. Using either a double or a single virus strategy, induction of luciferase expression was investigated in various cell lines, in mice muscle and in rat brain.

Results   Over 400-fold induction can be reached with PC12 and NHA cells using a double virus strategy. Comparison of the background activity of different minimal inducible promoters revealed a significant difference between TK* and CMV* promoters both with the cell culture and the *in vivo* experiments. Interestingly, a single virus strategy permitted an induction exceeding 600-fold with human astrocyte primary cells. Moreover, the E1-E4-defective adenovirus-mediated tet-on system can be quickly switched off and turned back on again. Depending on the cell line, the level of rtTA derived by the single virus strategy differed, resulting in different efficiencies. Experiments performed in rat *striatum* and mouse muscle confirmed the importance of rtTA expression and minimal promoter used on both doxycycline-independent expression and induction efficiency. Under appropriated rtTA expression, a 32-fold induction is observed in mouse muscle.

Conclusions   In the recombinant adenovirus context, the CMV* but not the TK* promoter is sensitive to transcriptional interference resulting in high doxycycline-independent expression. By paying attention to the rtTA expression, moderate and high induction can be obtained *in vivo* and *in vitro* accordingly. Copyright © 2002 John Wiley & Sons, Ltd.

Keywords   E1-E4-defective adenovirus vectors; tet-on regulation; rtTA synthesis

Introduction

Gene therapy is a promising approach for the treatment of either innate or acquired diseases and represents a major challenge for the new century. Among vectors that are used to transfer DNA into cells, adenoviruses

have several advantages, particularly in applications concerning the central nervous system (CNS). Indeed, adenoviruses can infect dividing as well as resting cells, and gene transfer into the brain has been widely reported. Moreover, adenovirus vectors transfect glial and neuronal cells at the injection site and can also be transported in a retrograde manner via axons to a projecting brain area far away from this site [1]. This latter property could be very useful for Parkinson's disease (PD), as virus injection into the *striatum* results in transgene expression in both *striatum* and *substantia nigra*. The usefulness of adenovirus vectors for PD has been demonstrated using GDNF, a neurotrophic factor that prevents the death of nigro-striatal dopaminergic neurons [2]. The major limiting factor with first-generation adenovirus vectors (E1-defective) is their immunogenicity that triggers both inflammation and a cytotoxic response against the transfected cell. It has been suggested that this phenomenon leads in a few days to transgene extinction due to cell death and the negative effects of several cytokines on viral promoters [3]. As viral proteins were nevertheless expressed in infected cells with E1-defective adenovirus [4], deletion from the adenovirus genome of other regions involved in the replication process has been proposed. The E4 region is crucial for virus replication and E1-E4-defective adenoviruses were generated in a transcomplementing cell line [5]. These recombinant adenoviruses were tested for gene transfer in murine immunocompetent liver and showed a prolonged transgene expression due to lower viral protein expression and the absence of RCA during production [6–8]. Interestingly, E1-E4-defective adenoviruses have also been shown to be efficient for gene therapy of brain diseases, as stereotaxic injection in rat *striatum* was associated with an attenuated immune response and prolonged transgene expression (J. F. Dedieu, pers. commun.).

A very important feature of efficient gene therapy is the control of transgene expression. If the use of tissue-specific promoters permits the targeting of gene expression, transgene regulation can only be obtained with artificial systems. Among these, a tetracycline-derived, so-called "tet system", is widely used. This system exists in two opposite configurations. The first, called "tet off", leads to gene repression when tetracycline is added [9]. The second, called "tet on", acts in the opposite way, since tetracycline addition triggers gene expression [10]. Both configurations are based on two separate elements: (i) a tetracycline-responsive transactivator made from the fusion protein between the tetracycline bacterial repressor and the herpes virus VP16 transactivator (tTA or rtTA), and (ii) a cluster of seven repeats of the tetracycline operator (Op7) upstream from a minimal promoter driving the targeted gene. Recently, an improved tet-on system, in which a repressor element decreased the background level in the absence of an inducer, has been developed. In the absence of tetracycline, the silencer domain of the KRAB protein fused with the tetracycline repressor (tetR) binds the operator and decreases the background activity of the minimal promoter. Tetracycline addition triggers the release of this silencer protein from operator sequences and permits the binding of the rtTA transactivator, resulting in gene expression activation [11].

Materials and methods

Cell lines

PC12 cells were maintained in RPMI 1640 medium supplemented with 10% FCS and 5% horse serum. Normal human astrocytes (NHA) were provided from Clonetics and cultured in astrocyte growth medium following the supplier's protocol.

Construction of transcription units

Schuttle plasmids were generated by cloning transcription units in pXL3234 (Kn^R plasmid) containing a multiple cloning site between the left adenovirus ITR and the pIX gene [12]. Minimal Op7.TK* promoter was excised from pUHD10.7 (kindly given by Dr Bujard) by SmaI-BglII digestion and ligated in the corresponding sites of the luciferase-encoding plasmid pGl3 basic (Promega). The Op7.TK*-luc transcription unit was recovered by XmaI-BamHI digestion and ligated in AgeI-BglII digested pXL3234 to generate the pXL3529 schuttle plasmid. Minimal Op7.CMV* promoter was excised from pUHD10.3 (kindly given by Dr Bujard) by XhoI-BglII and ligated in the corresponding sites of pGl3 basic. The Op7.CMV*-luc transcription unit was recovered by XmaI-BamHI digestion and ligated in AgeI-BglII digested pXL3234 to generate the pXL3530 schuttle plasmid. The RSV-rtTA unit was constructed by the ligation of the NheI-ScaI fragment of the rtTA encoding pXL3357 (Aventis) in corresponding sites of pXL3507 (Aventis), thus generating the pXL3531 schuttle plasmid. For the single Ad.TK*luc construction, the RSV-rtTA-luc-Op7.TK* unit was generated by the ligation of the NotI-SalI fragment of pXL3531 in the corresponding sites of pXL3529 thus generating the pXL3532 schuttle plasmid. For the single Ad-CMV*luc, the tetR-Krab was recovered by BamHI-StuI digestion of pBabe [11] and ligated in the corresponding sites of pRL.PGK (Aventis). Recovery of the tetR.KRAB-IRES-rtTA-pPGK unit was obtained by partial XbaI digestion. This fragment cloned in pXL3589 (Aventis) permitted recombination in the E3 region of the adenoviral backbone.

Production of recombinant adenovirus (RAds)

Recombinant adenoviruses were produced by "EDRAG" double recombination in *E. coli* [12]. Briefly, shuttle plasmids (Kn^R) containing the transcription units described

above were transfected in an *E. coli* strain containing a plasmid (tet^R) harbouring the whole adenovirus genome (except for the E1 region which was replaced with β-gal and the E3 and E4 regions which were deleted). After tetracycline and kanamycine selection, the presence of the transgene in white colonies was determined by restriction analysis. PacI sequences present at both extremities permit lineation of the recombinant E1-E4-deleted adenovirus genome; E1-E4-defective adenoviruses were produced by transfecting the E1-E4 transcomplementing IGRP2 cells as described previously [5]. Viral particles were purified by CsCl banding and titration was determined by high-performance liquid chromatography (HPLC) [13]. All the experiments were performed using a unique viral stock preparation.

In vitro RAd infection

One day before infection, 24-well plates were seeded with 10^5 PC12 cells or 5×10^4 normal human astrocyte cells (NHAs).

Double virus strategy

Cells were infected with either Ad.TK*-luc or Ad.CMV*-luc at 1000 vp/cell and co-infected with different amounts of Ad.RSV-rtTA as indicated. Two days after infection, luciferase expression in the presence of 1 µg/ml doxycycline (Sigma) was determined.

Single virus strategy

Cells were infected at 1000 vp/cell with single Ad-TK*luc. rtTA addition was performed by co-infecting with increasing amounts of Ad.RSV-rtTA as indicated. Reversibility of induction was monitored for 3 days with PC12 for 1 µg/ml doxycycline removed on day 1 and re-introduced on day 2. For NHA cells, luciferase expression was monitored for 8 days. Doxycycline (1 µg/ml) was added for the first 2 days, removed for the next 2 days, re-introduced on day 4 and removed again on day 6. Luciferase expression was determined in 10 µl of the 100 µl cell lysate (Promega cell lysis buffer) for 10 s in a Berthold luminometer. The induction rate was calculated by dividing the level of luciferase expression by the level of background expression for each condition tested.

In vivo RAd infection

Young adult female Sprague-Dawley rats (Charles River Breeding Laboratories) were stereotaxically injected in the *striatum* (A = +1.2; L = +2.5) at three different points (V = −5; −4.6 and −4.2) with 10^9 vp per injection point (0.25 µl/min). Doxycycline (Sigma) was added at 1 mg/ml in drinking water. On the day indicated, the rats were sacrificed and, after dissection, the *striata* were

lysed in 200 µl of cell lysis buffer (Promega). Luciferase expression was determined in a volume of 20 µl for 10 s in a Berthold luminometer. Results are given as an average for a group of four animals and the error bar represents the 95% confidence interval.

Single Ad.CMV*-luc was injected into mice *Tibialis cranialis* with increasing amounts of Ad.CMV-rtTA. On day 0, the mice were anesthetised with injections of xylazine (3.6 mg/kg) and ketamine (120 mg/kg). *Tibialis cranialis* muscle from the right leg was injected with 1×10^9 viral particles of single Ad.CMV*luc alone in 30 µl of 20 mM tris buffer at pH 8.4 in 10% glycerol or in association with 0.5×10^9; 1×10^9; 2×10^9; or 5×10^9 viral particles of Ad.CMV-rtTA. Doxycycline (Sigma) was added at 1 mg/ml in drinking water. For the control, non-inducible particles of adenovirus encoding luciferase driven by the whole CMV promoter were injected alone. Four days after the virus injection, animals were sacrificed. Muscles were harvested in 1 ml lysis buffer (Promega) containing protease inhibitors (Boehringer) and homogenised with a Fastprep Bio101 apparatus (Savant) and centrifuged for 10 min at 9000 g at 4 °C. Luciferase activity was determined in a Berthold luminometer in 10 µl of supernatant. Results are given as average of RLU/total muscle for group of six mice and the error bar represents the 95% confidence interval.

Results

Several E1-E4-deleted adenovirus vectors harbouring the luciferase gene under the control of tetracycline-inducible promoter and/or rtTA tetracycline-sensitive transactivator have been constructed (Figure 1). Both the double virus strategy and the single virus strategy were tested.

Double virus strategy

The double virus strategy consists of using one virus encoding the rtTA under the control of an RSV promoter (Ad.RSV-rtTA) and a second virus encoding luciferase under the control of an inducible TK* or CMV* promoter (Ad.TK*luc and Ad.CMV*luc; Figure 1). An optimum ratio between transactivator virus and inducible virus was determined using this strategy. This parameter was assessed on PC12 cells by adding a constant amount of Ad.TK*luc or Ad.CMV*luc and a varying amount of Ad.RSV-rtTA. The results clearly showed that rtTA was the limiting factor for luciferase induction on PC12, as a 400-fold induction was reached when rtTA-encoding virus was added in 10-fold excess (Figure 2a). Moreover, on PC12 cells, luciferase background expression was two orders of magnitude less when the TK* promoter was used instead of the CMV* promoter. More than three orders of magnitude in luciferase expression between uninduced Ad.TK*luc and induced Ad.CMV*luc was obtained when these viruses were added with an
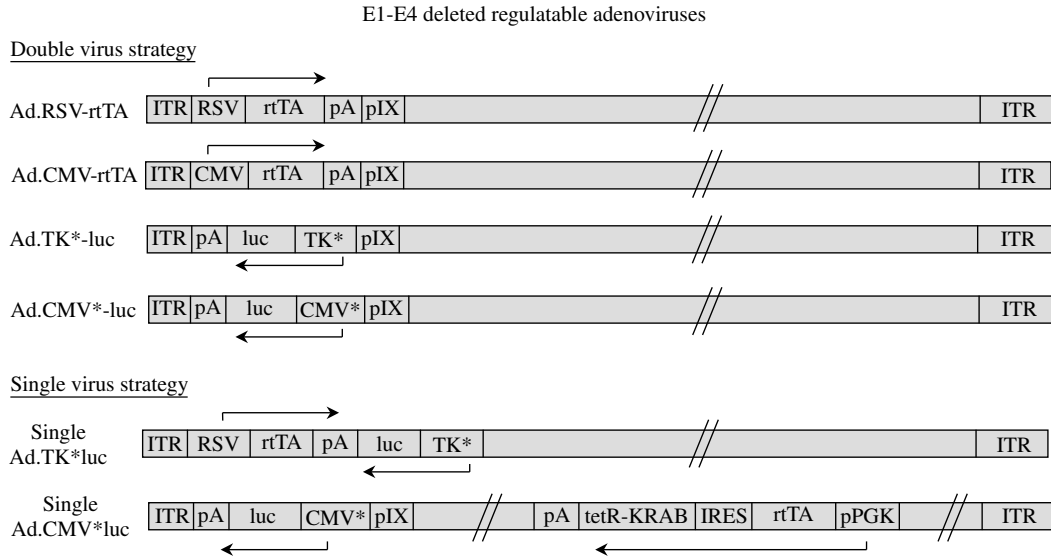
Figure 1. Schematic representation of regulatable E1-E4-deleted adenovirus vectors. Transgenes were inserted into the E1 region between the left ITR and the pIX protein of the adenovirus and into the E3 region for the vector harbouring the KRAB system [11]. Arrows indicate the direction of translation. (pA: SV40 polyadenylation sequence; CMV* and TK*: minimal CMV and TK promoter under the control of seven tetracycline operator repeats; IRES: internal ribosome entry site of the encephalomyocarditis virus; pPGK: phosphoglycerokinase promoter; ITR: inverted terminal repeat; luc: luciferase gene)
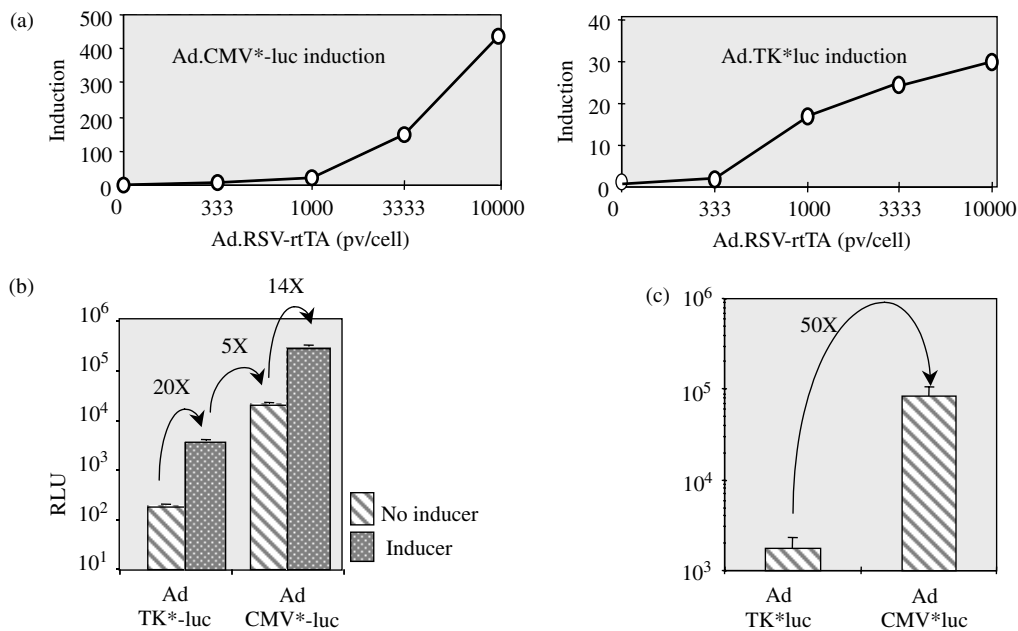
Figure 2. Comparison of TK* and CMV* promoters. (a) PC12 cells were infected with either Ad.TK*-luc or Ad.CMV*-luc at 1000 vp/cell and co-infected with different amounts of Ad.RSV-rtTA as indicated. Two days after infection, luciferase expression was determined and the induction rate in the presence of doxycycline (1 μg/ml) is shown. (b) Comparison of the level of luciferase expression on PC12 cells co-infected with Ad.TK*-luc + Ad.RSV-rtTA or Ad.CMV*-luc + Ad-RSV-rtTA (1000 vp/cell for each virus) in the presence or absence of inducer. (c) Luciferase background expression of Ad.TK*-luc and Ad.CMV*-luc (3×10^9 vp) co-injected with equimolar amounts of Ad.RSV-rtA in rat *striatum*. Seven days after injection, luciferase expression in the absence of inducer was determined in rat *striata* for a group of four animals

equimolar amount of Ad.RSV-rtTA (Figure 2b). Such results are very interesting especially for *ex vivo* cell engineering before transplantation. Features of the TK* and CMV* inducible promoters were also investigated *in vivo* and differences in background expression by these promoters were confirmed in rat *striatum*. TK* promoter exhibited a very low level of background expression

whereas CMV* promoter triggered a 50-fold increase in leakage of luciferase expression (Figure 2c). This leakage was not due to a non-specific binding of rtTA to the minimal promoter in the absence of inducer, as the background level of Ad.TK*luc or Ad.CMV*luc virus alone was the same in the absence of the rtTA-encoding virus (data not shown).

Single virus strategy

For clinical trials, a single adenovirus harbouring both rtTA and an inducible gene would be of great interest. Tet-regulated gene expression has been successfully employed in many mammalian cell cultures and transgenic mice. Gene therapy applications, especially applications concerning the regulated expression of neurotrophic factors, potentially toxic when expressed at high dose, are hampered by the residual basal activity in the non-induced state. For this purpose we present two approaches in which the expression of the transgene in non-induced conditions is maximally minimised. The luciferase gene was chosen as a reporter gene in this study for easy quantitative analysis of the promoter regulation studies. In the first approach, the minimal TK* promoter was inserted downstream of the seven TetO sequences and upstream of the reporter gene. As shown by the two virus strategy experiments, the luciferase background expression was much lower with this promoter than with a CMV* promoter. The rtTA and luciferase genes were cloned in a "head-to-head" configuration (single Ad.TK*-luc; Figure 1) with the minimal promoter away from the ITR region to avoid its transactivating effect [14].

In a second approach, activation by rtTA is combined with repression in the non-induced state. For this purpose the transactivator rtTA and the repressor are expressed in the same cell on the same virus but are controlled by the inducer in opposite ways. Indeed, the chimeric repressor TetR-Krab [11] binds in the absence of inducer to the tetracycline operator via its TetR domain and silences the downstream minimal promoter via the silencer Krab. Added inducer triggers both repressor withdrawal from the operator and activation of the promoter by binding of the rtTA to the operator. The TetR-Krab system was added in a bicistronic configuration with rtTA. This system, where both transregulators are co-expressed as monocistronic constructs, was proved to be efficient in mammalian cells where the basal activity was significantly repressed by TetR-Krab without significant reduction in the luciferase expression level in the induced state [15]. The TetR-Krab transcriptional unit is placed in the E3 region of the recombinant

adenovirus (Figure 1) far away from the operators sequences in order to avoid silencing of its own promoter, as repression by TetR-Krab is observable even when tet operator sequences are placed more than 3 kb away from the transcriptional initiation site of a eukaryotic promoter [16]. In the single virus configuration, several parameters could influence the efficiency of induction. Among these the choice of the promoter encoding the transactivator is critical. The RSV and the PGK promoters were chosen since they permitted long-term expression of transgene in E1-E4-defective adenovirus (J. F. Dedieu, pers. commun.).

An inducer range assay showed that doxycycline at 1 μg/ml seemed to be the optimum concentration for induction of single Ad.TK*luc on every cell line tested, although high concentrations of doxycycline, unlike minocycline, exhibited toxicity (data not shown). We have determined the effect of the addition of Ad.RSV-rtTA to the single Ad.TK*luc (Figure 3). With PC12 cells, the addition of Ad.RSV-rtTA did not significantly increase single Ad.TK*luc induction (around 15-fold for the single virus alone). In contrast, with human astrocytes (NHAs), the addition of Ad.RSV-rtTA to the single Ad.TK*luc virus clearly changed the induction efficiency. In these cells, the single virus alone permitted a 80-fold induction whereas the addition of Ad.RSV-rtTA increased the induction rate in a vp-dependent manner. When Ad.RSV-rtTA was used in 10-fold excess, an induction rate as high as 620-fold was reached representing an 8-fold increase in protein expression when compared with that obtained with single Ad.TK*luc alone. These data indicated that single Ad.TK*luc was designed in a *quasi optimal* manner for PC12 cells but the expression of rtTA by this virus in human astrocytes was not sufficient to reach full induction of the minimal promoter. Experiments performed on other primary cell lines (HUVEC, SMC) exhibited the same feature (data not shown). Interestingly, when rtTA was expressed in excess, Ad.TK*-luc and single Ad-TK*luc plateau at a comparable level with both NHA and PC12 cells. The weak and cell-specific difference in doxycycline-independent luciferase activity observed between Ad.TK*-luc and single Ad.TK*-luc is not dependent on rtTA synthesis.
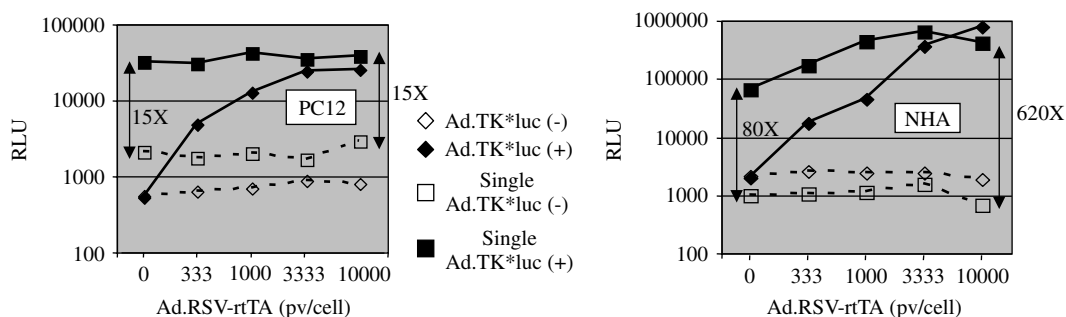
Figure 3. Determination of rtTA expression with PC12 and human astrocyte cells. Cells were infected with 1000 vp/cell of either Ad.TK*-luc or single Ad.TK*luc and co-infected with increasing amounts of Ad.RSV-rtTA. One day after infection, luciferase expression was determined and the induction rate was calculated by dividing the level of luciferase expression in the presence (+) of 1 μg/ml doxycycline by the expression level in the absence (−) of inducer
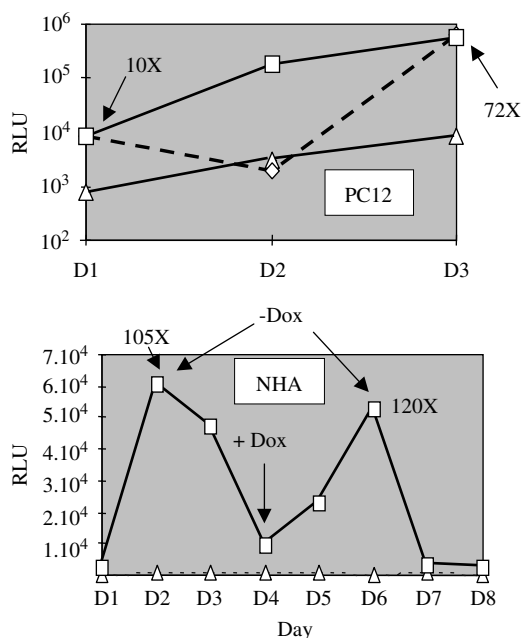
Reversibility of induction

One important advantage of the tet switch system is its reversibility. The time taken for induction, extinction and re-induction of our regulatable adenovirus was determined by adding or removing the inducer at different stages for different periods of time. Luciferase expression was tested daily with PC12 and NHA cells (Figure 4). The time of induction and extinction differed by 1–2 days between PC12-transformed cells and NHA primary cells infected with single Ad.TK*-luc, but, in both cases, the system was completely turned on and off. The longer period of time observed for NHAs to return to background levels could be due to the slower metabolism of these cells, increasing the half-life of luciferase.

In vivo experiments

Recombinant adenoviruses encoding neurotrophic factors have been described as good candidates for Parkinson's disease treatment [2]. To avoid side effects resulting from an over-expression of the neurotrophic factor in animals, a tight regulation of transgene expression is required. In order to determine if the E1-E4-defective adenovirus-mediated tet-on system can be used in the *striatum*, the single Ad.TK*luc (Figure 5a) and the single

Ad.CMV*-luc (Figure 5b) were stereotaxically injected into rat brain. High background expression, but weak induction, was observed in rat *striatum* with single Ad.CMV*-luc suggesting that both rtTA and TetR-KRAB were not sufficiently expressed. With the single Ad.TK*-luc, the background expression in the absence of inducer was very low and a 8-fold induction was observed at day 4 in the presence of inducer. The level of luciferase expression under induction slightly decreased at day 8 whereas background expression increased. The limited induction rate observed in this experiment could be due to an insufficient level of rtTA synthesis *in vivo* or to an insufficient doxycycline concentration in the brain.

Experiments performed in mice muscle permitted the investigation of the role of rtTA. As injection of the single Ad.TK*-luc yielded no detectable luciferase expression (data not shown), we investigated the behaviour of single Ad.CMV*luc. In mice muscle (Figure 5c), the single Ad.CMV*luc alone was weakly inducible ($4\times$) whereas the addition of small amounts of Ad.CMV-rtTA (ratio 1:2) led to a 32-fold induction of luciferase expression in the presence of inducer. Interestingly, under doxycycline induction, the intramuscular level of luciferase expression reached a plateau whatever the amount of Ad.CMV-rtTA virus co-injected with inducible virus. This result showed that rtTA expression at a 1:2 ratio (Ad.CMV-rtTA/single Ad.CMV*luc) was enough to saturate the tet-on system. The increased background level demonstrated that over-expression of the transactivator triggered promoter activation in the absence of inducer and that tetR-KRAB was not sufficiently expressed to thwart this phenomenon. Under induction, luciferase expression at a 1:2 ratio was comparable to that obtained by an adenovirus vector encoding luciferase under a whole CMV promoter.
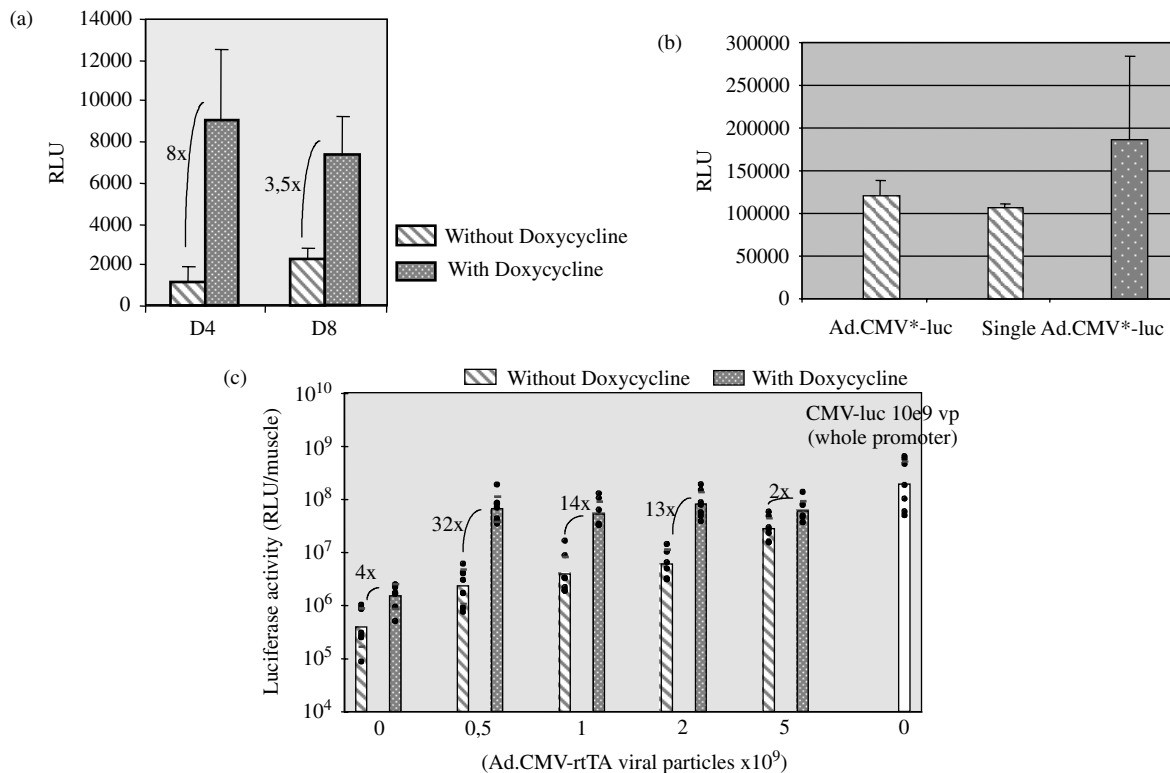
Discussion

The six different E1-E4-deleted adenovirus vectors described in this study have highlighted the respective roles of different components involved in the tet-on regulation process. We have described the feature of a tet-on system in adenovirus vectors, characterised the *in vitro* and *in vivo* background expression according to the minimal promoter used, and pointed out the effect of rtTA synthesis on induction efficiency.

The choice of inducible minimal promoter is critical and its use will depend on the applications required. It has been reported by the Bujard laboratory that CMV* but not TK* promoter was very sensitive to transcriptional interference. The difference in doxycycline-independent luciferase activity between the TK* and the CMV* promoter in our study is likely due to the sensitivity of the CMV* promoter to transcriptional interference in the E1-E4 adenovirus landscape. The CMV* promoter triggering a high background could be useful when constitutive transgene expression is needed and the inducer could be added only when over-expression is desired. This

Figure 4. Reversibility of induction of single Ad.TK*luc. PC12 or human astrocyte cells were infected with 1000 vp/cell of single Ad.TK*luc. For PC12 cells, luciferase expression was monitored for 3 days in the absence of inducer (empty triangles), in the presence of 1 μg/ml doxycycline (empty squares) and for 1 μg/ml doxycycline removed on day 1 and re-introduced on day 2 (dashed line). For NHA cells, luciferase expression was monitored for 8 days. Doxycycline (1 μg/ml) was added and withdrawn as indicated by the arrows. The induction rate is calculated by dividing the level of luciferase expression by the level of background expression of the virus in the absence of inducer

Figure 5. *In vivo* experiments. (a) Single Ad.TK*luc (3 × 10^9 vp) was stereotaxically injected into the *striatum* of Sprague-Dawley rats. The animals (group of four) received either no inducer or 1 mg/ml doxycycline in their drinking water. On day 4 or 8, the rats were sacrificed and luciferase expression was determined. (b) Ad.CMV*-luc or single Ad.CMV*-luc (3 × 10^9 vp) was stereotaxically injected into the *striatum* of Sprague-Dawley rats. The animals (group of four) received either no inducer or 1 mg/ml doxycycline in their drinking water. On day 4, the rats were sacrificed and luciferase expression was determined. (c) Single Ad.CMV*luc was injected in mice *Tibialis cranialis* with increasing amounts of Ad.CMV-rtTA virus. The animals received either no inducer or 1 mg/ml doxycycline in their drinking water. For the control, non-inducible particles of adenovirus encoding luciferase driven by the whole CMV promoter were injected alone. Four days after the virus injection, animals were sacrificed and luciferase activity was determined. Results are given as mean (group of six mice) and error bar represents the 95% confidence interval

approach could be used for secreted proteins such as human antitrypsin or erythropoietin [17]. On the other hand, the non-leaky TK* promoter could be used for toxic protein expression (e.g apoptogenic proteins). Indeed, the viral production process in the absence of inducer would result in high vector yields and, after injection, the toxic protein would be induced by addition of tetracycline.

Regulation of transgene expression by the tet switch system has already been described in a single genome with E1-defective adenoviruses, but only under the tet-off configuration [18–21]. Moreover, previous studies have already demonstrated the usefulness of tet-off tyrosine hydroxylase regulatable adenovirus vectors either in *ex vivo* strategies or after direct injection of the virus into the brain [18,20]. For clinical trials, the tet-on system may be more suitable as the transgene expression can be switched off just by stopping inducer addition, thus making this system safer. It has recently been reported that the Ad-mediated tet-on system is "functionally inferior" to the Ad tet-off system [22,23]. Nevertheless, we have designed a single adenovirus mediated tet-on system, optimal for specific cell lines. In other cell lines such as human astrocyte cells, this single tet-on mediated adenovirus alone permitted a 80-fold induction, whereas

a more than 600-fold induction was reached when rtTA-encoding adenoviruses were added. This observation indicated that rtTA synthesis differs according to the cell lines and that the choice of the promoter used to encode the transactivator is critical. Recently, it has been demonstrated that a single Ad-mediated tet-off system expressing the tTA under the control of cell-type-specific promoters can be used *in vivo* [24]. Glial fibrillary acidic protein (GFAP) and neuronal specific enolase (NSE) promoters have permitted the expression and regulation of the transgene only in restricted brain cells. Even if the strength of these promoters is not as high as viral promoters, we hypothesise that this strategy could be adapted to an Ad-mediated tet-on system.

rtTA is less sensitive to doxycycline than tTA and inducer concentration could be a limit for tet-on regulation, especially in the brain. Nevertheless, it has been previously reported that both tet-on and tet-off configurations permitted the switching of transgene expression in the hippocampus [23]. Moreover, since our work was completed, a new generation of rtTAs more sensitive to doxycycline has appeared, thus creating an opportunity to overcome this potential limitation [25]. Using this novel generation of rtTAs, we can speculate that

the 600-fold induction we obtained in human astrocyte cells and the 32-fold induction we observed in mice muscle could be improved and make possible the use in gene therapy trials of a single adenovirus-mediated tet-on system.

Acknowledgements

References

1. Bohn MC, Choi-Lundberg DL, Davidson BL, *et al*. Adenovirus-mediated transgene expression in nonhuman primate brain. *Hum Gene Ther* 1999; **10**: 1175–1184.
2. Choi-Lundberg DL, Lin Q, Chang YN, *et al*. Dopaminergic neurons protected from degeneration by GDNF gene therapy. *Science* 1997; **275**: 838–841.
3. Qin L, Ding Y, Pahud DR, *et al*. Adenovirus-mediated gene transfer of viral interleukin-10 inhibits the immune response to both alloantigen and adenoviral antigen. *Hum Gene Ther* 1997; **8**: 1365–1374.
4. Yang Y, Nunes FA, Berencsi K, *et al*. Cellular immunity to viral antigens limits E1-deleted adenoviruses for gene therapy. *Proc Natl Acad Sci* 1994; **91**: 4407–4411.
5. Yeh P, Dedieu JF, Orsini C, *et al*. Efficient dual transcomplementation of adenovirus E1 and E4 regions from a 293-derived cell line expressing a minimal E4 functional unit. *J Virol* 1996; **70**: 559–565.
6. Wang Q, Greenburg G, Bunch D, *et al*. Persistent transgene expression in mouse liver following in vivo gene transfer with a delta E1/delta E4 adenovirus vector. *Gene Ther* 1997; **4**: 393–400.
7. Gao GP, Yang Y, Wilson JM. Biology of adenovirus vectors with E1 and E4 deletions for liver-directed gene therapy. *J Virol* 1996; **70**: 8934–8943.
8. Dedieu JF, Vigne E, Mafhouz I, *et al*. Long term delivery into the livers of immunocompetent mice with E1/E4 defective adenoviruses. *J Virol* 1997; **71**: 4626–4637.
9. Gossen M, Bujard H. Tight control of gene expression in mammalian cells by tetracycline-responsive promoters. *Proc Natl Acad Sci* 1992; **89**: 5547–5551.
10. Gossen M, Freundlieb S, Bender G, *et al*. Transcriptional activation by tetracyclines in mammalian cells. *Science* 1995; **268**: 1766–1769.
11. Rossi F, Guicherit O, Spicher A, *et al*. Tetracycline-regulatable factors with distinct dimerization domains allow reversible growth inhibition by p16. *Nat Med* 1999; **20**: 389–393.
12. Crouzet J, Naudin L, Orsini C, *et al*. Recombinational construction in *E. coli* of infectious adenoviral genomes. *Proc Natl Acad Sci* 1997; **94**: 1414–1419.
13. Blanche F, Cameron B, Barbot A, *et al*. An improved anion-exchange HPLC method for the detection and purification of adenoviral particles. *Gene Ther* 2000; **7**: 1055–1062.
14. Steinwaerder DS, Lieber A. Insulation from viral transcriptional regulatory elements improves inducible transgene expression from adenovirus vectors *in vitro* and *in vivo*. *Gene Ther* 2000; **7**: 556–567.
15. Forster K, Helbl V, Lederer T, *et al*. Tetracycline-inducible expression systems with reduced basal activity in mammalian cells. *Nucleic Acids Res* 1999; **27**: 708–710.
16. Deuschle U, Meyer WK, Thiesen HJ. Tetracycline-reversible silencing of eukaryotic promoters. *Mol Cell Biol* 1995; **15**: 1907–1914.
17. Bohl D, Naffakh N, Heard JM. Long-term control of erythropoietin secretion by doxycycline in mice transplanted with engineered primary myoblasts. *Nat Med* 1997; **3**: 299–305.
18. Corti O, Horellou P, Colin P, *et al*. Intracerebral tetracycline-dependent regulation of gene expression in grafts of neural precursors. *Neuroreport* 1996; **7**: 1655–1659.
19. Ridet JL, Corti O, Pencalet P, *et al*. Toward autologous ex vivo gene therapy for the central nervous system with human adult astrocytes. *Hum Gene Ther* 1999; **10**: 271–280.
20. Corti O, Sanchez-Capelo A, Colin P, *et al*. Long-term doxycycline-controlled expression of human tyrosine hydroxylase after direct adenovirus-mediated gene transfer to a rat model of Parkinson's disease. *Proc Natl Acad Sci* 1999; **96**: 12 120–12 125.
21. Hu SX, Ji W, Zhou Y, *et al*. Development of an adenovirus vector with tetracycline-regulatable human tumor necrosis factor alpha gene expression. *Cancer Res* 1997; **57**: 3339–3343.
22. Mizuguchi H, Hayakawa T. Characteristics of adenovirus-mediated tetracycline-controllable expression system. *Biochim Biophys Acta* 2001; **1568**: 21–29.
23. Harding TC, Geddes BJ, Murphy D, *et al*. Switching transgene expression in the brain using an adenoviral tetracycline-regulatable system. *Nat Biotechnol* 1998; **6**: 553–555.
24. Smith-Arica JR, Morelli AE, Larregina AT, *et al*. Cell-type-specific and regulatable transgenesis in the adult brain: adenovirus-encoded combined transcriptional targeting and inducible transgene expression. *Mol Ther* 2000; **6**: 579–587.
25. Urlinger S, Baron U, Thellmann M, *et al*. Exploring the sequence space for tetracycline-dependent transcriptional activators: novel mutations yield expanded range and sensitivity. *Proc Natl Acad Sci* 2000; **14**: 7963–7968.

Vol. 77, No. 8

NOTES

Adenovirus Dodecahedron Allows Large Multimeric Protein Transduction in Human Cells

P. Fender,[1]* G. Schoehn,[1,2] J. Foucaud-Gamen,[3] E. Gout,[1] A. Garcel,[1] E. Drouet,[3] and J. Chroboczek[1]

Institut de Biologie Structurale[1] and Laboratoire Européen de Biologie Moléculaire,[2] 38027 Grenoble, and Faculté de Pharmacie, Domaine de la Merci, 38 La Tronche,[3] France

Adenovirus dodecahedron is a virus-like particle composed of only two viral proteins of human adenovirus serotype 3 that are responsible for virus attachment and internalization. We show here that this dodecameric particle, devoid of genetic information, efficiently penetrates human cells and can deliver large multimeric proteins such as immunoglobulins.

Human adenoviruses (Ads) are nonenveloped viruses responsible for respiratory, ocular, and enteric infections. Their icosahedral capsid, containing the 36-kpb double-stranded DNA genome, is composed of three major proteins: the hexon, the penton (Pt) base, and the fiber. At the 12 vertices of the capsid, the protruding fiber is noncovalently attached to the Pt base, thus forming the Pt complex. It has been reported that the fiber interacts with a high affinity with a primary receptor and that the subsequent interaction of the Pt base RGD motif with cellular integrins triggers endocytosis (17). A 42-kDa protein, called the coxsackievirus and Ad receptor (CAR), is recognized by at least one serotype of each of the six subgroups of Ad except for the serotypes belonging to subgroup B (i.e., Ad3) (1, 12). Even though that Ad capsid is composed of at least 11 proteins, it has been shown that Pt alone can penetrate into human cell lines, thus making of this complex a potential vector for DNA delivery (2, 5, 7, 8, 16). Remarkably, Ad3 but not Ad5 Pt expressed in the baculovirus system led to the formation of symmetric complexes of 12 Pts called dodecahedron (Dd). We have previously shown that the non-CAR-binding Ad3-Dd can be used as a gene transfer vector (2), and we show here that this virus-like particle is also able to transduce large multimeric proteins into human cells.

Dd internalization. Coexpression of Ad3 Pt base and fiber proteins in the baculovirus system led to the formation of a symmetric dodecameric particle (2, 14), Pt-Dd (Fig. 1a). This complex results from the interaction between the pentameric base proteins, as attested by the Dd formation upon expression of base proteins alone (Bs-Dd; Fig. 1a). The respective roles of the fiber and the Pt base protein in Ad3 Dd entry into HeLa cells was assessed by immunofluorescence. HeLa cells grown in a 96-multiwell plate (Falcon) at 2×10^4 cells per well were incubated in 100 μl of phosphate-buffered saline (PBS) with a range of Dd concentrations. After 1 h at 37°C, cells were
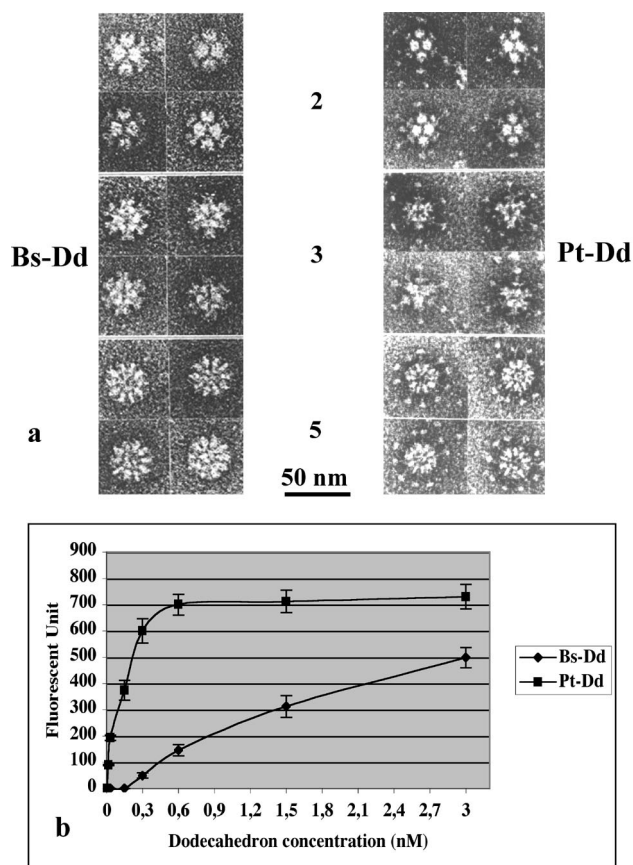
FIG. 1. Dd structure and function. (a) Negative-stain micrographs of purified Bs-Dd and Pt-Dd. Views along the two-, three-, and five-fold axes of Dds are shown. (b) Fluorescence quantification of Dd entry into HeLa cells after 1 h of incubation at 37°C. Incoming Bs-Dd or Pt-Dd was quantified by indirect immunofluorescence (at 485 and 535 nm) in permeabilized cells with an antibody directed against the Ad3 Pt base protein and an FITC-conjugated secondary antibody.

* Corresponding author. Mailing address: Institut de Biologie Structurale, 41 Rue Jules Horowitz, 38027 Grenoble, France. Phone: 33-4-38-78-96-28. Fax: 33-4-38-78-54-94. E-mail: fender@ibs.fr.
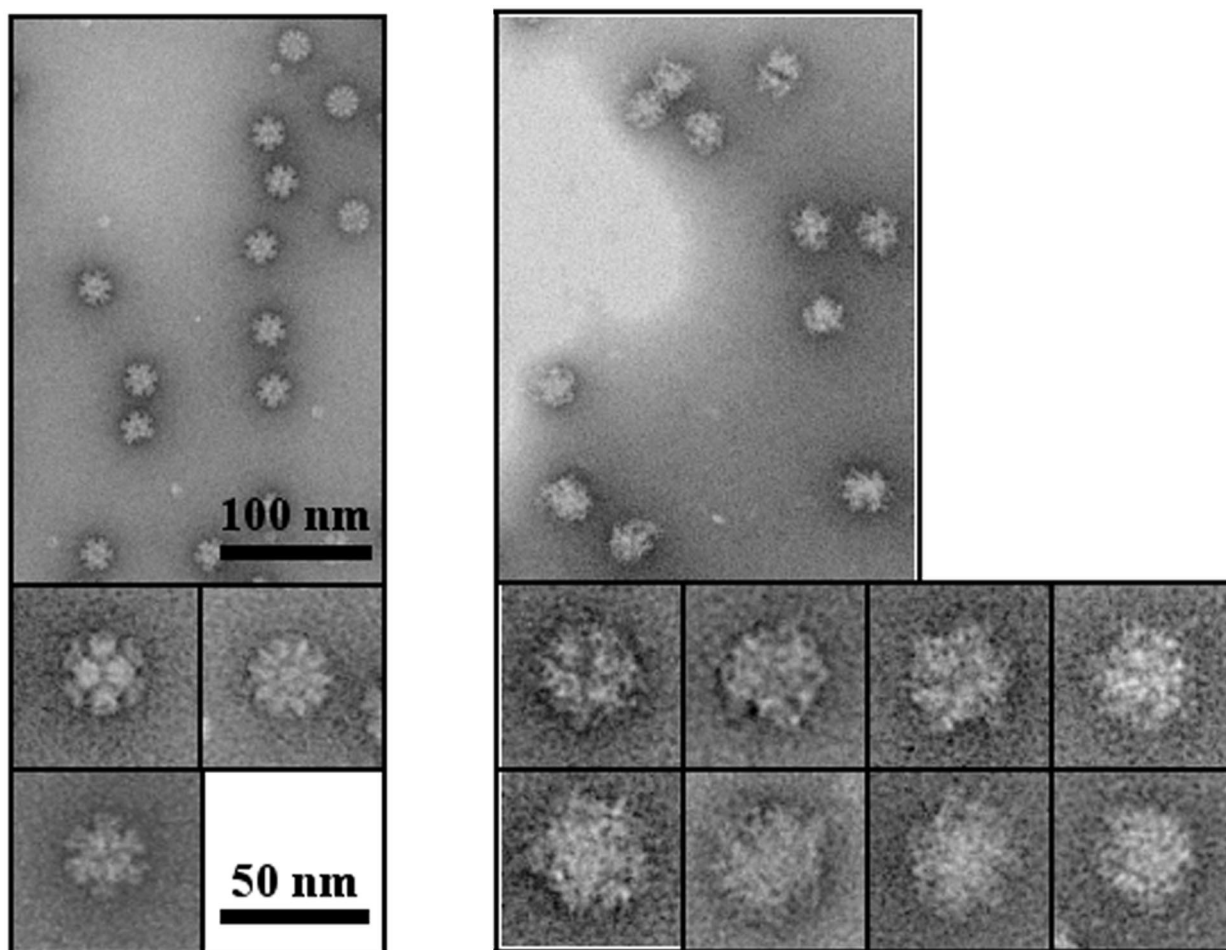
FIG. 2. Negative-stain electron microscopy of Bs-Dd (left panel) and Bs-Dd–5C12 complex (right panel). Proteins were purified by using a 15 to 40% sucrose density gradient, and a portion of the fractions corresponding to Bs-Dd or Bs-Dd–5C12 complexes was analyzed.

permeabilized, and the amount of Dd present in the cells was estimated by using a rabbit polyclonal serum recognizing the Ad3 Pt base, followed by incubation with a goat anti-rabbit secondary fluorescein isothiocyanate (FITC)-labeled antibody (Santa Cruz). After PBS washes, fluorescence quantification was performed by using a plate reader fluorimeter (485 and 535 nm; Wallac). The antibody background was subtracted, and the mean of three measurements is shown in Fig. 1b. The Bs-Dd was capable of entering human cells, suggesting that a direct interaction between the RGD motifs of the Pt base and the cellular integrins or between the Pt base and another cellular component (5) is sufficient for cell entry. However, the presence of fiber in the Pt-Dd dramatically increased the level of Dd entry, suggesting a more efficient two-step endocytosis mediated by this protein.

MAb production and characterization. Monoclonal antibodies (MAbs) have been produced against ion-exchange chromatography-purified Bs-Dd according to the classical protocol (6). Two retained hybridomas were analyzed by Western blot and enzyme-linked immunosorbent assay (ELISA). The 5C12 hybridoma recognized both Bs-Dd and Pt-Dd only in their native forms (as determined by ELISA), indicating that the recognized epitopes are exposed on the Dd surface and that

the presence of the fiber does not interfere with MAbs binding to the base protein. In contrast, the 5F5 clone, which was strongly reactive toward the sodium dodecyl sulfate-denatured base protein (detection of 0.1 ng of denatured base in a Western blot), recognized only weakly the native Dd by ELISA.

Electron microscopy study of Bs-Dd–5C12 complex. MAb-Dd complexes were obtained by incubation of purified Dds with purified MAbs. After sucrose gradient (15 to 40%) density centrifugation (4 h at $200,000 \times g$ in a TLS55 rotor [Beckman]), 5C12 MAb was found at the bottom of the tube, together with Dd, whereas the 5F5 MAb that is unable to strongly bind native Dd remained in the upper part of the gradient (data not shown). An aliquot of purified Bs-Dd–5C12 complex was applied to the carbon on mica and negatively stained with 1% silicotungstate (pH 7.0) for electron microscopy (Fig. 2). Micrographs were obtained under low-dose conditions by using a JEOL 1200 EX II microscope at 100 kV and a nominal magnification of ×40,000. The fuzzy outline and the increased size of Bs-Dd–5C12 versus Bs-Dd alone suggest that the particle is decorated by immunoglobulin G.

MAb entry into HeLa cells with Dd as a vector. In order to find out whether MAbs can be delivered to the cell by Dd,
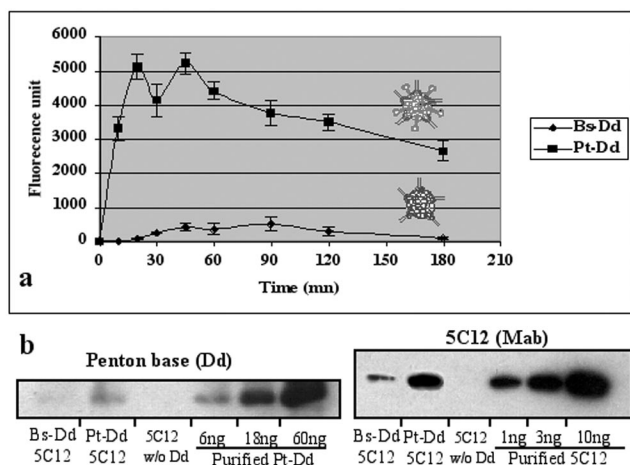
FIG. 3. 5C12 entry into HeLa cells. (a) Kinetic experiment. Bs-Dd–5C12 or Pt-Dd–5C12 complexes (0.6 nM) were incubated with HeLa cells for different times at 37°C. Transduced 5C12 antibody was quantified in permeabilized cells by using a secondary anti-mouse FITC-labeled antibody. Background signal raised by 5C12 antibody alone was subtracted. (b) Dd and MAbs quantification. Lysis extract of HeLa cells incubated for 1 h at 37°C with a 0.6 nM concentration of Pt-Dd–5C12, Bs-Dd–5C12, or 5C12 without Dd was analyzed by Western blot with either anti-Ad3 base serum and anti-rabbit HRP-labeled antibody (recognition of internalized Dd) or anti-mouse HRP-labeled antibody (recognition of transduced 5C12 MAb). Estimation of the amount of protein was performed by comparison to a range of purified Dd or 5C12.

Dd-MAb complexes (0.6 nM with respect to Dd) were incubated for different times with living HeLa cells in a 96-multiwell plate (Falcon) at 2×10^4 cells per well. After methanol permeabilization, the level of MAb entry was determined by using a fluorescent secondary antibody directed against the mouse monoclonal antibody. After PBS washes, fluorescence quantification was performed by using a plate reader fluorimeter (485 and 535 nm; Wallac). The antibody background was subtracted, and the mean of three measurements is shown in Fig. 3a. Bs-Dd permitted a limited transduction of 5C12 MAbs with a maximum level obtained at 90 min, whereas Pt-Dd permitted a very efficient transduction of 5C12 MAbs, with a maximum reached after 20 min only. These results show that the fiber in Pt-Dd improved considerably the protein transduction efficiency and also reduced the time needed by the Pt-Dd–MAb complex to bind and enter the cells.

The approximate amount of MAbs and Pt-Dd present inside the HeLa cell was determined by Western blot analysis. HeLa cells grown in a 96-multiwell plate (Falcon) at 2×10^4 cells per well were transduced for 1 h at 37°C with either 0.6 nM concentrations of Bs-Dd–5C12 or Pt-Dd–5C12 complexes or with 5C12 alone. After washes with PBS, cells were lysed in 100 μl of cell lysis buffer (Promega), and 10-μl aliquots were boiled and subjected to sodium dodecyl sulfate-polyacrylamide gel electrophoresis, together with known amounts of either purified Pt-Dd or 5C12 MAb. After transfer to a polyvinylidene difluoride membrane, the blot was treated with either anti-mouse horseradish peroxidase (HRP) antibody (visualization of transduced 5C12) or anti-Pt base antibody and anti-rabbit HRP antibody (visualization of internalized Dd). Estimation of Dd and 5C12 present inside the cell was performed by band

scanning (Molecular Analyst; Bio-Rad), and the results were scaled to the number of cells per well (Fig. 3b). About 6 ng of Pt-Dd and 3 ng of 5C12 MAbs were found in 2×10^4 HeLa cells, representing an average of 5×10^4 Pt-Dd and 5.7×10^5 MAbs per cell. This result indicates an average ratio of about 12 MAbs per Dd, suggesting a stoichiometric process of MAb attachment to Dd. This experiment shows an efficient and stable interaction of 5C12 MAb with Dd, as well as very efficient cell transduction of attached MAbs. As expected, the amount of Bs-Dd was much lower than that of Pt-Dd. Since we determined by ELISA that equivalent amounts of 5C12 MAb were bound to Bs-Dd and Pt-Dd (data not shown), the 10-fold-smaller amount of antibody transduced by Bs-Dd is consistent with the lower penetration efficiency of this particle (Fig. 3).

MAb localization upon transduction. MAb localization in transduced cells was monitored by confocal microscopy. About 10^5 HeLa cells were incubated for different periods of time with a 0.6 nM concentration of the Pt-Dd–5C12 complex. After a given period of entry, cells were washed and permeabilized and 5C12 MAb was detected by using an FITC-labeled secondary antibody (Fig. 4). Laser scanning confocal microscopy was performed on an MRC600 (Bio-Rad). Incubation times as short as 5 min were sufficient to detect some Pt-Dd–5C12 complexes bound to the plasma membrane and, after 10 min of incubation, a green signal surrounding the cells was observed. Consistent with the kinetic experiment (Fig. 3a), complex internalization began after 20 min (Fig. 4D). After 1 h of incubation, MAbs were detected close to the nucleus, whereas a control experiment performed with 5C12 antibody without Dd gave no signal, thus attesting that MAbs delivery into the cells is mediated by the Pt-Dd (Fig. 4E and A, respectively). Moreover, incubation of Dd with the 5F5 MAb (which was unable to recognize native Dd) on a HeLa cell produced no signal as in Fig. 4A, thus confirming that protein delivery occurs only when the MAb is attached to Dd. A similar experiment of confocal microscopy done with Bs-Dd–5C12 complexes confirmed the weaker and delayed transduction of 5C12 in HeLa cells observed in Fig. 3a (data not shown).

Activity of the transduced protein. It has been reported that the cell entry of subgroup B Ads (i.e., Ad3 and Ad7) is different from that of the subgroup C Ads (i.e., Ad2 and Ad5). The major difference lies in the ability of subgroup C Ads to escape endosomes, whereas subgroup B Ads accumulate in late endosomes and to a small extent in lysosomes prior to their cytosol escape (9, 10). It was therefore important to assess whether the activity of the transduced protein is retained during the trafficking process. For this, we developed an enzyme delivery system. Purified Pt-Dd and Bs-Dd were biotinylated with 1 mM Sulfo-NHS-LC-LC-biotin (Pierce). After removal of the unbound biotin, a 0.6 nM concentration of biotinylated Bs-Dd or Pt-Dd was incubated for 30 min in PBS with a 0 to 15 nM concentration of streptavidin conjugated to HRP (SptAv-HRP; Jackson Laboratories). HeLa cells grown in a 96-multiwell plate (2×10^4 cells per well) were then incubated with the complexes and, after 1 h at 37°C, the cells were lysed in 100 μl of cell lysis buffer (Promega). The enzyme activity was determined by photometry at 492 nm after the addition of 100 μl of the colorimetric peroxidase substrate o-phenylenediamine (3 mg/ml; Sigma). Nonbiotinylated Dd incubated with 0 to 15 nM of StpAv-HRP was used for background substraction. The
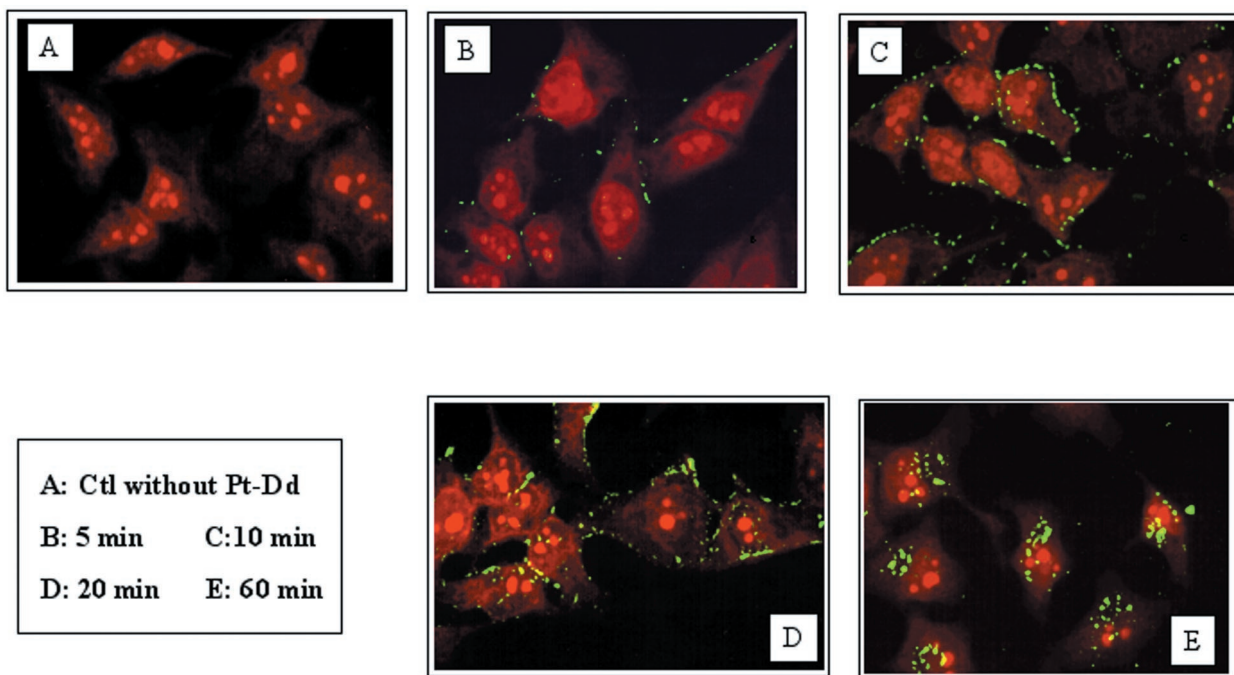
FIG. 4. MAb localization upon transduction into HeLa cells as determined by confocal microscopy. Pt-Dd–5C12 complexes (0.6 nM) were incubated for different times at 37°C. Cells were washed, and transduced MAbs were detected by using a secondary FITC-labeled mouse antibody (green signal). Cells nuclei were counterstained with propidium iodide (red signal).

experiment was performed in triplicate, and the results are expressed as the mean of the values (Fig. 5). This experiment shows an exogenous peroxidase activity in cells incubated with biotinylated Dd–StpAv-HRP, thus demonstrating that enzyme was delivered by biotinylated Dd and that at least a part of the transduced proteins remained active 1 h after transduction. During biotinylation of Pt-Dd, fiber protein is also biotinylated which could, in part, neutralize its function, and it can possibly explain the two- to threefold difference in transduction effi-

FIG. 5. Biological activity of the transduced protein. Complexes made of either biotinylated Dd (Bs-Dd* or Pt-Dd*), both at 0.6 nM, and streptavidin-HRP (0 to 15 nM) were incubated with HeLa cells for 1 h at 37°C. Cells were lysed, and peroxidase activity was determined at 492 nm by using the colorimetric peroxidase substrate o-phenylene-diamine.

ciency of Pt-Dd and Bs-Dd in this experiment compared to the 10-fold difference observed with MAb delivery (Fig. 3).

MAb delivery into human cells by Dd shows that this particle can act as a protein transduction vector. Protein transduction technology represents an alternative to gene transfer technology when no gene insertion into genome is required (3, 11, 15). This technology may be appropriate for restricted applications; it is also potentially a basis for an entirely new form of therapy and may allow us to overcome some of the technical hurdles of gene therapy. Protein transduction could be useful for the efficient antigen loading of dendritic cells for a range of vaccination purposes, including anti-tumor immune therapy. Interestingly, both Dd and the Ad virion contain 12 Pts and efficiently enter human cells. However, contrary to the complete Ad capsid, the Dds are compact particles devoid of any viral DNA. Consequently, Ad Dd might be a safe alternative vector to use instead of the whole Ad. In order to deliver proteins other than MAbs into the cells by Dd, a strategy aiming to fuse the protein of interest to a single-chain antibody derived from 5C12 can be considered. Moreover, it has been recently observed that the two PPxY motifs present in the Ad Pt base sequence interacted with WW domains of several proteins (4). As reported for polyomavirus-like particle, in which the WW domain has been inserted in order to target PPxY motif (13), we can hypothesize that the fusion of therapeutic protein to WW domains might permit its attachment to the Dd, thus allowing its transduction into the target cell.

REFERENCES

1. **Bergelson, J. M., J. A. Cunningham, G. Droguett, E. A. Kurt-Jones, A. Krithivas, J. S. Hong, M. S. Horwitz, R. L. Crowell, and R. W. Finberg.** 1997. Protein structure and isolation of a common receptor for coxsackie B viruses and adenoviruses 2 and 5. Science **275:**1320–1323.
2. **Fender, P., R. W. Ruigrok, E. Gout, S. Buffet, and J. Chroboczek.** 1997. Adenovirus dodecahedron, a new vector for human gene transfer. Nat. Biotechnol. **15:**52–56.
3. **Ford, K. G., B. E. Souberbielle, D. Darling, and F. Farzaneh.** 2001. Protein transduction: an alternative to genetic intervention? Gene Ther. **8:**1–4.
4. **Galinier, R., E. Gout, H. Lortat-Jacob, J. Wood, and Chroboczek, J.** 2002. Adenovirus protein involved in virus internalization recruits ubiquitin-protein ligases. Biochemistry **41:**14299–14305.
5. **Hong, S. S., B. Gay, L. Karayan, M. C. Dabauvalle, and P. Boulanger.** 1999. Cellular uptake and nuclear delivery of recombinant adenovirus penton base. Virology **262:**163–177.
6. **Kohler, G., and C. Milstein.** 1975. Continuous cultures of fused cells secreting antibody of predefined specificity. Nature **256:**495–497.
7. **Medina-Kauwe, L. K., N. Kasahara, and L. Kedes.** 2001. 3PO, a novel nonviral gene delivery system using engineered Ad5 penton proteins. Gene Ther. **8:**795–803.
8. **Medina-Kauwe, L. K., M. Maguire, N. Kasahara, and L. Kedes.** 2001. Nonviral gene delivery to human breast cancer cells by targeted Ad5 penton proteins. Gene Ther. **8:**1753–1761.
9. **Miyazawa, N., P. L. Leopold, N. R. Hackett, B. Ferris, S. Worgall, E. Falck-Pedersen, and R. G. Crystal.** 1999. Fiber swap between adenovirus subgroups B and C alters intracellular trafficking of adenovirus gene transfer vectors. J. Virol. **73:**6056–6065.
10. **Miyazawa, N., R. G. Crystal, and P. L. Leopold.** 2001. Adenovirus serotype 7 retention in a late endosomal compartment prior to cytosol escape is modulated by fiber protein. J. Virol. **75:**1387–1400.
11. **Morris, M. C., J. Depollier, J. Mery, F. Heitz, and G. Divita.** 2001. A peptide carrier for the delivery of biologically active proteins into mammalian cells. Nat. Biotechnol. **19:**1173–1176.
12. **Roelvink, P. W., A. Lizonova, J. G. Lee, Y. Li, J. M. Bergelson, R. W. Finberg, D. E. Brough, I. Kovesdi, and T. J. Wickham.** 1998. The coxsackievirus-adenovirus receptor protein can function as a cellular attachment protein for adenovirus serotypes from subgroups A, C, D, E, and F. J. Virol. **72:**7909–7915.
13. **Schmidt, U., R. Rudolph, and G. Böhm.** 2001. Binding of external ligands onto an engineered virus capsid. Protein Eng. **14:**769–774.
14. **Schoehn, G., P. Fender, J. Chroboczek, and E. A. Hewat.** 1996. Adenovirus 3 penton dodecahedron exhibits structural changes of the base on fibre binding. EMBO J. **15:**6841–6846.
15. **Schwartz, J. J., and S. Zhang.** 2000. Peptide-mediated cellular delivery. Curr. Opin. Mol. Ther. **2:**162–167.
16. **Smith, C. C., M. Kulka, and L. Aurelian.** 2000. Modified adenovirus penton base protein (UTARVE) as a non-replicating vector for delivery of antisense oligonucleotides with antiviral and/or antineoplastic activity. Int. J. Oncol. **17:**841–850.
17. **Wickham, T. J., P. Mathias, D. A. Cheresh, and G. R. Nemerow.** 1993. Integrins $\alpha_v\beta_3$ and $\beta_v\beta_5$ promote adenovirus internalization but not virus attachment. Cell **73:**309–319.

Recombinant adenoviruses and adenovirus penton vectors: from DNA transfer to direct protein delivery into cell

Review Article

Pascal Fender

Institut de Biologie Structurale, (CNRS/CEA), Grenoble, France

_____

Correspondence: Pascal Fender, Institut de Biologie Structurale, 41 rue Jules Horowitz, 38027 Grenoble; FRANCE; Tel: 33 4 38 78 96 28; Fax: 33 4 38 78 54 94; e-mail: fender@ibs.fr

Summary

Recombinant adenovirus (rAd) is one of the most frequently used vectors with 171 human gene therapy trials involving 644 patients in 2002. Its success stems mainly from the capacity of rAd to efficiently penetrate various cell lines or tissues and from the ease of producing large amounts of this vector on industrial scale. Recently, in parallel to gene transfer by viral vectors, a new technology aiming to deliver proteins rather than genetic material in human cells has emerged, using small vehicle peptides often derived from viral proteins. In the first part of this review, I summarize the different types of rAd vectors used for gene transfer, their advantages and their limits. In the second part, I summarize the main vectors used for direct protein delivery into human cells and I show how an amazing nanoparticle called "adenovirus dodecahedron" can be used for this emerging therapeutic area.

I. DNA transfer

DNA transfer by adenovirus (Ad) can be achieved using two different strategies. The first consists in modifying the Ad genome in order to introduce a transgene encoding the therapeutic protein, which will then be delivered to target cells by virus penetration. Such vectors are called: recombinant adenoviruses (rAd). The second strategy using Ad capsid proteins as vectors allows non-encapsidated plasmid DNA to be introduced into cells.

A. Recombinant adenoviral vectors

Gene therapy is a promising approach for the treatment of either innate or acquired diseases. Among vectors that are used to transfer DNA into cells, Ads have several advantages. They can infect dividing as well as resting cells with high efficiency and can be easily produced, purified and concentrated to high titres. In addition, a sizeable part of the viral genome, non-essential for virus development in cell cultures used for the vector replication, can be removed, permitting the insertion of the majority of various cDNAs encoding the therapeutic gene.

Numerous gene therapy trials have been performed, in particular for cancer treatment, using different therapeutic genes (tumor suppressor, thymidine kinase, cytokines…). A considerable effort has also been deployed in the area of central nervous system diseases, as Ads infect non-dividing cells and can be transported by the retrograde route from the injection point to distant locations.

In the first generation of rAd vectors, the E1 region involved in the initiation of the virus replication cycle is deleted, in order to avoid formation of recombinant replicative particles (RCA). The major limiting factor of such vectors is immunogenicity, which triggers both inflammation and a cytotoxic response against the transfected cells. It has been observed that this phenomenon results in transgene extinction a few days post-application, due to cell death and to the negative viral promoter regulation by some cytokines (Qin et al, 1996). Surprisingly, viral proteins can be still expressed in cells infected with E1-defective rAd (Yang et al, 1994). Therefore, it has been proposed to delete from the adenovirus genome additional regions involved in the replication process. The E4 region is crucial for virus replication and E1-E4-defective rAds were generated in a transcomplementing cell lines (Yeh et al, 1996), where

vectors are produced by double recombination in E. coli (Crouzet et al, 1997; **Figure 1**). These rAds were tested for gene transfer in murine immuno-competent liver and showed a prolonged transgene expression due to lower viral protein expression as well as the absence of RCA during production (Gao et al, 1996, Dedieu et al, 1997, Wang et al, 1997). Interestingly, E1-E4-defective rAds have also been shown to be efficient for gene therapy of brain diseases. The local injection (with a stereotaxic pump) in rat striatum was associated with an attenuated immune response and prolonged transgene expression (Do Thi et al, 2004).

Recently, the elaboration of helper-dependent rAds called gutless vectors represent a very promising development area in gene therapy. Use of the helper Ad encoding all adenoviral proteins made possible the encapsidation of up to 30 000 base pairs transgenes in rAd containing only the two inverted terminal repeats (ITRs) and the encapsidation sequence ( ) of the original virus. In order to improve the yield of recombinant gutless vector production, the helper virus encapsidation sequence has been flanked by two loxP sequences permitting excision of this sequence in the presence of the Cre recombinase.

Serial passages of both gutless rAd and helper virus in 293 cells expressing the Cre recombinase resulted in an increased gutless rAd titre whereas the helper virus titre remained constantly low, limiting rAd stock contamination by this undesired particle (Parks et al, 1996). The resulting gutless vectors harbouring no viral coding regions elicit no cytotoxic immune response against Ad-infected cells, thus permitting a prolonged expression of the transgene as attested by -antitrypsin expression in baboons for over 50 weeks (Morral et al, 1999).

B. Adenovirus pentons and dodecahedra

The use of recombinant adenovirus for gene therapy has been tempered by strong immune responses that develop to the virus and virus-infected cells. In addition, notwithstanding that the rAd are replication-defective, they introduce into the recipient cell together with the gene of interest viral genes that might lead to fortuitous recombination if the recipient is infected by wild-type adenovirus. The use of an Ad structural complex called the penton has been proposed as an alternative vector for
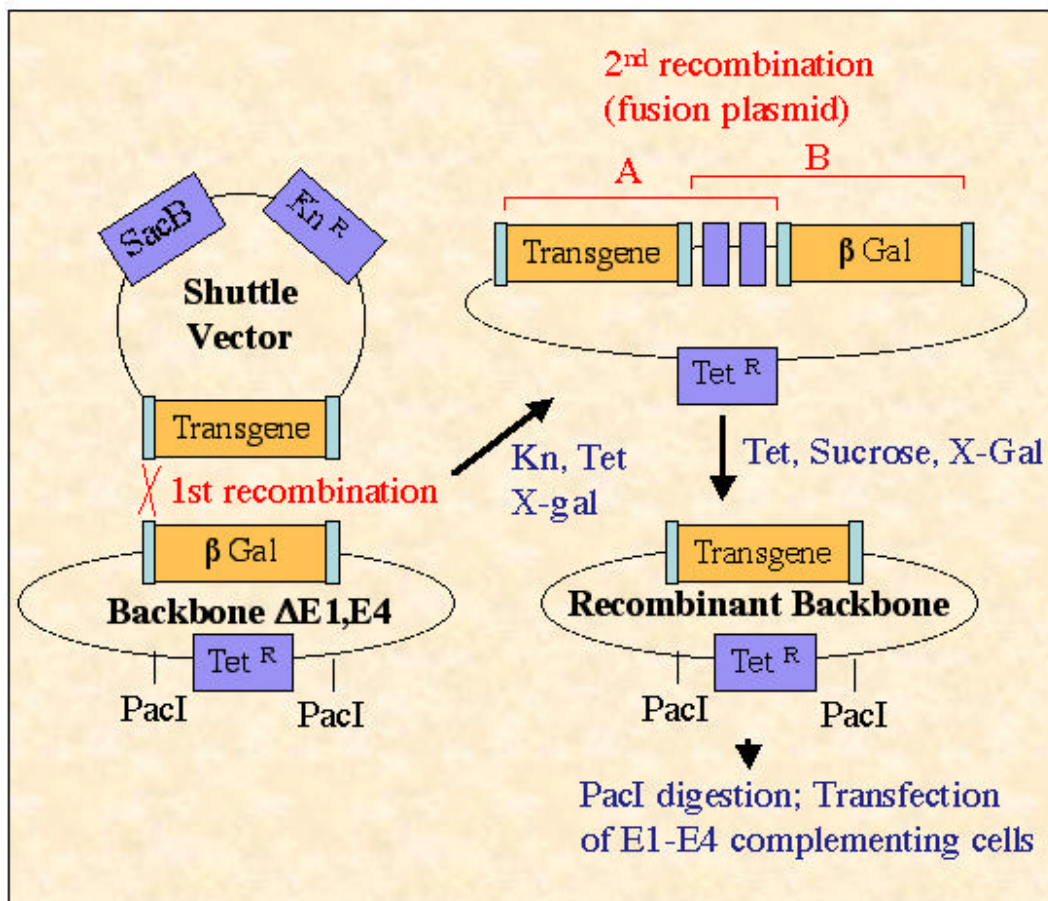
Figure 1: Principle of recombinant adenovirus production. Shuttle vector with the transgene cloned between the left ITR and the pIX sequences of adenovirus is transfected in recombination competent E. coli containing the E1-/E4- adenovirus backbone. Selection with Kanamycin (Kn) and Tetracyclin (Tet) results in the survival of a ß-galactosidase positive plasmid fusion. A second selection in presence of Tet and sucrose (that confere sensitivity to SacB positive bacteria) lead to the selection of either -Gal positive backbone (case A) or the desired recombinant backbone (case B). After PacI digestion, the recombinant backbone is transfected in a E1, E4 complementing cell line.

human gene therapy. The penton is a complex of two oligomeric proteins, a penton base and fiber. This complex located on the 12 vertices of the Ad capsid **(Figure 2)** is responsible for cell attachment, internalisation, and virus escape into the cytoplasm. The penton retains many of the advantages of adenovirus for gene transfer such as efficiency of entry and wide a range of cell and tissue targets. Because it consists of two proteins instead of at least 11 contained in an Ad virion, it is potentially a safer alternative to rAd. Interestingly, for some Ad serotypes such as human adenovirus of serotype 3 (Ad3), twelve pentons are capable of interacting together in a symmetric manner thus forming a sub-viral nanoparticle called dodecahedron (Dd) (Norrby et al, 1966). Expression of the Ad3 penton base alone or its co-expression with fiber protein using the baculovirus system leads respectively to the formation of base-dodecahedron (Bs-Dd) and penton-dodecahedron (Pt-Dd) **(Figure 2)**. The Dds structures solved by cryo-microscopy revealed that these particles contain an internal cavity with a volume close to 100 nm^3 (Schoehn et al, 1996).

Adenoviruses use primary receptors for high affinity interaction with invaded cell. We have recently shown that Ad3 dodecahedra recognize two types of receptors. The first is the Ad3 receptor (Sirena et al, *in press*) and, in addition, they have a capacity to strongly interact with cell surface glycoaminoglycans (Vives et al, Virology *in press*). This explains the remarkable penetration efficiency of Dds observed for a wide spectrum of cells. It has been proposed to use these particles as a gene transfer vector. In theory, the Dds internal cavity can only accommodate small oligonucleotides of about 100-mers. To overcome this limitation and attach DNA externally to the particle, a bi-functional peptide capable of interacting with both Dds and plasmid DNA (thanks to a polylysine stretch) has been designed, resulting in efficient gene expression in cells transfected by this system (Fender et al, 1997). Under certain conditions, this system permitted a gene expression comparable to that obtained with RAds *in vitro* and superior to cells transfected with cationic lipids. Following the same idea it has been reported that other penton base serotypes like Ad7 can transfect cells *in vitro* in an integrin-dependent manner. (Bal et al, 2000)

A modified version of this vector has been examined using the non-dodecameric Ad5 penton base fused to heregulin and a stretch of 10 lysines (HerPBK10). The rationale for this idea was to conserve the endocytotic properties of the Ad penton base (internalisation and endosomolytic activity) together with the targeting of HER-2/3 or HER2/4 heterodimeric receptors which are over-expressed in certain aggressive breast cancers (Medina-Kauwe et al, 2001).

II. Protein delivery

To date, direct protein delivery in the cell is mainly based on the use of small protein or peptide vectors. However, adenovirus capsid protein complexes can also be engineered to become a novel protein transduction vector.
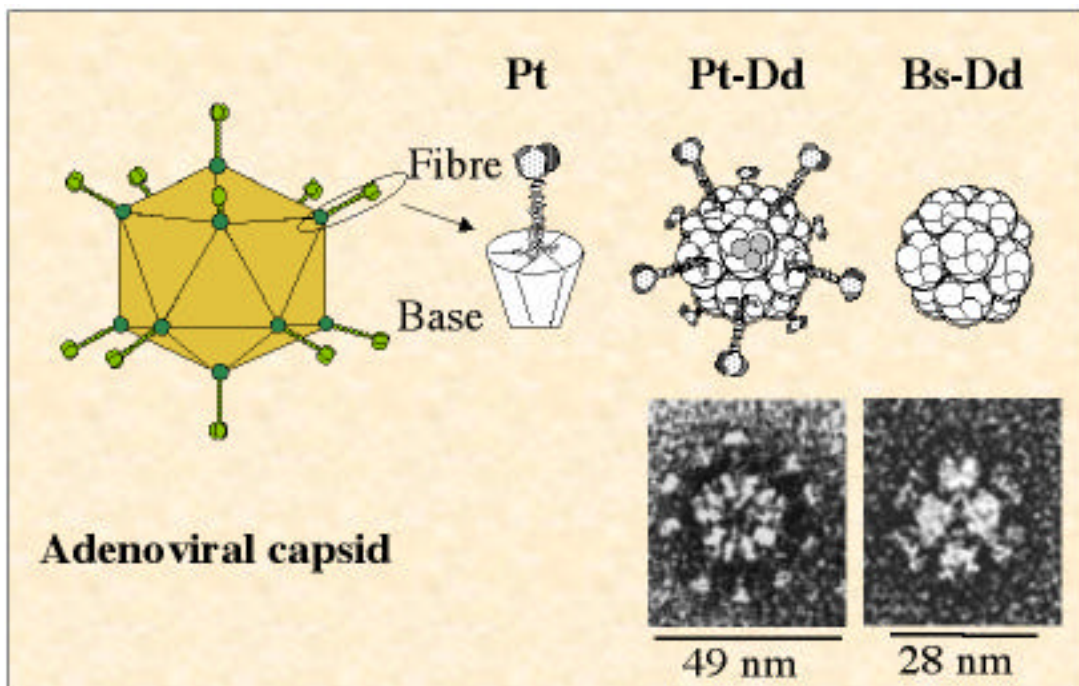
Figure 2: Adenovirus pentons and dodecahedron. Diagram of the icosahedric adenovirus capsid (left). A non-covalent complex of the fiber and the penton base protein called the penton (Pt) is found at each of the twelve virion vertices. The trimeric fibre is responsible for primary receptor recognition and enables the interaction of the pentameric penton base with cellular integrins. Human Ad3 pentons are capable of interacting together through the penton base and form a highly symmetric complex made of 12 units. The fibre is not required for this process as attested by the formation of both penton dodecahedron (Pt-Dd) and base dodecahedron (Bs-Dd).

A. Transduction peptides

A number of obstacles currently limit the effectiveness of gene therapy. One of the most formidable is the delivery of the desired genes to a sufficient number of target cells to elicit a therapeutic response. Recently, a series of virus-encoded and some regulatory proteins were found to be able to cross biological membranes. For example, peptides derived from the *Drosophila* Antennapedia homeodomain are internalised by cells in culture (Derossi et al, 1994) and transferred to cell nuclei where they can directly and specifically interfere with transcription (Le Roux et al, 1995, Derossi et al, 1996). The HIV-1 Tat protein was reported to be rapidly taken up by the cell *in vitro* where it can specifically transactivate the HIV-LTR (Frankel and Pabo 1988, Green and Loewenstein 1988). The Tat protein is composed of 86 amino acids and contains a highly basic region and a cysteine-rich region. It was found that Tat-derived peptides as short as 11 amino acids are sufficient for transduction of proteins (Fawell et al, 1994, Nagahara et al, 1998). The precise mechanism by which the 11-amino acid transduction domain crosses lipid bilayers was for a long time poorly understood but a recent study demonstrated that Tat or Antenapedia peptide endocytosis was promoted by interaction with cellular glycosaminoglycans (Console et al, 2003). A Tat-galactosidase fusion protein that was delivered efficiently into brain tissue and skeletal muscle *in vivo* has been generated recently (Schwarze et al, 1999). These findings suggest that protein therapies may be successfully developed provided that problems caused by immune response and toxicity that might be associated with long-term expression of novel proteins *in vivo* can be solved.

The herpes simplex virus type 1 tegument protein VP22 was also reported to exhibit a unique property of spreading between neighbouring cells. VP22 is a basic, 38-kDa phosphorylated protein encoded by the viral UL49 gene (Knopf and Kaerner 1980, Elliot and Meredith 1992). The transport of VP22 occurs *via* a mechanism potentially involving actin microfilaments. VP22 is exported from the cytoplasm of expressing cells and imported into neighbouring cells where it accumulates in the nucleus (Elliot et al, 1997). These properties aroused interest in VP22 as a delivery vehicle for therapeutic proteins (Dilber et al, 1999). VP22-directed delivery of proteins could be achieved either by transfection of genes encoding VP22 with a fused target protein gene, or by exogenous application of a protein extract containing VP22-fusion (Elliot et al, 1997).

However, the initial enthusiasm for results obtained with these peptides is tempered by a recent controversy whereby the nuclear homing of such fusion proteins was shown to be an artefact occurring during cell permeabilisation step (Lundberg and Johasson 2001).

B. Protein delivery using Ad dodecahedron

We are convinced that the high endocytotic capacity of adenoviruses can be used for direct protein delivery.

Sub-viral particles, dodecahedra, which retain the endocytotic features of Ad and are devoid of genetic material are ideal candidates for this purpose. The proof of the principle of using Dds for protein delivery has been made with a large multimeric protein (Fender et al, 2003). In this study, a monoclonal antibody against the penton base was shown to be efficiently delivered to cells by Dds. On average about $5,7 \cdot 10^5$ Mabs was found per cell using Pt-Dd vector while the efficiency of Bs-Dd in such transfer was lower. In order to attach other proteins to Dd, we are currently developing a system based on WW domains. Indeed, WW domains were found to interact with Ad penton base protein, which is a building block of Dd (Galinier et al, 2003). These domains, containing a linear sequence of about 35 amino-acids including two conserved tryptohanes (W), are known to interact with PPxY motifs in partner proteins (Sudol et al, 1995) and two such motifs are conserved in penton base sequences. In a novel study, we have shown that three WW domains fused in tandem to any protein enable fusion protein attachment to Dds and its subsequent delivery into human cells (**Figure 3**, manuscript in preparation). The use of WW domains as an adaptor to attach the protein of interest to our particles makes of Dds a versatile vector for proteins delivery. The efficiency of this new system is surprisingly high with an average of 10^7 WW-fused proteins imported per cell. Moreover, contrary to the results obtained for Mabs delivery with Dd, a comparable amount of protein is delivered by both Pt-Dd and Bs-Dd showing that the WW domain does not neutralize our vectors.

III. Conclusion

Its remarkable penetration efficacy has made adenovirus one of the most used gene therapy vectors. Several different types of rAds vectors have been designed, helped by the available knowledge of Ad genetics. The major problem with rAd vectors, their immunogenicity, has been at least partially overcome with the appearance of gutless rAd devoid of viral coding sequences. The alternative approach that benefits from virus endocytotic efficacy without the viral genome is to use the adenovirus capsid protein responsible for viral internalisation. Several studies have reported that the Ad penton base alone or penton base-derived dodecameric particle can be modified to attach plasmid DNA thus leading to transgene expression *in vitro*.

Very recently, another therapeutic approach based on direct protein delivery has appeared. Obviously, this kind of approach cannot be used for applications, like hereditary diseases, that require a sustained protein activity. However, it can be used in a particular therapeutic window where a temporary but massive protein delivery is sufficient. Among the possible applications of protein transduction, cancer therapy with toxins or apoptotic proteins would be one of the major challenges. However, the most promising uses for this new technology are *ex vivo* applications. In this vein, the delivery of antigens to prime dendritic cells for cancer vaccination or the delivery of pro-proliferating proteins to expand primary cells *in*
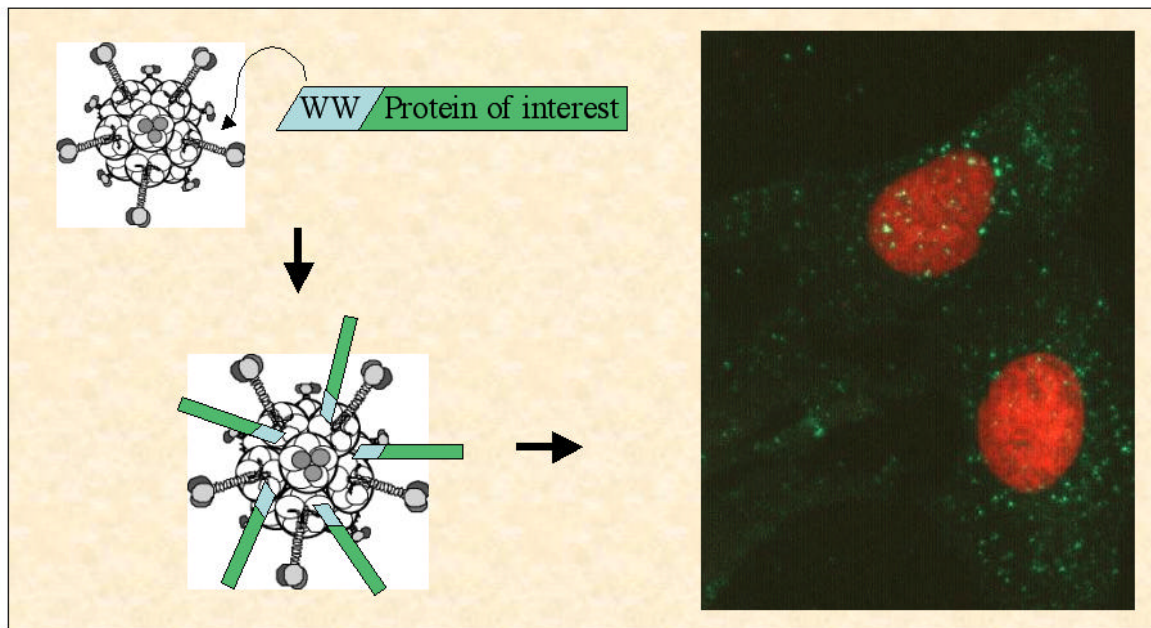
Figure 3: WW motifs can be use as a universal adaptor. The protein to be delivered to the cell is fused with WW domains to permit its attachment to the dodecahedron vector. The resulting complex is efficiently delivered into the cell as reflected by the green immuno-fluorecence detection of the protein of interest in HeLa cells (nuclei are counterstained in red)

vitro before a safe re-injection to the patient could be considered. Once again, Ad-derived vectors like the Ad3 dodecahedron could play an important role in this restricted but valuable area.

References

Bal HP, Chroboczek J, Schoehn G, Ruigrok RW, Dewhurst S. **(2000)** Adenovirus type 7 penton purification of soluble pentamers from Escherichia coli and development of an integrin-dependent gene delivery system. **Eur J Biochem** 267, 6074-81

Console S, Marty C, Garcia-Echeverria C, Schwendener R, Ballmer-Hofer K. **(2003)** Antennapedia and HIV transactivator of transcription (TAT) "protein transduction domains" promote endocytosis of high molecular weight cargo upon binding to cell surface glycosaminoglycans. **J Biol Chem** 278, 35109-14.

Crouzet J, Naudin, L., Orsini C, Vigne E, Ferrero L, Le Roux A, Benoit P, Latta M, Torrent C, Branellec D, Denefle P, Mayaux JF, Perricaudet M, Yeh P. **(1997)** Recombitional construction in E.coli of infectious adenoviral genomes. **Proc Natl Acad Sci** 94, 1414-1419.

Dedieu JF, Vigne E., Dedieu JF, Vigne E, Torrent C, Jullien C, Mahfouz I, Caillaud JM, Aubailly N, Orsini C, Guillaume JM, Opolon P, Delaere P, Perricaudet M, Yeh P. **(1997)** Long term delivery into the livers of immunocompetent mice with E1 /E4 defective adenoviruses. **J.Virol** 71, 4626-4637.

Derossi, D., Calvet, S., Trembleau, A., Brunissen, A., Chassaing, G, Prochiantz, A. **(1996)** Cell internalization of the third helix of the Antennapedia homeodomain is receptor-independent **J. Biol. Chem** 271, 18188-18193

Derossi, D., Joliot, A. H., Chassaing, G. **(1994)** The third helix of the Antennapedia homeodomain translocates through biological membranes **J. Biol. Chem**. 269, 10444-10450.

Dilber, M. S., Phelan, A., Aints, A., Mohamed, A. J., Elliott, G., Edvard Smith, S. C. I., O'Hare, P. **(1999)** Intercellular delivery of thymidine kinase prodrug activating enzyme by the herpes simplex virus protein, VP22. **Gene Ther**. 6, 12-21

Do Thi NA, Saillour P, Ferrero L, Dedieu JF, Mallet J, Paunio T. **(2004)** Delivery of GDNF by an E1,E3/E4 deleted adenoviral vector and driven by a GFAP promoter prevents dopaminergic neuron degeneration in a rat model of Parkinson's disease. **Gene Ther,** in press.

Elliott, G. D., Meredith, D. M. **(1992)** The herpes simplex virus type 1 tegument protein VP22 is encoded by gene UL49. **J. Gen. Virol.** 73, 723-726

Elliott, G., O'Hare, P. **(1997)** Intercellular trafficking and protein delivery by a herpesvirus structural protein. **Cell** 88, 223-233

Fawell, S., Seery, J., Daikh, Y., Moore, C., Chen, L. L., Pepinsky, B., Barsoum, J. **(1994)** Tat-mediated delivery of heterologous proteins into cells. **Proc. Natl. Acad. Sci** 91, 664-668

Fender P, Ruigrok RW, Gout E, Buffet S, Chroboczek J. **(1997)** Adenovirus dodecahedron, a new vector for human gene transfer. **Nat Biotechnol** 15, 52-6

Fender P, Schoehn G, Foucaud-Gamen J, Gout E, Garcel A, Drouet E, Chroboczek J. **(2003)** Adenovirus dodecahedron allows large multimeric protein transduction in human cells. **J Virol**. 77, 4960-4.

Frankel A. D, Pabo, C. O. **(1988)** Cellular uptake of the tat protein from human immunodeficiency virus **Cell** 55, 1189-1193

Galinier R, Gout E, Lortat-Jacob H, Wood J, Chroboczek J. **(2002)** Adenovirus protein involved in virus internalization recruits ubiquitin-protein ligases. **Biochemistry** 41, 14299-305

Gao GP, Yang Y, Wilson JM. **(1996)** Biology of adenovirus vectors with E1 and E4 deletions for liver-directed gene therapy. **J. Virol** 70, 8934-43

Green, M, Loewenstein, P. M. **(1988)** Autonomous functional domains of chemically synthesized human immunodeficiency virus tat trans-activator protein **Cell** 55, 1179-1188

Knopf, K. W., Kaerner, H. C. **(1980)** A herpes simplex virus type 1 mutant with a deletion in the polypeptide-coding sequences of the ICP4 gene **J. Gen. Virol**. 46, 405-414

Le Roux, I., Duharcourt, S., Volovitch, M., Prochiantz, A. and Ronchi, E. **(1995)** Promoter-specific regulation of gene expression by an exogenously added homedomain that promotes neurite growth **FEBS Lett.** 368, 311

Lundberg M, Johansson M.. **(2001)** Is VP22 nuclear homing an artefact? **Nat Biot** 19, 713-314

Medina-Kauwe LK, Kasahara N, Kedes L. **(2001)** 3PO, a novel nonviral gene delivery system using engineered Ad5 penton proteins. **Gene Ther** 8, 795-803.

Medina-Kauwe LK, Maguire M, Kasahara N, Kedes L. **(2001)** Nonviral gene delivery to human breast cancer cells by targeted Ad5 penton proteins. **Gene Ther** 8, 1753-61

Morral N, O'Neal W, Rice K, Leland M, Kaplan J, Piedra PA, Zhou H, Parks RJ, Velji R, Aguilar-Cordova E, Wadsworth S, Graham FL, Kochanek S, Carey KD. **(1999)** Administration of helper-dependent adenoviral vectors and sequential delivery of different vector serotype for long-term liver-directed gene transfer in baboons. **Proc Natl Acad Sci**, 12816-21

Nagahara, H., Vocero-Akbani, M. A., Snyder, E., Ho, A., Latham, G. D., Lissy, A. N., Becker-Hapak, M., Ezhevsky, A. S., Dowdy, F. S. **(1998)** Transduction of full-length TAT fusion proteins into mammalian cells: TAT-p27Kip1 induces cell migration **Nat. Med.** 4, 1449-1452

Norrby E **(1966)** The relationship between the soluble antigens and the virion of adenovirus type 3. II. Identification and characterization of an incomplete hemagglutinin. **Virology** 4, 608-17.

Parks RJ, Chen L, Anton M, Sankar U, Rudnicki MA, Graham FL. **(1996)** A helper-dependent adenovirus vector system: removal of helper virus by Cre-mediated excision of the viral packaging signal. **Proc Natl Acad Sci** 93, 13565-70

Pomeranz, L, Blaho, J. **(1999)** Modified VP22 localizes to the cell nucleus during synchronized herpes simplex virus type 1 infection **J. Virol.** 73, 6769-6781

Qin L, Ding Y, Pahud DR, Robson ND, Shaked A, Bromberg JS. **(1997)**. Adenovirus-mediated gene transfer of viral interleukin-10 inhibits the immune response to both alloantigen and adenoviral antigen. **Hum Gene Ther** 8, 1365-74.

Schoehn G, Fender P, Chroboczek J, Hewat EA. **(1996)** Adenovirus 3 penton dodecahedron exhibits structural changes of the base on fibre binding. **EMBO J** 15, 6841-6

Schwarze, R. S., Ho, A., Vocero-Akbani, A., Dowdy, F. S. **(1999)** In vivo protein transduction: delivery of a biologically active protein into the mouse **Science** 385, 1569-1572.

Sudol M, Chen HI, Bougeret C, Einbond A, Bork P. **(1995)** Characterization of a novel protein-binding module--the WW domain. **FEBS Lett**. 369, 67-71. Review.

Wang Q, Greenburg G, Bunch D, Farson D, Finer MH. **(1997)** Persistent transgene expression in mouse liver following in vivo gene transfer with a delta E1/delta E4 adenovirus vector. **Gene Ther** 4, 393-400

Yang Y, Nunes FA, Berencsi K, Furth EE, Gonczol E, Wilson JM. **(1994).** Cellular immunity to viral antigens limits E1-deleted adenoviruses for gene therapy. **Proc Natl Acad Sci** 91, 4407-4411.

Yeh P, Dedieu JF, Orsini C, Vigne E, Denefle P, Perricaudet M **(1996).** Efficient dual transcomplementation of adenovirus E1 and E4 regions from a 293-derived cell line expressing a minimal E4 functional unit. **J. Virol** 70, 559-65.

Dr. Pascal Fender

VIROLOGY

Heparan sulfate proteoglycan mediates the selective attachment and internalization of serotype 3 human adenovirus dodecahedron

Romain R. Vivès, Hugues Lortat-Jacob, Jadwiga Chroboczek, and Pascal Fender[*]

Institut de Biologie Structurale, CNRS-CEA-UJF, 38027 Grenoble, France

Abstract

During adenovirus type 3 (Ad3) infection cycle, the penton (Pt) of the viral capsid, a noncovalent complex of fiber and penton base proteins, is produced in large excess and self-assembles to form a highly organized dodecahedral structure, termed dodecahedron (Dd). The physiological role of these particles is poorly understood, but we have recently reported that they can penetrate cells with high efficiency and thus may constitute an attractive tool for gene or protein delivery approaches. Surprisingly, Dd displayed the ability to enter cells non-permissive to Ad3, suggesting the existence of additional internalization modes. In this study, we show that Ad3 Dd binds to cell surface heparan sulfate (HS) through high affinity interaction with the penton base. Furthermore, binding to HS was found to be the prerequisite for a novel and Dd specific entry pathway that could not be used by Ad3. Overall, these data provide new insights in the possible role of Dd during viral infection and potential therapeutic applications.
© 2004 Elsevier Inc. All rights reserved.

Keywords: Heparan sulfate; Adenovirus dodecahedron; Receptor; Cell attachment; Internalization; Vector

Introduction

Heparan sulfate proteoglycans (HSPGs) are glycoproteins ubiquitously expressed at the surface of mammalian cells and in extracellular matrices. During the past 15 years, progress in the study of these molecules has highlighted their central role in most biological processes including cell proliferation, cell adhesion, chemoattraction, inflammation, wound healing, coagulation, matrix assembly, embryo development ... (Delehedde et al., 2002; Esko and Selleck, 2002; Gallagher, 2001; Iozzo and San Antonio, 2001). HSPG properties are mostly mediated by the O-linked heparan sulfate (HS) polysaccharide chains present on the protein core that bind and regulate a wide range of proteins through motifs of specific saccharide sequence (Lindahl et al., 1998). Binding of proteins to HS serves a range of

functional purposes, from simple immobilization and localization to specific regulation of signal transduction, as initially demonstrated for basic fibroblast growth factor (bFGF) signaling (Lundin et al., 2000; Pye et al., 1998). Besides its physiological functions, it is widely recognized that HS binding properties can also be exploited by a great number of pathogen microorganisms, particularly viruses, for attachment to the host cell surface (Sawitzky, 1996; Spillmann, 2001). Binding to HS is generally believed to promote infectivity by increasing local concentration of pathogens at the cell surface and thus favoring access to specific entry receptors. Hence, HS can play the role of a viral attachment receptor, as described for adenoviruses type 2 and 5 (Dechecchi et al., 2000, 2001), adeno-associated parvovirus-2 (AAV-2) (Summerford and Samulski, 1998), several members of the herpes virus family (Shukla and Spear, 2001), Flavivirus including hepatitis C (Germi et al., 2002) and Dengue (Chen et al., 1997) virus, Sindbis virus (Byrnes and Griffin, 1998) or human T cell leukemia virus type-1 (Q. Sattentau, personal communication). However, several studies have recently highlighted a deeper role of HS in infection mechanisms, for which a direct participation in viral entry was demonstrated. This has been described at least for herpes simplex virus-1 (HSV-1), for which viral fusion with the cell membrane is triggered by the binding of

the viral glycoprotein D to rather rare HS motifs, in cooperation with other viral envelope proteins (Shukla et al., 1999; Spear et al., 2000). Finally, HS expressed on nonpermissive cells can capture, protect, and transmit viruses such as HIV, with increased infectivity, to cells permissive for the replication. This kind of novel class of in-trans receptor may have a deep impact on the tropism and dissemination of the virus in vivo (Bobardt et al., 2003).

Human adenoviruses (Ads) are a large family of non-enveloped viruses responsible for respiratory, ocular, and enteric infections. They share a common structural organization, in which the 36 kb dsDNA genome is concealed within a 90-nm icosahedral capsid composed of three major proteins: the trimeric hexon, the pentameric base, and the trimeric fiber. The last two form a noncovalent complex called the penton (Pt), which protrudes from each of the 12 vertices of the capsid (Ginsberg et al., 1966; Valentine and Pereira, 1965).

Ad penton is the major structural element responsible for viral attachment and entry into host cells. It has been demonstrated that purified penton alone was able to enter human epithelial cells (Fender et al., 1997; Hong et al., 1999). The infection process involves a first interaction of the fiber with a high affinity primary receptor that will facilitate subsequent binding of the penton base to cellular integrins and eventually trigger endocytosis (Mathias et al., 1994; Wickham et al., 1993). For most Ads, a 42-kDa protein of tight junctions, termed coxsackievirus and adeno-virus receptor (CAR), is the primary receptor for infection (Bergelson et al., 1997). Members of Ad subgroup B, including adenovirus type 3 (Ad3), do not use CAR (Roel-vink et al., 1998; Segerman et al., 2003). Recently, CD46 has been identified as the primary receptor used by several subgroup B Ads, but not Ad3 (Gaggar et al., 2003). How-ever, this latter observation concerning Ad3 appears to be challenged by a recent work from another group (Greber and Hemmi, personal communication, manuscript submitted).

During Ad infectious cycle, free pentons are produced in excess and released with the virus progeny. The physiolog-ical relevance of this remains unclear, but a recent study suggested that free penton proteins enhanced infectivity by disturbing tight junctions and thus favored virus spreading (Walters et al., 2002). In contrast with most Ads, expression of Ad3 penton resulted in the formation of a highly organized dodecahedral structure (49 nm in diameter), in which the 12 penton base proteins interact with each other (Fig. 1) (Schoehn et al., 1996). Although its physiological role is not known, this complex, termed penton-dodecahe-dron (Pt-Dd), displayed high efficiency ability to bind and enter human epithelial cells, thus indicating that no other Ad protein was required during early endocytosis.

We have recently demonstrated that Ad3 Pt-Dd could constitute a good tool for gene or protein delivery (Fender et al., 1997, 2003). However, potential applications require the clarification of the mechanisms involved in cell attachment and entry. Intriguingly, we found that the expression of Ad3
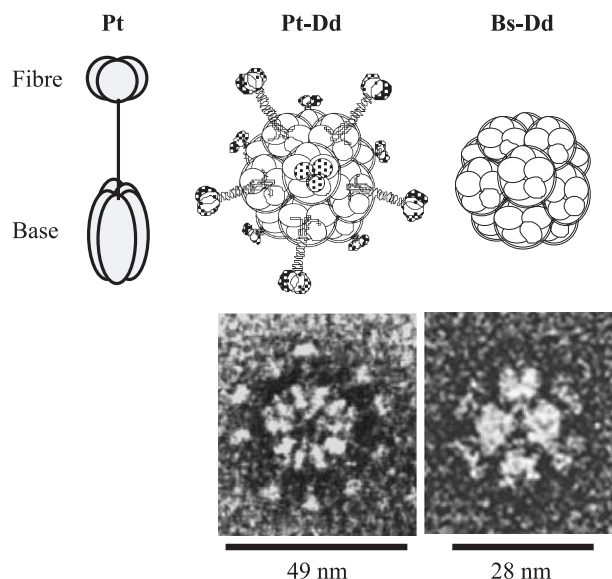
Fig. 1. Structure of Ad3 penton and Ad3 Dds. Schematic representation of Ad3 penton (Pt), which comprises the pentameric penton base (Bs) and the trimeric fiber. Self-association of Pt or Bs results in the formation of highly organized dodecahedral complexes, termed, respectively, Pt-Dd and Bs-Dd. The structure of Pt-Dd and Bs-Dd is represented schematically, along with the respective electron microscopy pictures.

penton base alone also yielded dodecahedral structures, termed base-dodecahedron (Bs-Dd, see Fig. 1). These smaller particles (28 nm in diameter) could also get into human cells, though with lower efficiency than Pt-Dd, indicating that the fiber plays an important role for cell attachment or entry (Fender et al., 2003), but that the existence of alternative internalization pathways had to be considered. In this study, we provide evidence that HS is a receptor involved in binding and entry of Dd into cells.

Results

Ad3 Dds use cell surface GAGs for attachment to CHO cells

To study novel Dd internalization pathways, we first investigated the ability of Ad3 Dd to bind to the surface of Ad3 nonpermissive cells, that is, cells that would not express Ad3 primary receptor. CHO-K1 cells were incubat-ed with Pt-Dd at 4 °C and in presence of NaN_3 to prevent Dd internalization. After washing, bound dodecahedron was detected by FACS analysis, using a set of anti-Dd primary and FITC-conjugated secondary antibodies. No background was observed for control assays performed in absence of primary antibody (data not shown). Results showed that Pt-Dd efficiently bound to CHO-K1 cell surface, as indicated by a shift of the cell-associated fluorescence peak (Fig. 2A). However, no Dd binding could be detected on CHO-2241 cells, a mutant clone defective in glycosaminoglycan (GAG) synthesis, at both concentrations tested (Fig. 2B). These data suggested that Dd interaction with the CHO cell surface

A

B

Fig. 2. FACScan analysis of Pt-Dd binding to CHO-K1 and CHO-2241 cells. CHO-K1 (A) and CHO-2241 (B) cells were incubated at 4 °C with 0, 25, or 120 nM of Pt-Dd (dotted, gray, and black lines, respectively), followed by successive incubations with anti-Pt-Dd primary antibody and FITC-conjugated secondary antibody. FL1-H: fluorescence intensity.
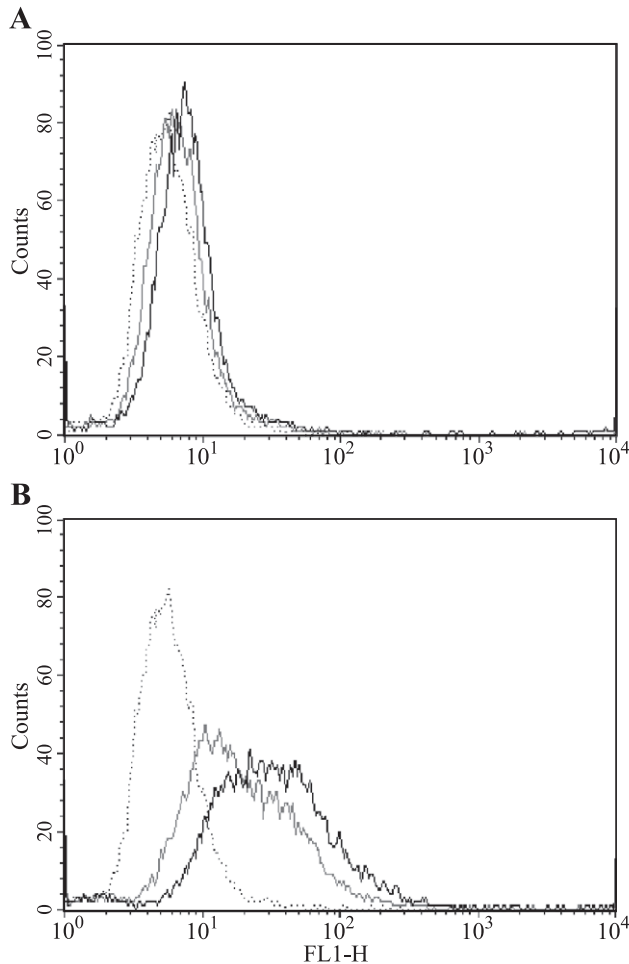
involved GAGs, and that no other appropriate attachment receptors were present on these cells. To confirm such hypothesis, CHO-K1 and CHO-2241 cells were incubated with FITC-labeled Dd and observed by laser confocal microscopy (Fig. 3). On CHO-K1 cells, a green halo resulting from bound Dd could be clearly seen at the cell surface (Fig. 3A). In contrast, no cell-associated green fluorescence could be distinguished on CHO-2241 cells, indicating absence of Dd attachment. Interestingly, similar observations were made for experiments performed with FITC-labeled Bs-Dd. This indicated that Dd binding to CHO cells was fiber independent. Such a mechanism is distinct from the putative Ad3 primary attachment process, which by analogy with subgroup C Ads, should require the fiber. Finally, the involvement of GAGs suggested by the above data was confirmed by competition assays with exogenous heparin. Preincubation of Dd with the polysaccharide before cell exposure indeed abrogated Dd attachment, with a dramatic reduction observed at heparin concentration as low as 0.01 µg/ml (Fig. 3B).

Ad3 Dd binding to GAGs is restricted to HS and heparin

The nature of cell surface GAGs actually involved in Dd binding was then determined, using filter binding analysis. Pt-Dd was incubated with biotinylated heparin (Hpb), after which the reaction mixture was drawn through a nitrocellulose membrane. Free Hpb was washed away, while Pt-Dd-bound Hpb remained trapped on the membrane and was detected by exposing the blots to peroxydase conjugated extravidin, followed by ECL detection (Fig. 4). The absence of signal for the negative control (Fig. 4, top lane, row 1) confirmed that free heparin was not retained by the nitrocellulose membrane. In contrast, binding of Hpb to Pt-Dd was clearly shown by a spot of strong density (Fig. 4, top lane, row 3). The Pt-Dd/Hpb interaction could be inhibited with an excess of non-biotinylated heparin or HS resulting, respectively, in total or severe signal loss (Fig. 4, top lane, rows 4 and 5, respectively). However, chondroitin 4-*O*-sulfate (CS-A), Dermatan sulfate (DS), and chondroitin 6-*O*-sulfate (CS-C) failed to compete with Hpb (Fig. 4, top lane, rows 6–8), indicating that Dd GAG-binding properties were restricted to heparin and HS. Experiments performed with Bs-Dd yielded a similar binding pattern (Fig. 4, bottom lane), with spots of equivalent intensity, thus further supporting a location of the heparin/HS binding site on the base protein of Ad3 Dd.

Ad3 Dds bind heparin with high affinity and form very stable complexes

Ad3 Dd interaction with heparin was then studied, using surface plasmon resonance (spr) analysis. For each sample, a set of sensorgrams was obtained by injection of a range of Pt-Dd or Bs-Dd concentrations (from 0 to 60 µg/ml) over both heparin-immobilized and negative control surfaces, and on-line subtraction of the recorded signals (Figs. 5A and 5B, respectively). Sensorgrams indicated potent interaction of both Pt-Dd and Bs-Dd to heparin, with significant signal being observed even at the lowest concentration tested (2.5 µg/ml, i.e., 0.52 and 0.69 nM, for Pt-Dd and Bs-Dd, respectively).

Preliminary kinetic analysis of the sensorgrams revealed a complex binding process, which could not be fitted to any obvious model of ligand–receptor interaction (data not shown). This is in agreement with the complexity of the Dd structure, in which the 12 penton bases, each composed of 5 identical monomers, display 60 potential heparin binding sites and thus could bind heparin in many different ways. Such multivalency is likely to cause strong avidity. Kinetic analysis of the sensorgram dissociation phases, using the BIAevaluation 3.1 software, yielded apparent dissociation rate constants (k_{off}) of 5.6×10^{-5} and 9.3×10^{-5} s^{-1} for Pt-Dd and Bs-Dd, respectively, indicating that Ad3 Dd formed highly stable complexes with heparin. To analyze the Dd–heparin interaction in more detail, we generated data in which the association phase was allowed to

A

B
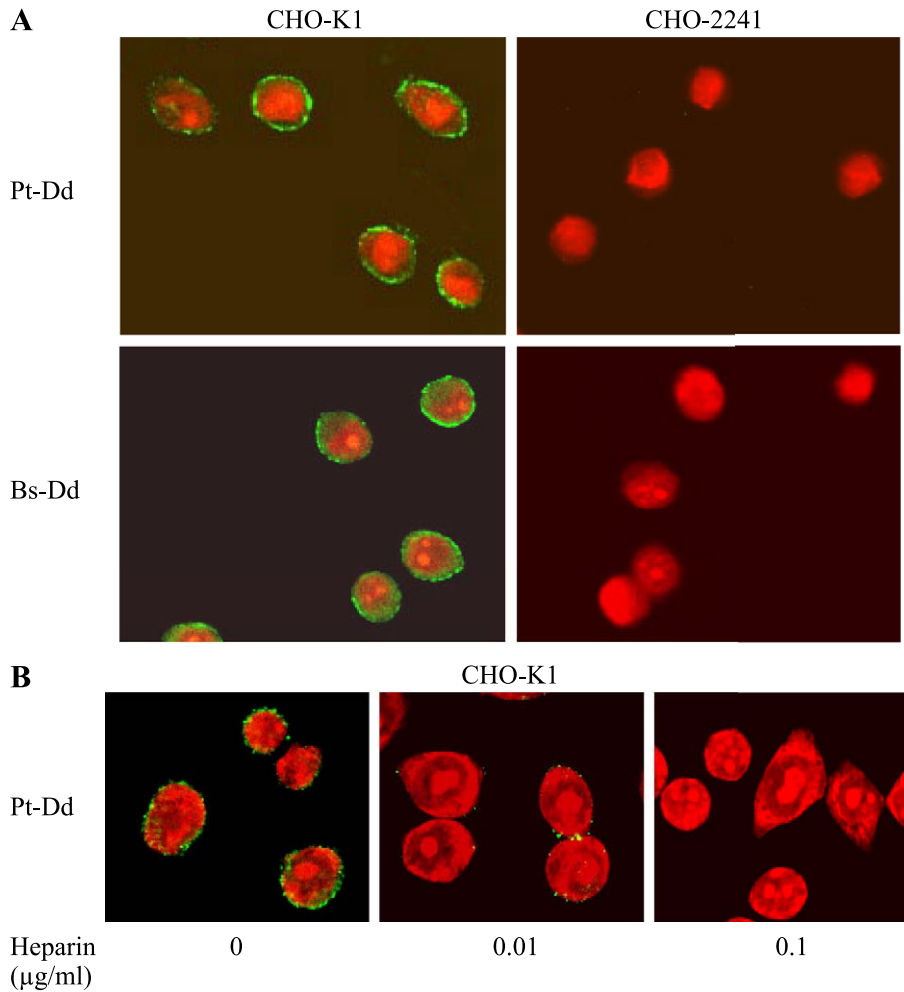
Fig. 3. Analysis of Dd binding to CHO-K1 and CHO-2241 cells by confocal microscopy. (A) CHO-K1 and CHO-2241 cells were incubated for 2 h at 4 °C with 1 nM of FITC-labeled Pt-Dd or Bs-Dd (green signal). After permeabilization, cell nuclei were counter-stained with propidium iodide (red signal). (B) Before CHO-K1 cell incubation, FITC-labeled Pt-Dd (1 nM) was pre-incubated with heparin (0, 0.01, or 0.1 μg/ml) for 30 min at room temperature.

proceed to equilibrium (20 min injections, Figs. 5A and 5B). Equilibrium data were extracted from sensorgrams that displayed a clear binding plateau, that is, for concentrations

Fig. 4. GAG specificity of Dd interaction. Filter binding analysis of Dd/GAG interaction. Pt-Dd/Bs-Dd were incubated with (rows 3–8) or without (row 2) biotinylated heparin (Hpb), in absence (row 3) or presence of a 10-fold excess of non-biotinylated competing GAG, including Hp, HS, CS-A, DS, and CS-C (rows 4–8, respectively). Negative control (Hpb in absence of Dd) is shown on the top lane, row 1.

of 10 μg/ml and above, and these were plotted according to the Scatchard representation (Figs. 5C and 5D) to provide an affinity value independently of the kinetic aspect of the binding. This confirmed the high affinity of these interactions, with calculated Kd values in the nanomolar range: 0.7 and 1.4 nM for Pt-Dd and Bs-Dd, respectively.

Cell surface HS is required for Ad3 Dd entry into CHO cells

Having highlighted the critical role of HS in Dd cell attachment, we then investigated a possible involvement in the cell internalization process. Here, incubation of CHO-K1 cells with FITC-Dd was performed in PBS for 1 h at 37 °C to allow internalization. Cell observation by confocal microscopy showed a very bright and punctuated intracellular signal, indicating that both Pt-Dd and Bs-Dd could efficiently enter CHO cells (Figs. 6A and 6B, respectively), despite absence of Ad3 primary receptor. Furthermore, Pt-Dd and Bs-Dd showed no difference in the endocytosis efficiency, thus supporting that this process
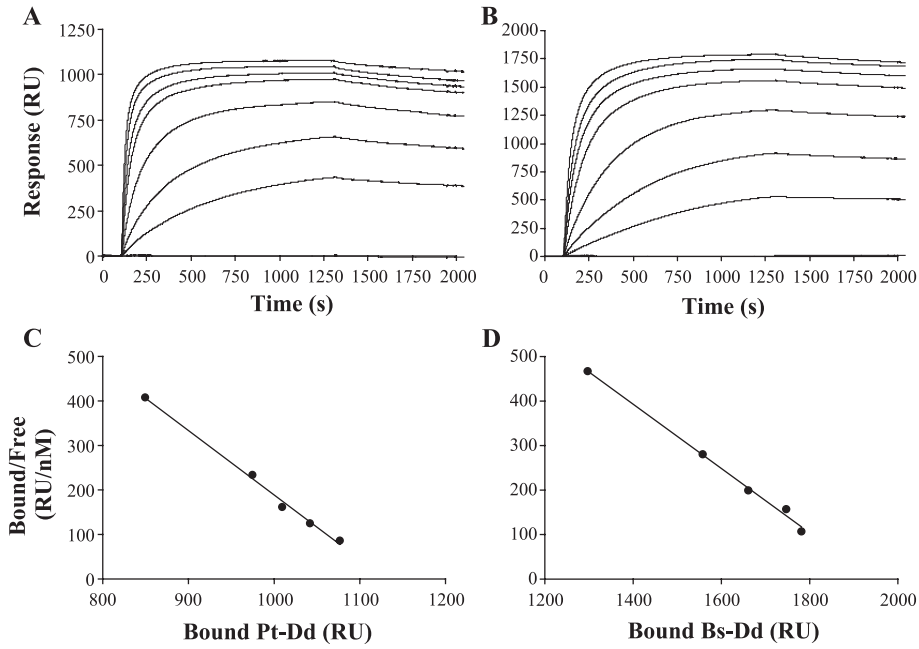
Fig. 5. Analysis of Pt-Dd and Bs-Dd binding to heparin by spr. Sensorgrams were obtained by injections of Pt-Dd (A) and Bs-Dd (B) at 0, 2.5, 5, 10, 20, 30, 40 and 60 μg/ml onto a heparin immobilized sensorchip. Data for which equilibrium was achieved were used for Scatchard analysis of the interaction (C and D, respectively).

was independent of the presence of the fiber. Addition of heparin (10 μg/ml) or cell treatment with chlorate that blocks GAG sulfation totally abolished cell internalization of both Pt-Dd (Figs. 6C and 6D, respectively) and Bs-Dd (data not shown). These results demonstrate that Dd binding to HS is a prerequisite for endocytosis of these particles into CHO cells.
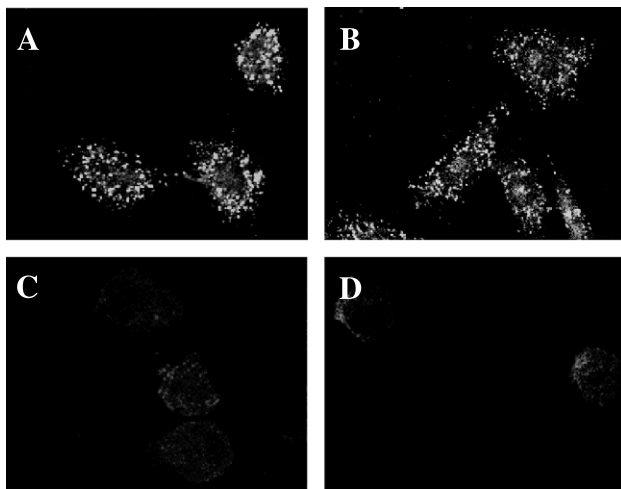
Fig. 6. HS-dependent Dd entry into Ad3 nonpermissive CHO-K1 cells. FITC-labeled Pt-Dd (A) and Bs-Dd (B) were incubated with HeLa cells for 1 h at 37 °C. After washing and fixation with 2% PFA, cells were observed by laser confocal microscopy. Pt-Dd internalization was inhibited by either pre-incubating Dd with 10 μg/ml of heparin (C) or treating cells with chlorate (D).
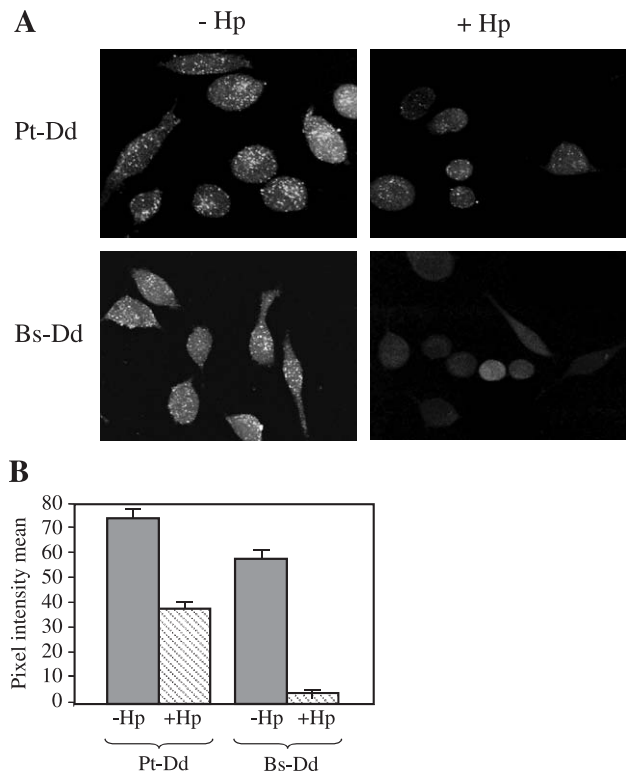
Fig. 7. Role of HS for Dd entry into Ad3 permissive HeLa cells. FITC-labeled Dd (1 nM) was pre-incubated or not with 10 μg/ml of heparin (Hp), then incubated with HeLa cells at 37 °C. After washing and fixation with 2% PFA, cells were observed by laser confocal microscopy (A). Cell fluorescence was quantified by photo-counting. The means of pixel intensity were determined from 12 individual cells (B).

HS constitutes an alternative pathway for Dd entry into Ad3 permissive HeLa cells

The role of HS in Dd cell attachment and internalization was defined on CHO-K1 cells, which are not the natural target of Ad3. To study this process in a more physiological context, we repeated our direct fluorescence assays on Ad3 permissive HeLa cells. FITC-Dd were incubated with HeLa cells for 1 h at 37 °C, before cell washing and fixation. In agreement with our previous study (Fender et al., 2003), results indicated that both Pt-Dd and Bs-Dd could enter HeLa cells, with slightly lower yields for the latter (Fig. 7). Addition of heparin resulted in a twofold reduction of Pt-Dd endocytosis, and a complete abrogation of Bs-Dd entry, as shown by cell fluorescence quantification (Fig. 7B). These data support the existence on HeLa cells of a fiber-independent, HS-mediated Dd internalization pathway, which is exclusively used by Bs-Dd and accounts for about half of Pt-Dd endocytosis.

Discussion

Due to its high ability to enter cells, Ad3-Dd has been thoroughly studied as a putative vector for gene and protein delivery. The advantage of such a structure is that it only comprises two distinct proteins, the base and the fiber, and is devoid of foreign nucleic acid. However, the mechanism of Dd cell attachment and entry remains poorly understood. By analogy with subgroup C adenoviruses, it is thought that Ad3 fiber head binds to a cell surface primary receptor, which will in turn facilitate interaction of Ad penton base RGD motif with $\alpha v \beta 3$ and $\alpha v \beta 5$ integrins and trigger subsequent endocytosis (Wickham et al., 1993). However, our previous data had already suggested the existence of a Ad3 primary receptor independent internalization pathway, as fiber devoid Bs-Dd was still able to bind to and enter cells, though to a lesser extent than Pt-Dd (Fender et al., 2003). Here, we provide evidence of a novel Dd cell attachment pathway, in which HS promotes binding and is required for cell entry.

The present study first showed that both Bs-Dd and Pt-Dd could bind to non-permissive CHO-K1 cells (Figs. 2 and 3). Interestingly, binding occurred with a similar efficiency for both Dd forms, suggesting that the fiber was not involved in this interaction. GAGs were identified as the docking site, because Dd attachment to CHO-K1 cells could be efficiently inhibited by competition with free heparin (Fig. 3B) and that both Bs-Dd and Pt-Dd failed to bind to GAG-deficient CHO-2241 cells (Fig. 3A). GAG-specific requirements for Ad3 Dd cell attachment were then investigated by filter binding analysis (Fig. 4). Our results indicated that both Bs-Dd and Pt-Dd bound to the biotinylated heparin with similar efficiency, thus further supporting the view that the base only participates to the binding. Competition performed with non-biotinylated GAGs showed

that only heparin and HS could significantly inhibit the interaction, although addition of CS-A, DS, or CS-C had no effect. These results demonstrated that the base protein of Dd specifically bound to HS amongst cell surface GAGs.

The Dd/heparin interaction was further characterized by spr analysis. Injections of Pt-Dd and Bs-Dd on a heparin-immobilized surface yielded sensorgrams with very similar features, that is, a strong association with the polysaccharide followed by a very slow dissociation phase (Fig. 5). Due to the complexity of the binding reaction, we did not attempt to fully describe the kinetic aspects of the interaction. However, the very slow dissociation phase observed indicated that the complexes formed were very stable. Kd values could be deduced from Scatchard analysis of the data obtained at the binding equilibrium. Pt-Dd and Bs-Dd bound heparin with similar affinity (0.7 and 1.4 nM, respectively). These particularly high affinities may result from an avidity mechanism caused by the multiplicity of HS binding sites present on the Dd. We recently reported that the trimerization of the Ad2 fiber protein elicited a 25-fold affinity increase for the CAR receptor, this being due to an avidity effect (Lortat-Jacob et al., 2001). Such a phenomenon has also been observed when comparing the binding to heparin of HIV virions and isolated gp120 (unpublished observation). Moreover, the high affinity values measured are consistent with the low heparin concentration (0.01 μg/ml) needed to inhibit Dd cell attachment (Fig. 3B). Interestingly, surface maximum occupancy of Pt-Dd was half that of Bs-Dd (42 and 18 heparin chains per Pt-Dd and Bs-Dd, respectively), this reflecting the radius differences of Dd particles (49 nm versus 28 nm, see Fig. 1) that may limit the maximum density that could be bound onto the heparin surface.

In addition to cell attachment, our data provided evidence that Dd binding to HS was the prerequisite of a novel cell internalization pathway. Such process involved interaction of the polysaccharide with the penton base, as both Pt-Dd and Bs-Dd failed to enter GAG-deficient CHO-2241 cells, but could penetrate CHO-K1 cells with similar efficiency (Fig. 6). HS requirement was further demonstrated by blockage of Dd cell entry, using exogenous heparin, or cell treatment with chlorate that prevents endogenous GAG sulfation (Cardin and Weintraub, 1989). This HS-dependent internalization pathway could be clearly distinguished from the conventionally assumed Ad3 cell entry process that required the binding of the fiber to the Ad3 primary receptor, as shown by our results on Dd entry into Ad3 permissive HeLa cells (Fig. 7). On these cells, preincubation of Dd with exogenous heparin completely abolished attachment and entry of fiber devoid Bs-Dd, indicating an exclusive use of the HS-dependent pathway, and significantly reduced the internalization of Pt-Dd, which nevertheless retained a partial ability to enter cells, most likely through the Ad3 primary receptor pathway. The mechanisms by which HS initiates Dd cell entry remain unclear. A first hypothesis is that HS could facilitate the binding of Dd with

entry receptors, such as integrins. The structural basis of HS interaction with the penton base has not been investigated yet. However, analysis of the protein sequence revealed several positively charged arginine and lysine residues gathered in clusters typical of HS binding sites. Interestingly, one of this cluster, $K_{337}QKR_{340}$, is found near the $R_{329}GD_{331}$ sequence believed to interact with integrins. The close proximity of these two putative binding sites could suggest that HS and integrins may act in synergy to trigger cell internalization. This would be in agreement with our data showing that αv integrins, which are expressed at the surface of CHO-2241 cells, could not mediate Dd attachment or entry on their own. Another hypothesis is that HSPGs themselves could mediate internalization of Dd, as observed for several ligands, including growth factors and lipoproteins (Reiland and Rapraeger, 1993; Williams and Fuki, 1997). Interestingly, work from Fuki et al. (1997) reported that this endocytosis process could be triggered by the clustering of HSPG transmembrane and cytoplasmic domains. For Dd, HSPG clustering is likely to be favored by the multiplicity of HS binding sites at their surface and thus could permit efficient endocytosis of these particles.

In contrast to the high affinity binding of Ad3 Dd to HS, the Ad3 virus does not interact with either heparin or HS (Dechecchi et al., 2000 and unpublished data). Such a discrepancy raises several questions from a structural and a functional point of view. Pt-Dd and Ad3 viral capsid both comprise 12 pentons protruding in a similar manner from the particle. However, in the former, pentons directly interact with each other, while they are separated by hexons on the virus. It is possible that the HS binding site on the penton base is located near the penton–hexon interface, and thus the hexon on the virus partially or fully overlaps HS binding residues. Alternatively, the HS binding site could be created by the penton–penton interface that occurs on the Dd. Such situation has been already described for several dimerized chemokines, for which the HS binding site was formed at the protein–protein interface (Lortat-Jacob et al., 2002). Another hypothesis is that the negatively charged hexon, which is the major component of the viral capsid, but is not found on the Dd, may significantly influence the surface electrostatic potential and thus prevent possible interaction of the base with polyanionic HS. This is supported by data reporting that Ad endocytosis is sensitive to the global charge of the capsid (Arcasoy et al., 1997; Shayakhmetov and Lieber, 2000). Other Ads do use HS for cell attachment. In particular, HS has been recently described as an alternative receptor to CAR for wild-type Ad2/Ad5 (Dechecchi et al., 2000, 2001). In this study, a BBxB consensus motif (Humphries and Silbert, 1988) within the Ad2 fiber shaft sequence was presented as a putative HS binding site. This basic cluster is absent in the Ad3 fiber, suggesting that Ad2 penton and Ad3 Dd interact with HS through distinct binding sites. Pt-Dd is naturally found during the Ad3 replication cycle and in vivo, large amounts of Pt-Dd are released at the cell lysis (Norrby, 1966). The physiological role of Dd during viral infection is still unknown, but its ability to bind to HS, a molecule involved in a huge array of biological functions, is likely to be critical. It has been recently shown that the excess of synthesized Ad2 fiber contributed to virus spreading by disrupting the junctional integrity mediated by CAR (Walters et al., 2002). In addition, the base protein is also known to trigger cell detachment (Boudin et al., 1979), supporting further the ability of penton components to interfere with cell adhesion processes. As HS participates to cell cohesion, its interaction with Ad3 Dd may also be involved in the weakening of cell–cell contacts and contribute to the viral dissemination.

In this study, we have identified HS as a major attachment receptor for Ad3 Dd to the cell surface, and as a trigger for endocytosis through a novel, fiber-independent pathway. Our data highlighted a major divergence between Ad3 and Ad3 Dd cell entry mechanisms that may have an important physiological significance. Clarifying the structural and functional features involved in Ad3 Dd/HS interaction will constitute a major challenge for the understanding of the role played by these particles during viral infection, and for a potential use, as a gene/protein delivery vector.

Material and methods

BIAcore 3000, B1 sensorchip, amine coupling kit, and HBS-EP buffer were purchased from BIAcore AB. FACScan is from Becton Dickinson. EMEM and Ham's F12 medium were from Gibco. Heparin of 9 kDa was a generous gift from Maurice Petitou (Sanofi-Synthélabo). Heparin of 6 kDa and chondroitins sulfate were supplied by Sigma. MRC-600 laser scanning confocal microscope was purchased from BioRad. Tissue culture reagents were from Gibco Lifesciences.

Cell culture

Chinese Hamster Ovary (CHO) cell lines K1 (GAG positive, American Type Culture Collection [ATCC] code CCL-61) and 2241 (GAG negative, pgsB-618, ATCC code CRL-2241) were obtained from the European Collection of Cultured Cells. Cells were cultured at 37 °C, under 5% CO_2 atmosphere, in Ham's F12 (for CHO cells) or EMEM (for HeLa cells), supplemented with 10% fetal calf serum (FCS), penicillin (50 IU/ml), and streptomycin (50 μg/ml). Chlorate treatment was performed by incubation of trypsinized cells for 36 h in EMEM, 2% FCS, 30 mM sodium chlorate (Cardin and Weintraub, 1989).

Production, purification, and labeling of Ad3 Dd

Both Pt-Bs and Bs-Dd were expressed using the baculovirus system. Particles were purified by sucrose density gradient, as previously described (Fender et al., 1997). Dd

(300 nM) were fluorescently labeled by incubation with 1 mM FITC, in 20 mM HEPES, pH 8, for 3 h at 4 °C. Free FITC was removed by dialysis against 20 mM HEPES, 150 mM NaCl, pH 8.

Flow cytometry analysis

Cells (2×10^6/ml) in FACS buffer (PBS, 1% BSA, 0.02% azide, 1 mM EDTA) were incubated with Pt-Dd (25 and 120 nM) for 45 min at 4 °C. After washing with FACS buffer, cells were incubated with primary anti-Dd Ab (1/1000, 1 h at 4 °C in FACS buffer, followed by washing), then with FITC-conjugated secondary antibody (1/200, 1 h at 4 °C in FACS buffer, followed by washing), and analyzed by flow cytometry.

Filter binding assay

The interaction of Ad3 Dd with heparin was analyzed by filter binding assay (Sadir et al., 2001). Ad3 Pt-Dd and Bs-Dd (100 ng) were co-incubated with biotinylated heparin (0.05 µg/ml) in 200 µl of Tris-buffered saline (TBS) for 45 min at room temperature. In competition assays, a 10-fold excess of non-biotinylated GAGs (0.5 µg/ml) was also added. Samples were then drawn through a nitrocellulose membrane using a vacuum-assisted dot-blot apparatus. The membrane was washed twice with 200 µl of TBS and blocked with 5% dry milk in TBS containing 0.05% Tween 20. Protein-bound biotinylated heparin was revealed by incubation of the membrane with extravidin peroxydase (0.5 µg/ml) and enhanced chemiluminescence (ECL) detection reagents, followed by autoradiography.

Heparin/Dd interaction analysis by surface plasmon resonance

Heparin (9 kDa) was biotinylated and immobilized on a B1 BIAcore sensorchip, as described before (Vives et al., 2002). Briefly, two flowcells were prepared by sequential injections of EDC/NHS, streptavidin, and ethanolamine. One of these flowcells served as negative control, while biotinylated heparin was injected on the other one, to get an immobilization level of 80–90 response units (RU). All spr experiments were performed, using HBS-EP buffer (10 mM HEPES, 150 mM NaCl, 3 mM EDTA, 0.005% surfactant P20, pH 7.4), at a flow rate of 10 µl/min. Interaction assays involved 20 min injections of different dodecahedron concentrations (ranging from 0 to 60 µg/ml) over the heparin and negative control surfaces, followed by a 10-min washing step with HBS-EP buffer to allow dissociation of the complexes formed. At the end of each cycle, the heparin surface was regenerated by sequential injections of 0.05% SDS (1 min) and 2 M NaCl (2.5 min). Sensorgrams shown correspond to on-line subtraction of the negative control to the heparin surface signal. Data from sensorgrams that reached binding equilibrium were used for Scatchard analysis.

Confocal microscopy

Cells grown overnight on coverslips (about 10^5 cells/slide) and washed in PBS were incubated with either FITC-labeled Pt-Dd or Bs-Dd (1 nM) for 2 h at 4 °C. For heparin competition assays, Dd were first incubated for 30 min at RT with 0.01 or 0.1 µg/ml of 6 kDa heparin. Cells were then permeabilized with cold methanol for 10 min at −20 °C and cell nuclei counter-stained with propidium iodide (5 µg/ml). For internalization assays, cells were incubated with either Pt-Dd or Bs-Dd (1 nM) in PBS for 1 h at 37 °C. After PBS washes, cells were fixed with 2% paraformaldehyde. Coverslips were then mounted for observation on a microscope slide with 1,4-diazabicyclo-octane.

References

Arcasoy, S.M., Latoche, J.D., Gondor, M., Pitt, B.R., Pilewski, J.M., 1997. Polycations increase the efficiency of adenovirus-mediated gene transfer to epithelial and endothelial cells in vitro. Gene Ther. 4 (1), 32–38.

Bergelson, J.M., Cunningham, J.A., Droguett, G., Kurt-Jones, E.A., Krithivas, A., Hong, J.S., Horwitz, M.S., Crowell, R.L., Finberg, R.W., 1997. Isolation of a common receptor for Coxsackie B viruses and adenoviruses 2 and 5. Science 275 (5304), 1320–1323.

Bobardt, M.D., Saphire, A.C., Hung, H.C., Yu, X., Van der Schueren, B., Zhang, Z., David, G., Gallay, P.A., 2003. Syndecan captures, protects, and transmits HIV to T lymphocytes. Immunity 18 (1), 27–39.

Boudin, M.L., Moncany, M., D'Halluin, J.C., Boulanger, P.A., 1979. Isolation and characterization of adenovirus type 2 vertex capsomer (penton base). Virology 92 (1), 125–138.

Byrnes, A.P., Griffin, D.E., 1998. Binding of Sindbis virus to cell surface heparan sulfate. J. Virol. 72 (9), 7349–7356.

Cardin, A.D., Weintraub, H.J., 1989. Molecular modeling of protein-glycosaminoglycan interactions. Arteriosclerosis 9 (1), 21–32.

Chen, Y., Maguire, T., Hileman, R.E., Fromm, J.R., Esko, J.D., Linhardt, R.J., Marks, R.M., 1997. Dengue virus infectivity depends on envelope protein binding to target cell heparan sulfate. Nat. Med. 3 (8), 866–871.

Dechecchi, M.C., Tamanini, A., Bonizzato, A., Cabrini, G., 2000. Heparan sulfate glycosaminoglycans are involved in adenovirus type 5 and 2-host cell interactions. Virology 268 (2), 382–390.

Dechecchi, M.C., Melotti, P., Bonizzato, A., Santacatterina, M., Chilosi, M., Cabrini, G., 2001. Heparan sulfate glycosaminoglycans are receptors sufficient to mediate the initial binding of adenovirus types 2 and 5. J. Virol. 75 (18), 8772–8780.

Delehedde, M., Allain, F., Payne, S.J., Borgo, R., Vampouille, C., Fernig, D.G., Deudon, E., 2002. Proteoglycans in inflammation. Curr. Med. Chem. 1, 89–102.

Esko, J.D., Selleck, S.B., 2002. ORDER OUT OF CHAOS: assembly of ligand binding sites in heparan sulfate. Annu. Rev. Biochem. 71, 435–471.

Fender, P., Ruigrok, R.W., Gout, E., Buffet, S., Chroboczek, J., 1997.

Adenovirus dodecahedron, a new vector for human gene transfer. Nat. Biotechnol. 15 (1), 52–56.

Fender, P., Schoehn, G., Foucaud-Gamen, J., Gout, E., Garcel, A., Drouet, E., Chroboczek, J., 2003. Adenovirus dodecahedron allows large multimeric protein transduction in human cells. J. Virol. 77 (8), 4960–4964.

Fuki, I.V., Kuhn, K.M., Lomazov, I.R., Rothman, V.L., Tuszynski, G.P., Iozzo, R.V., Swenson, T.L., Fisher, E.A., Williams, K.J., 1997. The syndecan family of proteoglycans. Novel receptors mediating internalization of atherogenic lipoproteins in vitro. J. Clin. Invest. 100 (6), 1611–1622.

Gaggar, A., Shayakhmetov, D.M., Lieber, A., 2003. CD46 is a cellular receptor for group B adenoviruses. Nat. Med. 9 (11), 1408–1412.

Gallagher, J.T., 2001. Heparan sulfate: growth control with a restricted sequence menu. J. Clin. Invest. 108 (3), 357–361.

Germi, R., Crance, J.M., Garin, D., Guimet, J., Lortat-Jacob, H., Ruigrok, R.W., Zarski, J.P., Drouet, E., 2002. Cellular glycosaminoglycans and low density lipoprotein receptor are involved in hepatitis C virus adsorption. J. Med. Virol. 68 (2), 206–215.

Ginsberg, H.S., Pereira, H.G., Valentine, R.C., Wilcox, W.C., 1966. A proposed terminology for the adenovirus antigens and virion morphological subunits. Virology 28 (4), 782–783.

Hong, S.S., Gay, B., Karayan, L., Dabauvalle, M.C., Boulanger, P., 1999. Cellular uptake and nuclear delivery of recombinant adenovirus penton base. Virology 262 (1), 163–177.

Humphries, D.E., Silbert, J.E., 1988. Chlorate: a reversible inhibitor of proteoglycan sulfation. Biochem. Biophys. Res. Commun. 154 (1), 365–371.

Iozzo, R.V., San Antonio, J.D., 2001. Heparan sulfate proteoglycans: heavy hitters in the angiogenesis arena. J. Clin. Invest. 108 (3), 349–355.

Lindahl, U., Kusche-Gullberg, M., Kjellen, L., 1998. Regulated diversity of heparan sulfate. J. Biol. Chem. 273 (39), 24979–24982.

Lortat-Jacob, H., Chouin, E., Cusack, S., van Raaij, M.J., 2001. Kinetic analysis of adenovirus fiber binding to its receptor reveals an avidity mechanism for trimeric receptor–ligand interactions. J. Biol. Chem. 276 (12), 9009–9015.

Lortat-Jacob, H., Grosdidier, A., Imberty, A., 2002. Structural diversity of heparan sulfate binding domains in chemokines. Proc. Natl. Acad. Sci. U.S.A. 99 (3), 1229–1234.

Lundin, L., Larsson, H., Kreuger, J., Kanda, S., Lindahl, U., Salmivirta, M., Claesson-Welsh, L., 2000. Selectively desulfated heparin inhibits fibroblast growth factor-induced mitogenicity and angiogenesis. J. Biol. Chem. 275 (32), 24653–24660.

Mathias, P., Wickham, T., Moore, M., Nemerow, G., 1994. Multiple adenovirus serotypes use alpha v integrins for infection. J. Virol. 68 (10), 6811–6814.

Norrby, E., 1966. The relationship between the soluble antigens and the virion of adenovirus type 3. II. Identification and characterization of an incomplete hemagglutinin. Virology 30 (4), 608–617.

Pye, D.A., Vives, R.R., Turnbull, J.E., Hyde, P., Gallagher, J.T., 1998. Heparan sulfate oligosaccharides require 6-O-sulfation for promotion of basic fibroblast growth factor mitogenic activity. J. Biol. Chem. 273 (36), 22936–22942.

Reiland, J., Rapraeger, A.C., 1993. Heparan sulfate proteoglycan and FGF receptor target basic FGF to different intracellular destinations. J. Cell Sci. 105 (Pt. 4), 1085–1093.

Roelvink, P.W., Lizonova, A., Lee, J.G., Li, Y., Bergelson, J.M., Finberg, R.W., Brough, D.E., Kovesdi, I., Wickham, T.J., 1998. The coxsackievirus–adenovirus receptor protein can function as a cellular attachment protein for adenovirus serotypes from subgroups A. C, D, E, and F. J. Virol. 72 (10), 7909–7915.

Sadir, R., Baleux, F., Grosdidier, A., Imberty, A., Lortat-Jacob, H., 2001. Characterization of the stromal cell-derived factor-1alpha-heparin complex. J. Biol. Chem. 276 (11), 8288–8296.

Sawitzky, D., 1996. Protein-glycosaminoglycan interactions: infectiological aspects. Med. Microbiol. Immunol. (Berl.) 184 (4), 155–161.

Schoehn, G., Fender, P., Chroboczek, J., Hewat, E.A., 1996. Adenovirus 3 penton dodecahedron exhibits structural changes of the base on fiber binding. EMBO J. 15 (24), 6841–6846.

Segerman, A., Arnberg, N., Erikson, A., Lindman, K., Wadell, G., 2003. There are two different species B adenovirus receptors: sBAR, common to species B1 and B2 adenoviruses, and sB2AR, exclusively used by species B2 adenoviruses. J. Virol. 77 (2), 1157–1162.

Shayakhmetov, D.M., Lieber, A., 2000. Dependence of adenovirus infectivity on length of the fiber shaft domain. J. Virol. 74 (22), 10274–10286.

Shukla, D., Spear, P.G., 2001. Herpesviruses and heparan sulfate: an intimate relationship in aid of viral entry. J. Clin. Invest. 108 (4), 503–510.

Shukla, D., Liu, J., Blaiklock, P., Shworak, N.W., Bai, X., Esko, J.D., Cohen, G.H., Eisenberg, R.J., Rosenberg, R.D., Spear, P.G., 1999. A novel role for 3-O-sulfated heparan sulfate in herpes simplex virus 1 entry. Cell 99 (1), 13–22.

Spear, P.G., Eisenberg, R.J., Cohen, G.H., 2000. Three classes of cell surface receptors for alphaherpesvirus entry. Virology 275 (1), 1–8.

Spillmann, D., 2001. Heparan sulfate: anchor for viral intruders? Biochimie 83 (8), 811–817.

Summerford, C., Samulski, R.J., 1998. Membrane-associated heparan sulfate proteoglycan is a receptor for adeno-associated virus type 2 virions. J. Virol. 72 (2), 1438–1445.

Valentine, R.C., Pereira, H.G., 1965. Antigens and structure of the adenovirus. J. Mol. Biol. 13 (1), 13–20.

Vives, R.R., Sadir, R., Imberty, A., Rencurosi, A., Lortat-Jacob, H., 2002. A kinetics and modeling study of RANTES(9-68) binding to heparin reveals a mechanism of cooperative oligomerization. Biochemistry 41 (50), 14779–14789.

Walters, R.W., Freimuth, P., Moninger, T.O., Ganske, I., Zabner, J., Welsh, M.J., 2002. Adenovirus fiber disrupts CAR-mediated intercellular adhesion allowing virus escape. Cell 110 (6), 789–799.

Wickham, T.J., Mathias, P., Cheresh, D.A., Nemerow, G.R., 1993. Integrins alpha v beta 3 and alpha v beta 5 promote adenovirus internalization but not virus attachment. Cell 73 (2), 309–319.

Williams, K.J., Fuki, I.V., 1997. Cell-surface heparan sulfate proteoglycans: dynamic molecules mediating ligand catabolism. Curr. Opin. Lipidol. 8 (5), 253–262.

ELSEVIER

Rapid Communication

Synthesis, cellular localization, and quantification of penton-dodecahedron in serotype 3 adenovirus-infected cells

P. Fender[a,*], A. Boussaid[a], P. Mezin[b], J. Chroboczek[a]

[a]Institut de Biologie Structurale, 41, rue Horowitz, 38027 Grenoble, France
[b]Centre Hospitalier Universitaire, BP217, 38043 La Tronche, France

Abstract

Adenovirus penton is a non-covalent complex composed of the penton base and fiber proteins, localized at the twelve vertices of the icosahedral virus capsid. In cells infected by adenovirus serotype 3 (Ad3), penton is found not only in the virus capsid but also self-assembled in dodecahedra formed through interactions between the twelve penton bases. In this study, the intracellular trafficking of penton proteins from the cytoplasm to the nucleus has been followed, and the nuclear re-arrangement induced by viral infection has been observed by electron microscopy of ultrathin sections. The amount of dodecahedra has been assessed in relation to the number of Ad3 infectious virions produced during the Ad3 replication cycle. It appears that dodecahedra are produced in a large excess over viral infectious particles and that they are located intranuclearly along the nuclear membrane of Ad3-infected cells at late times of infection.
© 2005 Elsevier Inc. All rights reserved.

Keywords: Adenovirus; Ad3; Dodecahedron; Nuclear localization; Ultrathin sections; Quantification

Introduction

Human adenoviruses (Ads) are non-enveloped viruses causing respiratory, ocular, and enteric infections. Their icosahedral capsid, containing the 36 kpb dsDNA genome, is composed of three major proteins, the hexon, the penton base, and the fiber. At the twelve vertices of the capsid, the protruding fiber together with the penton base embedded in the capsid form a complex called penton (Pt). Ad penton is the major structural element responsible for viral attachment and entry into host cells. Interestingly, in some Ad serotypes, penton proteins (penton base and fiber) are over-expressed during replicative cycle and can be purified from Ad-infected cell either separately or in form of penton complex (Boulanger and Puvion, 1973). Pentons in the complete virion are separated by hexon proteins but amazingly, in some serotypes, pentons can self-assemble

into dodecameric particles called adenovirus dodecahedra (Ad-Dd). This has been reported for the first time for Ad3-infected cells (Norrby, 1966) and later the presence of Ad-Dd has been observed for other Ad serotypes. Ad-Dd can be also obtained by the penton expression in the baculovirus system thus demonstrating that other adenoviral components are not required for dodecahedra formation (Fender et al., 1997). The structure of these particles has been solved by cryo-electromicroscopy (Schoehn et al., 1996) and it has been reported that Ad-Dd enters human cells with a high efficiency, likely through interaction of the fiber with the Ad3 primary receptor (CD46) (Gaggar et al., 2003; Sirena et al., 2004), but also through direct interaction of the penton base with heparan sulphate (Vives et al., 2004).

Despite all these functional and structural data, the formation, the localization, and the quantification of Ad3-Dd produced during the adenoviral replicative cycle are not well established. Here, we report the kinetics and the site of penton synthesis in Ad3-infected cells. In addition, we present the data concerning the amount of Ad-Dd produced in comparison with the infectious virus and we provide

information on the respective nuclear localization of Ad3 and Ad-Dd.

Results

Penton synthesis during the Ad3 replicative cycle

For the determination of the kinetics of penton synthesis during the Ad3 replicative cycle, HeLa cells were infected with Ad3 at MOI 1 for different periods of time. Infected cells were lysed and analyzed by Western blot using an anti-Pt-Dd serum that recognized SDS-denatured penton base and fiber proteins. Although the anti-Pt-Dd serum is able to detect less that 1 ng of protein, neither fiber nor penton base protein could be detected before 12 h of infection (Fig. 1A). As expected for late viral proteins, the penton synthesis started at 12 h p.i. as attested by the detection of the monomeric forms of the penton base at 60 kDa and a faint signal for the fiber at 35 kDa. Penton protein expression increased rapidly between 12 and 24 h and seemed to stabilize after 24 h.

Cellular localization of pentons during the Ad3 replication cycle

The expression and localization of penton proteins in Ad3-infected cells were studied by confocal microscopy using anti-Pt-Dd serum and anti-rabbit FITC-labeled secondary antibody while nuclei were counterstained in red by propidium iodide (Fig. 1B). At 12 h p.i., penton proteins were observed solely in the cytoplasm of Ad3-infected cells indicating entry into the late stage of the Ad replication cycle. Interestingly, at this stage, no dodecahedra were found in the heavy fractions of sucrose gradient density suggesting that dodecamerization of penton does not take place in the cytoplasm (data not shown). Four hours later (16 h p.i.), although penton synthesis was still detectable in the cytoplasm, the majority of the signal was observed in the nucleus where the diffuse yellow signal reflected the co-localization of penton proteins with the cellular DNA. At 24 h p.i., no detectable penton signal was seen in the cytoplasm, indicating that Ad late proteins are not sufficiently expressed to be detectable under these experimental conditions. Interestingly, the diffuse green penton signal
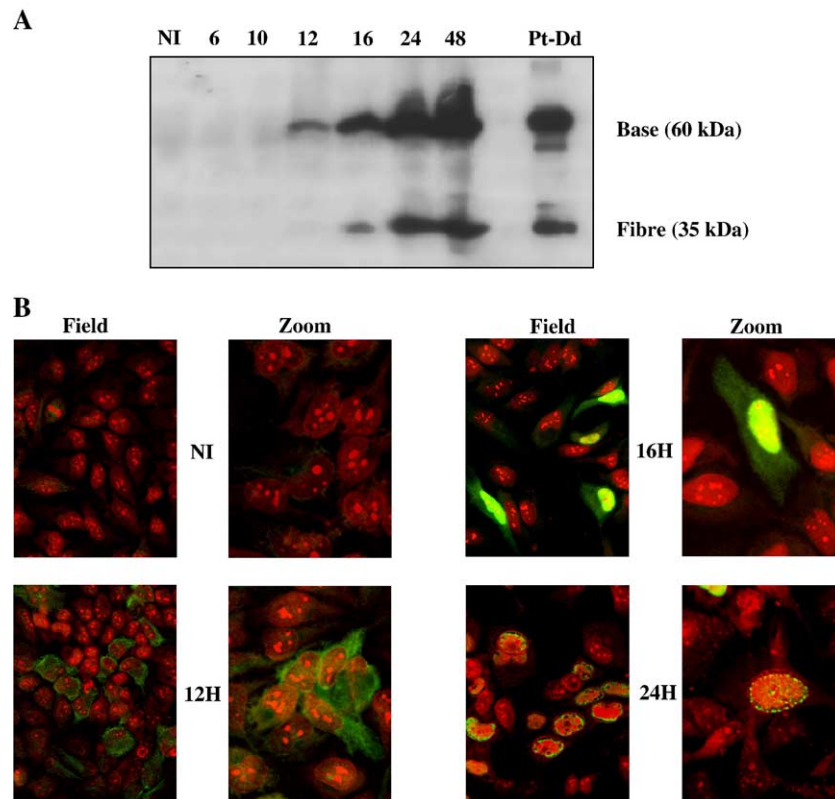
Fig. 1. Kinetics and localization of penton proteins in Ad3-infected HeLa cells. (A) Expression of penton base and fiber proteins monitored by Western blot with anti-Pt-Dd serum recognizing both monomeric penton base and monomeric fiber. Time post-infection is shown on the figure. NI—lysate from non-infected cells; Pt-Dd—purified penton dodecahedron expressed in the baculovirus system. (B) Localization of penton proteins, monitored by immunofluorescence. Ad3-infected HeLa cells were permeabilized at indicated times of infection and incubated with anti-Pt-Dd. Penton proteins are seen in green with a FITC-conjugated antibody while the nuclei are counterstained in red with propidium iodide. Picture acquisitions were performed at the same exposure settings on MRC600 (Bio-Rad) LASER confocal microscopy.

seen at 16 h in the nucleus was now punctated and predominantly located at the nuclear membrane of the infected cells (Fig. 1B, last panel). Taken together, these results show that penton proteins are expressed in the cytoplasm and transported to the nucleus where they tend to localize close to the nuclear membrane later in infection.

Specific location of encapsidated and non-encapsidated pentons in infected cell

At 24 h p.i., a complete cycle of adenovirus replication has occurred yielding progeny virions in infected cells. Penton can then be found either incorporated in the progeny virions (encapsidated pentons) or can remain free in form of dodecahedron (non-encapsidated pentons). To determine whether the penton signal seen at the nuclear membrane is due to the dodecahedron or to the virus, an immunofluorescence study was performed using either anti-Pt-Dd or anti-hexon antibodies. While the anti-Pt-Dd serum will interact with both virions and dodecahedra, the latter antibody will recognize virions but not the Dd. Interestingly,

the signal raised with anti-hexon was also punctated but arranged all over the infected cell nucleus (Fig. 2A, left panel). Of note, a majority of hexon synthesized in the Ad3-infected cells is used for the formation of 240 hexon capsomers of virions since infection by Ad3 contrary to that by Ad2 does not produce a large excess of free hexon (White et al., 1969, Boulanger and Puvion, 1973). It seems plausible that the weak intranuclear signal observed with anti-Pt-Dd antibody (Fig. 2A, middle panel) is due to encapsidated pentons whereas the bright perinuclear signal raised by this antibody is likely emitted by non-encapsidated pentons. To confirm this hypothesis, ultrathin sections of Ad3-infected HeLa cell have been observed by electron microscopy (Fig. 2B). As previously described for other Ad serotypes (Henry et al., 1971), the Ad3 progeny viruses are seen concentrated in form of nuclear inclusions, possibly explaining the large punctate signal observed with the anti-hexon antibody in the immunofluorescence study. It is relevant that individual Dd with about 3-fold smaller diameter than that of virus cannot be directly detected by this technique. Nevertheless, the punctate signals observed
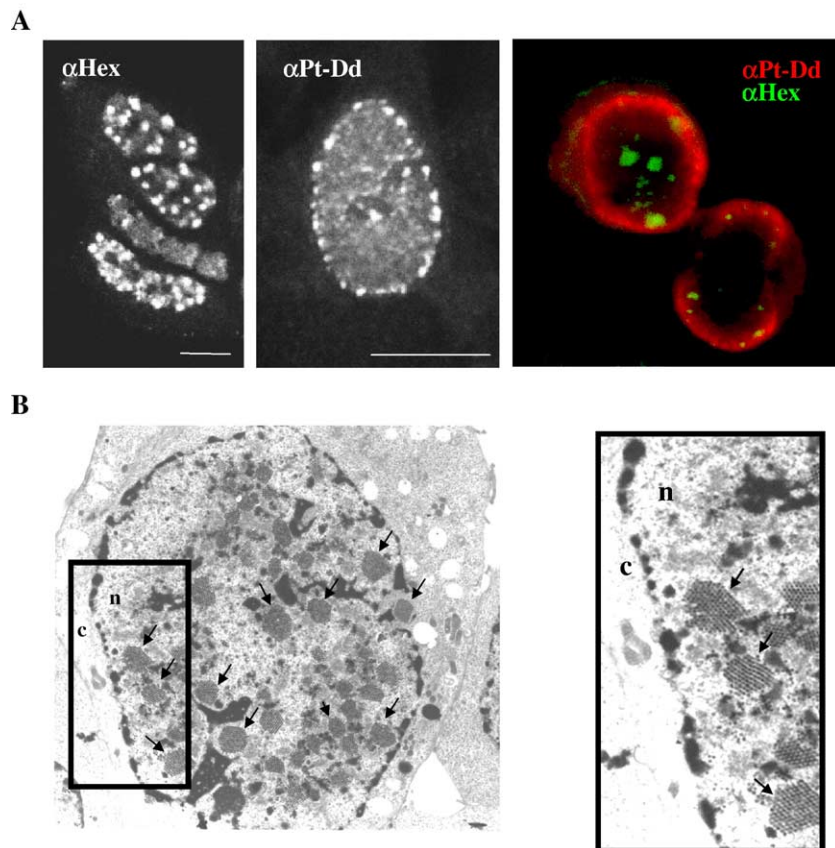
Fig. 2. Location of free and encapsidated penton complexes in Ad3-infected HeLa cells at 24 h p.i. (A) Immunofluorescent detection of Ad3 virions and Pt-Dd. Virions were detected with anti-hexon antibody (left panel) and dodecahedra with anti-Pt-Dd antibody (middle panel). Signal revealed with FITC-labeled secondary antibody were observed by LASER confocal microscopy—scale bar: 10 μm. Colored panel shows the respective localization of dodecahedron (revealed in red with an anti-penton base antibody) and of the virus (in green revealed with an anti-hexon antibody). (B) Ultrathin sections. On the left panel, arrows indicate intranuclear inclusions of virus. The framed portion of the thin section presented in the left panel is shown blown-up in the right panel. Cytoplasm is denoted by letter c, and the nucleus by letter n. A dark intranuclear punctate signal lining the nuclear membrane can be seen on the right panel. The hexon signal observed in A (left panel) stems most likely from the intranuclear inclusions observed in B (right panel), while Pt-Dd signal in A (right panel) is due predominantly to the condensed dark material seen in the ultrathin section along the nuclear membrane (B, right panel).

on Fig. 2A with anti-Pt-Dd (middle panel) can be correlated with the dark punctate structures seen at the perinuclear membrane space of infected cells nuclei on ultrathin sections (Fig. 2B, right panel). It can be thus concluded that a large excess of penton is synthesized during the Ad3 replicative cycle and that this non-encapsidated pentons tends to accumulate in the nucleus lining the external side of the nuclear membrane at late stage of infection.

Estimation of dodecahedra and infectious virus in Ad3-infected cell

We have elaborated a strategy enabling both the quantification of Dd and the titration of Ad3 to be performed on the same batch of infected cells (Fig. 3). Lysate recovered from HeLa cell infected for 24 h has been either subjected to sucrose gradient ultracentrifugation to separate Dds from the virus particles or applied to cesium chloride gradient to purify Ad3 virions. As expected, Dd was localized in the 28–38% part of the sucrose gradient density with very low contamination by virus particles as attested by electron microscopy (below 0.5%, data not shown). These fractions were then pooled and different volumes were run on SDS-PAGE in the presence of known amounts of purified Dd, and subjected to Western blot with anti-Pt-Dd serum. By comparing the band intensity of our sample to that of the purified Dd range, we found a total amount of 45 µg of Dds in the lysate of 10^7 cells meaning that, on average, 7.5×10^5

	Dodecahedron		Infectious virus	Ratio
	amount (ng)	particles	FFU total	(Dds/Virus)
Assay 1	50	$8,3.10^{12}$	$1,6.10^6$	$5,2.10^6$
Assay 2	42	$7,0.10^{12}$	$1,3.10^6$	$5,4.10^6$
Assay 3	44	$7,3.10^{12}$	$1,2.10^6$	$6,1.10^6$
Average	**45**	**$7,5.10^{12}$**	**$1,4.10^6$**	**$5,5.10^6$**
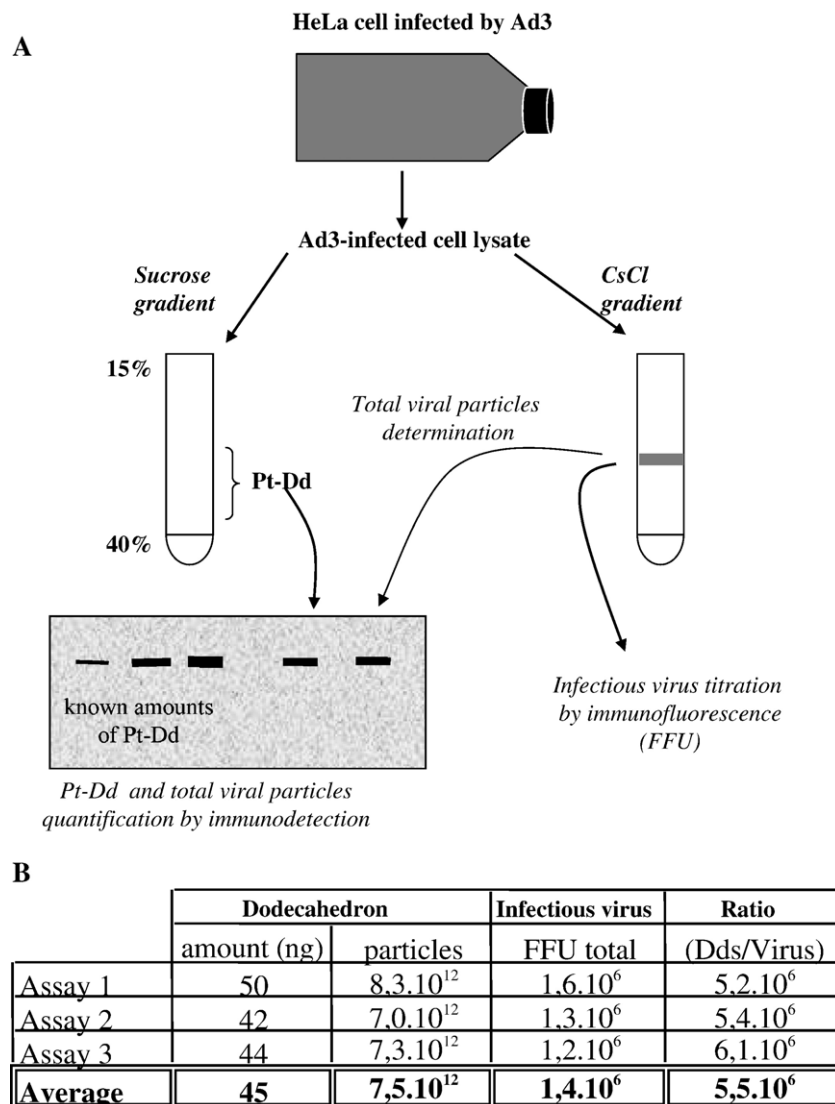
Fig. 3. Titration of infectious virus and quantification of Pt-Dd and total viral particles. (A) Principle: Ad-infected HeLa cells were lysed after 24 h of infection. A part of the lysate was centrifuged on a 15–40% sucrose gradient to recover Pt-Dd. Quantification of Dd was performed by Western blot using anti Pt-Dd serum. For this, aliquots of Pt-Dd produced during the Ad3 cycle were run on SDS-PAGE and compared to known amounts of Pt-Dd expressed in the baculovirus system and purified. For the infectious virus titration, Ad3 was purified on a cesium chloride gradient and titrated by FFU determination. (B) Results obtained in three independent experiments. Dodecahedron particle molecular weight of 3.6×10^6 Da was used in calculations.

particles were found per cell. This amount is likely to be underevaluated as some cells were not infected.

Infectious Ad3 particles were titrated by fluorescent forming unit (FFU) determination. For this, adenoviruses were purified from infected cell lysate by cesium chloride gradient centrifugation in order to eliminate Dds and other contaminants that could interfere with Ad3 infection. Results of three independent experiments demonstrated that a total of 1.4×10^6 FFU were present in the lysate. These results show that there is a large excess of Dd over infectious Ad3 particles in infected cells with an average of 5.5×10^6 Dds per one infectious virus. Total viral particles have also been assessed by Western blot by comparing the penton base band displayed by the virus to that of a range of known amounts of purified dodecahedron, as described in Fig. 3. With a ratio of 26,000 non-infectious viral particles per infectious virus, it has been calculated that about 200-fold more Dds than total viral particles are found in Ad3-infected cell, at 24 h p.i.

Discussion

Adenovirus penton base is a major player not only in adenovirus entry but also during the adenovirus replication cycle. Indeed, even if it has been known for long time that penton base has a critical role in viral endocytosis (Wickham et al., 1993), another role for this protein has been reported more recently. Due to their strictly conserved PPxY sequence in their N-terminus, human adenovirus penton bases interact with WW domain-containing proteins such as the ubiquitin ligases family (Galinier et al., 2002, Chroboczek et al., 2003). In our study, we showed that neo-synthesized penton as a typical late product appears in the cytoplasm of infected cell 12 h p.i and its synthesis increases steadily until 24 h, as reflected by the kinetic study (Fig. 1). During this period, the penton is susceptible to interact with several cytoplasmic protein partners including WW-containing proteins before being transferred to the nucleus where the virus assembly takes place. Interestingly, the diffuse penton base signal seen inside the nucleus at 16 h p.i. seems to become arranged along the nuclear membrane 8 h later. At 24 h p.i., one cycle of the virus replication has been accomplished and thus virion progeny is already present in the nucleus of infected cell (White et al., 1969; Boudin et al., 1979).

It has been reported that a highly symmetric particle made of twelve penton bases is produced in Ad3-infected cells (Norrby, 1966). This particle, called adenovirus dodecahedron (Dd), is well characterized from the structural point of view (Schoehn et al., 1996; Zubieta et al., 2005) as well as functionally (Fender et al., 1997; Vives et al., 2004) but little is known about its formation. In this study, we bring new elements showing that this particle is likely assembled in the nucleus as no Dd can be recovered from

cell infected for 12 h when penton base is expressed in the cell cytoplasm but not yet found in the nucleus (Fig. 1B). Nuclear assembly of virus-like particles has already been described for other viruses such AAV or polyomavirus (Hoque et al., 1999; Johne and Muller, 2004).

Another point investigated in this work is the total number of Ad-Dd produced per infected cell and how it correlates with the virus titer. Surprisingly, Ad3 infection in cell culture yielded very low titer of infectious virus. This low number is somewhat in contradiction with the number and the size of adenoviruses para-crystals (nuclear inclusion) seen in the nucleus of Ad3-infected cells (Fig. 2B, right panel). A ratio of about 26,000 non-infectious viral particles per infectious particle has been determined. Such a low yield of infectious Ad3 might suggest that the virion maturation requires an additional step taking place during normal cell lysis and which does not occur in freeze–thaw cycles. However, whatever the number of defective and infectious viruses, a massive amount of Dd is found in the nucleus of Ad3-infected cell and we have investigated their distribution. Remarkably, these complexes that at 16 h p.i. are randomly spread all over the nucleus, are arranged inside the nucleus along the nuclear membrane at 24 h p.i. This distribution contrasts with the virion nuclear inclusions that are found in different area of the nucleus as seen by immunofluorescence with anti-hexon antibody and confirmed on infected cell ultrathin sections (Fig. 2). The mechanism leading to such localization of Dd is not known and unfortunately the size of the particle does not permit obtaining precise details of their organization on ultrathin sections.

The amount of dodecameric particles produced in infected cell nuclei has been estimated. On average, 7.5×10^5 particles are found per infected cell representing a ratio of 5.5×10^6 Dds per infectious virus. Such an excess of pentons synthesized during the Ad3 replication cycle strongly suggests that Dd has a role in virus strategy. It is relevant that the Ad2 penton base protein is know to triggers cell detachment (Boudin et al., 1979) and we have reported that Ad3-Dd interacts with high affinity with heparan sulfate that participates in cell cohesion (Vives et al., 2004). It can be hypothesized that during cell lysis, the release of massive amounts of Dd can affect cell cohesion and/or that competition with virus for its receptor during secondary infection contributes to virus escape and spreading as reported for the Ad2 fiber (Walters et al., 2002). With regards to our results, it can also be hypothesized that Dd plays a role in the nucleus of infected cells. It could be envisaged that Dd localizes with nuclear pore complex and regulates nuclear import and export. Taken together, our results show that only a low proportion of Ad3 penton proteins migrating from cytoplasm to the nucleus is used for virion formation while the major part self-assembles in form of Dd and accumulates along the nuclear membrane reinforcing the idea of the crucial role of this particle in the Ad3 life cycle.

Materials and methods

Cells and virus

HeLa cells were cultured at 37 °C, under 5% CO_2 atmosphere, in EMEM (BioWhittaker), supplemented with 10% fetal calf serum (FCS), penicillin (50 IU/ml), and streptomycin (50 μg/ml). Ad3 stock was purified from a lysate of HeLa cells infected at MOI 1 for 48 h, by double banding on CsCl gradient according to Kanegae et al. (1994). This stock was dialyzed against Tris 20 mM pH 7.4–150 mM NaCl and stored in presence of 20% glycerol at −20 °C.

Pt-Dd expression and detection

Pt-Dd was expressed in the baculovirus system and purified on sucrose density gradient, as previously described (Fender et al., 1997). Pt-Dds were detected by Western blot using anti-Pt-Dd serum (diluted at 1/40,000 in PBS–0.1% Tween-20) and a subsequent incubation with anti-rabbit HRP-conjugated antibody at 1/5000 (Jackson).

Virus titration and Dd quantification

HeLa cells grown in a 25-cm^2 dish (about 10^7 cells) were infected with Ad3 at MOI 1. At the indicated time after infection, cells were washed with PBS and lysed by three freeze/thaw cycles in 1 ml hypotonic buffer (Tris 20 mM pH 7.5–50 mM NaCl). The cell lysate was recovered after 5 min centrifugation at $400 \times g$ and one part was used for titration of infectious virus while the other part was used for Dd quantification (summarized in Fig. 3).

Ad3 titration

Titration of Ad3 infectious particles was performed by immunofluorescence. Serial virus dilutions prepared in 250 μl of EMEM without serum were incubated for 1 h with HeLa cells in a 24-multiwell plate (10^5 cells/well). Then, 750 μl of EMEM containing 10% SVF was added for an additional 23H. Cells were then washed with PBS and permeabilized for 10 min with 250 μl of cold methanol. After several PBS washes, the wells were incubated for 1 h with 250 μl anti-Pt-Dd rabbit polyclonal serum diluted at 1/1000 in PBS–0.1% Tween-20 for 1 h and subsequently incubated for 1 h with FITC-labeled goat anti-rabbit antibody (Jackson) diluted at 1/250 in the same buffer. Green fluorescent cells were counted in triplicate and the results were averaged and scaled in order to obtain the titer of infectious particle in FFU/ml. Total particles of adenovirus has been quantified by Western blot, using an anti-Bs-Dd antibody (recognizing Ad3 penton base). Penton base signal corresponding to boiled viruses was compared to that of known amounts of purified Bs-Dd.

Dodecahedron quantification

Dodecahedron was purified from 100 μl cell lysate on a 15–40% sucrose gradient (prepared in 20 mM Tris, pH 7.4–150 mM NaCl–10% glycerol) by 4 h centrifugation at $200,000 \times g$ in a TLS-55 rotor (Beckman). Ten fractions were collected from the top of the gradient. Fractions 6 to 9 containing purified dodecahedron (28–38% sucrose) were pooled and analyzed by electron microscopy. Different volumes of this pool were then boiled in the presence of SDS and run on a 12% PAGE-SDS gel together with known amounts of purified Pt-Dd. After electro-transfer on a PVDF membrane, a Western blot was performed with anti Pt-Dd serum as described above. The amount of Dd was assessed by the comparison of band intensity and results were scaled to the total cell number. Results are expressed as the mean of three independent experiments.

Confocal microscopy

HeLa cells were grown overnight on glass coverslips (about 10^5 cell/cm^2) in EMEM medium supplement with 10% FCS at 37 °C under 5% CO_2 atmosphere. Cells were infected with Ad3 at MOI 1 in 250 μl EMEM without serum. After 1 h at 37 °C, the inoculum was removed, cells were washed, and 750 μl EMEM containing 10% FCS was added. After different periods post-infection (p.i.), the medium was removed, cells were rinsed with PBS and then permeabilized with cold methanol for 10 min. Immuno-fluorescence detection of penton was performed by incubation of coverslips with anti-Pt-Dd rabbit polyclonal serum at 1/1000 in 50 μl PBS–0.1% Tween-20 and a subsequent incubation with FITC-labeled goat anti-rabbit antibody (Jackson), diluted 1/250 in the same buffer. Cell nuclei were counterstained with propidium iodide (5 μg/ml). A similar experiment was performed with mouse monoclonal anti-Ad3 hexon antibody (Chemicon) at 1/100 and FITC-labeled anti-mouse antibody. Localization of Dd and adenoviruses in the same cell was performed by using an anti-Bs-Dd rabbit polyclonal serum (recognizing only the penton base) at 1/1000 and an anti-Ad3 hexon antibody at 1/100. Penton base signal was revealed in red by rhodamine-labeled anti-rabbit antibody and hexon signal in green by FITC-labeled antibody. Laser scanning confocal microscopy was performed on MRC600 (Bio-Rad).

Epon inclusion and thin sections of infected cells

HeLa cells grown in a Labtek chamber slide (Nunc) were infected with Ad3 at MOI 1 for 24 h. Cells were fixed with 2.5% glutaraldehyde in 100 mM HEPES buffer pH 7.4, post-fixed with 1% osmium tetraoxide and dehydrated with ethanol. Ultrathin sections (80 nm) of infected cells embedded in Epon were performed and collected on carbon-coated grids. Grids were stained with saturated uranyl acetate in 50% ethanol and then with 1 M lead citrate. Observations were made with Philips CM10 microscope at 80 kV.

Acknowledgments

References

Boudin, M.L., Moncany, M., D'Halluin, J.C., Boulanger, P., 1979. Isolation and characterisation of Adenovirus type 2 Vetex capsomer (Penton Base). Virology 92, 125–138.

Boulanger, P.A., Puvion, F., 1973. Large-scale preparation of soluble adenovirus hexon, penton and fiber antigens in highly purified form. Eur. J. Biochem. 39 (1), 37–42.

Chroboczek, J., Gout, E., Favier, A.L., Galinier, R., 2003. Novel partner proteins of adenovirus penton. Curr. Top. Microbiol. Immunol. 272, 37–55 (Review).

Fender, P., Ruigrok, R.W., Gout, E., Buffet, S., Chroboczek, J., 1997. Adenovirus dodecahedron, a new vector for human gene transfer. Nat. Biotechnol. 15 (1), 52–56.

Gaggar, A., Shayakhmetov, D.M., Lieber, A., 2003. CD46 is a cellular receptor for group B adenoviruses. Nat. Med. 9 (11), 1408–1412.

Galinier, R., Gout, E., Lortat-Jacob, H., Wood, J., Chroboczek, J., 2002. Adenovirus protein involved in virus internalization recruits ubiquitin–protein ligases. Biochemistry 41 (48), 14299–14305.

Henry, C.J., Slifkin, M., Merkow, L.P., Pardo, M., 1971. The ultrastructure and nature of adenovirus type 2-induced paracrystalline formations. Virology 44 (1), 215–218.

Hoque, M., Ishizu, K., Matsumoto, A., Han, S.I., Arisaka, F., Takayama, M., Suzuki, K., Kato, K., Kanda, T., Watanabe, H., Handa, H., 1999. Nuclear transport of the major capsid protein is essential for adeno-associated virus capsid formation. J. Virol. 73 (9), 7912–7915.

Johne, R., Muller, H., 2004. Nuclear localization of avian polyomavirus structural protein VP1 is a prerequisite for the formation of virus-like particles. J. Virol. 78 (2), 930–937.

Kanegae, Y., Makimura, M., Saito, I., 1994. A simple and efficient method for purification of infectious recombinant adenovirus. Jpn. J. Med. Sci. Biol. 47 (3), 157–166.

Norrby, E., 1966. The relationship between the soluble antigens and the virion of adenovirus type 3: II. Identification and characterization of an incomplete hemagglutinin. Virology 30 (4), 608–617.

Schoehn, G., Fender, P., Chroboczek, J., Hewat, E.A., 1996. Adenovirus 3 penton dodecahedron exhibits structural changes of the base on fibre binding. EMBO J. 15 (24), 6841–6846.

Sirena, D., Lilienfeld, B., Eisenhut, M., Kalin, S., Boucke, K., Beerli, R.R., Vogt, L., Ruedl, C., Bachmann, M.F., Greber, U.F., Hemmi, S., 2004. The human membrane cofactor CD46 is a receptor for species B adenovirus serotype 3. J. Virol. 78 (9), 4454–4462.

Vives, R.R., Lortat-Jacob, H., Chroboczek, J., Fender, P., 2004. Heparan sulfate proteoglycan mediates the selective attachment and internalization of serotype 3 human adenovirus dodecahedron. Virology 321 (2), 332–340.

Walters, R.W., Freimuth, P., Moninger, T.O., Ganske, I., Zabner, J., Welsh, M.J., 2002. Adenovirus fiber disrupts CAR-mediated intercellular adhesion allowing virus escape. Cell 110 (6), 789–799.

White, D., Matthew, D., Scarff, D., Maizel, J., 1969. The polypeptides of adenovirus. Virology 3, 395–406.

Wickham, T.J., Mathias, P., Cheresh, D.A., Nemerow, G.R., 1993. Integrins alpha v beta 3 and alpha v beta 5 promote adenovirus internalization but not virus attachment. Cell 73 (2), 309–319.

Zubieta, C., Schoehn, G., Chroboczek, J., Cusack, S., 2005. The structure of the human adenovirus 2 penton. Mol. Cell 17 (1), 121–135.

Heparan Sulphate Proteoglycans and Viral Vectors : Ally or Foe?

Romain R. Vivès, Hugues Lortat-Jacob and Pascal Fender*

Institut de Biologie Structurale, 41 rue Jules Horowitz 38027 Grenoble, France

Abstract: The attachment of viruses to the host cell surface is a critical stage that will largely condition cell permissivity and productive infection. The understanding of such mechanisms is therefore essential for gene therapy applications involving viruses, as this step will influence both targeting and delivery efficiency of the gene of interest. Viral attachment depends upon the recognition and binding of viral envelope/capsid proteins to specific cellular receptors that can be from very diverse origins. Amongst them are heparan sulphate proteoglycans (HSPGs), a family of glycoproteins which, through the large binding properties of their heparan sulphate (HS) polysaccharide chains, serve as attachment receptor for a great number of viruses. The aim of this review is to provide an update on the multiple roles of HSPGs during viral infection, with a special focus on viruses used as gene delivery vectors. Consequences of HS binding for gene therapy applications will be assessed, as well as the various strategies that have been developed to potentiate the advantages or to overcome the drawbacks resulting from viral vector interaction with HS.

Keywords: Proteoglycan, glycosaminoglycan, heparan sulphate, adenovirus, AAV, virus, viral vector, receptor, endocytosis, targeting, gene therapy.

1. HEPARAN SULPHATE PROTEOGLYCAN (HSPG): A MULTIFACETED MOLECULE AT THE CELL SURFACE

1.1 Proteoglycans and Glycosaminoglycans

Proteoglycans (PGs) are ubiquitous glycoproteins, widely distributed in animal tissues, that are involved in a multitude of biological processes, including cell proliferation and differentiation, embryo development, inflammation, migration, chemoattraction, and viral attachment [Bernfield *et al.,* 1999; Delehedde *et al.,* 2002; Iozzo *et al.,* 2001; Liu *et al.,* 2002; Perrimon *et al.,* 2000] . They are characterised by a protein core, on which one or several glycosaminoglycan (GAG)-type polysaccharide chains are covalently attached. PGs are generally classified according to the nature of their polysaccharide chains, their location and their function. PGs can first be expressed in intracellular compartments. This is the case of Serglycin that is found in mast cell secretory granules released upon inflammation and that helps packaging their protein content. PGs can also be extracellular (examples are Perlecan, Aggrecan, Decorin…) and are then generally associated with roles in the cohesion and remodelling of the extracellular matrix, or protein storage. Finally, a last class of PGs are associated to the cell surface, where they provide binding sites for a large number of proteins, have been shown to participate to most cell processes and are exploited by many pathogens for binding to the cell surface. These PGs fall in two main families: syndecans, a four member family of type I transmembrane proteins, and glypicans (Glypican-1 to -6), which are extracellular proteins bound to the cell surface by the mean of a phosphatidylinositol lipid anchor (Fig. **1**). In addition, proteins occasionally bearing GAG chains have been observed, including type III Transforming Growth Factor (TGF) receptor, or cell adhesion molecule CD44.

A number of evidence suggests that PG core protein directly participates to various cell functions [Yoneda *et al.,* 2003; Zimmermann *et al.,* 1999] . Syndecan protein core is involved in the regulation of the cytoskeleton organisation and formation of focal adhesion. Moreover, syndecan cytoplasmic domain can be phosphorylated and thus, may initiate cascades of signalling events. However, it is widely recognised that most of HSPGs' large biological activities are primarily due to the ability of their GAG chains to interact with a wide range of protein ligands [Esko *et al.,* 2002; Gallagher, 2001; Lyon *et al.,* 1998] . GAGs are a family of highly sulphated (with the exception of hyaluronic acid), complex polysaccharides. The structural basis of GAG saccharide backbone is a disaccharide unit, comprising a hexosamine and an uronic acid, that can be variably sulphated (for review, see [Esko *et al.,* 2001; Lindahl *et al.,* 1998]). The nature of the hexosamine (glucosamine or galactosamine), uronic acid (glucuronic or iduronic acid) and the degree of sulphation define the type of GAGs. For instance, HS which is the major GAG species found at the cell surface, is a polymer of glucosamine and glucuronic/iduronic acid. In HS, sulphation occurs at C-2, C-6 and occasionally C-3 of the amino sugar, and at C-2 of the uronic acid (mostly iduronic acid) (Fig. **1**). Remarkably, disaccharide unit sulphation does not occur uniformly along the chain. This is particularly marked in HS, for which sulphation is mostly restricted to specialised regions of the polysaccharide called S domains. Consequently, HS features a unique molecular organisation, with homogeneous, non or low sulphated regions alternating with hypervariable highly sulphated S domains. Within these domains are found motifs of precise saccharide sequence and sulphation pattern that constitute protein binding sites. On proteins, a positively charged area

*Address correspondence to this author at the Institut de Biologie Structurale, 41 rue Jules Horowitz 38027 Grenoble; France; Tel: (33) 4 38 78 95 78; Fax: (33) 4 38 78 54 94; Email: fender@ibs.fr
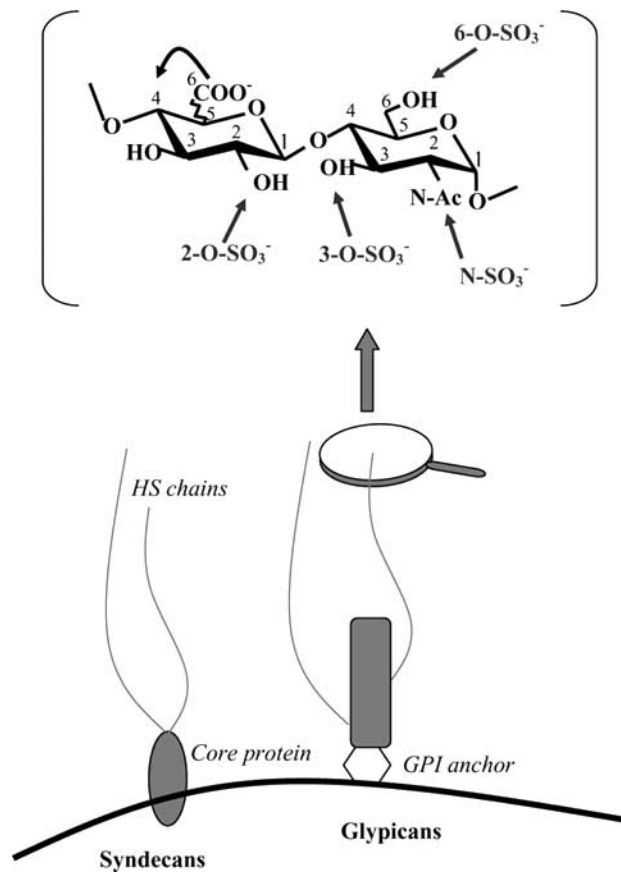
Fig. (1). Cell surface HSPGs.
Cell surface HSPGs are divided in two main families: transmembrane syndecans and GPI-anchored glypicans. HSPG main feature is the presence, on the protein ectodomain, of HS chains. HS is linear polysaccharide constituted by the repetition of a disaccharide motif, comprising an uronic acid and a glucosamine, that can be variably sulphated. Within the chain, oligosaccharide motifs of precise sugar sequence and sulphation pattern constitute binding sites for a multitude of proteins.

usually characterises the HS binding region. It often consists of a BBXB or BBBXXB type sequence (where B stands for a basic and X for any other amino acid), but can also include conformational epitopes comprising distant amino acids clusterised through the folding of the protein [Vives *et al.,* 2004a] . Interaction with HS can influence protein activity through many ways. Binding of antithrombin III (AT-III) to HS induces conformational changes that turn the protein into an active form, able to bind and inhibit coagulation factor Xa [Petitou *et al.,* 2003] . HS can act as a template that brings proteins together and directs formation of biologically active complexes. A well-studied example of such mechanism is that of HS binding independently both thrombin and AT-III to favour their interactions [Petitou *et al.,* 1999; Petitou *et al.,* 2001] . HS has been shown to induce chemokine dimerisation, a process that may be critical for cell signalling and formation of chemotactic gradients. HS can act as a corepector for a number of growth factors, including fibroblast growth factors (FGFs), for which binding to the polysaccharide is necessary for induction of productive cell re-

sponse [Rapraeger *et al.,* 1991; Yayon *et al.,* 1991] . In contrast, HS can inhibit ligand-receptor recognition as for interferon [Sadir *et al.,*1998] . Finally, HS has been involved in the storage and protection of proteins against proteolysis [Sadir *et al.,* 2004] .

1.2 Role of HSPGs in Viral Infection

1.2.1 PGs Serve as High Affinity Receptor

HS, because of its potent interactive properties and wide tissue distribution, has been exploited as a prevalent source of cell surface docking sites by a great number of pathogens (for reviews, see [Rostand *et al.,* 1997; Spillmann, 2001]). These comprise parasites, such as *Plasmodium falciparum* [Ancsin *et al.,* 2004] or *Toxoplasma gondii* [Carruthers *et al.,* 2000] , bacteria, including *Bordetella pertussis* [Geuijen *et al.,* 1998] , *Staphylococcus aureus* [Fallgren *et al.,* 2001] and *Helicobacter pylori* [Utt *et al.,*1997] and many viruses, such as Human Immunodeficiency Virus type 1 (HIV-1) [Patel *et al.,* 1993] , Herpes viruses [Shukla *et al.,* 2001] , Dengue virus [Chen *et al.,* 1997] , Foot and Mouth Disease Virus [Jackson *et al.,* 1996] and adenoviruses [Dechecchi *et al.,* 2001; Dechecchi *et al.,* 2000] . Binding to HS has usually been associated with increased infectivity and studies showed that many viruses could very easily adapt to the use of HS, after a few passages on cells in culture [Klimstra *et al.,* 1998; Lee *et al.,* 2002] . Elimination of cell surface HS using sulphation inhibitors (sodium chlorate) or HS degrading enzymes (heparinases) has been associated with increased cell resistance to infection, resulting from a reduction in the virus ability to bind to the cell surface. HS has thus been regarded as an ubiquitous virus attachment receptor that facilitated concentrations at the cell surface and access to specific entry receptors (Fig. **2a**).

Such an implication has been well established in the case of adenovirus. Human adenoviruses (Ads) are a large family of non-enveloped viruses responsible for respiratory, ocular and enteric infections. Their 36 kb dsDNA genome is concealed within a 90 nm icosaedral capsid composed of three major proteins : the trimeric hexon, the pentameric base and the trimeric fibre. The last two form a non-covalent complex called the penton, which protrudes from each of the 12 vertices of the capsid [Ginsberg *et al.,* 1966; Valentine *et al.,*1965] (Fig. **3**). The infection process involves a first interaction of the fibre with a high affinity primary receptor, that will facilitate subsequent binding of the penton base to cellular integrins and eventually trigger endocytosis [Mathias *et al.,* 1998; Wickham *et al.,* 1993] . It has been first demonstrated that most adenovirus serotypes, including Ad5, use a protein termed Coxsackievirus and Adenovirus Receptor (CAR) as the primary receptor for infection [Bergelson *et al.,* 1997; Roelvink *et al.,* 1998] . This interaction is mediated by the distal globular "head-domain" of the fibre (Fig. **3**). Recently, Decchechi *et al.,* reported that the adenovirus fibre was also able to interact with HS and thus, that this sulphated polysaccharide is another primary receptor for Ads. Indeed, addition in the culture medium of a HS competitor, such as heparin, reduced Ad2 and Ad5 binding by 50% [Dechecchi *et al.,* 2000] and a similar reduction was achieved by treating cells with heparin lyases, but not chondroitin lyases. Moreover, whereas competition assays using soluble CAR only lead to a 50% reduction of Ad5 binding on HS expressing
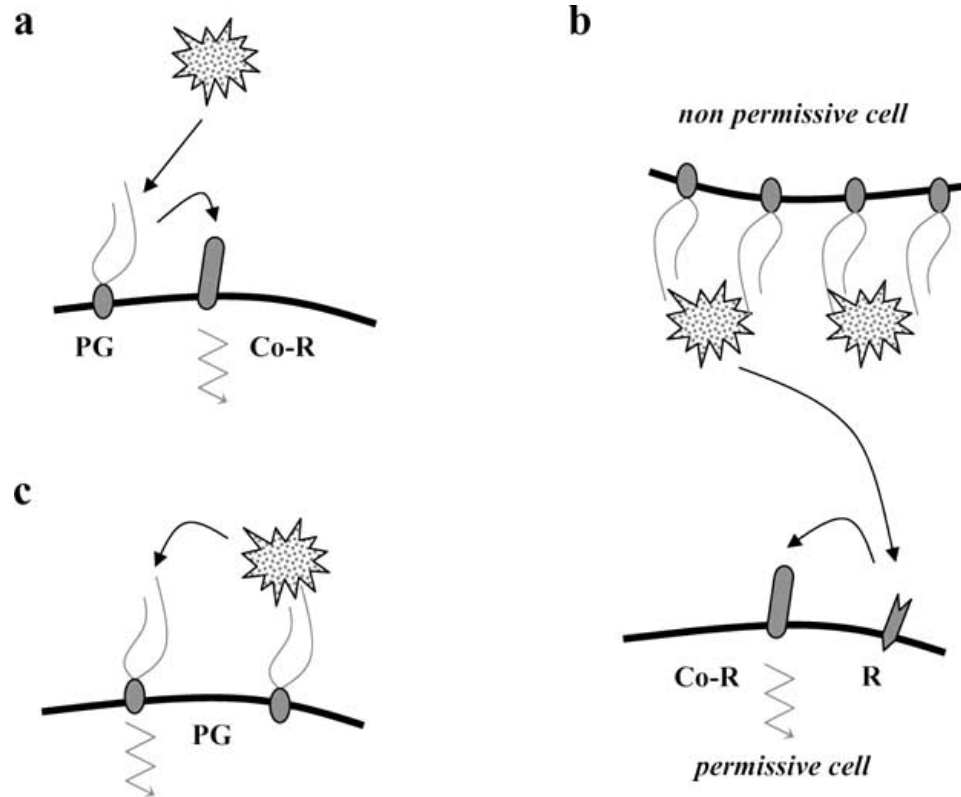
Fig. (2). HSPGs and their roles in viral entry.
HSPGs play multiple roles during viral infection (a) PGs serve as high affinity primary receptor that enables virus docking and facilitates subsequent interaction with specific entry receptors. (b) PGs can be involved in storage and protection of viruses at the surface of non-permissive cells, and then mediate "*in trans*" infection by presenting these viruses to attachment and entry receptors on permissive cells. (c) For some viruses, PGs can participate to both virus attachment and entry processes. (PG: Proteoglycan; R:receptor; Co-R: Co-receptor).
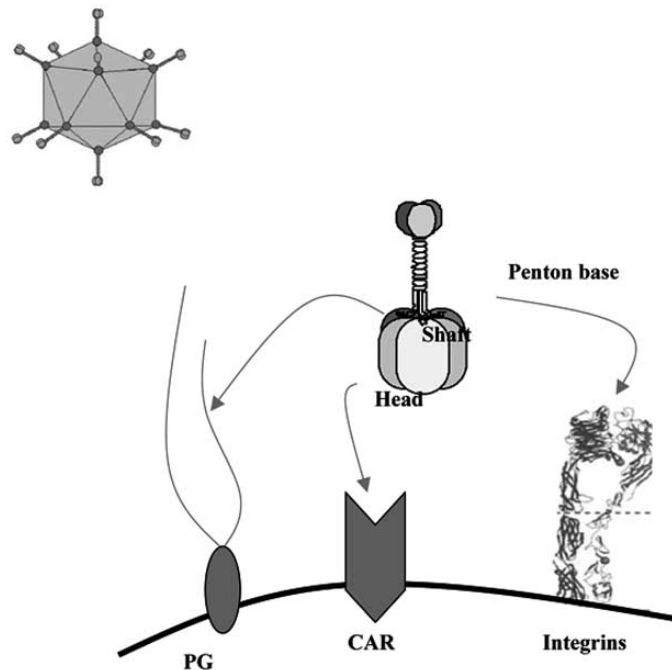
Fig. (3). Interaction of Adenovirus with its receptors: the French « ménage à trois ».
The trimeric fibre is composed of an elongated shaft and a globular head domain. The latter interacts with the CAR receptor, whereas the shaft can bind to with HS. This primary attachment enables the subsequent interaction of the pentameric penton base with integrins that will eventually trigger endocytosis. The fibre and penton base are located at each of the twelve vertices of the capsid.

cells, full inhibition could be achieved on Raji GAG-defective cells. Further work from the same group also demonstrated that HS played the role of attachment receptor for Ad2 and Ad5 on cells, such as CHO-K1, that do not express CAR but exhibit HS on their surface [Dechecchi *et al.,* 2001]. Interestingly, they also showed that GAG expression at the cell surface varied according to the degree of confluency and that sparse cells which expressed more HS on their surface were more susceptible to Ad infection. Ad molecular determinants involved in HS recognition have not been identified yet, though the presence of a HS binding consensus sequence has been highlighted within the shaft domain of Ad-5 fibre. However, a recent study suggests that adenovirus-HS interaction could be indirectly mediated by blood factors such as the coagulation factor IX or the complement component C4 binding protein. In this hypothesis, the blood factor interacts in one hand with the adenovirus fibre head and in the other hand with HS [Shayakhmetov *et al.,* 2005]. Whatever the mechanism, a virus–like particle produced in great excess during the Ad3 replication cycle [Norrby, 1966] could also interact with the polysaccharide. This particle called penton-dodecahedron (Pt-Dd) is made of twelve penton bases interacting through their base in a symmetric manner, with the fibre protruding outside. The formation of this structure is only due to the penton base, as dodecahedron lacking the fibre (Bs-Dd) could be produced in the baculovirus system [Fender *et al.,* 1997]. Interestingly, both Pt-Dd and Bs-Dd interact with HS with an affinity in the nanomolar range, indicating that the base protein is involved in HS binding and that the fibre does not interfere with this process [Vives *et al.,* 2004b]. The functional aspects of both dodecahedron production during the viral cycle, and strong interaction with HS are unknown. However, as these particles can be utilised for protein transduction, their ability to interact with HS is of large interest in this context (see paragraph 2.3).

Another interesting example of HS-using viruses is that of adenovirus associated virus (AAV). AAVs were discovered associated to adenovirus infection [Blacklow *et al.,* 1968]. Their replication is dependent on a helper virus, such as adenovirus or herpesvirus. However, AAVs can enter cells on their own. Three different AAV-2 receptors have been reported so far: HSPGs [Summerford *et al.,* 1998]; the FGF receptor 1 (FGFR1) [Qing *et al.,* 1999] and integrins v 5 [Summerford *et al.,* 1999], although the involvement of this latter receptor has been challenged in other studies. In any case, AAV-2 binding to HSPGs is critical for entry into cells. Indeed, studies showed that relatively low concentrations of soluble heparin (5 µg/ml) nearly completely inhibited the binding of AAV-2 to HeLa cells, whereas other GAGs such as dermatan sulphate, or chondroitin sulphate A and C, had negligible effect on the virus binding [Summerford *et al.,*1998]. In agreement with this, enzymatic digestion of cells by heparin lyases reduced viral adsorption on HeLa cells by 80%. Moreover, the use of CHO mutants that do not express HSPG or express undersulphated GAGs at their surfaces confirmed the role of HSPG as a primary attachment receptor for AAV-2. Binding to GAGs involves the VP capsid proteins, and may explain the broad tropism of the virus.

For many viruses, the role of HS as a low specificity, preliminary attachment receptor has been reported and

clearly documented, at least in cell culture. However, it should be noted that HS-binding activity can emerge as a result of virus adaptation to replication in cultured cells, in which viral variants carrying substitutions of positively charged instead of acid or neutral amino acids in the attachment protein, have been selected. If this makes difficult the extrapolation of the conclusions raised from laboratory strains to primary isolates, this also indicates that viruses have an advantage to attach cell through HS, a situation likely to be the case for viral vectors that have been propagated and amplified on cultured cells.

1.2.2 PGs are Involved in Virus Storage and Protection

Evidences have also indicated that HS could play more intricate roles in the mechanisms of viral infection. It has been recently observed that HIV-1 ability to bind to HS was related to viral tropism. HIV-1 infection of a host cell is based on the recognition of two distinct classes of cell surface molecules: the primary receptor CD4 and a coreceptor, mostly chemokine receptors CXCR4 and CCR5. The use of one coreceptor or the other defines viral tropism: R5 strains (using CCR5 as a coreceptor) preferentially infect monocytes and macrophages, while CXCR4-using strains target CD4+ T-lymphocytes. The ability to bind to HS seems to be restricted to X4 strains [Moulard *et al.,* 2000]. Such tropism specific property may explain physiological differences observed *in vivo*. In particular, the preferential 'trapping' of X4 viruses onto cell surface HSPGs could lead to selective exhaustion of these viral phenotypes observed in the early stage of the infection. Such a phenomenon may help to explain the preferential transmission and early dominance of R5 viruses over X4 viruses *in vivo*. In support to this, a study has recently shown that non permissive endothelial cells could trap HIV at their surface *via* interaction with their HS, store it for several days without loss of infectivity (whereas free virus would be rapidly inactivated) and transfer it to circulating T lymphocytes through a mechanism of "in trans" infection (Fig. **2b**). Furthermore, another recent study has suggested that HS interaction with HIV-1 envelope glycoprotein gp120 could interfere with gp120 binding to the virus coreceptors, a process that is the prerequisite of virus-cell membrane fusion [Vives *et al.,* 2005]. Although the precise role of HS in the regulation of HIV-1 entry remains unclear, these results strongly suggest a participation of the polysaccharide in late, post-binding events of the infection process.

1.2.3 PGs Participate to Both Virus Attachment and Entry Processes

For other viruses, such as vaccinia virus and HSV-1, a direct role of HS in cell entry mechanisms has already been demonstrated. For the latter, HS is implicated at two distinct stages of the infection. HS participates to cell attachment *via* interactions with viral envelope glycoproteins gB and gC, [Shukla *et al.,* 1999] but is also one of the entry receptor recognised by glycoprotein gD [Liu *et al.,* 2002]. More interestingly, binding to gD was shown to be dependent upon precise and rare saccharide motifs on the HS chains comprising a 3-O-sulphated glucosamine residue (Fig. **2c**). This finding suggests therefore the existence of two different strategies for the use of HS by viruses: the traditionally recognised "low specificity" binding, for which abundance and charge content of HS provide both efficient attachment and

large infection tropism, and an emerging "high specificity" approach, in which viruses would bind to defined saccharide epitopes involved in more critical steps of the infection and enabling a cell targeting restricted to those expressing such motifs. Better insights into this last strategy may of great importance for both understanding viral infection mechanisms and engineering new viral vectors for gene therapy applications.

In this context, defining the molecular determinants of HS interaction with viral proteins has become more and more critical. Structural characterisation of protein/GAG interactions still remains a challenging issue. Nevertheless, great progress in the field can be mentioned and have involved a number of innovative approaches. Structural determinants of HS interaction with viral proteins, such as AAV-2 capsid protein [Kern *et al.,* 2003], pseudorabbies gC [Trybala *et al.,* 1998] , HSV-1 gC [Mardberg *et al.,* 2001] , HIV gp120 [Moulard *et al.,* 2000; Vives *et al.,* 2005] , or vaccinia virus A27L [Ho *et al.,* 2005] , have been clarified, with the help of site directed mutagenesis or surface pasmon resonance analysis. Identification of HS critical 3-O-sulphate group for binding to HSV-1 gD glycoprotein (see above) was first achieved, following the observation that expression of specific HS 3-O-sulfotransferases involved in the biosynthesis of the polysaccharide were associated with cell permissivity to the virus [Shukla *et al.,* 1999] . Later on, screening of oligosaccharide libraries enabled the isolation and characterisation of a HS structural motif binding to gD [Liu *et al.,* 2002] . In another interesting work, the full structure of FMDV virus in complex with a heparin oligosaccharide was elucidated by X-Ray crystallography [Fry *et al.,* 1999] . Very recently, a complex involving heparin and the Ross River virus has been analysed by electron cryo-microspcopy [Zhang *et al.,* 2005] . These two studies provided detailed mapping of the polysaccharide/virus interface.

2. TAMPERING WITH HS BINDING PROPERTIES OF VIRAL VECTORS: APPLICATIONS IN GENE THERAPY

In the context of gene therapy, interaction of recombinant viruses with HS can be looked at with two opposite points of view. On one hand, the large HS dependent hepatic tropism reported for recombinant virus injected in preclinical trials can be considered as a negative effect of this interaction. Indeed, for *in vivo* experiments, the massive retention of transfer vectors by the liver prevents an efficient targeting of others organs or tumours. On the other hand, adapting viral vectors to the use of HS can be beneficial to broaden the tropism to cells that would not be permissive otherwise. Such approach has been proved efficient in *ex vivo* experiments or for direct injections into target tissues.

2.1 Targeting HSPGs: How to Broaden Gene Delivery

For several applications, the interaction of viral vectors with HS is beneficial and it can even be desirable to artificially improve this interaction. Increasing the binding of recombinant adenovirus (RAd) to the polysaccharide has been successfully achieved by insertion of short, positively charged HS binding motifs within the exposed region of the capsid. It has been first elegantly reported that the suppression of the fibre stop codon led to the translation of the en-

coding mRNA polyA tail, resulting in the addition of a polylysine sequence at the C-terminus (in the head domain) of the fibre [Wickham *et al.,* 1996] . Such kind of C-terminus insertion has been improved further by the cloning of a stretch of 7 lysines, downstream a flexible Glycine-Serine arm (AdpK7) [Wickham *et al.,* 1997] . On the basis of the high-resolution structure of the fibre head domain [Xia *et al.,* 1994] , the polylysine stretch was also inserted within the very exposed and flexible HI loop of this domain. However, HS interaction resulting from this latter insertion appeared to be slightly less efficient, compared to insertions at the fibre C-terminus [Koizumi *et al.,* 2003]. Nevertheless, whatever the insertion site, these approaches consistently improved vector entry, with yields varying amongst cell types. For epithelial cells that are naturally easily infected by Ads, the use of modified RAd harbouring HS binding motifs resulted in a very modest increase of cell transduction (1 to 2 fold increase). In contrast, entry efficiency was dramatically increased for cells that are normally not permissive to wild type Ads, including macrophages, smooth muscle cells or endothelial cells. This increase was the result of RAd ability to bind to HS, as AdpK7 entry into cells that do not express the CAR receptor was totally abolished by cell treatment with heparinase, whereas chondroitinase or neuraminidase treatment had no effect.

Such strategy aiming at increasing cell transduction levels is not restricted to *ex vivo* applications. It has been demonstrated that Adpk7 could penetrate human glioblastoma cells 70 times more efficiently than the unmodified Rad, suggesting a possible use of this vector for direct injections in tumours. In addition, primary endothelial cells, such as HuVEC, that are known to be poorly infected by adenovirus, are 50 times more sensitive to AdpK7. This latter observation suggests again potential therapeutical applications. Improved targeting of endothelial cells could be of interest in anti-angiogenic strategies, aiming at restricting tumour growth and metastasis spreading, or in the prevention of restenosis as the endothelium is lesioned during angioplasty. Interestingly, cell entry efficacy could be further enhanced by combining the addition of HS binding motifs with modifications enabling recognition of other cell surface molecules. It has indeed been reported that AdpK7 harbouring a RGD peptide displayed an increased transduction efficiency on human cervix carcinoma, both in cell culture assays and in *in vivo* experiments [Rein *et al.,* 2004] . Addition of HS binding motifs has not been restricted to the fibre protein. Another capsid protein, the minor pIX protein, has also been engineered to comprise a polybasic sequence within their ectodomain [Dmitriev *et al.,*2002]. Advantages are the higher number of pIX trimers (80 copies versus 12 fibre trimers) and their repartition at the virion facets, [Fabry *et al.,* 2005] . However, modification of this cimenting protein was shown to partially disturb the stability of the virion architecture.

Another aspect that may favour the development of viral vectors with a tropism for HS is the recent observation that HS may be responsible for HIV ability to cross the blood brain barrier (BBB). Contrary to other retroviruses, HIV can infect resting cells including, in particular, cells of the central nervous system. Although this property has not been exploited yet in gene therapy, stereotaxic injections of HIV have been widely reported [Blomer *et al.,* 2002] . A study

has recently shown that HSPGs were involved in HIV brain invasion. Interaction of HS with basic domains of HIV gp120 enables capture of the virus at the surface of CD4 negative endothelial cells and migration through the BBB [Bobardt *et al.,* 2004] . This transcytosis process is not fully understood, but cannot be inhibited by the natural ligands of CXCR4 or CCR5 coreceptors (SDF-1a, RANTES or MIP). Moreover, virus lacking gp120 failed to cross this biological membrane, reinforcing the idea of a CD4 independent binding of gp120 to HSPGs. In support to this, previous studies reported that syndecans greatly enhanced HIV binding on both CD4+ cells, such as macrophages or T-lymphocytes, and CD4- cells, including HuVEC and human genital epithelial cells [Bobardt *et al.,* 2003; Patel *et al.,* 1993; Saphire *et al.,* 2001; Wu *et al.,* 2003] . The adaptation of viral vectors to the use of a HS mediated BBB cross-over pathway would represent a major step forward for the delivery of neurotrophic factors in neurodegenerative diseases.

2.2. Detargeting HSPGs: How to Increase Specificity

For gene therapy applications aiming specific tissues such as metastasis, interaction with HS could represent a major drawback, as viral vectors may be diverted from their targets and trapped within HS rich organs, such as the liver. To overcome this, HS detargeting strategies have been developed, mainly for adenovirus and AAV based vectors. To target Ad5 derived vectors to a specific receptor, the invalidation of both CAR and integrin tropism is not sufficient. It has been demonstrated that this vector still displayed a very pronounced hepatic tropism [Martin *et al.,* 2003] and thus, that the abolition of Ad5 HS binding properties was required to enable efficient targeting of specific markers. To do this, the basic sequence found in the shaft of Ad5 fibre was first mutated. Resulting RAds showed a 50% transduction reduction in rat liver [Nicol *et al.,* 2004] . Combining this fibreshaft mutation to fibre-head mutations that prevented CAR recognition resulted in a dramatic decrease (95%) of adenovirus transfer to the liver. A 99% reduction of rat liver transduction could even be achieved by a further deletion of the RGD motif required for integrin binding [Nicol *et al.,* 2004] . Altogether, these data show that HS is one of the major factor responsible for Rad hepatic tropism, but also that other receptors are involved in this process. These results have been further supported by *in vivo* trials in non-human primates that demonstrated the importance of HS binding on tissue targeting. Indeed, while RAds harbouring mutations for CAR recognition displayed no significant modifications of their bio-distribution (mostly in liver and spleen), a dramatic change was observed for RAds lacking HS binding motifs, with a significant decrease in delivery for all examined organs [Smith *et al.,* 2003] . Hence, the design of new vectors may require appropriate modifications to achieve HS detargeting and allow efficient "retargeting" towards specific markers.

Abrogation of HS binding properties has also been considered for AAV-2 based vectors. One interesting property of AAV-2 lies on the fact that its genome is integrated at a specific site into human chromosome 19 [Kotin *et al.,* 1990; Samulski *et al.,* 1991]. Although this feature is lost in AAVs vectors their non-immunogenic properties have made of this virus one of the most promising viral vectors for gene therapy.

The broad range of cells permissive to AAV-2 is another advantage for gene transfer applications, such as *ex-vivo* DNA delivery or direct injection into an organ or a tissue. On the contrary, the low binding specificity of this vector is a clear limitation for delivery through intravenous injections. A number of studies aimed at redirecting AAV-2 to specific target cells by inserting motifs in the VP capsid. AAV-2 vector with a VP protein harbouring an endothelial-specific peptide inserted at the level of residue 587 was able to enter HuVEC, using a HS-independent pathway, as addition of soluble heparin had no effect on transduction efficiency [Nicklin *et al.,* 2001] . In contrast to wt-AAV-2, such modified virus was not retained on a heparin column, indicating that the peptide insertion had induced structural modifications that altered the heparin binding site. Another work reported that the deletion of six residues at position 586-591 (GN<u>R</u>QAA) of the VP protein resulted in the loss of HSPG recognition. Interestingly, the insertion of a peptide (NG<u>R</u>AHA) identified by phage display to specifically target CD13, a receptor expressed in the angiogenic vasculature and many tumour cell lines, restored binding to HSPG interaction and thus, demonstrated the involvement of R588 in the interaction [Grifman *et al.,* 2001] . Several studies have also reported the insertion of a RGD peptide into the VP protein, at different positions, without impairing the virus titre. This addition of a RGD motif increased only moderately the transduction of cells expressing both integrins and HSPGs, including HeLa cells, but dramatically enhanced transduction in cells that expressed low levels of HSPG, such as Raji cells. Interestingly, Ovarian carcinoma cell (SKOV-3) that are poorly transduced by wt-AAV-2 are permissive to RGD-AAV vectors [Shi *et al.,* 2003] . Surprisingly, contrary to wt-AAV, RGD-AAVs were not susceptible to addition of soluble heparin, indicating that the "RGD pathway" was completely independent from HSPG. Such strategy is promising, especially for the targeting of tumours that overexpress integrins [Albelda *et al.,* 1990; Gladson *et al.,* 1991; Lessey *et al.,* 1995] . Recently, the HS binding site on AAV-2 capsid has been fully characterised [Kern *et al.,* 2003; Opie *et al.,* 2003] . In correctly assembled VP trimers, a number of basic residues (R484, R487, K532 in one site and R585, R588 in another site of the VP capsid proteins) are gathered in clusters that form the HS binding domain (Fig. **4**). Interestingly, mutation of residue R475 that is not exposed at the capsid surface strongly reduced binding of AAV-2 to heparin, this being most likely due to an indirect structural effect that disturbs the correct assembly of VP subunits and the subsequent formation of the HS binding clusters. Mutations on residues of the HS binding site have been performed to alter AAV tropism for the polysaccharide. An *in vivo* experiment was undertaken in immuno-competent mice by injection in the tail vein of a wild-type or a double mutated (R484E, R585E) recombinant AAV-2 encoding for luciferase. Three weeks after injection, luciferase activity was detected predominantly in the liver, heart and to a lesser extent in kidney of mice treated with wild type vector, whereas the luciferase activity was only detected in the heart, for animals injected with the mutated vector. For these animals, luciferase activity detected in the heart was fifteen times higher than for wild type AAV-2 treated mice [Kern *et al.,* 2003].
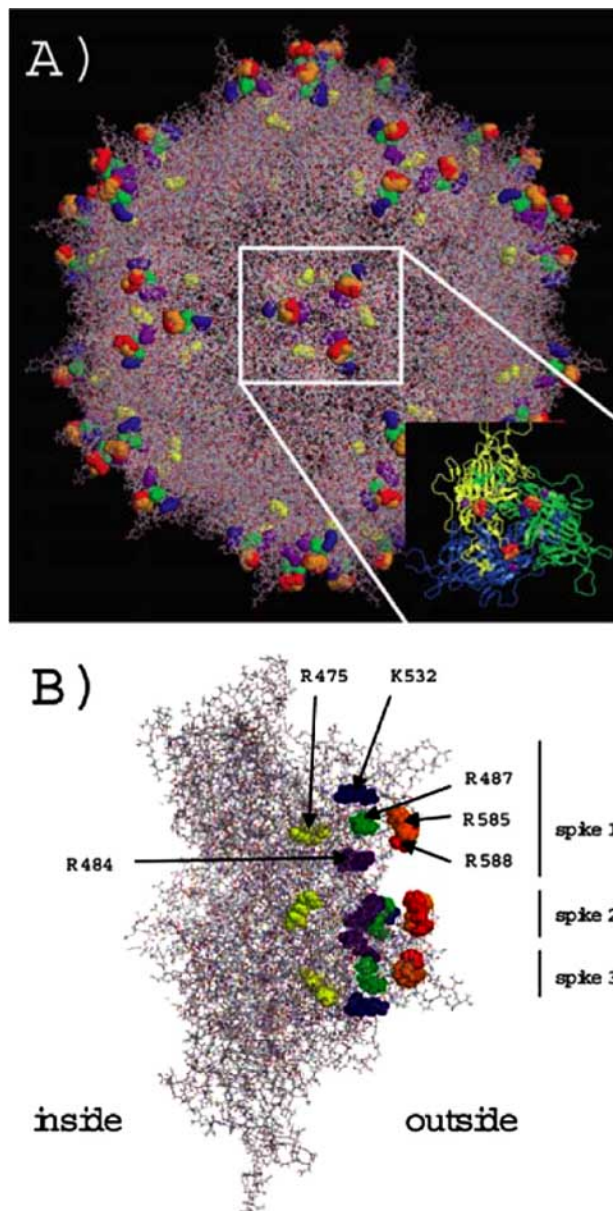
Fig. (4). Clustering of basic residues forms HS binding sites on the AAV capsid.

(a) The amino acids involved in heparin binding are grouped in three clusters at the threefold spike region of the capsid: R585 (orange), R588 (red), R484 (purple), R487 (green), K532 (blue) and R475 (yellow). (b) A side view of a VP trimer shows the surface exposure of the basic clusters at the inner shoulder of the threefold spikes and along a channel-like structure between the threefold spikes.

(Reproduced from Kern *et al.,* 2003 with permission).

A last interesting example on how HS can constitute an obstacle in gene therapy is that of retrovirus vectors. Retroviruses are the most utilised vectors in gene therapy. Their success is mainly based on their ability to integrate the gene of interest in the cellular genome, this providing a hereditary correction of the phenotype to daughter cells. Such feature is particularly used for *ex vivo* correction of cells before re-

implantation [Cavazzana-Calvo *et al.,* 2000]. Binding of retroviruses to widely express receptors, such as HS, is thus critical for both *in vivo* and *ex vivo* applications. It has been shown that the envelope of retroviruses can feature HSPGs that were recovered from the plasma membrane of the infected cell during the budding process of the progeny virions. These negatively charged molecules embedded in the virion could have a negative effect on cell attachment, as they generate small electrostatic forces that may repel the virus from the cell surface. To overcome this problem, retroviral vectors have been treated with positively charged molecule like polybrene [Davis *et al.,* 2002]. This treatment clearly improved direct interaction of the virus with the targeted cell. In another approach designed for *ex vivo* applications, the retrovirus vector was complexed with HS and allowed to bind to fibronectin (FN) coated plates. The HS-fibronectin interaction resulted in neutralisation of the molecule charges and contributed to immobilising the vector at the surface of the plate. As the traction force that cell exerts on the substrate was considerably larger than the repulsive force of the virion, retroviral vector penetration would then occur [Lei *et al.,* 2002] . This two step mechanism showed more efficiency than the direct interaction of polybrene-treated retroviral vectors with cells.

2.3. HSPGs and Protein/Peptide Vectors

Recently, a series of virus-encoded and regulatory proteins showed the ability to cross biological membranes. For example, peptides derived from the Drosophila Antennapedia homeodomain are internalised by cells in culture [Derossi *et al.,* 1994] and transferred to the cell nucleus where they can directly and specifically interfere with the transcription [Derossi *et al.,* 1996; Le Roux *et al.,* 1995] . HIV-1 Tat protein is rapidly taken up by the cell *in vitro* and can specifically transactivate the HIV-LTR [Frankel *et al.,* 1988; Green *et al.,*1988] . The Tat protein is composed of about one hundred amino acids including a highly basic region and a cysteine-rich region. It was shown that Tat-derived peptides as short as 11 amino acids are sufficient for transduction of proteins [Fawell *et al.,* 1994; Nagahara *et al.,* 1998] . A Tat-galactosidase fusion protein could be efficiently delivered into brain tissue and skeletal muscle *in vivo* [Schwartz *et al.,*, 2000] . For a long time, the precise mechanism by which the 11-amino acid transduction domain could cross lipid bilayers was poorly understood, but a recent study demonstrated that Tat or Antenapedia peptide endocytosis was promoted by interaction with cellular glycosaminoglycans [Console *et al.,* 2003] . This has also been described for other viral trans-activators. The Zebra protein of the Epstein Barr Virus (EBV), has recently been shown to enter lymphoid cells through a HS dependant pathway [Mahot *et al.,* 2005]. Similarly, the Rep68 protein of AAV-2 has been reported to enter cells, through clathrin-dependent endocytosis mediated by HS, and to reach the nucleus where it regulates viral promoters [Awedikian *et al.,* 2005] . Altogether, these results show that HS mediated cell entry is a mechanism shared by several viral proteins.

Beside these viral peptides, a virus-like particle derived from adenovirus called dodecahedron (Dd) has been developed for protein delivery into cells. A clear advantage of this sub-viral particle is that it retains adenovirus endocytotic

features but is devoid of genetic material. The proof of concept of Dd use for protein delivery has been made for large multimeric proteins, such as a monoclonal antibody [Fender *et al.,* 2003] . Recently, a universal adaptor has been developed to make of Dd a versatile vector for protein transduction [Garcel *et al.,* in press]. The efficiency of this new system is surprisingly high, with an average of 10^7 proteins of interest imported per cell. This efficacy can be explained, in part, by the ability of Dd to bind with high affinity to cellular HS, this interaction mediating cell entry through a fibre independent internalisation pathway [Vives *et al.,* 2004b] . This confers to Dd the ability to enter a wide range of cell lines, including cells that are not permissive to adenovirus.

CONCLUSION

Understanding the mechanisms by which HS participates to viral infection has become a critical issue for gene therapy applications, as increasing evidence show that the binding of viral vectors to HS can dramatically influence cell entry efficiency, tropism and biodistribution. On one hand, this interaction can be beneficial, as the broad expression of HS by a variety of cells enables ubiquitous delivery of the therapeutic genes. With this respect, efforts have been made to engineer viral vectors with increased affinity for this polysaccharide. Addition of polybasic sequences in their capsid protein yielded promising results, with a dramatic increase in transduction efficiency for cells that would normally be poorly permissive to the virus. On the other hand, for *in vivo* applications, injection of viral vectors in the bloodstream often results in the accumulation of the virus in HS rich organs, such as the liver, which thus prevents efficient delivery to a specific target tissue. Hence, new strategies were developed to "detarget" the vectors from their natural receptors, including HS, and retarget them for the recognition of specific ligand. With the recent finding that HSV-1 entry into cells could be mediated by rare HS motifs of precise sulphation pattern, a new view has emerged on the role of this polysaccharide during viral infection. Binding to HS can also be highly specific and may be used to drive infection towards the only tissues expressing particular saccharide epitopes at their surface. Further insights into the structural basis of virus-HS recognition will be crucial for the design of viral vectors with improved specificity and efficiency.

ABBREVIATIONS

AAV   =   Adenovirus-Associated Virus

Ad   =   Adenovirus

Bs-Dd =   Base-Dodecahedron

CAR   =   Coxsackie and Adenovirus Receptor

Dd   =   Dodecahedron

EBV   =   Epstein Barr Virus

FMDV   =   Foot and Mouth Virus

GAGs   =   Glycosaminoglycans

HIV   =   Human Immunodeficiency Virus

HS   =   Heparan Sulphate

HSPGs =   Heparan Sulphate Proteoglycans

HSV   =   Herpes Simplex Virus

LTR   =   Long Terminal Repeat

PGs   =   Proteoglycans

Pt-Dd =   Penton-Dodecahedron

RAd   =   Recombinant Adenovirus

REFERENCES

Albelda, S.M., Mette, S.A., Elder, D.E., Stewart, R., Damjanovich, L., Herlyn, M., and Buck, C.A. (1990) Integrin distribution in malignant melanoma: association of the beta 3 subunit with tumor progression. *Cancer Res.,* **50**: 6757-64.

Ancsin, J.B., and Kisilevsky, R. (2004) A binding site for highly sulfated heparan sulfate is identified in the N terminus of the circumsporozoite protein: significance for malarial sporozoite attachment to hepatocytes. *J. Biol. Chem.,* **279**: 21824-32.

Awedikian, R., Francois, A., Guilbaud, M., Moullier, P., and Salvetti, A. (2005) Intracellular route and biological activity of exogenously delivered Rep proteins from the adeno-associated virus type 2. *Virology,* **335**: 252-63.

Bergelson, J.M., Cunningham, J.A., Droguett, G., Kurt-Jones, E.A., Krithivas, A., Hong, J.S., Horwitz, M.S., Crowell, R.L., and Finberg, R.W. (1997) Isolation of a common receptor for Coxsackie B viruses and adenoviruses 2 and 5. *Science,* **275**: 1320-3.

Bernfield, M., Gotte, M., Park, P.W., Reizes, O., Fitzgerald, M.L., Lincecum, J., and Zako, M. (1999) Functions of cell surface heparan sulfate proteoglycans. *Annu. Rev. Biochem.,* **68**: 729-77.

Blacklow, N.R., Hoggan, M.D., Kapikian, A.Z., Austin, J.B., and Rowe, W.P. (1968) Epidemiology of adenovirus-associated virus infection in a nursery population. *Am. J. Epidemiol.,* **88**: 368-78.

Blomer, U., Ganser, A., and Scherr, M. (2002) Invasive drug delivery. *Adv. Exp. Med. Biol.,* **513:** 431-51.

Bobardt, M.D., Salmon, P., Wang, L., Esko, J.D., Gabuzda, D., Fiala, M., Trono, D., Van der Schueren, B., David, G., and Gallay, P.A. (2004) Contribution of proteoglycans to human immunodeficiency virus type 1 brain invasion. *J. Virol.,* **78**: 6567-84.

Bobardt, M.D., Saphire, A.C., Hung, H.C., Yu, X., Van der Schueren, B., Zhang, Z., David, G., and Gallay, P.A. (2003) Syndecan captures, protects, and transmits HIV to T lymphocytes. *Immunity,* **18**: 27-39.

Carruthers, V.B., Hakansson, S., Giddings, O.K., and Sibley, L.D. (2000) Toxoplasma gondii uses sulfated proteoglycans for substrate and host cell attachment. *Infect. Immun.,* **68**: 4005-11.

Cavazzana-Calvo, M., Hacein-Bey, S., de Saint Basile, G., Gross, F., Yvon, E., Nusbaum, P., Selz, F., Hue, C., Certain, S., Casanova, J.L., Bousso, P., Deist, F.L., and Fischer, A. (2000) Gene therapy of human severe combined immunodeficiency (SCID)-X1 disease. *Science,* **288**: 669-72.

Chen, Y., Maguire, T., Hileman, R.E., Fromm, J.R., Esko, J.D., Linhardt, R.J., and Marks, R.M. (1997) Dengue virus infectivity depends on envelope protein binding to target cell heparan sulfate. *Nat. Med.,* **3**: 866-71.

Console, S., Marty, C., Garcia-Echeverria, C., Schwendener, R., and Ballmer-Hofer, K. (2003) Antennapedia and HIV transactivator of transcription (TAT) "protein transduction domains" promote endocytosis of high molecular weight cargo upon binding to cell surface glycosaminoglycans. *J. Biol. Chem.,* **278**: 35109-14.

Davis, H.E., Morgan, J.R., and Yarmush, M.L. (2002) Polybrene increases retrovirus gene transfer efficiency by enhancing receptor-independent virus adsorption on target cell membranes. *Biophys. Chem.,* **97**: 159-72.

Dechecchi, M.C., Melotti, P., Bonizzato, A., Santacatterina, M., Chilosi, M., and Cabrini, G. (2001) Heparan sulfate glycosaminoglycans are receptors sufficient to mediate the initial binding of adenovirus types 2 and 5. *J. Virol.,* **75**: 8772-80.

Dechecchi, M.C., Tamanini, A., Bonizzato, A., and Cabrini, G. (2000) Heparan sulfate glycosaminoglycans are involved in adenovirus type 5 and 2-host cell interactions. *Virology,* **268**: 382-90.

Delehedde, M., Allain, F., Payne, S.J., Borgo, R., Vampouille, C., Fernig, D.G., and Deudon, E. (2002) Proteoglycans in Inflammation. *Curr. Med. Chem.,* **1:** 89-102.

Derossi, D., Calvet, S., Trembleau, A., Brunissen, A., Chassaing, G., and Prochiantz, A. (1996) Cell internalization of the third helix of the Antennapedia homeodomain is receptor-independent. *J. Biol. Chem.,* **271**: 18188-93.

Derossi, D., Joliot, A.H., Chassaing, G., and Prochiantz, A. (1994) The third helix of the Antennapedia homeodomain translocates through biological membranes. *J. Biol. Chem.,* **269**: 10444-50.

Dmitriev, I.P., Kashentseva, E.A., and Curiel, D.T. (2002) Engineering of adenovirus vectors containing heterologous peptide sequences in the C terminus of capsid protein IX. *J. Virol.,* **76**: 6893-9.

Esko, J.D., and Lindahl, U. (2001) Molecular diversity of heparan sulfate. *J. Clin. Invest.,* **108**: 169-73.

Esko, J.D., and Selleck, S.B. (2002) Order Out of Chaos: Assembly of Ligand Binding Sites in Heparan Sulfate. *Annu. Rev. Biochem.,* **71:** 435-71.

Fabry, C.M., Rosa-Calatrava, M., Conway, J.F., Zubieta, C., Cusack, S., Ruigrok, R.W., and Schoehn, G. (2005) A quasi-atomic model of human adenovirus type 5 capsid. *EMBO J.,* **24**: 1645-54

Fallgren, C., Andersson, A., and Ljungh, A. (2001) The role of glycosaminoglycan binding of staphylococci in attachment to eukaryotic host cells. *Curr. Microbiol.,* **43**: 57-63.

Fawell, S., Seery, J., Daikh, Y., Moore, C., Chen, L.L., Pepinsky, B., and Barsoum, J. (1994) Tat-mediated delivery of heterologous proteins into cells. *Proc. Natl. Acad. Sci. USA,* **91**: 664-8.

Fender, P., Ruigrok, R.W., Gout, E., Buffet, S., and Chroboczek, J. (1997) Adenovirus dodecahedron, a new vector for human gene transfer. *Nat. Biotechnol.,* **15**: 52-6.

Fender, P., Schoehn, G., Foucaud-Gamen, J., Gout, E., Garcel, A., Drouet, E., and Chroboczek, J. (2003) Adenovirus dodecahedron allows large multimeric protein transduction in human cells. *J. Virol.,* **77**: 4960-4.

Frankel, A.D., and Pabo, C.O. (1988) Cellular uptake of the tat protein from human immunodeficiency virus. *Cell,* **55**: 1189-93.

Fry, E.E., Lea, S.M., Jackson, T., Newman, J.W., Ellard, F.M., Blakemore, W.E., Abu-Ghazaleh, R., Samuel, A., King, A.M., and Stuart, D.I. (1999) The structure and function of a foot-and-mouth disease virus-oligosaccharide receptor complex. *EMBO J.,* **18**: 543-54.

Gallagher, J.T. (2001) Heparan sulfate: growth control with a restricted sequence menu. *J. Clin. Invest.,* **108**: 357-61.

Garcel, A., Gout, E., Timmins, J., Chroboczek, J., and Fender, P. Protein transduction into human cells by adenovirus dodecahedron using WW domains as universal adaptors. *J. Gene Med.,* in press.

Geuijen, C.A., Willems, R.J., Hoogerhout, P., Puijk, W.C., Meloen, R.H., and Mooi, F.R. (1998) Identification and characterization of heparin binding regions of the Fim2 subunit of Bordetella pertussis. *Infect Immun.,* **66**: 2256-63.

Ginsberg, H.S., Pereira, H.G., Valentine, R.C., and Wilcox, W.C. (1966) A proposed terminology for the adenovirus antigens and virion morphological subunits. *Virology,* **28**: 782-3.

Gladson, C.L., and Cheresh, D.A. (1991) Glioblastoma expression of vitronectin and the alpha v beta 3 integrin. Adhesion mechanism for transformed glial cells. *J. Clin. Invest,* **88**: 1924-32.

Green, M., and Loewenstein, P.M. (1988) Autonomous functional domains of chemically synthesized human immunodeficiency virus tat transactivator protein. *Cell,* **55**: 1179-88.

Grifman, M., Trepel, M., Speece, P., Gilbert, L.B., Arap, W., Pasqualini, R., and Weitzman, M.D. (2001) Incorporation of tumor-targeting peptides into recombinant adeno-associated virus capsids. *Mol. Ther.,* **3**: 964-75.

Ho, Y., Hsiao, J.C., Yang, M.H., Chung, C.S., Peng, Y.C., Lin, T.H., Chang, W., and Tzou, D.L. (2005) The Oligomeric Structure of Vaccinia Viral Envelope Protein A27L is Essential for Binding to Heparin and Heparan Sulfates on Cell Surfaces: A Structural and Functional Approach Using Site-specific Mutagenesis. *J. Mol. Biol.,* **349**: 1060-71.

Iozzo, R.V., and San Antonio, J.D. (2001) Heparan sulfate proteoglycans: heavy hitters in the angiogenesis arena. *J. Clin. Invest.,* **108**: 349-55.

Jackson, T., Ellard, F.M., Ghazaleh, R.A., Brookes, S.M., Blakemore, W.E., Corteyn, A.H., Stuart, D.I., Newman, J.W., and King, A.M. (1996) Efficient infection of cells in culture by type O foot-and-mouth disease virus requires binding to cell surface heparan sulfate. *J. Virol.,* **70**: 5282-7.

Kern, A., Schmidt, K., Leder, C., Muller, O.J., Wobus, C.E., Bettinger, K., Von der Lieth, C.W., King, J.A., and Kleinschmidt, J.A. (2003) Identification of a heparin-binding motif on adeno-associated virus type 2 capsids. *J. Virol.,* **77**: 11072-81.

Klimstra, W.B., Ryman, K.D., and Johnston, R.E. (1998) Adaptation of Sindbis virus to BHK cells selects for use of heparan sulfate as an attachment receptor. *J. Virol.,* **72**: 7357-66.

Koizumi, N., Mizuguchi, H., Utoguchi, N., Watanabe, Y., and Hayakawa, T. (2003) Generation of fiber-modified adenovirus vectors containing heterologous peptides in both the HI loop and C terminus of the fiber knob. *J. Gene. Med.,* **5**: 267-76.

Kotin, R.M., Siniscalco, M., Samulski, R.J., Zhu, X.D., Hunter, L., Laughlin, C.A., McLaughlin, S., Muzyczka, N., Rocchi, M., and Berns, K.I. (1990) Site-specific integration by adeno-associated virus. *Proc. Natl. Acad. Sci. USA,* **87**: 2211-5.

Le Roux, I., Duharcourt, S., Volovitch, M., Prochiantz, A., and Ronchi, E. (1995) Promoter-specific regulation of gene expression by an exogenously added homedomain that promotes neurite growth. *FEBS Lett.,* **368**: 311-4.

Lee, E., and Lobigs, M. (2002) Mechanism of virulence attenuation of glycosaminoglycan-binding variants of Japanese encephalitis virus and Murray Valley encephalitis virus. *J. Virol.,* **76**: 4901-11.

Lei, P., Bajaj, B., and Andreadis, S.T. (2002) Retrovirus-associated heparan sulfate mediates immobilization and gene transfer on recombinant fibronectin. *J. Virol.,* **76**: 8722-8.

Lessey, B.A., Albelda, S., Buck, C.A., Castelbaum, A.J., Yeh, I., Kohler, M., and Berchuck, A. (1995) Distribution of integrin cell adhesion molecules in endometrial cancer. *Am. J. Pathol.,* **146**: 717-26.

Lindahl, U., Kusche-Gullberg, M., and Kjellen, L. (1998) Regulated diversity of heparan sulfate. *J. Biol. Chem.,* **273**: 24979-82.

Liu, J., Shriver, Z., Pope, R.M., Thorp, S.C., Duncan, M.B., Copeland, R.J., Raska, C.S., Yoshida, K., Eisenberg, R.J., Cohen, G., Linhardt, R.J., and Sasisekharan, R. (2002) Characterization of a heparan sulfate octasaccharide that binds to herpes simplex virus type 1 glycoprotein D. *J. Biol. Chem.,* **277**: 33456-67.

Liu, J., and Thorp, S.C. (2002) Cell surface heparan sulfate and its roles in assisting viral infections. *Med. Res. Rev.,* **22**: 1-25.

Lyon, M., and Gallagher, J.T. (1998) Bio-specific sequences and domains in heparan sulphate and the regulation of cell growth and adhesion. *Matrix Biol.,* **17**: 485-93.

Mahot, S., Fender, P., Vives, R.R., Caron, C., Perrissin, M., Gruffat, H., Sergeant, A., and Drouet, E. (2005) Cellular uptake of the EBV transcription factor EB1/Zta. *Virus Res.,* **110**: 187-93.

Mardberg, K., Trybala, E., Glorioso, J.C., and Bergstrom, T. (2001) Mutational analysis of the major heparan sulfate-binding domain of herpes simplex virus type 1 glycoprotein C. *J. Gen. Virol.,* **82**: 1941-50.

Martin, K., Brie, A., Saulnier, P., Perricaudet, M., Yeh, P., and Vigne, E. (2003) Simultaneous CAR- and alpha V integrin-binding ablation fails to reduce Ad5 liver tropism. *Mol. Ther.,* **8**: 485-94.

Mathias, P., Galleno, M., and Nemerow, G.R. (1998) Interactions of soluble recombinant integrin alphav beta5 with human adenoviruses. *J. Virol.,* **72**: 8669-75.

Moulard, M., Lortat-Jacob, H., Mondor, I., Roca, G., Wyatt, R., Sodroski, J., Zhao, L., Olson, W., Kwong, P.D., and Sattentau, Q.J. (2000) Selective interactions of polyanions with basic surfaces on human immunodeficiency virus type 1 gp120. *J. Virol.,* **74**: 1948-60.

Nagahara, H., Vocero-Akbani, A.M., Snyder, E.L., Ho, A., Latham, D.G., Lissy, N.A., Becker-Hapak, M., Ezhevsky, S.A., and Dowdy, S.F. (1998) Transduction of full-length TAT fusion proteins into mammalian cells: TAT-p27Kip1 induces cell migration. *Nat. Med.,* **4**: 1449-52.

Nicklin, S.A., Buening, H., Dishart, K.L., de Alwis, M., Girod, A., Hacker, U., Thrasher, A.J., Ali, R.R., Hallek, M., and Baker, A.H. (2001) Efficient and selective AAV2-mediated gene transfer directed to human vascular endothelial cells. *Mol. Ther.,* **4**: 174-81.

Nicol, C.G., Graham, D., Miller, W.H., White, S.J., Smith, T.A., Nicklin, S.A., Stevenson, S.C., and Baker, A.H. (2004) Effect of adenovirus serotype 5 fiber and penton modifications on *in vivo* tropism in rats. *Mol. Ther.,* **10**: 344-54.

Norrby, E. (1966) The relationship between the soluble antigens and the virion of adenovirus type 3. II. Identification and characterization of an incomplete hemagglutinin. *Virology,* **30**: 608-17.

Opie, S.R., Warrington, K.H., Jr., Agbandje-McKenna, M., Zolotukhin, S., and Muzyczka, N. (2003) Identification of amino acid residues in the capsid proteins of adeno-associated virus type 2 that contribute to heparan sulfate proteoglycan binding. *J. Virol.,* **77**: 6995-7006.

Patel, M., Yanagishita, M., Roderiquez, G., Bou-Habib, D.C., Oravecz, T., Hascall, V.C., and Norcross, M.A. (1993) Cell-surface heparan sulfate proteoglycan mediates HIV-1 infection of T-cell lines. *AIDS Res. Hum. Retroviruses,* **9**: 167-74.

Perrimon, N., and Bernfield, M. (2000) Specificities of heparan sulphate proteoglycans in developmental processes. *Nature,* **404**: 725-8.

Petitou, M., Casu, B., and Lindahl, U. (2003) 1976-1983, a critical period in the history of heparin: the discovery of the antithrombin binding site. *Biochimie,* **85**: 83-9.

Petitou, M., Herault, J.P., Bernat, A., Driguez, P.A., Duchaussoy, P., Lormeau, J.C., and Herbert, J.M. (1999) Synthesis of thrombin-inhibiting heparin mimetics without side effects. *Nature,* **398**: 417-22.

Petitou, M., Imberty, A., Duchaussoy, P., Driguez, P.A., Ceccato, M.L., Gourvenec, F., Sizun, P., Herault, J.P., Perez, S., and Herbert, J.M. (2001) Experimental proof for the structure of a thrombin-inhibiting heparin molecule. *Chemistry,* **7**: 858-73.

Qing, K., Mah, C., Hansen, J., Zhou, S., Dwarki, V., and Srivastava, A. (1999) Human fibroblast growth factor receptor 1 is a co-receptor for infection by adeno-associated virus 2. *Nat. Med.,* **5**: 71-7.

Rapraeger, A.C., Krufka, A., and Olwin, B.B. (1991) Requirement of heparan sulfate for bFGF-mediated fibroblast growth and myoblast differentiation. *Science,* **252**: 1705-8.

Rein, D.T., Breidenbach, M., Wu, H., Han, T., Haviv, Y.S., Wang, M., Kirby, T.O., Kawakami, Y., Dall, P., Alvarez, R.D., and Curiel, D.T. (2004) Gene transfer to cervical cancer with fiber-modified adenoviruses. *Int. J. Cancer,* **111**: 698-704.

Roelvink, P.W., Lizonova, A., Lee, J.G., Li, Y., Bergelson, J.M., Finberg, R.W., Brough, D.E., Kovesdi, I., and Wickham, T.J. (1998) The coxsackievirus-adenovirus receptor protein can function as a cellular attachment protein for adenovirus serotypes from subgroups A, C, D, E, and F. *J. Virol.,* **72**: 7909-15.

Rostand, K.S., and Esko, J.D. (1997) Microbial adherence to and invasion through proteoglycans. *Infect. Immun.,* **65**: 1-8.

Sadir, R., Forest, E., and Lortat-Jacob, H. (1998) The heparan sulfate binding sequence of interferon-gamma increased the on rate of the interferon-gamma-interferon-gamma receptor complex formation. *J. Biol. Chem.,* **273**: 10919-25.

Sadir, R., Imberty, A., Baleux, F., and Lortat-Jacob, H. (2004) Heparan sulfate/heparin oligosccharides protect stromal cell-derived factor-1 (SDF-1)/CXCL12 against proteolysis induced by CD26/dipeptidyl peptidase IV. *J. Biol. Chem.,* **279**: 43854-60

Samulski, R.J., Zhu, X., Xiao, X., Brook, J.D., Housman, D.E., Epstein, N., and Hunter, L.A. (1991) Targeted integration of adeno-associated virus (AAV) into human chromosome 19. *EMBO J.,* **10**: 3941-50.

Saphire, A.C., Bobardt, M.D., Zhang, Z., David, G., and Gallay, P.A. (2001) Syndecans serve as attachment receptors for human immunodeficiency virus type 1 on macrophages. *J. Virol.,* **75**: 9187-200.

Schwartz, J.J., and Zhang, S. (2000) Peptide-mediated cellular delivery. *Curr. Opin. Mol. Ther.,* **2**: 162-7.

Shayakhmetov, D.M., Gaggar, A., Ni, S., Li, Z.Y., and Lieber, A. (2005) Adenovirus binding to blood factors results in liver cell infection and hepatotoxicity. *J. Virol.,* **79**: 7478-91.

Shi, W., and Bartlett, J.S. (2003) RGD inclusion in VP3 provides adeno-associated virus type 2 (AAV2)-based vectors with a heparan sulfate-independent cell entry mechanism. *Mol. Ther.,* **7:** 515-25.

Shukla, D., Liu, J., Blaiklock, P., Shworak, N.W., Bai, X., Esko, J.D., Cohen, G.H., Eisenberg, R.J., Rosenberg, R.D., and Spear, P.G. (1999) A novel role for 3-O-sulfated heparan sulfate in herpes simplex virus 1 entry. *Cell,* **99:** 13-22.

Shukla, D., and Spear, P.G. (2001) Herpesviruses and heparan sulfate: an intimate relationship in aid of viral entry. *J. Clin. Invest.,* **108**: 503-10.

Smith, T.A., Idamakanti, N., Marshall-Neff, J., Rollence, M.L., Wright, P., Kaloss, M., King, L., Mech, C., Dinges, L., Iverson, W.O., Sherer, A.D., Markovits, J.E., Lyons, R.M., Kaleko, M., and Stevenson, S.C. (2003) Receptor interactions involved in adenoviral-mediated gene delivery after systemic administration in non-human primates. *Hum. Gene. Ther.,* **14**: 1595-604.

Spillmann, D. (2001) Heparan sulfate: anchor for viral intruders? *Biochimie,* **83**(8)**,** 811-7.

Summerford, C., Bartlett, J.S., and Samulski, R.J. (1999) AlphaVbeta5 integrin: a co-receptor for adeno-associated virus type 2 infection. *Nat. Med.,* **5**: 78-82.

Summerford, C., and Samulski, R.J. (1998) Membrane-associated heparan sulfate proteoglycan is a receptor for adeno-associated virus type 2 virions. *J. Virol.,* **72**: 1438-45.

Trybala, E., Bergstrom, T., Spillmann, D., Svennerholm, B., Flynn, S.J., and Ryan, P. (1998) Interaction between pseudorabies virus and heparin/heparan sulfate. Pseudorabies virus mutants differ in their interaction with heparin/heparan sulfate when altered for specific glycoprotein C heparin-binding domain. *J. Biol. Chem.,* **273**: 5047-52.

Utt, M., and Wadstrom, T. (1997) Identification of heparan sulphate binding surface proteins of Helicobacter pylori: inhibition of heparan sulphate binding with sulphated carbohydrate polymers. *J. Med. Microbiol.,* **46**: 541-6.

Valentine, R.C., and Pereira, H.G. (1965) Antigens and structure of the adenovirus. *J. Mol. Biol.,* **13**: 13-20.

Vives, R.R., Crublet, E., Andrieu, J.P., Gagnon, J., Rousselle, P., and Lortat-Jacob, H. (2004a) A novel strategy for defining critical amino acid residues involved in protein/glycosaminoglycan interactions. *J. Biol. Chem.,* **279**: 54327-33.

Vives, R.R., Imberty, A., Sattentau, Q.J., and Lortat-Jacob, H. (2005) Heparan sulfate targets the HIV-1 envelope glycoprotein gp120 coreceptor binding site. *J. Biol. Chem.,* **280**:**,** 21353-7.

Vives, R.R., Lortat-Jacob, H., Chroboczek, J., and Fender, P. (2004b) Heparan sulfate proteoglycan mediates the selective attachment and internalization of serotype 3 human adenovirus dodecahedron. *Virology,* **321**: 332-40.

Wickham, T.J., Mathias, P., Cheresh, D.A., and Nemerow, G.R. (1993) Integrins alpha v beta 3 and alpha v beta 5 promote adenovirus internalization but not virus attachment. *Cell,* **73**: 309-19.

Wickham, T.J., Roelvink, P.W., Brough, D.E., and Kovesdi, I. (1996) Adenovirus targeted to heparan-containing receptors increases its gene delivery efficiency to multiple cell types. *Nat. Biotechnol.,* **14**: 1570-3.

Wickham, T.J., Tzeng, E., Shears, L.L., 2nd, Roelvink, P.W., Li, Y., Lee, G.M., Brough, D.E., Lizonova, A., and Kovesdi, I. (1997) Increased *in vitro* and *in vivo* gene transfer by adenovirus vectors containing chimeric fiber proteins. *J. Virol.,* **71**: 8221-9.

Wu, Z., Chen, Z., and Phillips, D.M. (2003) Human genital epithelial cells capture cell-free human immunodeficiency virus type 1 and transmit the virus to CD4+ Cells: implications for mechanisms of sexual transmission. *J. Infect. Dis.,* **188**: 1473-82.

Xia, D., Henry, L.J., Gerard, R.D., and Deisenhofer, J. (1994) Crystal structure of the receptor-binding domain of adenovirus type 5 fiber protein at 1.7 A resolution. *Structure,* **2**: 1259-70.

Yayon, A., Klagsbrun, M., Esko, J.D., Leder, P., and Ornitz, D.M. (1991) Cell surface, heparin-like molecules are required for binding of basic fibroblast growth factor to its high affinity receptor. *Cell,* **64**: 841-8.

Yoneda, A., and Couchman, J.R. (2003) Regulation of cytoskeletal organization by syndecan transmembrane proteoglycans. *Matrix Biol.,* **22**: 25-33.

Zhang, W., Heil, M., Kuhn, R.J., and Baker, T.S. (2005) Heparin binding sites on Ross River virus revealed by electron cryo-microscopy. *Virology,* **332**: 511-8.

Zimmermann, P., and David, G. (1999) The syndecans, tuners of transmembrane signaling. *FASEB J.,* **13 Suppl,** S91-S100.

Available online at www.sciencedirect.com

SCIENCE @ DIRECT°

JMB

ELSEVIER

Structure of the Dodecahedral Penton Particle from Human Adenovirus Type 3

P. Fuschiotti[1], G. Schoehn[2], P. Fender[3], C. M. S. Fabry[2], E. A. Hewat[1] J. Chroboczek[4], R. W. H. Ruigrok[2] and J. F. Conway[1]*

[1]*Laboratoire de Microscopie Electronique Structurale Institut de Biologie Structurale UMR 5075 CNRS-CEA-UJF 38027 Grenoble cedex, France*

[2]*Institut de Virologie Moléculaire et Structurale FRE 2854 CNRS-UJF, BP181 38042 Grenoble cedex 9, France*

[3]*Laboratoire d'Enzymologie Moléculaire, Institut de Biologie Structurale, UMR 5075 CNRS-CEA-UJF, 38027 Grenoble cedex, France*

[4]*Laboratoire de Biophysique Moléculaire, Institut de Biologie Structurale, UMR 5075 CNRS-CEA-UJF, 38027 Grenoble cedex, France*

*Corresponding author

The sub-viral dodecahedral particle of human adenovirus type 3, composed of the viral penton base and fiber proteins, shares an important characteristic of the entire virus: it can attach to cells and penetrate them. Structure determination of the fiberless dodecahedron by cryo-electron microscopy to 9 Å resolution reveals tightly bound pentamer subunits, with only minimal interfaces between penton bases stabilizing the fragile dodecahedron. The internal cavity of the dodecahedron is ∼80 Å in diameter, and the interior surface is accessible to solvent through perforations of ∼20 Å diameter between the pentamer towers. We observe weak density beneath pentamers that we attribute to a penton base peptide including residues 38–48. The intact amino-terminal domain appears to interfere with pentamer–pentamer interactions and its absence by mutation or proteolysis is essential for dodecamer assembly. Differences between the 9 Å dodecahedron structure and the adenovirus serotype 2 (Ad2) crystallographic model correlate closely with differences in sequence. The 3D structure of the dodecahedron including fibers at 16 Å resolution reveals extra density on the top of the penton base that can be attributed to the fiber N terminus. The fiber itself exhibits striations that correlate with features of the atomic structure of the partial Ad2 fiber and that represent a repeat motif present in the amino acid sequence. These new observations offer important insights into particle assembly and stability, as well as the practicality of using the dodecahedron in targeted drug delivery. The structural work provides a sound basis for manipulating the properties of this particle and thereby enhancing its value for such therapeutic use.

© 2005 Elsevier Ltd. All rights reserved.

Keywords: adenovirus; dodecahedron; penton; fiber; cryo-electron microscopy

---

Present addresses: P. Fuschiotti, Department of Immunology, University of Pittsburgh, Room E1040, Biomedical Science Tower, 200 Lothrop Street, Pittsburgh, PA 15261, USA; J. F. Conway, Department of Structural Biology, University of Pittsburgh, Room 2047, Biomedical Science Tower 3, 3501 5th Ave, Pittsburgh, PA 15260, USA.

Abbreviations used: Ad2, Ad3, Ad5, adenovirus serotypes 2, 3 and 5, respectively; Bs-Dd, dodecahedra constructed from adenovirus penton base protein alone; Pt-Dd, dodecahedra of pentons, i.e. penton base and fiber proteins; EM, electron microscopy; cryoEM, cryo-electron microscopy; Mab, monoclonal antibody.

E-mail address of the corresponding author: jxc100@pitt.edu

Introduction

Adenoviruses are a large family of non-enveloped DNA viruses that infect a wide range of human and animal cell types, most commonly causing respiratory disease but also gastroenteritis or conjunctivitis. Their characteristic morphology includes an icosahedral capsid with a diameter of 900–1000 Å, pentameric capsomers (penton bases) at the vertices and hexavalent trimers (hexons) populating the facets in a pseudo-$T=25$ arrangement.[1] A trimeric fiber protein extends 100–300 Å (according to serotype) from the outer capsid surface and is attached non-covalently to each penton base forming the penton. Several other minor structural proteins are involved in stabilizing
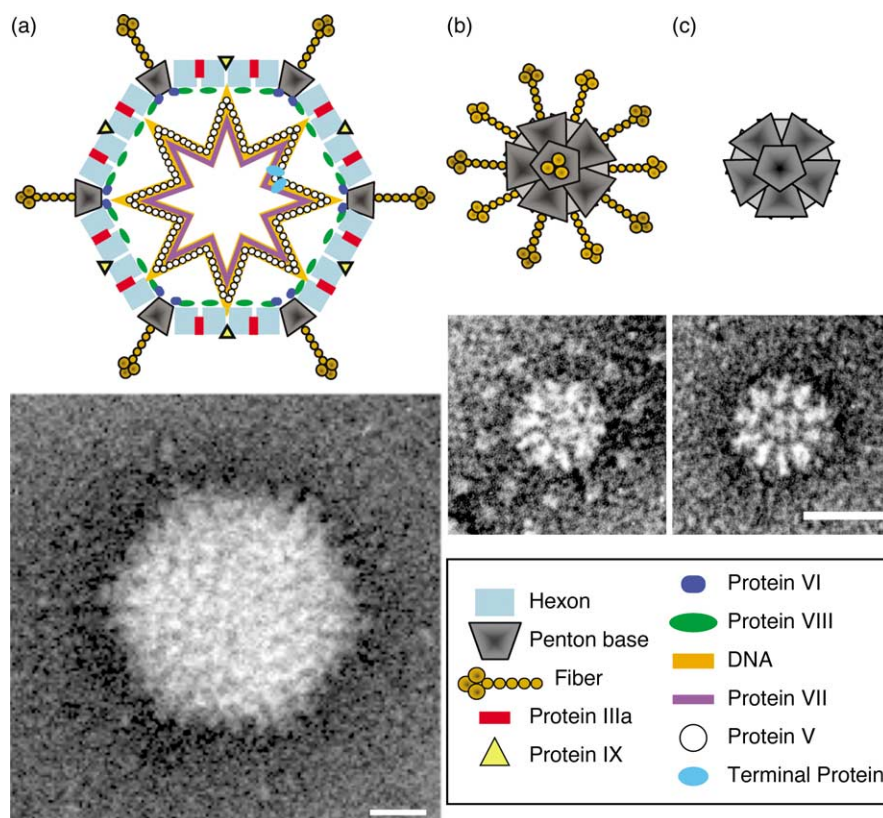
Figure 1. Schematics of adenovirus and its dodecahedron. (a) Diagram of adenovirus, including the major structural proteins: hexon (light blue), penton base (grey) and the trimeric fiber (gold) that extends outwards ending in a knob. Additional minor capsid proteins include the hexon "cementing" proteins IIIa (red bars), IX (yellow triangles), protein VIII associated with the hexons (green oval) and protein VI associated with the penton base (blue ovals). DNA is represented as an extended string (although in reality it is more compact than indicated here) and coated with associated proteins. Beneath is a negative-stain EM image of a viral particle. (b) Representation of the sub-viral dodecahedral particle with fiber bound (Pt-Dd) viewed down a 5-fold axis and a negative stain EM image from expressed penton base and fiber proteins where some fibers are visible, particularly the distal knobs. (b) The dodecahedral particle without fiber (Bs-Dd) and corresponding EM image. The bars represent 200 Å.

the capsid (Figure 1). The distal knob-domain of the fiber is necessary for cell recognition. Most subgroups (A–F, excluding B) bind the Coxsackie and adeno-virus receptor (CAR),[2,3] an integral membrane protein of the tight junction in epithelial cells.[4] The interaction between the fiber and CAR is implicated both in viral entry and egress.[5] Several subgroup B adeno-viruses utilize another cell surface receptor, CD46,[6,7] but the primary receptor for another subgroup B member, adenovirus serotype 3 (Ad3), is still not known. Cell entry is gained by endocytosis, in most serotypes through RGD-loops extending from the penton base that bind to the αvβ3 or β5 integrins.[8,9] The penton base also has a role in release from endosomes and decapsidation.[10,11]

Models of the adenovirus capsid have been built by combining available crystallographic structures of the capsomers with lower resolution density maps of the entire capsid from cryo-electron microscopy (cryoEM). A model of the subgroup C Ad2 capsid was partially built from the trimeric hexon[12] and capsid reconstruction.[1] This model accounted for ~60% of the protein in the virion and offered insights into hexon–hexon and hexon–

penton base interfaces, as well as indicating potential locations for some of the minor proteins. More recent updates include cryo-electron microscopy density maps of the Ad2 and Ad12 capsids to 21 Å resolution where surface features such as the RGD receptor binding loops were localized through binding MAbs or small receptor fragments.[13,14] However, much detail was lacking, including the structure of the penton base, its interaction with the fiber and the role of the symmetry-mismatch between these two components. Our recent cryoEM study on the Ad5 capsid has extended the resolution to 10 Å, allowing more detailed modeling of the capsomer interfaces and localization of minor structural proteins by comparison of native and deletion mutant capsids.[15]

For certain adenovirus serotypes, penton bases can self-assemble into a sub-viral particle called dodecahedron that comprises 12 copies of the penton arranged on a T=1 icosahedral lattice[16,17] and may include fiber molecules (penton dodeca-hedron, Pt-Dd) or not (base dodecahedron, Bs-Dd) (Figure 1). Analysis of the dodecahedral particle of Ad3 by cryoEM to a resolution of ~30 Å revealed

the overall shape of the particle and allowed an estimation of the dimensions of the internal cavity.[18] Comparison between particles including the fiber molecule (Pt-Dd) and those without (Bs-Dd) revealed apparent redistribution of density at the outermost surface of the penton at the presumed location of the mobile integrin-binding RGD loops. The fiber itself, however, was poorly resolved, possibly as a consequence of intrinsic flexibility, limited number of particles included in the reconstruction (30) or from bending imposed by a restricted depth of ice formed during preparation for microscopy. Subsequently, the dodecahedron was shown to enter cells efficiently using the same mechanism as adenovirus,[19,20] confirming the localization of the infection mechanisms to the penton's two constituent proteins, penton base and fiber. We have previously proposed the dodeca-hedron as an alternative to adenovirus for therapeutic delivery.[19,20] One of the potential advantages over the intact virus particle is that it cannot provoke infection directly or through recombination, as it harbors none of the viral genome. A second is the possibility of a weaker immune response compared to adenovirus because of its reduced protein content, thereby enhancing the success of multiple applications. In addition, recent work has shown that dodecahedra can penetrate a wider range of cells than the virus by entering through a heparin sulfate pathway.[21] However, the internal cavity of the dodecahedron is too small to accommodate more than ∼100 bp of DNA and is thus too small to carry a gene, although it could accommodate drugs. Specific targeting to non-native receptors is possible through modification of the cell-recognition domains on the fiber, or combining fibers and penton bases from different adenovirus serotypes.[22]

Recently, a crystallographic model of the Ad2 penton base was reported. An expressed 48 N-terminal truncated form of the penton exposed to crystallization conditions lead to formation of dodecahedral particles in the crystal.[23] Interes-tingly, the full-length Ad2 penton base did not spontaneously form dodecahedra. The core of the structure is a jellyroll motif, an eight-stranded antiparallel β-barrel that is common to capsid proteins of certain virus families, with an extensive insertion of 308 residues (54% of the protein) between two β-strands of the jellyroll, and a second insertion of 54 residues between another pair of strands. The first insertion includes two external loops, one of which (the RGD loop) contains the integrin-binding RGD domain and is highly vari-able between serotypes in sequence and length. It is also flexible and none of the 74 residues of the loop were modeled in the crystal structure. The second loop (variable loop) is shorter, also variable between serotypes, and projects from the outer surface of the penton base into solvent. The binding pattern of the Ad2 fiber was revealed in a second dodecahedron structure including residues 11–21 from the N-terminal part of the fiber protein as five monomers bound to the penton base, albeit

in non-stoichiometric quantities since the fiber molecule is a trimer.

The available adenovirus penton base protein sequences are highly conserved outside these external loops, suggesting that the bulk of the penton base has a common fold. The Ad2 penton protein differs in sequence from that of Ad3 at the amino terminus and at the two external loops, where the Ad3 protein is some 34 residues shorter in the RGD loop and nine residues longer in the variable loop. These three variable regions are perhaps the most important outside of the con-served interface residues that direct subunit and penton–hexon organization. The amino terminus is located internally to the capsid[15] and holds two conserved motifs of the form PPxY that may potentially interact with host cell ubiquitine ligases containing WW domains[24] presumably before incorporation into the capsid or after partial decapsidation. The RGD loop is a co-receptor binding site involved in endocytosis, and the second loop has unknown function but is clearly serotype specific.

Here we report on our work extending the structural characterization of the Ad3 dodeca-hedron by cryo-electron microscopy, including a more detailed visualization of the fiber and its interface with, and effects on, the penton base. We model the cryoEM density with the atomic coordinates of the Ad2 dodecahedron to compare the core structures and to identify the location of residues unique to the Ad3 penton sequence as well as part of the 48 amino-terminal residues not visualized by crystallography.

Results and Discussion

Although we published previously that dodeca-meric particles consisting of Ad3 penton base or Ad3 penton base plus fiber formed spontaneously upon expression,[18,20] new purification methods of recombinant protein produced in insect cells led to assembly of few particles, some incomplete, and with a much higher proportion of free penton bases (Figure 2(a)). We explain this discrepancy by first noting that the atomic structure of the Ad2 penton base dodecahedron was derived from protein that was N-terminally truncated, with the first 48 amino acid residues missing.[23] The internal space in this dodecahedron may be approximated by a sphere with diameter of 80 Å, sufficient to accommodate 225 kDa of tightly packed protein but which is too small to accommodate the 317 kDa of truncated peptides (60 copies of 48 residues). Clearly, dodecahedra cannot assemble from full-length penton base protein. Secondly, we observed that when full-length Ad3 penton base (Figure 2(c), lane 1) was kept for two weeks at room tempera-ture, almost all the protein had assembled into dodecahedra (Figure 2(b)) and that the protein had been spontaneously degraded to a smaller size (Figure 2(c), lane 2). N-terminal sequencing showed
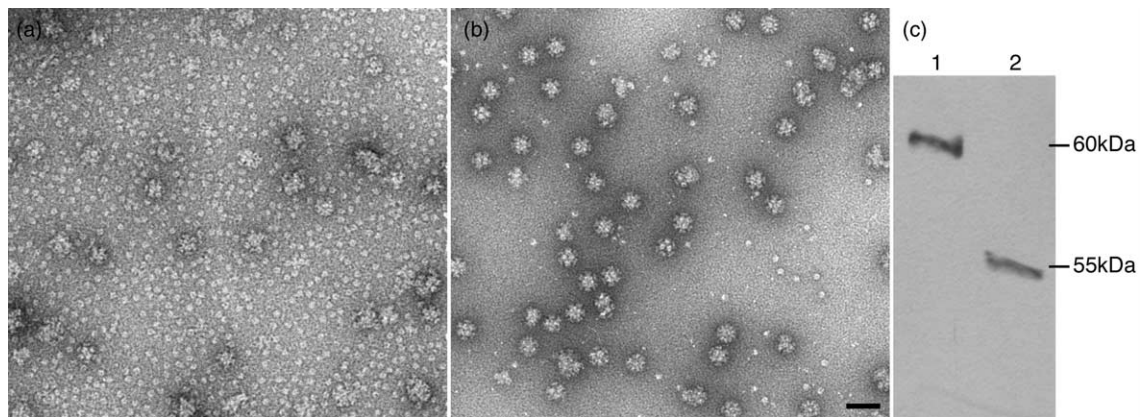
Figure 2. Negative stained images of expressed penton base. (a) Expressed penton base visualized immediately after expression and purification. Mainly free pentameric bases are visible with also some more or less complete dodecahedra. (b) Same sample as in (a) but visualized after two weeks at room temperature, having lost the first 37 residues. Most of the particles are well-formed dodecahedra. Only a few free penton bases are visible in the background. The scale bar represents 30 nm. (c) An SDS-PAGE gel of the two samples visualized in a, lane 1, and b, lane 2.

that the protein was N-terminally truncated between residues 37 and 38 (Figure 3). This 11 residue extension over the truncated Ad2 protein visualized by crystallography totals only 73 kDa (i.e. 60 copies of 11 residues) and is well able to pack into an 80 Å radius cavity. We conclude that our previous work on the Ad3 dodecahedron most probably involved N-terminally truncated protein resulting from inadvertent and unsuspected

proteolysis. In the experiments shown here, all penton base protein was cleaved at the same site (residues 37–38), but in principle one would expect that dodecahedra could be formed from a mixture of cleaved and full-length protein.

The observation of dodecahedra in lysates of cells infected by Ad3[25] but not from cells infected by Ad2 may be due to the fact that the cleaved site is not conserved between the two serotypes (Figure 3) and
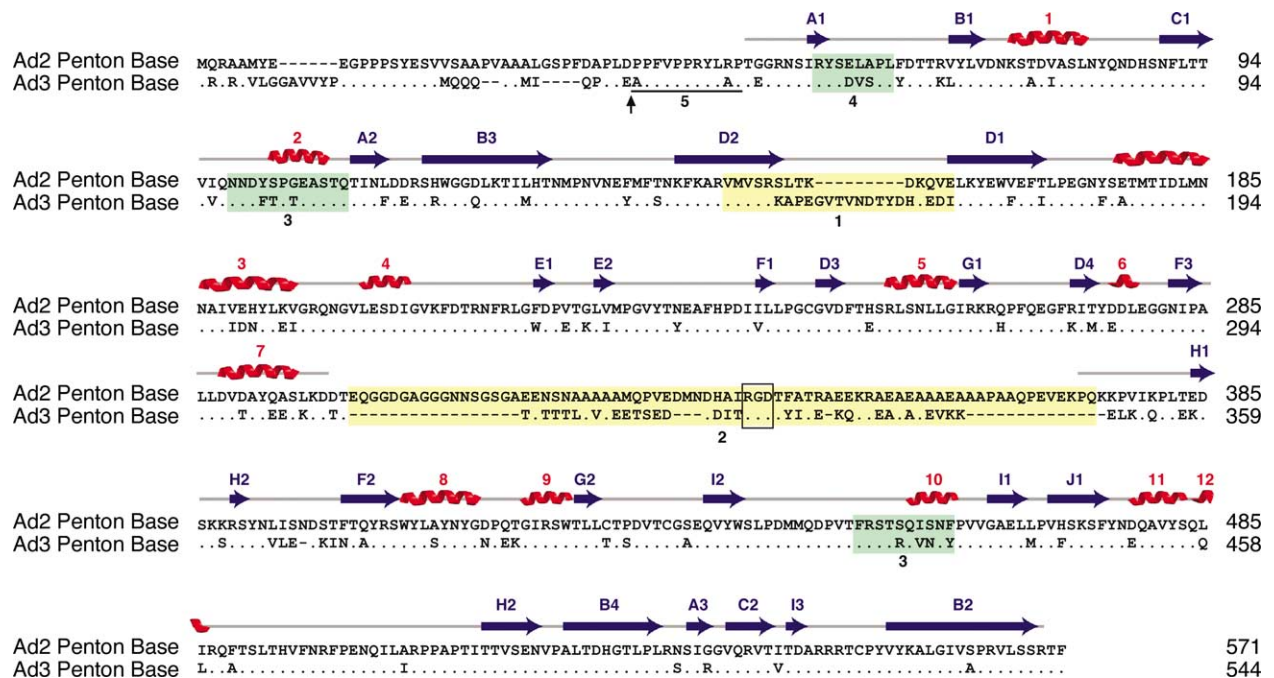
Figure 3. Sequence alignment of penton base proteins from human adenoviruses 2 and 3. Secondary structures in the Ad2 penton base are denoted above the sequence by blue arrows (β-strands) and red helices (α-helices). The RGD region (numbered 2, RGD is boxed into a black square) and the variable loop (numbered 1) are highlighted in orange whereas the regions involved in particle dodecamerization are in green and numbered 3 (two 2-fold related connections) and 4 (one connection on the 2-fold axis). The black arrow indicates the site of proteolysis allowing dodecahedron formation.[23] The number 5 and the black line above indicate residues 38–49 that are present in the Ad3 dodecahedron visualized in Figure 2(b) but not in the Ad2 dodecahedron X-ray structure. Regions 1–5 are also indicated in Figure 5.

that the Ad3 penton base is more readily cleaved in infected cells. During infection of cells by Ad2 there is production of a large excess of soluble fiber that is thought to be necessary to undo the tight junctions between cells involving the Ad2 receptor CAR.[5] Ad3 does not infect the same cells as Ad2 and uses a different receptor from CAR.[3] The fact that Ad3 dodecahedra are found in large quantities in Ad3-infected cells most likely means that these structures also play an as yet unknown role in the infection process.[26]

Electron cryo-microscopy and image analysis yielded models of the dodecahedron made from penton base only (Bs-Dd) and dodecahedron made of complete pentons (Pt-Dd) (Figure 4). The Bs-Dd particle was resolved at 9 Å but for the Pt-Dd particle only 16.5 Å was achieved as a consequence of both a smaller dataset of images as well as higher background noise due to the larger diameter particle being embedded in thicker ice. The Bs-Dd density map (Figure 4(d) and (e)) reveals tight packing of subunits in the penton bases but a looser association between penton bases. Although at lower resolution, the Pt-Dd map (Figure 4(f) and (g)) shows very strong density for the fiber up to the fiber head. Keeping in mind the improper imposition of 5-fold symmetry on the trimeric fiber molecule, several observations can be made. Firstly, the density level in the fiber is similar to that in the penton base, indicating that the fiber is coincident with the icosahedral 5-fold axis and so does not lose strength due to the imposed and inappropriate averaging. This strength of the fiber density is remarkable in comparison to that visualized in previous work[18] and likely results from embedding the particles in thicker ice, thus avoiding bending of the fibers, as well as correction of image distortions generated by the microscope (contrast transfer function).[27] We note that the Quantifoil grids used here appear to have rims of thick carbon around the holes that leads to thicker ice than for the "lacy" home made holey carbon films used previously. Secondly, we observe that the extent of the fiber is well delimited: small bridges of density connect it to the penton base (arrows in Figure 4(g)), and at the distal end the transition from strong to smeared density is sudden. Extending the radius of selection for the raw images does not result in any further extension of the fiber density in the reconstruction (results not shown), thus indicating the onset of either flexibility or a kink at the visible distal end. Such flexibility was observed before for negatively stained fibers of Ad2 that were seen to have a triangular shaped head with the fiber shaft lying flat on the carbon support film.[28] Flexibility of the fiber near the head and near the base probably assists in favorable positioning for receptor binding.[29] Finally, the fiber density shows an axial banding pattern with a spacing of about 15 Å. This feature will be discussed below.

The atomic structure of the Ad2 penton base was fit into the EM density maps of Ad3 Bs-Dd and Pt-Dd (Figure 5(a)–(d)). The atomic model fits very well (see Materials and Methods) apart from two loop areas where the EM density is too wide, as indicated in Figure 5(a) and (b) by 1 for the variable loop[15,23] and by 2 for the RGD loop (see also the sequence in Figure 3). The extra EM density in loop 1 is about 950 Å^3 in volume and can accommodate about 800 Da, slightly less than required for the eight amino acid insertion in the Ad3 penton base compared to that of Ad2. Less can be said about loop 2, the RGD loop, since most of it is invisible in the atomic structure of the Ad2 penton base[23] and in the 10 Å Ad5 structure.[15] Consequently, extra volume is visualized in the EM density maps corresponding to the RGD loop despite its shorter length than for Ad2 (Figure 3). This volume appears further from the penton's axis of symmetry in the Pt-Dd structure than for Bs-Dd, presumably a consequence of the fiber binding the penton base (see below).

The Ad3 dodecahedron is stabilized by three contacts between each pair of pentons. Two of these (marked 3 in Figure 5(c)–(f)) are related by the 2-fold axis and one (marked 4 in Figure 5(d) and (f)) is situated on the 2-fold axis. The corresponding positions in the Ad2 sequence are also marked by 3 and 4 in Figure 3. Because the quasi-atomic model of the Ad3 dodecahedron is made using the Ad2 X-ray structure, it is difficult to say exactly which amino acids interact across the Ad3 penton–penton interface. However, the atomic structure of the Ad2 penton base falls exactly inside the Ad3 EM density, implying that both types of penton base use the same structural elements to form the dodecahedron. Further, the high degree of homology between the sequences in these regions suggests that many of the same contacts may be made.

The EM structure shows additional density attached to the inside surface of the dodecahedron at the position of the N-terminal residue 49 of the Ad2 atomic structure (Figure 5(g) and (h); the N-terminal residue 49 is marked by an asterisk (*) and the extra density is marked by the number 5). We attribute this to the presence of 11 additional N-terminal residues present in the Ad3 penton base protein used for the cryoEM reconstructions, and it is a further indication that the N terminus of the penton base is sequestered inside the dodecahedron, and by inference inside the virus particle as well. Data obtained by cryoEM for the Ad5 capsid also showed extra density present under the penton and was likewise attributed to the N-terminal 48 residues of the penton base.[15] A corollary of these observations is that the N-terminal PPxY sequences that interact with cellular ubiquitine protein ligases[24,30] are not accessible in intact particles nor after assembly of new virus particles.

Model for the fiber density and its attachment to the base

The penton base is a pentamer but the fiber molecule that binds it is a trimer. There are five binding sites on the penton base for the N-terminal
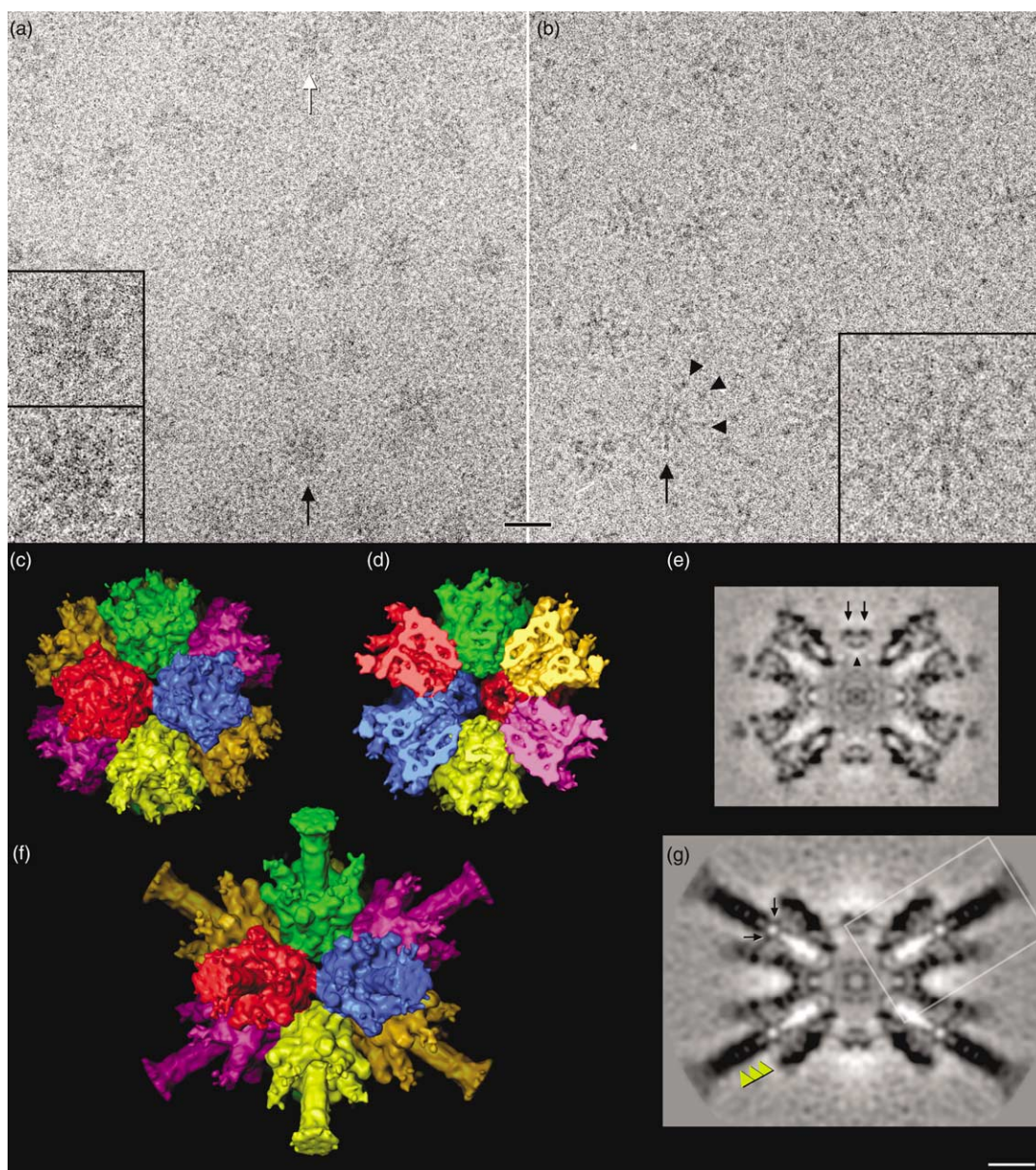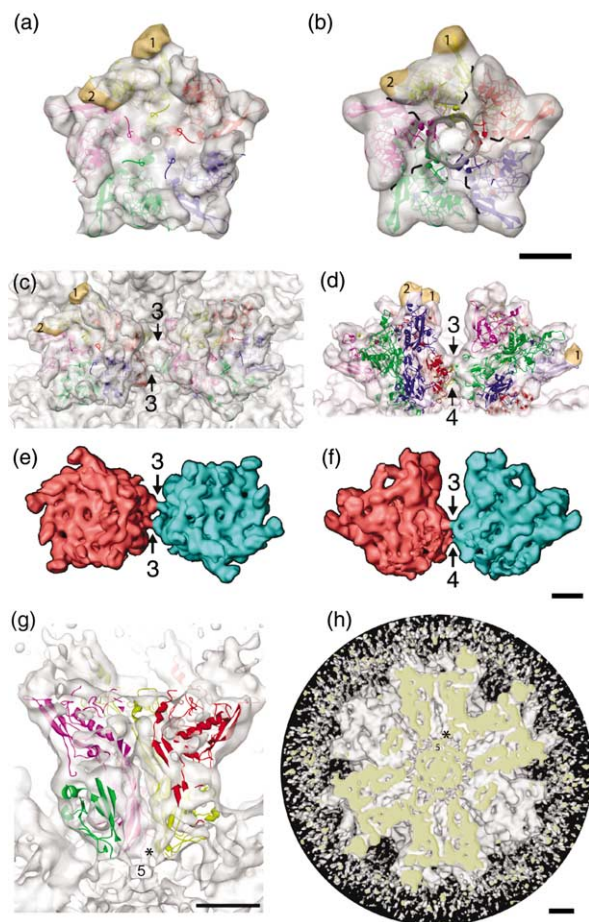
Figure 4. Structures of the Ad3 penton base dodecahedron with and without fiber. cryoEM images of Bs-Dd (a) and Pt-Dd (b), where arrowheads indicate fiber knobs. Several particles indicated by arrows are inset at double scale. The scale bar represents 250 Å. Surface representations of the Bs-Dd particle reconstruction viewed down a 2-fold axis and calculated from the cryoEM images are shown in (c), exterior view, and (d), interior view where the front half has been computationally removed. The penton bases are symmetrically identical, but colorized differently by a simple segmentation across the icosahedral 2-fold axes to aid in interpretation. The most peripheral density appears to be partially complete loops that may lose visibility due to flexibility. Gaps between penton bases are about 20 Å across and would allow solvent access to the interior. The interior cavity is about 80 Å in diameter and lined by the inwardly protruding loops of the penton bases. The central section corresponding to the sectioning plane in (d) is shown in grey-scale (protein is black) in (e). Densities 3 and 4 on the icosahedral 2-fold axis, and near or on the interface between penton bases, are marked with arrows and an arrowhead, respectively. These bridges are visualized in more detail in Figure 5. Equivalent views of the Pt-Dd particle are shown in (f), exterior view, and (g), central section, where density connections between the strong fiber density and the penton base are indicated with arrows. Also note the banding pattern along the axis of the fiber density, with a spacing of about 15 Å (yellow arrow heads). The boxed region is reproduced in Figure 6. An animation of the surface views is available on-line (Supplementary Data). The scale bar represents 50 Å.

tail of the fiber.[23] Therefore, when the fiber binds to the base, the fiber N termini will occupy at most three of the five available sites, an interesting example of symmetry mismatch but with unknown purpose. Because icosahedral symmetry is imposed upon the dodecahedron during the image reconstruction process, the density at the vertices, including that of the trimeric fiber, is 5-fold

Figure 5. Quasi-atomic model of the Ad3 dodecahedron using the atomic structure of the Ad2 penton base. (a) Fit of the Ad2 penton base X-ray structure (PDB accession number 1X9P) into the Ad3 penton base EM density. The fit is nearly perfect at this resolution with only two unoccupied regions visible in the EM map. The first, marked 1, corresponds to the variable loop (see Figure 3) while the second, 2, is the RGD loop. (b) Fit of the fiber peptide, Ad2 penton base complex X-ray structure (PDB accession number 1X9T), into the Ad3 penton EM density. Extra densities are marked as in (a). The peptide that mimics the N terminus of the fiber (amino acid residues 10–20) is drawn in black. (c) and (d) Visualization of the contacts between two penton bases across the 2-fold axis. (c) Top-view along the icosahedral 2-fold axis, and (d) a perpendicular side view. The sequences involved in the different contacts are marked 3 and 4 as in Figure 3. Extra densities compared to the Ad2 X-ray structure are marked 1 and 2 as in (a) and (b). (e) and (f) The contact densities between penton bases are indicated in these surface views that have been rendered from a density map limited to 11 Å and contoured at a stringent level to highlight stronger densities. Arrows and numbers indicate features corresponding to those of (c) and (d) and in Figure 3. The boundaries between penton bases have been slightly adjusted from the simple 2-fold positions of Figure 4 by inspection of the density and respecting the 2-fold axis. The lower connection (4) is apparently weaker and is not quite continuous at this stringent contour level. (g) Same view of the Ad2 penton base X-ray data fitted into the Ad3 penton base as in (d) but the EM map is contoured at a lower threshold (i.e. more density is visible). It is then possible to see that the N-terminal part of the X-ray data (represented by an

averaged. When the EM density for Bs-Dd is subtracted from the density for Pt-Dd, several regions remain (colored light blue in Figure 6(a)), corresponding to the fiber as well as any penton base densities that are flexible in Bs-Dd but more rigid in Pt-Dd. On the top of the base, five spokes of density radiate azimuthally outwards, each consisting of three blobs. The center-most two blobs correspond to the density observed in the complete Ad5 capsid and also in the crystal structure of the Ad2 penton base plus an N-terminal fiber peptide, and are likely made up of Ad3 fiber residues 10-SFNPVYPYEDE-21.[15,23] The third blob is situated towards the outside of the penton base against the RGD loop and is either due to a stabilizing effect of the fiber N terminus on the flexible loop or comprises the nine N-terminal residues of the fiber tail. The volume of this blob of density, 1000 Å,[3] can contain 850 Da of protein, enough for most of the nine N-terminal Ad3 fiber tail residues (1-MAKRARLST-9). In a previous analysis[18] we interpreted the volume difference between Bs-Dd and Pt-Dd near the RGD loop as movement by this loop because at the low resolution of that analysis we could only see that the midpoint of the mass of this loop changed position. Only higher resolution data would confirm our hypothesis about the identity of the outer-most blue blobs.

The cross-section of the EM density of the fiber in Figure 4(g) shows a series of striations along its length. The distances between these striations is 15($\pm$2) Å and thus could correspond to the 15 amino acid pseudo-repeats in the fiber shaft.[28,31–33] Indeed, when the atomic structure of the distal shaft and knob region of the trimeric Ad2 fiber[31] is 5-fold averaged, a similar pattern of striations is observed from averaging of the repeating three pairs of antiparallel β-strands that are close to the fiber axis (Figure 6(b); β-strands and corresponding striations are arrowed). Analysis of the sequence of the Ad2 and Ad3 fibers shows that they have N-terminal tails of similar length (45 residues for Ad3 and 46 for Ad2) followed by three shaft repeats in common.[32] Although the short Ad3 fiber has only six repeats in total compared to the 22 for the longer Ad2 fiber,[32,34] the regular spacing of repeats can be directly compared with those of Ad2 that are present in the crystal structure of the fiber (Figure 6(b)). The cross-section of the fiber density of Ad3 Pt-Dd shows five clear bands, with the sixth striation from the last repeat being smeared out, as is the density for the knob, implying some flexibility is likely between the fifth and sixth repeat. The distance between the first striation and the inner-most blob of blue density shown in Figure 6(a) is about 15 Å and is evidently made up of the proline

asterisk (*)) is now connected to a small cylindrical density inside the dodecahedron. We attribute this density to residues 38–49 (region 5 in Figure 3). (h) Same view as in (g) but for the entire dodecahedron. The cutting slice is colored in beige and region 5 and * are indicated under one penton base. The bars represent 25 Å.
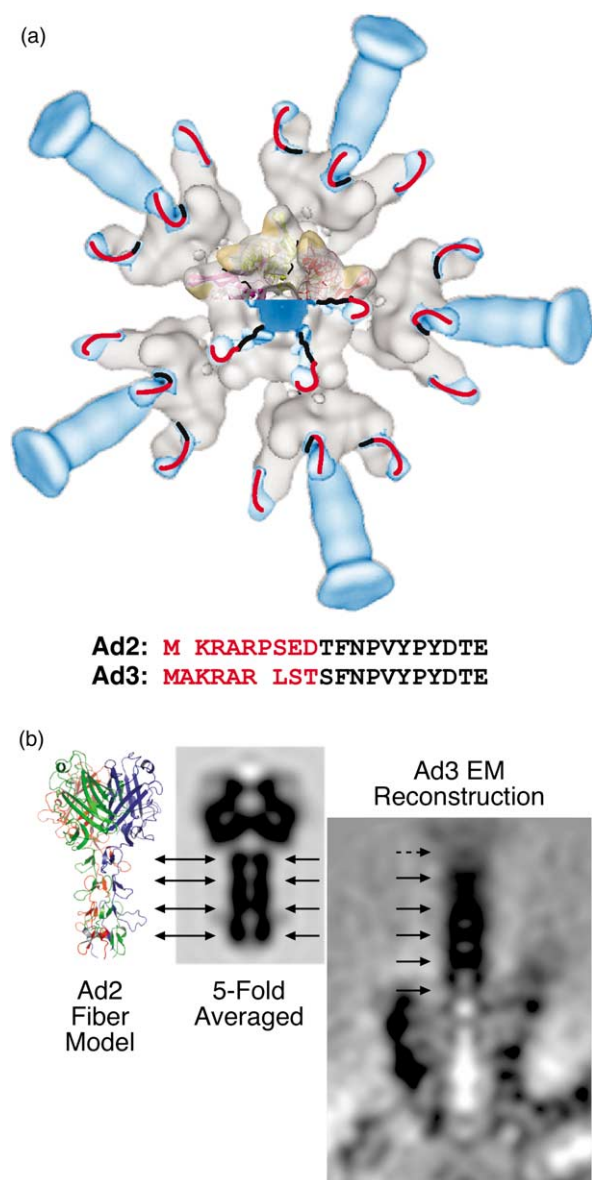
Figure 6. (a) The fiber of adenovirus. Difference mapping between Pt-Dd and Bs-Dd structures filtered at 18 Å resolution. Bs-Dd is in grey and the difference density is in blue. One half of the central penton shows the same fit as in Figure 5(b). The N-terminal fiber peptide (residues 11–21 of the Ad2 fiber[23]) is in black and superposes exactly with extra density visible in Pt-Dd (the two radially oriented cylinders of blue density). We interpret a third blue density localized on the outside part of the RGD loop (region 2 in Figures 3 and 5) as the N-terminal part of the fiber (Ad3 fiber residues 1–9) that is modeled by a red line connected to the black line (Ad2 fiber residues 11–21 seen in the crystal structure; Figure 5(b)). The sequence alignment of the first 20 amino acid residues of the Ad2 and Ad3 fibers indicates in black the amino acids that were modeled in the Ad2 crystallographic structure of the penton base with the bound fiber peptide, and in red those that were disordered. (b) Comparison of fiber density from the crystallographic structure of the Ad2 fiber head domain (residues 312–582)[31] as indicated, and from the Ad3 Pt-Dd density map. The Ad2 atomic model is averaged to mimic the Ad3 icosahedral reconstruction by filtering to 16 Å followed by imposition of 5-fold symmetry about an axis

and glycine-rich sequence 21-SSSQHPFINPG FISPDGFTQSPNGV-45 that must form the well-defined link visible in the cross-section (Figure 4(g), arrows).

The loose packing between penton bases and the accessibility of the dodecahedron interior to solvent are features of the subviral particle that contrast sharply with the adenovirus capsid, where penton bases interact with hexon and other minor structural proteins to form a closed capsid. In addition, the insight into the need for truncation of the N-terminal 37 residues (48 for Ad2) in order to form dodecamers highlights another difference with the *in situ* penton base and has been crucial to understanding how to optimize particle production. These factors are important for our goal of developing the dodecahedron as a therapeutic vector (P.F. *et al*, unpublished results). Loose packing is more likely to allow our manipulation of the assembly status for the purpose of encapsidating a drug or other "cargo", although maintaining assembly buffer conditions will be crucial for particle stability. The large trefoil perforations also present an interesting challenge for retaining any packaged molecules, and clearly the size of the molecule must be sufficient to avoid diffusion through the pores. This may be achieved by polymerization of the molecules, thus increasing the diameter of the payload, or by modifying the interior surface of the dodecahedron cavity to attract the molecules but without affecting assembly. Finally, the need for truncation is essential for assembling particles in the first place, but also suggests that the amino termini might be suitable sites to introduce modifications for enhancing recruitment and retention of specific drugs and in sufficient quantity to be useful. Clearly much needs to be done to develop this system, but the structural work presented here gives some clear directions for future work.

Materials and Methods

Protein preparation

Adenovirus 3 dodecahedra were prepared using the baculovirus expression system as described.[20] Briefly, a double expression vector pAcUW31 (Clontech, Palo Alto, CA) was used for cloning the Ad3 penton base protein (60 kDa) and fiber protein (35 kDa) genes into the baculovirus genome. Infectivity titres were determined on monolayers of *Spodoptera frugiperda* (Sf21) cells by

parallel with the fiber shaft. The section view shows four parallel striations corresponding to β-sheet crossovers, as indicated by arrows, and large loops between the lowest sets of β-sheet crossovers correspond to wisps of density between the lowest two striations in the section. At right is a corresponding section through the Ad3 fiber density of the Pt-Dd structure (boxed region from Figure 4(g)) and in approximate alignment by the distal ends presents similar striations. In the Ad3 fiber five striations are visible corresponding to five N-terminal motifs[32] while that for the distal sixth crossover is too smeared out to be clearly defined (broken arrow).

standard procedures. *Trichoplusia ni* moth cells (High Five; Invitrogen) were infected with the recombinant baculovirus isolates at a multiplicity of infection of 5 plaque-forming units/cell. Lysates of infected High Five cells were separated on a 15%–40% (w/w) sucrose gradient containing 10 mM Tris–HCl, 150 mM NaCl, 10% glycerol, 2 mM EDTA (pH 6.6) for 18 h in a Beckman SW41 rotor at 40,000 rpm. Expressed protein was visualized by SDS-PAGE and Coomassie stain of the collected fractions at weights of 60 kDa and 35 kDa corresponding to the penton base protein and fiber protein, respectively. After the gradient, the protein-containing fractions localized in 38%–40% sucrose were dialyzed against 25 mM phosphate buffer (pH 6.6) and further purified by anionic exchange chromatography (Econo-Pac High Q Cartridge; BioRad) using a linear 0 to 1 M NaCl gradient in the phosphate buffer.

Electron microscopy

Particles were visualized by negative-stain EM to assess their assembly status using 1%(w/v) sodium silicotungstate (pH 7.0) as stain. cryoEM for structural analysis was performed according to standard low-dose methods. Bs-Dd particles were imaged on a JEOL JEM2010F microscope equipped with an Oxford CT3500 cryoholder operated at 200 kV and 50,000× nominal magnification. Pt-Dd particles were imaged with an FEI CM200 microscope with a Gatan 626 cryoholder operated at 200 kV and 38,000× nominal magnification. Quantifoil R2/1 grids (Quantifoil Micro Tools GmbH, Germany) were loaded with 4 μl of sample at 1 mg/ml, blotted and rapidly frozen in liquid ethane within a liquid nitrogen bath using a Zeiss cryo-plunger. Grids were maintained at liquid nitrogen temperatures during transfer into the microscope and imaged with low dose techniques on Kodak SO163 film. Fields were imaged twice at different defocus values with the closer-to-focus exposure being made first. Negatives were developed in full strength D19 for 12 min, screened by optical diffraction to reject those with weak or astigmatic power spectra, and digitized at a 7 μm sampling step on a Z/I Imaging PhotoScan (previously the Zeiss SCAI).

Image analysis

Particle images were selected manually from the digitized micrographs, corrected for contrast transfer function effects and processed as described[35] with several modifications as noted. The Bs-Dd micrographs (seven defocus pairs) yielded 5597 image pairs of which 1849 were selected for the final reconstruction; for Pt-Dd, 2141 image pairs were collected from six defocus pairs of micrographs, and 1071 were included in the final density map. Particle orientations were determined with the PFT protocol[36] with modifications (D.M. Belnap, J.B. Heymann & J.F.C., unpublished results), and three-dimensional density maps were calculated using Fourier–Bessel methods. Resolution was estimated by Fourier Shell Correlation[37] calculated between independent half-dataset maps, and applying a correlation limit of 0.3: for Bs-Dd this was at 9.3 Å and for Pt-Dd, 16.5 Å (see Supplementary Data, Figure 1). Density maps were manipulated with BSOFT utilities[38] and visualized with ROBEM (Rob Ashmore, Purdue University, Indiana), Amira (Mercury Computer Systems Inc, Merignac, France), and the UCSF Chimera software†.

Density maps have been deposited in the Macromolecular Structure Database‡ with accession numbers 1178 for Bs-Dd and 1179 for Pt-Dd.

Docking of the atomic structure of the Ad2 penton base into the Ad3 penton base dodecahedron

The atomic structures of the Ad2 penton base alone (PDB accession number 1X9P) and in complex with the N-terminal fiber peptide (PDB accession number 1X9T) were fit into the EM model for Ad3 Bs-Dd and Pt-Dd, respectively. The atomic structures were placed manually into one penton base using the program O.[39] The optimization procedure was carried out using URO[40] with the pentamer treated as a single molecule (i.e. only applying icosahedral 2-fold and 3-fold symmetry). The scale factor was also optimized to determine the real magnification of the microscopes. For Bs-Dd the quality of the final fit is given by a correlation coefficient of 80.4%, a crystallographic R factor of 44.5% and a quadratic misfit of 17.9. The fitted scale factor was 0.98 of the original, corresponding to a calibrated pixel size in the cryoEM images of 1.37 Å. For Pt-Dd the quality of the final fit after masking out the fiber shaft and head domains is given by a correlation coefficient of 93%, a crystallographic R factor of 41.9% and a quadratic misfit of 14.9. The computed scale was 0.93 of the original, or 1.72 Å/pixel.

Difference imaging

Both the Bs-Dd and Pt-Dd maps were converted into SPIDER format,[41] adjusted to a common pixel size of 1.72 Å and subsequently filtered to 18 Å resolution. The two maps were then normalized (same min/max and standard deviation) and the correct threshold calculated to include the expected molecular mass of the particle (excluding the fiber for Pt-Dd). Pt-Dd was subtracted from Bs-Dd but no significant positive densities were visible (not shown). When Bs-Dd was subtracted from Pt-Dd, positive difference density resulted as seen in Figure 6(a).

Five-fold averaging of the fiber

The PDB file corresponding to the distal region of the Ad2 fiber (residues 319–582; PDB accession number 1QIU) was loaded into SPIDER and filtered to 16 Å. 5-fold symmetry was imposed along the fiber shaft to allow comparison with the corresponding density in the cryoEM model. A central slice through the resulting density is shown in Figure 6(b).

Acknowledgements

---

† http://www.cgl.ucsf.edu/chimera/

‡ http://www.ebi.ac.uk/msd/

Supplementary Data

Supplementary data associated with this article can be found, in the online version, at doi:10.1016/j.jmb.2005.11.048

References

1. Stewart, P. L., Fuller, S. D. & Burnett, R. M. (1993). Difference imaging of adenovirus: bridging the resolution gap between X-ray crystallography and electron microscopy. *EMBO J*, **12**, 2589–2599.

2. Bergelson, J. M., Cunningham, J. A., Droguett, G., Kurt-Jones, E. A., Krithivas, A., Hong, J. S. *et al.* (1997). Isolation of a common receptor for Coxsackie B viruses and adenoviruses 2 and 5. *Science*, **275**, 1320–1323.

3. Roelvink, P. W., Lizonova, A., Lee, J. G., Li, Y., Bergelson, J. M., Finberg, R. W. *et al.* (1998). The coxsackievirus-adenovirus receptor protein can function as a cellular attachment protein for adenovirus serotypes from subgroups A, C, D, E, and F. *J. Virol.* **72**, 7909–7915.

4. Cohen, C. J., Shieh, J. T., Pickles, R. J., Okegawa, T., Hsieh, J. T. & Bergelson, J. M. (2001). The coxsackievirus and adenovirus receptor is a transmembrane component of the tight junction. *Proc. Natl Acad. Sci. USA*, **98**, 15191–15916.

5. Walters, R. W., Freimuth, P., Moninger, T. O., Ganske, I., Zabner, J. & Welsh, M. J. (2002). Adenovirus fiber disrupts CAR-mediated intercellular adhesion allowing virus escape. *Cell*, **110**, 789–799.

6. Gaggar, A., Shayakhmetov, D. M. & Lieber, A. (2003). CD46 is a cellular receptor for group B adenoviruses. *Nature Med.* **9**, 1408–1412.

7. Sirena, D., Lilienfeld, B., Eisenhut, M., Kalin, S., Boucke, K., Beerli, R. R. *et al.* (2004). The human membrane cofactor CD46 is a receptor for species B adenovirus serotype 3. *J. Virol.* **78**, 4454–4462.

8. Wickham, T. J., Mathias, P., Cheresh, D. A. & Nemerow, G. R. (1993). Integrins alpha v beta 3 and alpha v beta 5 promote adenovirus internalization but not virus attachment. *Cell*, **73**, 309–319.

9. Albinsson, B. & Kidd, A. H. (1999). Adenovirus type 41 lacks an RGD alpha(v)-integrin binding motif on the penton base and undergoes delayed uptake in A549 cells. *Virus Res.* **64**, 125–136.

10. Greber, U. F., Willetts, M., Webster, P. & Helenius, A. (1993). Stepwise dismantling of adenovirus 2 during entry into cells. *Cell*, **75**, 477–486.

11. Seth, P. (1994). Adenovirus-dependent release of choline from plasma membrane vesicles at an acidic pH is mediated by the penton base protein. *J. Virol.* **68**, 1204–1206.

12. Roberts, M. M., White, J. L., Grutter, M. G. & Burnett, R. M. (1986). Three-dimensional structure of the adenovirus major coat protein hexon. *Science*, **232**, 1148–1151.

13. Stewart, P. L., Chiu, C. Y., Huang, S., Muir, T., Zhao, Y., Chait, B. *et al.* (1997). Cryo-EM visualization of an exposed RGD epitope on adenovirus that escapes antibody neutralization. *EMBO J.* **16**, 1189–1198.

14. Chiu, C. Y., Mathias, P., Nemerow, G. R. & Stewart, P. L. (1999). Structure of adenovirus complexed with its internalization receptor, alphavbeta5 integrin. *J. Virol.* **73**, 6759–6768.

15. Fabry, C. M., Rosa-Calatrava, M., Conway, J. F., Zubieta, C., Cusack, S., Ruigrok, R. W. & Schoehn, G. (2005). A quasi-atomic model of human adenovirus type 5 capsid. *EMBO J.* **24**, 1645–1654.

16. Pettersson, U. & Hoglund, S. (1969). Sructural proteins of adenoviruses. 3. Purification and characterization of the adenovirus type 2 penton antigen. *Virology*, **39**, 90–106.

17. Norrby, E. (1968). Comparison of soluble components of adenovirus types 3 and 11. *J. Gen. Virol.* **2**, 135–142.

18. Schoehn, G., Fender, P., Chroboczek, J. & Hewat, E. A. (1996). Adenovirus 3 penton dodecahedron exhibits structural changes of the base on fibre binding. *EMBO J.* **15**, 6841–6846.

19. Fender, P., Schoehn, G., Foucaud-Gamen, J., Gout, E., Garcel, A., Drouet, E. & Chroboczek, J. (2003). Adenovirus dodecahedron allows large multimeric protein transduction in human cells. *J. Virol.* **77**, 4960–4964.

20. Fender, P., Ruigrok, R. W., Gout, E., Buffet, S. & Chroboczek, J. (1997). Adenovirus dodecahedron, a new vector for human gene transfer. *Nature Biotechnol.* **15**, 52–56.

21. Vives, R. R., Lortat-Jacob, H., Chroboczek, J. & Fender, P. (2004). Heparan sulfate proteoglycan mediates the selective attachment and internalization of serotype 3 human adenovirus dodecahedron. *Virology*, **321**, 332–340.

22. Mizuguchi, H. & Hayakawa, T. (2004). Targeted adenovirus vectors. *Hum. Gene Ther.* **15**, 1034–1044.

23. Zubieta, C., Schoehn, G., Chroboczek, J. & Cusack, S. (2005). The structure of the human adenovirus 2 penton. *Mol. Cell*, **17**, 121–135.

24. Galinier, R., Gout, E., Lortat-Jacob, H., Wood, J. & Chroboczek, J. (2002). Adenovirus protein involved in virus internalization recruits ubiquitin-protein ligases. *Biochemistry*, **41**, 14299–14305.

25. Norrby, E. (1969). The structural and functional diversity of Adenovirus capsid components. *J. Gen. Virol.* **5**, 221–236.

26. Fender, P., Boussaid, A., Mezin, P. & Chroboczek, J. (2005). Synthesis, cellular localization, and quantification of penton–dodecahedron in serotype 3 adenovirus-infected cells. *Virology*, **340**, 167–1673.

27. Conway, J. F. & Steven, A. C. (1999). Methods for reconstructing density maps of "single" particles from cryoelectron micrographs to subnanometer resolution. *J. Struct. Biol.* **128**, 106–118.

28. Ruigrok, R. W., Barge, A., Albiges-Rizo, C. & Dayan, S. (1990). Structure of adenovirus fibre. II. Morphology of single fibres. *J. Mol. Biol.* **215**, 589–596.

29. Wu, E., Pache, L., Von Seggern, D. J., Mullen, T. M., Mikyas, Y., Stewart, P. L. & Nemerow, G. R. (2003). Flexibility of the adenovirus fiber is required for efficient receptor interaction. *J. Virol.* **77**, 7225–7235.

30. Chroboczek, J., Gout, E., Favier, A. L. & Galinier, R. (2003). Novel partner proteins of adenovirus penton. *Curr. Top. Microbiol. Immunol.* **272**, 37–55.

31. van Raaij, M. J., Louis, N., Chroboczek, J. & Cusack, S. (1999). Structure of the human adenovirus serotype 2 fiber head domain at 1.5 Å resolution. *Virology*, **262**, 333–343.

32. Chroboczek, J., Ruigrok, R. W. & Cusack, S. (1995). Adenovirus fiber. *Curr. Top. Microbiol. Immunol.* **199**, 163–200.

33. Green, N. M., Wrigley, N. G., Russell, W. C., Martin, S. R. & McLachlan, A. D. (1983). Evidence for a repeating

cross-beta sheet structure in the adenovirus fibre. *EMBO J.* **2**, 1357–1365.

34. Signas, C., Akusjarvi, G. & Pettersson, U. (1985). Adenovirus 3 fiber polypeptide gene: implications for the structure of the fiber protein. *J. Virol.* **53**, 672–678.

35. Conway, J. F. & Steven, A. C. (1999). Methods for reconstructing density maps of single particles from cryo-electron micrographs to subnanometer resolution. *J. Struct. Biol.* **128**, 106–118.

36. Baker, T. S. & Cheng, R. H. (1996). A model-based approach for determining orientations of biological macromolecules imaged by cryoelectron microscopy. *J. Struct. Biol.* **116**, 120–130.

37. van Heel, M. (1987). Similarity measures between images. *Ultramicroscopy*, **48**, 95–100.

38. Heymann, J. B. (2001). Bsoft: image and molecular processing in electron microscopy. *J. Struct. Biol.* **133**, 156–169.

39. Jones, T. A., Zou, J. Y., Cowan, S. W. & Kjeldgaard, M. (1991). Improved methods for building protein models in electron density maps and the location of errors in these models. *Acta Crystallog. sect. A*, **47**, 110–119.

40. Navaza, J., Lepault, J., Rey, F. A., Alvarez-Rua, C. & Borge, J. (2002). On the fitting of model electron densities into EM reconstructions: a reciprocal-space formulation. *Acta Crystallog. sect. D*, **58**, 1820–1825.

41. Frank, J., Radermacher, M., Penczek, P., Zhu, J., Li, Y., Ladjadj, M. & Leith, A. (1996). SPIDER and WEB: processing and visualization of images in 3D electron microscopy and related fields. *J. Struct. Biol.* **116**, 190–199.

RESEARCH ARTICLE

Protein transduction into human cells by adenovirus dodecahedron using WW domains as universal adaptors

A. Garcel[1]
E. Gout[1]
J. Timmins[2]
J. Chroboczek[1]
P. Fender[1]*

[1]*Institut de Biologie Structurale, 41 rue Jules Horowitz, 38027 Grenoble, France*

[2]*European Synchrotron Radiation Facility (ESRF), Grenoble, France*

*Correspondence to: P. Fender, Institut de Biologie Structurale, 41 rue Jules Horowitz, 38027 Grenoble, France.
E-mail: fender@ibs.fr

Abstract

Background   Direct protein transduction is a recent technique that involves use of peptide vectors. In this study, we demonstrate that adenovirus dodecahedron (Dd), a virus-like particle devoid of DNA and able to penetrate cells with high efficiency, can be used as a vector for protein delivery.

Methods   Taking advantage of Dd interaction with structural domains called WW, we have elaborated a universal adaptor to attach a protein of interest to this vector.

Results   A tandem of three WW structural domains derived from the Nedd4 protein enables the formation of stable complexes with Dd, without impairing its endocytosis efficiency. Our protein of interest fused to the triple WW linker is delivered by the dodecahedron in 100% of cells in culture with on average more than ten million molecules per cell.

Conclusion   These data demonstrate the great potential of adenovirus dodecahedron in combination with WW domains as a protein transduction vector. Copyright © 2006 John Wiley & Sons, Ltd.

Keywords   adenovirus; dodecahedron; WW domain; protein transduction; vector; Nedd4

Introduction

Adenovirus penton is a non-covalent complex composed of the antenna-like fibre protein attached to the capsid-embedded penton base protein. Pentons are localised at the 12 vertices of the adenovirus capsid. It has been reported for most human adenovirus serotypes including adenovirus of serotype 3 (Ad3) that the high affinity interaction of the fibre with its primary receptor [1,2] triggers virus endocytosis through the subsequent interaction of the penton base RGD motif with cellular integrin [3,4]. Remarkably, during the Ad3 viral cycle, some pentons can self-assemble forming symmetric complexes called penton-dodecahedron (Pt-Dd) [5–7]. The formation of dodecahedron (Dd) is due solely to penton base interactions, as attested by the formation in the baculovirus expression system of symmetric particles made of base proteins only, called base-dodecahedron (Bs-Dd). Interestingly, both Bs-Dd and Pt-Dd penetrate human cells albeit with a higher efficiency for the particle containing the fibre. As these particles are devoid of genetic information, they are potentially good tools for gene transfer or protein delivery [7,8].

   Nedd4 is a protein belonging to the ubiquitin E3-ligase family. This modular protein is composed of a C2 domain mediating calcium-dependent attachment to the cellular membrane, four WW domains named WW1 to WW4,

and the catalytic HECT domain (homologous to E6-AP carboxy terminus) [9]. This catalytic domain mediates ubiquitination of proteins that are structurally recognised by the WW domains [10]. Target proteins recognised by the WW domain often display short proline-rich linear sequences, such as PTAP or PPxP [11]. It has been reported that interaction of Nedd4 with viral proteins is required at a late stage of infection (i.e. budding) for several enveloped viruses [12]. Surprisingly, it has been recently demonstrated that the non-enveloped human adenoviruses also interact with several WW-containing proteins. This interaction occurs through the recognition of two PPxY motifs that are strictly conserved in the N-terminus of the penton base protein [13,14].

Adenovirus dodecahedron is a good candidate for intracellular protein delivery; however, in order to attach proteins of interest to Dd, a module enabling attachment to the base protein is necessary. As both Bs-Dd and Pt-Dd contain 12 pentameric bases, they exhibit 60 tandems of WW-interacting PPxY motifs. In this study, the potential use of WW domains for attaching proteins to these dodecameric vectors has been evaluated. We report here that three WW domains derived from Nedd4 are able to attach proteins to Dds making these structural domains a universal adaptor module for protein transduction by our subviral particles.

Methods

Protein expression, purification and detection

Both Pt-Bs and Bs-Dd were expressed in the baculovirus system. Particles were purified by sucrose density gradient, as previously described [7]. The MBP-WW constructs were expressed in *E. coli* and purified on amylose resin (Biolabs), as previously described [15]. The maltose binding protein (MBP) tag was detected using anti-MBP serum (Biolabs) at 1/40 000 for enhanced chemiluminescence (ECL) and enzyme-linked immunosorbent assay (ELISA) and a subsequent incubation with anti-rabbit HRP 1/5000 (Jackson). Dds were detected using anti-Pt-Dd serum recognising both the fibre and the penton base protein at 1/40 000 and a subsequent incubation with anti-rabbit HRP conjugated antibody at 1/5000 (Jackson).

In the immunofluorescence study, the anti-MBP serum was used at 1/1000 for 1 h and was subsequently detected with either anti-rabbit FITC-labelled or anti-rabbit Tex-Red-labelled secondary antibody at 1/250 for 1 h. Pt-Dd used in the co-localisation experiment was previously FITC-labelled by incubating 300 nM of Pt-Dd with 1 mM FITC (Sigma), in 20 mM HEPES, pH 8, for 3 h at 4 °C. Free FITC was removed by dialysis against 20 mM HEPES, 150 mM NaCl, pH 8.

ELISA

Ninety-six multiwell plates were coated overnight at 4 °C with 100 µl of Bs-Dd or Pt-Dd (1 µg/ml in carbonate buffer, pH 9.6). Control wells were coated with buffer alone. After washes with phosphate-buffered saline (PBS), the plates were blocked with PBS/3% bovine serum albumin (BSA) for 1 h at 37 °C. Different concentrations of purified MBP-WW constructs ranging between 0 and 10 µg/ml were incubated for 1 h at room temperature (RT) in triplicate. MBP detection was performed as indicated above in PBS buffer containing 0.05% Tween 20 and 1% BSA. *o*-Phenylenediamine substrate (3 mg/ml, Sigma) was added and the reaction was stopped with 0.5 N sulphuric acid. Absorption at 490 nm was measured and the mean of the triplicate controls was subtracted from the mean of the triplicate assays, for each point tested.

Dd-MBP-WW complex formation

Purified Bs-Dd (100 µg), MBP-WW2,3,4 (200 µg), either separately or pre-incubated together for 1 h at RT in 500 µl PBS, were ultra-centrifuged on sucrose gradient density as previously described [7]. Fractions of 600 µl were collected from the top of the gradient and 10 µl of each were applied under vacuum on a PVDF membrane. Detection was performed with either anti-MBP or anti-Pt-Dd antibody as described above.

Immunofluorescence

HeLa cells were grown overnight on glass coverslips (about 10^5 cell/cm^2) in EMEM medium supplemented with 10% fetal calf serum (FCS), at 37 °C under 5% CO$_2$ atmosphere. Normal human astrocytes (NHA, clonetics) were cultured in astrocyte basal medium (Clonetics) following the supplier' recommendations. The coverslips were then incubated for 1 h at 37 °C with 50 µl of pre-warmed PBS containing either MBP-WW2,3,4 protein alone (2 µg) or in complex with Pt-Dd or Bs-Dd (1 µg). After PBS washes, cells were permeabilised in cold methanol for 10 min. Protein detection was performed as described above. Cell nuclei were counterstained with propidium iodide (5 µg/ml). Laser scanning confocal microscopy was performed with a MRC600 (Bio-Rad). Photographs shown in Figure 4a are the Z-serie projection of eight 0.5 µm cell sections.

Dds and MBP-WW2,3,4 quantification in transduced cells

HeLa cells grown on a 24-multiwell plate (10^5 cells/well) were incubated at 37 °C with 200 µl PBS containing various amounts of MBP-WW2,3,4 (0, 500, 1000, 3000, 5000 ng) either separately or pre-incubated for 1 h with 1000 ng of Pt-Dd. After 1 h, cells were washed and lysed

in 100 µl of cell lysis buffer (Promega). Samples (10 µl) were run on 12% sodium dodecyl sulphate polyacrylamide gel electrophoresis (SDS-PAGE) with a range of purified MBP-WW2,3,4 or Pt-Dd. After electrotransfer on PVDF membrane, proteins were detected with anti-MBP or anti-Pt-Dd antibody, as described above. The molecular weight of MBP-WW2,3,4 (63 kDa) and of the Ad3 penton base monomer (60 kDa, 60 monomers per Dd) make possible the calculation of the amount of these proteins per well.

Results

Respective implication of the different WW domains in binding to Dd

Three of the four WW domains derived from Nedd4 were cloned separately (WW2; WW3; WW4) or together (WW2,3,4) in fusion with the maltose binding protein (MBP) (Figure 1). In the present study, the MBP tag (45 kDa) is not only used for protein purification, but will also enable monitoring of these different constructs with anti-MBP antibody.

Specific interaction of Nedd4 WW domains with Dd was investigated using a modified ELISA method. A multiwell plate coated with Pt-Dd or Bs-Dd was incubated with different concentrations of purified WW proteins. Relative amounts of bound WW proteins were assessed by MBP tag detection, using anti-MBP antibody (Figure 2). All the single Nedd4 WW domains can interact independently with Pt-Dd with a slightly stronger interaction displayed by WW3 (similar results were obtained with Bs-Dd, data not plotted). However, for the construct expressing the

three WW domains together, a dramatic increase in protein binding is observed with both Pt-Dd (full line) and Bs-Dd (dashed line). The interaction reached saturation at a concentration above 2 nM of MBP-WW2,3,4. These observations suggest that, although the single WW domains can independently recognise the penton base, the three domains together likely interact in a cooperative
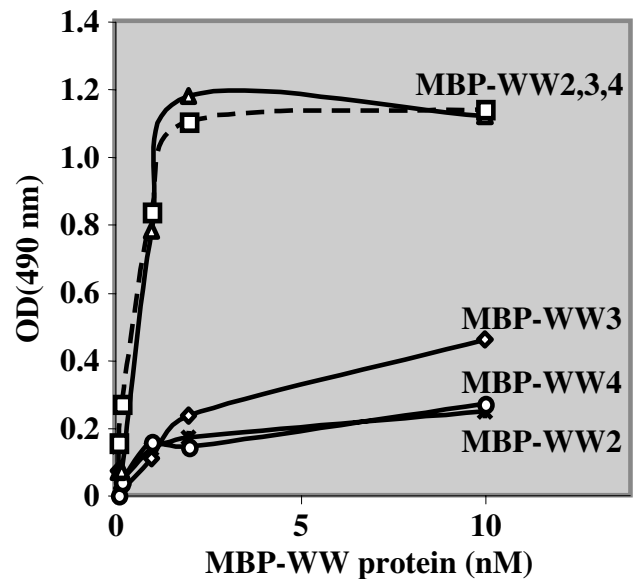

Figure 2. Characterisation of WW construct interaction with Dds by ELISA. Pt-Dd (full line) or Bs-Dd (dashed line) coated on a 96-multiwell plate was incubated for 1 h with different concentrations of WW constructs. Bound proteins were detected with anti-MBP and their relative amounts were assessed with a colorimetric substrate at 490 nm
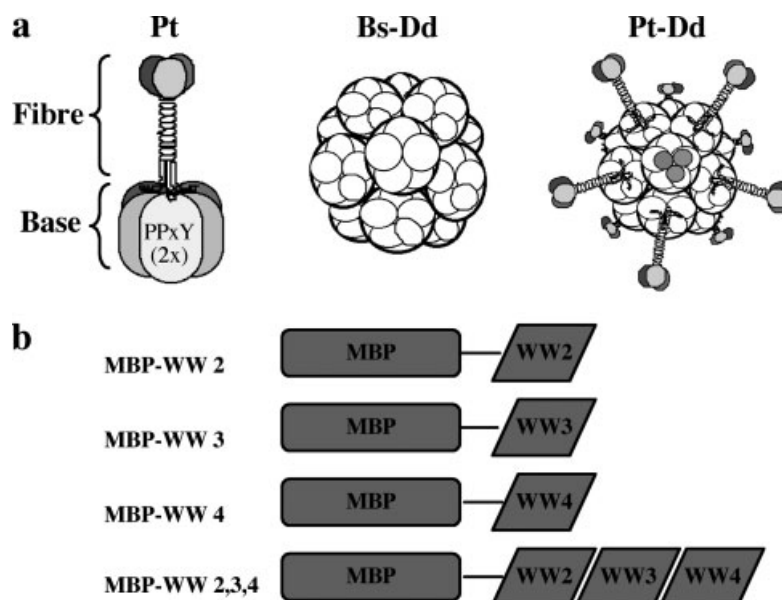

Figure 1. Schematic representation of Dd and WW constructs. (a) Adenovirus penton (Pt) is a non-covalent complex involved in Ad entry, composed of the trimeric fibre and the pentameric penton base (containing 2 PPxY motifs at the N-terminus of each monomer). Expression of Ad3 penton base alone in the baculovirus system leads to the formation of a highly symmetric complex termed base-dodecahedron (Bs-Dd). Co-expression with the Ad3 fibre gives a fibre-decorated particle termed penton-dodecahedron (Pt-Dd). (b) Nedd4-derived constructs are expressed in *E. coli* in fusion with the maltose binding protein (MBP: 45 kDa). Three out of the four Nedd4 WW domains (4 kDa) were expressed separately or together. Constructs containing WW1 domains were insoluble

manner to both kinds of Dd. Moreover, since no difference is observed for MBP-WW2,3,4 binding to Bs-Dd and Pt-Dd, it shows that the fibre does not interfere with WW domain binding to the penton base.

Purification of Dd/MBP-WW2,3,4 stable complexes

Isolation of Dd/MBP-WW2,3,4 complex was performed by sucrose gradient density centrifugation. Indeed, the high molecular weight of Dds (3600 and 4800 kDa for Bs-Dd and Pt-Dd, respectively) enables these particles to migrate towards the bottom fractions of the sucrose gradient density whereas MBP-WW2,3,4 (63 kDa) remains in the upper fractions. In this experiment, Bs-Dd (1.7 nmol of monomeric penton base protein) was incubated with MBP-WW2,3,4 protein (3.2 nmol) prior to ultracentrifugation on a 15–40% sucrose gradient density. After fractionation, a portion of each of the 20 fractions was analysed by dot-blot with either anti-MBP or anti-Pt-Dd antibody. As expected, Bs-Dd alone migrated to the bottom fractions of the gradient (Figure 3, top row, dots 12 to 20) while MBP-WW2,3,4 alone remained in the upper part (Figure 3, middle row, dots 4 to 8). When these proteins were pre-incubated together prior to centrifugation, a significant part of the MBP signal was then detected in the bottom fractions of the gradient density along with Bs-Dd (Figure 3, bottom row). This demonstrates the formation of a stable complex between Dd and MBP-WW2,3,4 that can be separated from free MBP-WW2,3,4 remaining in the upper fractions.

Protein delivery by Dd

Knowing that MBP-WW2,3,4 protein can form a stable complex with Dd, the delivery of this protein into cells was investigated using immunofluorescence. Pt-Dd or Bs-Dd was mixed with MBP-WW2,3,4 protein prior to incubation with HeLa cells. An equivalent amount of fusion protein was used as a control, in the absence of Dd. After 1 h at 37 °C, cells were washed, fixed, and the presence of the protein was detected in green using anti-MBP antibody while the nuclei were counterstained in red. A very bright

and punctate signal was seen in the cytoplasm of HeLa cells incubated with both Pt-Dd and Bs-Dd (Figure 4a, middle and right panels). No detectable signal was seen either in cells incubated with the MBP-WW2,3,4 alone (data not shown), or for Pt-Dd incubated with MBP protein not fused to WW domains (Figure 4a, left panel). These data show that the protein delivery was specifically mediated by Dd and through the WW adaptors.

In order to determine whether Dd and MBP-WW2,3,4 localise together in the cells at 1 h post-transduction, a co-localisation experiment was performed. For this purpose, FITC-labelled Pt-Dd was used and MBP-WW2,3,4 was detected in red with a rhodamine-conjugated antibody (Figure 4b). A pronounced yellow signal was obtained by merging the green Pt-Dd signal with the red signal of MBP-WW2,3,4. This shows that a large majority of the transduced proteins is still in the same cellular compartment as the vector.

Interestingly, the Dd-WW system enables a massive transfer of MBP-WW2,3,4 not only in other transformed cell lines like A549 (not shown), but also in human primary cells, such as endothelial cells (HuVEC) or NHA (Figure 4c).

Quantification of the protein of interest delivered by Dd into the cells

The respective amounts of Pt-Dd and MBP-WW2,3,4 protein transduced into HeLa cells was assessed by Western blot. Cells grown in a multiwell plate were transduced for 1 h at 37 °C with different amounts of MBP-WW2,3,4 protein (0 to 5000 ng), alone or in complex with Pt-Dd. After several washes, cells were lysed and analysed by Western blot using anti-MBP or anti-Pt-Dd serum (Figure 5). The intensities of the bands corresponding to the MBP-WW2,3,4 protein (upper panel) or to the penton base protein (lower panel) were compared to their respective range of purified proteins (on the right). As expected, no WW-MBP signal was seen for the control Pt-Dd alone or for the lowest concentrations of MBP-WW2,3,4 in the absence of Pt-Dd (Figure 5, upper panel, no Pt-Dd). Nevertheless, for high concentrations of MBP-WW2,3,4 alone (2000 and 5000 ng), faint bands were visible, suggesting the
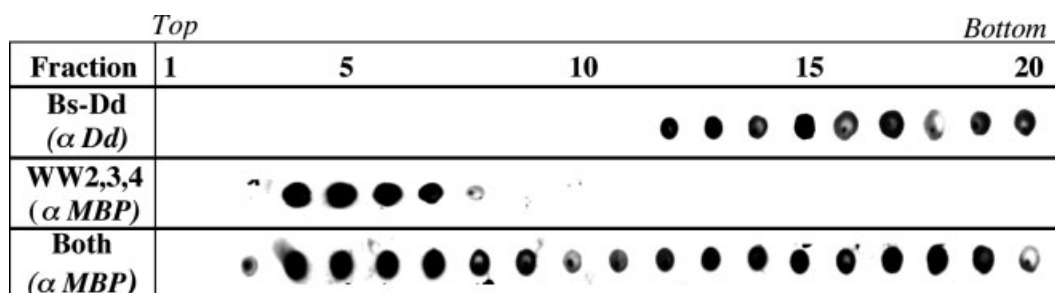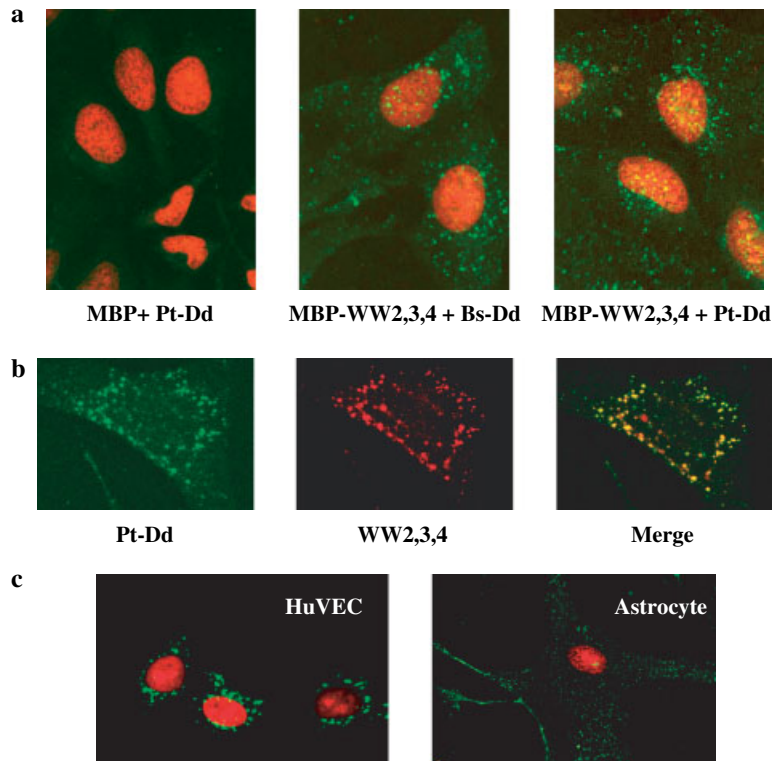

Figure 3. Isolation of Dd/WW2,3,4 complexes by sucrose gradient density. Bs-Dd and MBP-WW2,3,4 separately or incubated both together for 1 h (noted 'both') were run on sucrose gradient density (15–40%). After gradient fractionation from the top to the bottom, protein content in each fraction was analysed by dot-blot with αBs-Dd or αMBP, as indicated in the figure

Figure 4. Detection and localisation by confocal microscopy of MBP-WW2,3,4 protein and Dd translocated in HeLa cell or human primary cells. (a) HeLa cells were incubated for 1 h at 37 °C with MBP-WW2,3,4 in complex with Dds (middle and right panels) or with a control MBP not fused to WW domains (left panel). After cell permeabilisation, MBP-WW2,3,4 protein was detected in green with αMBP antibody while cell nuclei were counterstained by propidium iodide. Photographs are obtained by Z-serie projection of eight 0.5 μm sections. (b) MBP-WW2,3,4 protein in complex with FITC-labelled Pt-Dd was incubated with HeLa cells for 1 h before permeabilisation. Red signal reflects the MBP-WW2,3,4-transduced protein detected with anti-MBP and Texas-red secondary antibody while green signal is raised by FITC-Pt-Dd. The photograph on the right-hand side of the panel was obtained by merging the green Pt-Dd and the red MBP-WW2,3,4 signals demonstrating a significant co-localisation of the vector and the delivered protein. (c) Human endothelial and astrocyte primary cells (HuVEC and NHA) are efficiently transduced by the MBP-WW2,3,4 protein delivered by Bs-Dd. The MBP-WW2,3,4 protein is detected in green with anti-MBP and FITC-labelled secondary antibody and the nuclei are counterstained in red with propidium iodide
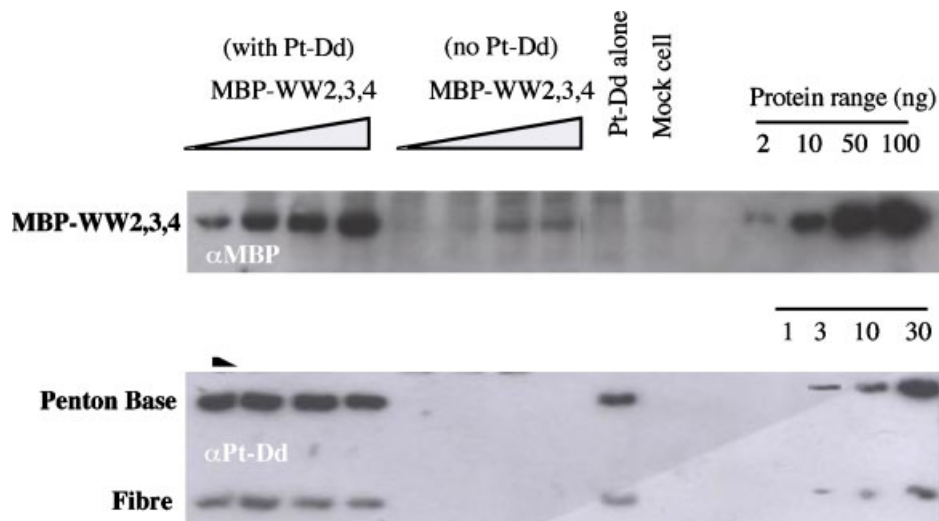
Figure 5. Quantification of the intracellular Pt-Dd and MBP-WW2,3,4 protein in HeLa cells. Cells grown in a multiwell plate were incubated for 1 h at 37 °C with either MBP-WW2,3,4 alone (500, 1000, 2000, 5000 ng; noted 'no Pt-Dd' in the figure) or in complex with a fixed amount of Pt-Dd (noted 'with Pt-Dd' in the figure). After washes, cells were lysed and analysed by Western blot with anti-MBP (upper panel) or anti-Pt-Dd antibody (lower panel). Quantification of Pt-Dd and MBP-WW2,3,4 proteins per cell was achieved by densitometry. For this purpose, the Pt-Dd and MPB-WW2,3,4 signals were compared to that of their respective range of known amounts of purified protein (on the right)

existence of a background internalisation of this protein by HeLa cells. However, when this protein were pre-incubated with Pt-Dd prior to addition to cells, a dramatic increase in MBP-WW2,3,4 transduction was observed for both low and high concentrations used (Figure 5, upper panel, with Pt-Dd). Interestingly, revelation with anti-Pt-Dd showed similar band intensity whatever the concentration of MBP-WW2,3,4 used (Figure 5, lower panel). This observation indicated that vector entry was not affected by the WW domains bound to its surface, thus showing that WW adaptors can be used with no neutralising effect on the vector.

The amount of both Pt-Dd and MBP-WW2,3,4 present in transduced cells was calculated by comparing signals obtained for the different assays to that of the purified protein ranges. It was estimated that on average 3.7×10^5 Pt-Dd are internalised into one cell. Under this condition, Pt-Dd has directed the delivery of 4.7×10^6 MPB-WW2,3,4 protein at the lowest concentration assayed and up to 1.9×10^7 molecules for the highest concentration tested without affecting cell viability, as determined by trypan blue exclusion (not shown). Under this last condition, 51 proteins of interest have been transduced by one Pt-Dd. Interestingly, this ratio is close to the number of penton base monomers constituting the dodecahedron (12 pentamers = 60 monomers), which might signify that one MBP-WW2,3,4 molecule is attached to each penton monomer. Moreover, no proteolysis product was observed for both the MBP-WW2,3,4 and the Pt-Dd vectors, demonstrating that this system is not affected during the internalisation process and the first hour after delivery.

Discussion

The utility of the penton base protein has already been described for gene delivery purposes [7,16–19]. In this work, we demonstrate that adenovirus dodecahedron (Dd) is also a valuable tool for direct protein delivery. In order to attach the protein of interest to the vector, we have taken advantage of the ability of Dd to interact with WW-containing proteins [13,14]. Indeed, we have shown in this study that a protein of interest fused to WW domains derived from the human Nedd4 protein can form a stable complex with Dd without impairing its endocytosis property. The proof-of-concept has been made using a 63 kDa protein (45 kDa for the protein of interest and 18 kDa for the three WW domains). However, it can be speculated that proteins of higher molecular weight could be delivered using this system as we have previously reported that a monoclonal antibody (160 kDa) directed against Dd was efficiently co-internalised with the vector [8]. Although the WW3 domain of Nedd4 seems predominant for the interaction with Dd, as previously reported for Nedd4 interaction with the VP40 protein of Ebola virus [15] or with its natural target, the epithelial sodium channel ENaC [20], this interaction is greatly enhanced by the presence of WW2 and WW4, suggesting a cooperative binding of these domains with dodecahedron. In order to further improve the Dd recognition by WW domains, it could be of interest to artificially generate a tandem of WW3 domains of Nedd4.

The confocal microscopy study shows that proteins fused to the WW2,3,4 domains of Nedd4 are efficiently and rapidly delivered into human cells. Importantly, 100% of the cells are transduced with the protein of interest delivered by either Pt-Dd or Bs-Dd. This high efficacy can be explained by the ability of both kinds of Dd to interact with heparan sulfate (HS). HS is widely expressed at the surface of most cell lines enabling Dd to enter cells that are not even accessible to the virus [21]. Furthermore, protein quantification revealed that, on average, each HeLa cell is transduced with 3.7×10^5 Pt-Dd that have delivered 1.9×10^7 proteins after a 1-h incubation period. This means an average ratio of 51 proteins of interest translocated per Dd, suggesting a quasi molar-occupancy of Dd by the protein, as each Dd is made of 60 monomers of penton base (12 pentamers). Cooperative binding of the WW domains to the vector observed in ELISA (Figure 2) might nevertheless take place as two PPxY sequences are conserved in all the N-terminal sequences of the adenovirus penton bases [13] (see Figure 1). However, a further structural investigation on Dd/WW is necessary to bring a detailed mechanism for this interaction. Indeed, the recent Ad2 penton base structure shows that the N-termini (deleted of the 50 first residues then of the two PPxY sequences) are buried close to the Dd cavity [22]. As the size of the cavity is too small to accommodate large proteins such as MBP-WW2,3,4 [6], it could be envisaged in the full-length penton base (i.e. with PPxY sequences) that the N-termini are flexible, rendering them accessible to WW interaction in the dodecameric structure.

To date, protein delivery has been described using peptides like the drosophila Antennapedia homeodomain [23] or viral peptides such as the Tat transactivator of HIV-1 [24,25], its shorter form of only 11 amino acids [26], or the VP22 protein from HSV-1 [27]. It is of interest to note that these peptides mediate protein transduction through interactions with glycosaminoglycans [28] and that Dd also interacts with this cellular component with an affinity in the nanomolar range [21]. This property not only enables the Dd to be efficiently taken up by Ad3 permissive cells (3.7×10^5 Dd per HeLa cells), but also to target Ad3 non-permissive cells, as this virus cannot exploit the glycosaminoglycan entry pathway [21]. Even if Dd cannot be compared to short peptides in terms of size, its use in protein delivery displays a number of advantages. Indeed, this cargo uses the very efficient adenovirus endocytosis pathway and it can be envisaged to change its tropism. We have previously demonstrated that the Ad2 long fibre can be inserted in the Ad3 Bs-Dd [7]. The Ad2 fibre recognises the CAR receptor [29], whereas the Ad3 fibre interacts

with another primary receptor [30,31], possibly CD46 [1,2]. Addition of Ad2 fibre could not only direct the vector to other cell types, but also change the fate of the delivered proteins, as it has been demonstrated that subgroup B (i.e. Ad3) and subgroup C (i.e. Ad5) fibres induced different trafficking routes [32]. In particular, it is known that adenovirus harbouring subgroup B fibres follows an endosomal route whereas the Ad5 fibre induces rapid escape of the virion from early endosomes [33]. From a targeting point of view, it might be interesting to abolish the natural tropism of the penton base for HS (work in progress) and specifically target different cell lines by introducing into Dds the fibre of different serotypes or by using modified recombinant fibres, as has been done for recombinant adenoviruses [34,35].

Direct protein delivery represents an alternative to gene transfer technology when gene insertion into the genome is not required [36,37]. Even though this strategy may be appropriate only for restricted purposes, this approach is of great interest for specific therapeutic or biotechnological applications that do not require a sustained protein activity like monogenic diseases but rather need only a 'hit' effect of the therapeutic protein that can take place either in the nucleus (i.e. transactivators) or in the cytoplasm (i.e. toxins). In this study, we show the proof-of-concept that the Dd-WW system might be of use in this restricted, but valuable area.

Acknowledgements

References

1. Gaggar A, Shayakhmetov DM, Lieber A. CD46 is a cellular receptor for group B adenoviruses. *Nat Med* 2003; **9**: 1408–1412.
2. Sirena D, *et al*. The human membrane cofactor CD46 is a receptor for species B adenovirus serotype 3. *J Virol* 2004; **78**: 4454–4462.
3. Wickham TJ, Mathias P, Cheresh DA, Nemerow GR. Integrins alpha v beta 3 and alpha v beta 5 promote adenovirus internalization but not virus attachment. *Cell* 1993; **73**: 309–319.
4. Mathias P, Galleno M, Nemerow GR. Interactions of soluble recombinant integrin alpha v beta5 with human adenoviruses. *J Virol* 1998; **72**: 8669–8675.
5. Norrby E. The relationship between the soluble antigens and the virion of adenovirus type 3. II. Identification and characterization of an incomplete hemagglutinin. *Virology* 1966; **30**: 608–617.
6. Schoehn G, Fender P, Chroboczek J, Hewat EA. Adenovirus 3 penton dodecahedron exhibits structural changes of the base on fibre binding. *EMBO J* 1996; **15**: 6841–6846.
7. Fender P, Ruigrok RW, Gout E, Buffet S, Chroboczek J. Adenovirus dodecahedron, a new vector for human gene transfer. *Nat Biotechnol* 1997; **15**: 52–56.
8. Fender P, *et al*. Adenovirus dodecahedron allows large multimeric protein transduction in human cells. *J Virol* 2003; **77**: 4960–4964.
9. Staub O, *et al*. WW domains of Nedd4 bind to the proline-rich PY motifs in the epithelial Na+ channel deleted in Liddle's syndrome. *EMBO J* 1996; **15**: 2371–2380.
10. Macias MJ, *et al*. Structure of the WW domain of a kinase-associated protein complexed with a proline-rich peptide. *Nature* 1996; **382**: 646–649.
11. Macias MJ, Wiesner S, Sudol M. WW and SH3 domains, two different scaffolds to recognize proline-rich ligands. *FEBS Lett* 2002; **513**: 30–37.
12. Garnier L, Wills JW, Verderame MF, Sudol M. WW domains and retrovirus budding. *Nature* 1996; **381**: 744–745.
13. Galinier R, Gout E, Lortat-Jacob H, Wood J, Chroboczek J. Adenovirus protein involved in virus internalization recruits ubiquitin-protein ligases. *Biochemistry* 2002; **41**: 14299–14305.
14. Chroboczek J, Gout E, Favier AL, Galinier R. Novel partner proteins of adenovirus penton. *Curr Top Microbiol Immunol* 2003; **272**: 37–55.
15. Timmins J, *et al*. Ebola virus matrix protein VP40 interaction with human cellular factors Tsg101 and Nedd4. *J Mol Biol* 2003; **326**: 493–502.
16. Medina-Kauwe LK, Kasahara N, Kedes L. 3PO, a novel nonviral gene delivery system using engineered Ad5 penton proteins. *Gene Ther* 2001; **8**: 795–803.
17. Medina-Kauwe LK, Maguire M, Kasahara N, Kedes L. Nonviral gene delivery to human breast cancer cells by targeted Ad5 penton proteins. *Gene Ther* 2001; **8**: 1753–1761.
18. Smith CC, Kulka M, Aurelian L. Modified adenovirus penton base protein (UTARVE) as a non-replicating vector for delivery of antisense oligonucleotides with antiviral and/or antineoplastic activity. *Int J Oncol* 2000; **17**: 841–850.
19. Carlisle RC. Use of adenovirus proteins to enhance the transfection activity of synthetic gene delivery systems. *Curr Opin Mol Ther* 2002; **4**: 306–312.
20. Lott JS, Coddington-Lawson SJ, Teesdale-Spittle PH, McDonald FJ. A single WW domain is the predominant mediator of the interaction between the human ubiquitin-protein ligase Nedd4 and the human epithelial sodium channel. *Biochem J* 2002; **361**: 481–488.
21. Vives RR, Lortat-Jacob H, Chroboczek J, Fender P. Heparan sulfate proteoglycan mediates the selective attachment and internalization of serotype 3 human adenovirus dodecahedron. *Virology* 2004; **321**: 332–340.
22. Zubieta C, Schoehn G, Chroboczek J, Cusack S. The structure of the human adenovirus 2 penton. *Mol Cell* 2005; **17**: 121–135.
23. Derossi D, Joliot AH, Chassaing G, Prochiantz A. The third helix of the Antennapedia homeodomain translocates through biological membranes. *J Biol Chem* 1994; **269**: 10444–10450.
24. Frankel AD, Pabo CO. Cellular uptake of the tat protein from human immunodeficiency virus. *Cell* 1988; **55**: 1189–1193.
25. Green M, Loewenstein PM. Autonomous functional domains of chemically synthesized human immunodeficiency virus tat transactivator protein. *Cell* 1988; **55**: 1179–1188.
26. Fawell S, *et al*. Tat-mediated delivery of heterologous proteins into cells. *Proc Natl Acad Sci U S A* 1994; **91**: 664–668.
27. Elliott G, O'Hare P. Intercellular trafficking and protein delivery by a herpes virus structural protein. *Cell* 1997; **88**: 223–233.
28. Console S, Marty C, Garcia-Echeverria C, Schwendener R, Ballmer-Hofer K. Antennapedia and HIV transactivator of transcription (TAT) "protein transduction domains" promote endocytosis of high molecular weight cargo upon binding to cell surface glycosaminoglycans. *J Biol Chem* 2003; **278**: 35109–35114.
29. Bergelson JM, *et al*. Isolation of a common receptor for coxsackie B viruses and adenoviruses 2 and 5. *Science* 1997; **275**: 1320–1323.
30. Roelvink PW, *et al*. The coxsackievirus-adenovirus receptor protein can function as a cellular attachment protein for adenovirus serotypes from subgroups A, C, D, E, and F. *J Virol* 1998; **72**: 7909–7915.
31. Segerman A, Arnberg N, Erikson A, Lindman K, Wadell G. There are two different species B adenovirus receptors: sBAR, common to species B1 and B2 adenoviruses, and sB2AR, exclusively used by species B2 adenoviruses. *J Virol* 2003; **77**: 1157–1162.

32. Miyazawa N, *et al*. Fiber swap between adenovirus subgroups B and C alters intracellular trafficking of adenovirus gene transfer vectors. *J Virol* 1999; **73**: 6056–6065.

33. Miyazawa N, Crystal RG, Leopold PL. Adenovirus serotype 7 retention in a late endosomal compartment prior to cytosol escape is modulated by fiber protein. *J Virol* 2001; **75**: 1387–1400.

34. Krasnykh VN, Douglas JT, van Beusechem VW. Genetic targeting of adenoviral vectors. *Mol Ther* 2000; **1**: 391–405.

35. Legrand V, Leissner P, Winter A, Mehtali M, Lusky M. Transductional targeting with recombinant adenovirus vectors. *Curr Gene Ther* 2002; **2**: 323–339.

36. Ford KG, Souberbielle BE, Darling D, Farzaneh F. Protein transduction: an alternative to genetic intervention? *Gene Ther* 2001; **8**: 1–4.

37. Schwartz JJ, Zhang S. Peptide-mediated cellular delivery. *Curr Opin Mol Ther* 2000; **2**: 162–167.